

# **Functional Characterization of Wheat ALMT1 Transporter and its Involvement in Extreme pH Stress Tolerance**

A thesis submitted in fulfillment of the requirements for the degree of  
Doctor of Philosophy

at

**University of Adelaide**



**Faculty of Sciences**

**School of Agriculture, Food and Wine**

Submitted by

**Muhammad Kamran**

14<sup>th</sup> June 2018

## Table of Contents

Abstract .....	4
Declaration.....	7
Acknowledgments .....	8
Dedication.....	10
List of Publications from this Thesis .....	11
List of Abbreviations .....	12
Chapter 1: Introduction and Literature Review      Role of ALMT1 transporter during alkaline pH stress.....	14
1.1 Introduction.....	14
1.2 What are alkaline soils? .....	15
1.2.1 Aluminium toxicity in alkaline soils.....	17
1.2.2 Healthy roots, healthy plants .....	18
1.2.3 Mechanism of root growth in alkaline soils.....	18
1.3 Anion channels have multifarious and integrated roles in plants .....	19
1.3.1 R-type anion channels are encoded by ALMTs.....	20
1.3.2 What are ALMTs? .....	21
1.3.3 The Role of ALMTs is diverse and not specific to Al resistance .....	22
1.3.4 Are ALMTs involved in signalling?.....	26
1.3.5 Links between ALMTs and plant hormones.....	26
1.3.6 TaALMT1 is more active at pH 9 than pH 4.5.....	27
1.4 Organic anion efflux is linked to alkaline soil tolerance – is this due to acidification of apoplast and avoidance of phosphorus and iron deficiency? .....	28
1.5 GABA is a ubiquitous molecule .....	29
1.5.1 GABA metabolism .....	30
1.5.2 The transcriptional link between GABA and ALMT1 .....	31
1.5.3 Is GABA a stress signal? .....	32
1.5.4 TaALMT1 is regulated by external GABA, but its activation also changes endogenous GABA levels.....	33
1.6 Research questions.....	35
1.7 Aims and objective .....	35
1.8 References.....	36
Chapter 2: RESEARCH ARTICLE      Aluminium-Activated Malate Transporters Can Facilitate GABA Transport.....	46
2.2 SUPPLEMENTAL MATERIAL.....	65
Chapter 3: RESEARCH ARTICLE      Role of TaALMT1 malate-GABA transporter in alkaline pH tolerance of wheat. ....	87
2.1 ABSTRACT.....	89
3.2 INTRODUCTION .....	90
3.3 RESULTS .....	92

3.4	DISCUSSION.....	106
3.5	MATERIALS AND METHODS.....	114
3.6	LITERATURE CITED .....	120
3.7	SUPPLEMENTAL MATERIAL.....	125
3.8	APPENDIX TO CHAPTER 3 .....	128
Chapter 4: General discussion and future directions .....		148
3.1	Alkaline tolerance mediated by TaALMT1.....	149
4.2	Root growth over 5 weeks is enhanced at high pH by the presence of the TaALMT1-V allele in ET8 plants but not in barley expressing TaALMT1 (Appendix Chapter 3). ....	150
4.3	Higher root exudation of malate and GABA occurs at alkaline pH in wheat and barley associated with the expression of TaALMT1 .....	151
4.4	TaALMT1 might also be involved in aluminium tolerance at alkaline pH.....	152
4.5	Exogenous GABA and muscimol blocked Al <sup>3+</sup> activated malate efflux at low pH, but the block didn't occur at high pH. ....	152
4.6	Is TaALMT1 calcium sensitive?.....	153
4.7	Research questions and future directions.....	153
4.7.1	What is the molecular mechanism (in a broader perspective) of alkaline soil tolerance? .....	153
4.7.2	Is TaALMT1-mediated GABA influx and efflux proton-coupled?.....	154
4.7.3	Can malate and GABA be complexed with aluminium at high pH?.....	157
4.7.4	What are the links between ALMTs and plant hormones?.....	157
4.8	References.....	159

## Abstract

The optimum soil pH for most cultivated plants ranges from pH 6 to 8. This range provides optimal nutrient availability and minimal effects of toxic ions. Soils with pH below 5.5 (acid) and above 8 (alkaline) pose challenges for plant growth and development due to ion toxicities and lack of nutrient availability or nutrient imbalances. Roots of some species such as *Triticum aestivum* (wheat) exude organic anions such as malate under acidic conditions, providing tolerance against free  $\text{Al}^{3+}$  which is highly toxic to roots. In wheat the transporter responsible for this exudation is the Aluminium Activated Malate Transporter (TaALMT1). This thesis examines the role of the TaALMT1 transporter in extreme pH stress tolerance.

Plant ALMTs are anion channels named after the first characterized member from wheat roots (TaALMT1). However, most ALMTs are not activated by  $\text{Al}^{3+}$ , but all those so far investigated are regulated by gamma-aminobutyric acid (GABA). Gamma-aminobutyric acid (GABA) regulation of anion flux through ALMT proteins requires a specific amino acid motif in ALMTs that shares similarity with a GABA-binding site in mammalian GABA<sub>A</sub> receptors. In wheat root apices a negative correlation between activation of TaALMT1 and endogenous GABA concentrations ( $[\text{GABA}]_i$ ) was previously identified. This is explored here further in both wheat root apices and in heterologous expression systems using inhibitors that are reported to change  $[\text{GABA}]_i$ : amino-oxyacetate (AOA) – a glutamate decarboxylase (GAD) and GABA transaminase (GABA-T) inhibitor, and vigabatrin – a GABA transaminase (GABA-T) inhibitor. It is demonstrated that activation of TaALMT1 reduces  $[\text{GABA}]_i$  because TaALMT1 facilitates GABA efflux. Though TaALMT1 is activated by  $\text{Al}^{3+}$  the released GABA does not complex  $\text{Al}^{3+}$ . TaALMT1 also facilitates GABA transport into cells, demonstrated by a yeast complementation assay and via  $^{14}\text{C}$ GABA uptake into *TaALMT1*-expressing *Xenopus laevis* oocytes; found to be a general feature of all ALMTs examined. Mutation of the GABA ‘motif’ (TaALMT1<sup>F213C</sup>) prevented both GABA influx and efflux in yeast and *Xenopus laevis* oocytes, and resulted in no correlation between malate efflux and  $[\text{GABA}]_i$ . It is concluded that ALMTs are likely to act as both GABA and anion transporters *in planta*. GABA and malate appear to interact with ALMTs in a complex manner to regulate each other’s transport, suggestive of a role for ALMTs in communicating metabolic status.

One of the potential roles for GABA is as a pH regulator. Being a zwitterion its exudation into acidic or alkaline solutions will tend to bring pH towards neutrality. Previous field studies have suggested that TaALMT1 in wheat may also confer tolerance to alkaline soil. Soil alkalinity reduces yield and is a major problem worldwide, but very little is known about the physiological mechanisms that allow some plants to tolerate alkaline conditions. Along with its

role in  $\text{Al}^{3+}$  tolerance at low pH, TaALMT1 is also activated by external anions at alkaline pH. Therefore it was hypothesized that TaALMT1 provides alkaline soil tolerance by exuding malate and GABA facilitating acidification of the rhizosphere. To test this hypothesis, a series of experiments were carried out using wheat NILs; ET8 ( $\text{Al}^{3+}$  tolerant, high expression of TaALMT1) and ES8 ( $\text{Al}^{3+}$  sensitive, low expression of TaALMT1) and *Xenopus laevis* oocytes expressing *TaALMT1*. Under alkaline conditions, root biomass was significantly higher in the ET8 plants compared to ES8 plants and was inhibited by the application of GABA. Shoot gas exchange also differed between NILs but continuous GABA application to roots interfered with shoot gas exchange. In alkaline conditions, a higher concentration of both malate and GABA was found in root exudates from root apices and whole seedling roots with high TaALMT1 expression which appears to decrease the rhizosphere pH more so in ET8 compared with ES8. *Xenopus laevis* oocytes expressing *TaALMT1* also acidified an alkaline media more rapidly than controls corresponding to higher GABA efflux. *TaALMT1* expression did not change under alkaline conditions but key genes involved in GABA turnover changed in accord with a high rate of GABA synthesis in ET8. It is concluded that TaALMT1 plays a role in alkaline soil tolerance by exuding malate and GABA, possibly coupled to proton efflux, facilitating rhizosphere acidification.

To further explore the role of TaALMT1 in alkaline soil tolerance, transgenic Golden Promise barley plants expressing TaALMT1 (TaALMT1-GP) were treated with pH 6 and pH 9 nutrient solutions over 5 weeks of growth. There was no significant effect of TaALMT1 expression on shoot and root growth relative to GP wildtype in alkaline conditions. However, root fresh mass was more sensitive to pH for TaALMT1-GP with a significantly larger root fresh mass at pH 9 compared with pH 6. GABA application significantly reduced both root and shoot growth independently of TaALMT1 expression. Malate and GABA efflux was higher in TaALMT1-GP plants than for GP plants at pH 9, however, the opposite was the case at pH 6. GABA application affected malate efflux with different effects between TaALMT1-GP and GP. Malate efflux from root apices over 1 h was not significantly different between TaALMT1-GP and GP and both genotypes increased malate efflux at high pH. However, GABA efflux was significantly higher in TaALMT1-GP than GP at pH 9 in buffered solution. It is concluded that the expression of TaALMT1 may be interfering with the endogenous systems that allow barley to tolerate alkaline soils and that future experiments will require the use of null segregants as the appropriate controls rather than wildtype (GP) background.

Preliminary experiments were also undertaken to test the effects of externally applied sodium aluminate, calcium, GABA and muscimol, and selected hormones using wheat (ET8 and ES8 NILs) and Barley (TaALMT1-GP and GP, aluminate only) at alkaline pH. Sodium

aluminate treatment significantly increased malate and GABA efflux above the already elevated level at pH 9 in plants with high expression of TaALMT1, suggestive of TaALMT1 involvement. Root growth was also higher in response to sodium aluminate in both ET8 and TaALMT1-GP compared with ES8 and GP respectively. Elevated external calcium significantly increased  $\text{Al}^{3+}$ -activated malate efflux in ET8 compared with ES8 with an optimum at 3 mM  $\text{CaCl}_2$ . In response to external jasmonic acid (JA) and brassinosteroid (BR) at pH 4.5, ET8 showed a higher  $\text{Al}^{3+}$ -activated malate efflux compared to ES8. However, in contrast to malate, GABA efflux was significantly reduced by BR and JA compared with the  $\text{Al}^{3+}$  treatment alone. Root growth was significantly reduced in response to JA plus  $\text{Al}^{3+}$  compared with  $\text{Al}^{3+}$  alone. However, BR plus  $\text{Al}^{3+}$  significantly enhanced root growth compared to  $\text{Al}^{3+}$  treatment alone.

Overall, it is concluded that: 1) TaALMT1 is not only regulated by GABA but also mediates its transport, which is a general feature of ALMTs. 2) TaALMT1 plays a role in alkaline soil tolerance by exuding malate and GABA and facilitating rhizosphere acidification. 3) External application of high concentrations of GABA (10 mM) to roots results in inhibited root growth and alters leaf gas exchange possibly by interactions with other ALMTs. In addition, the following preliminary conclusions are subject to carrying out experiments with TaALMT1 expressed in heterologous systems: 1) TaALMT1 might be calcium sensitive. 2) TaALMT1 may play a role in aluminium tolerance in alkaline conditions. 3) There may be complicated hormonal control over TaALMT1 activity and selectivity.

## Declaration

I certify that this work contains no material which has been accepted for the award of any other degree or diploma in my name, in any university or other tertiary institution and, to the best of my knowledge and belief, contains no material previously published or written by another person, except where due reference has been made in the text. In addition, I certify that no part of this work will, in the future, be used in a submission in my name, for any other degree or diploma in any university or other tertiary institution without the prior approval of the University of Adelaide and where applicable, any partner institution responsible for the joint-award of this degree.

I acknowledge that copyright of published works contained within this thesis resides with the copyright holder(s) of those works.

I also give permission for the digital version of my thesis to be made available on the web, via the University's digital research repository, the Library Search and also through web search engines, unless permission has been granted by the University to restrict access for a period of time.

I acknowledge the support I have received for my research through the provision of an Australian Government Research Training Program Scholarship.

Muhammad Kamran

13<sup>th</sup> June 2018

## Acknowledgments

I would like to express my special appreciation and thanks to my principal supervisor Prof Stephen Tyerman for giving me the opportunity to study with him and for his continuous support, constructive guidance and motivation during the course of this study. I remember all those days and many hours you spent with me for discussing results and further experiments. I am also grateful to him for critically reading my work and for supporting my research ideas. Steve, I feel so lucky that I was one of your students and I believe that I could not have had a better mentor and supervisor.

I thank my co-supervisor Dr. Jay Kumar Bose for critically reading my work and help in experiments. I am also grateful to Dr Jay for the training he provided me with MIFE. Many thanks for being my co-supervisor in this process and for encouraging attitude and useful discussions.

This work would not have been possible without the help and support I got from various people. I thank Dr Sunita Ramesh for providing training, guidance and sharing knowledge throughout my PhD. I have able to learn a lot from her which helped me to broaden my knowledge in Plant Biology. Sunita, kindly accept my sincere gratitude and appreciation for all the help I got during my PhD. I am immensely grateful to Wendy Sullivan for her support and help during the course of this study. I acknowledge the support from Gilliham and Steve Lab members, specially Asmini Athman, Ali Mafakheri, and Dr. Rebecca Vandeleur.

I thank the Australian government and the University of Adelaide for providing financial support through the provision of an Australian Government Research Training Program Scholarship (RTP) and Australian Postgraduate Award (APA). I also thank Professor Matthew Gilliham for the guidance he provided in getting these scholarships. I thank the Australian Research Centre, Centre of Excellence in Plant Energy Biology, for generously providing financial support to this project.

I would like to thank Prof Shafiq Ur Rehman and Dr. Amana Khatoon for their sincere advice and encouragement to pursue a career as a research scientist in Plant Biology. I am immensely grateful to Dr. Abdul Latif Khan for his continuous motivation and for showing me a possible PhD pathway. I also thank my brother Dr. Qari Muhammad Imran for his valuable discussions during the course of this study.

I offer my sincerest gratitude to my family for unconditional support and encouragement throughout my study abroad. Deepest thanks to both my parents and parents-in-law for believing in me and for encouraging me to fulfill my dreams.

Finally, I am deeply thankful to my wife Maria Kamran for her patience and for providing me with an enormous amount of support and encouragement during the pursuit of this degree. Thank you Maria, for being with me through the challenging journey, for your love and ongoing support in difficult times. Thanks to my son Hassan Muhammad Kamran for his patience, especially, when I spent after-hours and weekends to complete PhD tasks. Dear Hassan, I know daddy didn't play much with you but for sure, soon, daddy is going to submit thesis and he will play with you as much as you want.

Muhammad Kamran

June 2018

## **Dedication**

To my father Aurang Zeb who couldn't see this achievement, but he has been an inspiration for me to go beyond the limitations. And to my mother Farzana Begum who encouraged me to fulfil my father's dream and for her unconditional love.

## List of Publications from this Thesis

### Journal publications

1. Ramesh SA, **Kamran M**, Sullivan W, Chirkova L, Okamoto M, Degryse F, McLauchlin M, Gilliam M and Tyerman SD. (2018) Aluminium-Activated Malate Transporters Can Facilitate GABA Transport. **The Plant Cell**. 30: 1147–1164
2. **Kamran M**, Ramesh SA, Bose J, Gilliam M, Tyerman SD. (2018) Role of TaALMT1 malate-GABA transporter in alkaline pH tolerance of wheat. Submitted to **Plant Physiology** (under review process).

### Conference presentations

1. **Kamran M**, Ramesh SA, Gilliam M, Bose J and Tyerman SD. (2017) Role of TaALMT1 malate-GABA transporter in alkaline pH tolerance of wheat. COMBIO. Adelaide, Australia.
2. Ramesh SA, **Kamran M**, Sullivan W, Gilliam M and Tyerman SD. (2017) The role of gamma aminobutyric acid (GABA) in abiotic stress tolerance in plants. COMBIO. Adelaide, Australia.
3. **Kamran M**, Tyerman SD and Gilliam M. (2015) Wheat root tolerance to high pH. COMBIO. Melbourne, Australia.
4. **Kamran M**, Tyerman SD and Gilliam M. (2015) Root growth and high pH tolerance. Post Graduate Symposium. University of Adelaide, Waite Campus, Australia

## List of Abbreviations

ALMT 1	Aluminium Activated Malate Transporter 1
AOA	Amino-oxyacetate
OA	Organic acid
GABA	Gamma-aminobutyric acid
TaALMT1	Wheat aluminium activated malate transporter 1
NIL	Near isogenic line
AUX1	Auxin transporter protein 1
PKS5	SOS2-like protein kinase 5
J3	Arabidopsis DnaJ homologous protein 3
PIN	PIN-formed auxin efflux transporter family
ABA	Abscisic acid
R-type	Rapid type
S-type	Slow type
SLAC	Slowly activating anion channel family
QUAC	Quick anion channel
WT	Wild type
FAO	Food and Agriculture Organization of the United Nations
GP	Golden promise barley
TCA	Tricarboxylate acid cycle
<i>A</i>	Assimilation rate (Photosynthesis)
<i>E</i>	Transpiration rate
<i>g<sub>s</sub></i>	Stomatal conductance
3MPA	3-Mercaptopropionic acid
GAD	Glutamate decarboxylase
ROS	Reactive oxygen species
RNAseq	RNA sequencing
ha	Hectare
JA	Jasmonic Acid
BR	Brassinosteroids
ACC	1-Aminocyclopropane-1-carboxylic acid (ACC)
BY2	Cultivar Bright Yellow - 2 of the tobacco plant
SSDH	Succinic semialdehyde dehydrogenase
CaM	calcium (Ca <sup>2+</sup> )/calmodulin

STOP1	Sensitive to proton toxicity1
GABA-T	Gamma-aminobutyric acid aminotransferase
UPLC	Ultra-High-Performance Liquid Chromatography
M, mM, $\mu$ M, nM	Molar, milli molar, micro molar, nano molar
NADP	Nicotinamide adenine dinucleotide phosphate
GAT1	GABA influx transporter 1
OE	Over expresser
TEVC	Two-electrode voltage clamp
cRNA	Complementary RNA
EAAT	excitatory amino acid transporters
BTP	1,3-Bis[tris(hydroxymethyl)methylamino] propane
MES	2-(N-morpholino) ethanesulfonic acid
MS	Murashige and Skoog's
ISE	Ion selective electrode
PCR	Polymerase chain reaction
cDNA	Complementary DNA
mV	Milli volts
qPCR	Quantitative PCR
MIFE	Microelectrode ion flux estimation

## Chapter 1: Introduction and Literature Review

### Role of ALMT1 transporter during alkaline pH stress

#### 1.1 Introduction

Alkaline soils are a global problem that can severely affect crop productivity worldwide. According to one estimate, up to 831 million ha of the world's land is saline, of which 434 million ha is affected by soil alkalinity (Jin et al., 2006; Xu et al., 2013). In Australia, soil alkalisation (Wong et al., 2008) has become an increasingly important problem; about 30% of soils in Australia are sodic of which 86% are alkaline (Rengasamy and Olsson, 1991). Alkaline soils cause soil toxicity, and nutrient deficiency thereby negatively impacting crop growth and productivity. Several studies have been published about mechanisms of alkaline soil tolerance in plants and the main focus has been the plasma membrane H<sup>+</sup>-ATPase and its relationship with auxin and ethylene (Fuglsang et al., 2007; Yang et al., 2010; Xu et al., 2012; Xu et al., 2013; Li et al., 2015). The H<sup>+</sup>-ATPase is also a key component of aluminium tolerance allowing cytosolic pH regulation and charge balance for organic anion secretion at low pH (Zhang et al., 2017). There is also the requirement to reduce excess ROS under alkali stress as shown in rice and wheat (Guo et al., 2014; Meng et al., 2017; Zhang et al., 2017). There are no reports suggesting alternative mechanisms that plants use to tolerate alkaline soils and the potential combination with aluminium.

To survive against various environmental stresses, plants exude different compounds which help to keep the rhizosphere environment favourable for plant growth and development. For example, in acidic soils, Al<sup>3+</sup> toxicity is a serious problem affecting root growth. Several plant species have evolved mechanisms to alleviate Al<sup>3+</sup> toxicity by triggering organic acid (OA) anions exudation from root apices, e.g. malate and citrate. These OA anions chelate Al<sup>3+</sup> in the rhizosphere (and/or in the apoplast), resulting in the formation of non-toxic Al<sup>3+</sup> complexes thereby preventing the entry of phototoxic Al<sup>3+</sup> into the root tissue (Ma et al., 2001; Ryan et al., 2001; Kochian et al., 2004). This phenomenon was the basis for the identification and characterization of the first member of the Aluminium-activated Malate Transporter proteins (ALMT) family (Sasaki et al., 2004).

Gamma-aminobutyric acid (GABA) is a non-protein amino acid and a major inhibitory neurotransmitter in mammalian brains (Palacios et al., 1981; Owens and Kriegstein, 2002). In plants, both abiotic (hypoxia, heat, cold, drought, aluminium) and biotic (herbivory, infection) stresses results in rapid accumulation of GABA (Shelp et al., 2012). For the last 20 years, scientists have tried to determine whether GABA is an endogenous signal in plants, but the

definitive proof was lacking until the recent discovery by Ramesh et al (2015) that provided the first evidence for a signalling role of GABA in plants. Plant ALMTs have a GABA binding motif that acts as a GABA receptor to regulate these anion channels (Ramesh et al., 2015). At low pH (pH 4.5), endogenous GABA concentrations were high in the root tips of Al-tolerant wheat (ET8) but decreased in presence of  $Al^{3+}$ . Interestingly, endogenous GABA concentrations decreased with increasing pH and anion efflux via TaALMT1 from wheat could be activated by exogenous anions (e.g. malate, sulphate, chloride) at alkaline pH in the absence of  $Al^{3+}$  (Ramesh et al., 2015). Previously, it has been shown that, among all amino acids exuded from wheat roots, GABA showed the highest efflux (Warren, 2015). This raised the question as to why wheat plants allow such a large carbon loss via GABA exudation. To answer this question, Gilliham and Tyerman (2016) hypothesized that GABA might be involved in cell to cell communication of metabolic status. They proposed that ALMTs can sense and signal metabolic status of a cell thorough GABA and translate this information into a physiological response via changes in membrane potential (Gilliham and Tyerman, 2016).

The role of TaALMT1 in  $Al^{3+}$  tolerance in acid soils is well established (Ryan et al., 2011). Intriguingly, wheat genotypes with a higher level of TaALMT1 expression produced greater yields under alkaline soils (McDonald et al., 2013; Eagles et al., 2014), suggesting TaALMT1 improves alkaline soil tolerance through an unknown mechanism which needs to be further investigated. The ET8 NIL has the Type V allele of *TaALMT1* (TaALMT1-V) associated with high expression of *TaALMT1* in root apices and greater malate efflux, while ES8 NIL possesses the Type I allele of TaALMT1 (TaALMT1-I) associated with low expression of *TaALMT1* and low malate efflux (Ryan et al., 1995; Sasaki et al., 2004; Raman et al., 2005; Ryan et al., 2010). However, a recent study comparing these two NILs concluded that there was no evidence of increased alkaline tolerance from possession of the TaALMT1 high expression allele (Silva et al. 2018). This review aims to cover mechanisms of root growth in alkaline soils, the regulation of malate efflux from roots via TaALMT1 and the role of GABA signalling *in planta*.

## **1.2 What are alkaline soils?**

Alkaline soils are generally defined as soils having a pH greater than pH 8 (Brautigan et al., 2014). According to Guerinot et al (2007), alkaline soils makeup one-third of the world's soils (Figure 1).

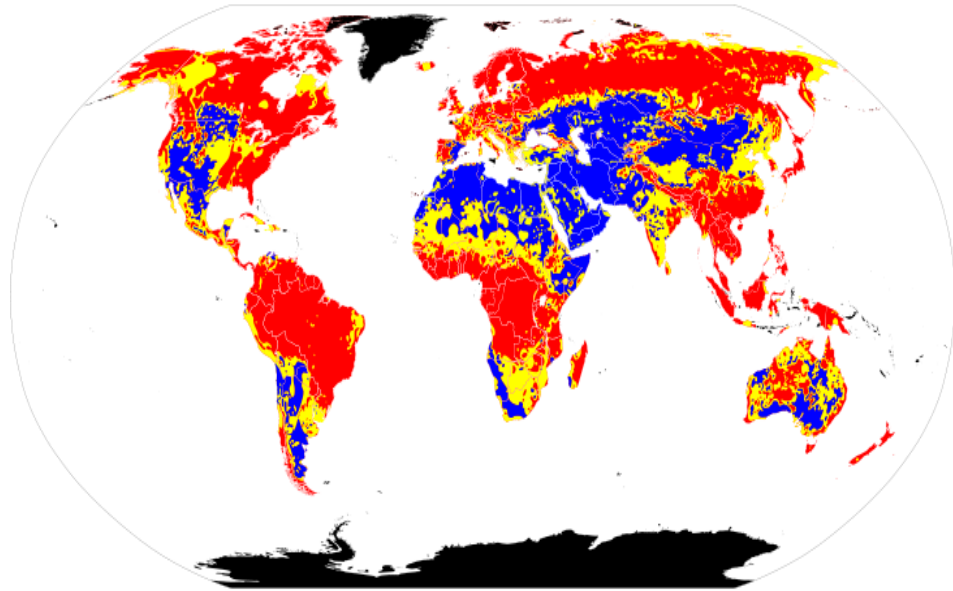


**Figure 1:** Distribution of world's alkaline soils (blue areas)

Adopted from [http://commons.wikimedia.org/wiki/File:World\\_Soil\\_pH.svg](http://commons.wikimedia.org/wiki/File:World_Soil_pH.svg)

In Australia, 30% of the cropping land is affected by alkaline soils (de Caritat et al., 2011) (Figure 2). The situation is more severe in South Australia, where over 80% of the soils in the cereal zone have an alkaline subsoil with pH ranging from 8 to 10.5 (Ma et al., 2003). In particular, alkaline soils impose a number of physical (e.g. photosynthesis, metabolic balance of reactive oxygen species, microfilament depolymerization and membrane selectivity) and chemical limitations (e.g iron (Fe) deficiency and cellular ionic homeostasis) that result in poor root growth, nutrition and water uptake (Shi and Sheng, 2005; Yang et al., 2007; Zhang and Mu, 2009; Zhou et al., 2010; Liu and Guo, 2011). To improve crop growth in alkaline soils through molecular plant breeding, a thorough understanding of the mechanisms alkaline soil tolerance is clearly needed (Xu et al., 2013).

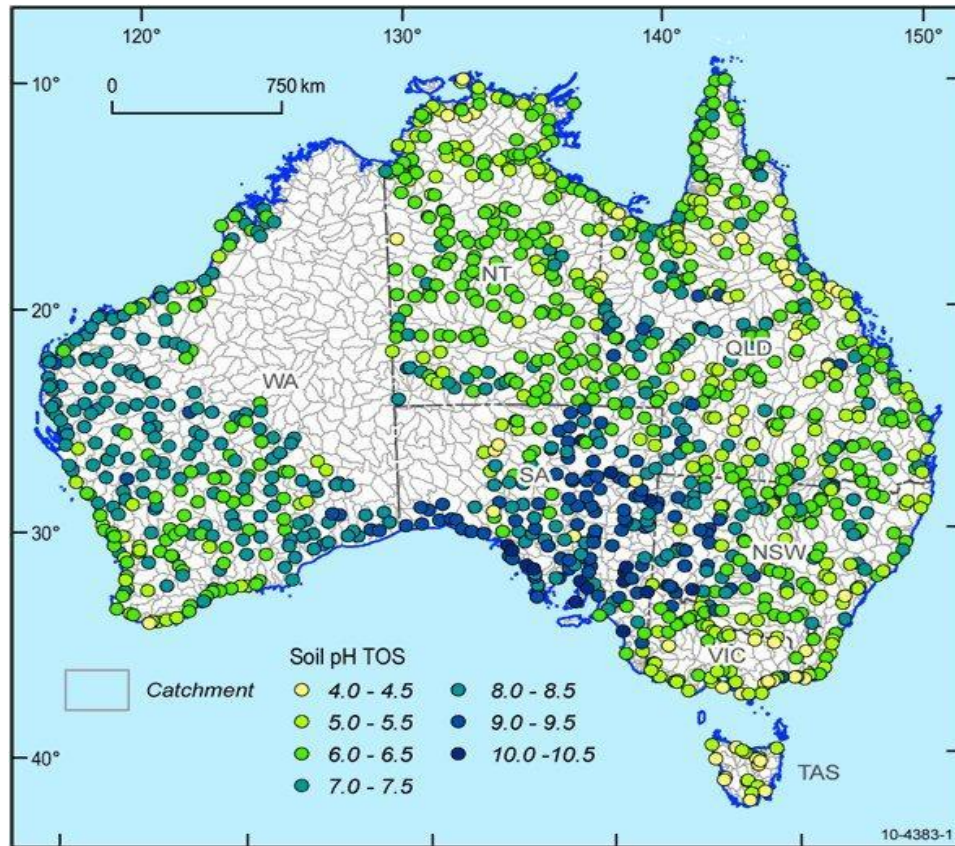


**Figure 2:** pH map (TOS, Top Outlet Sediment) of Australian soils developed by Geoscience Australia. A large number of blue dots (high pH soils) can be seen clearly in SA, WA, Vic, NSW and QLD. Adapted from Geoscience Australia, <http://www.ga.gov.au/ausgeonews/ausgeonews201003/soil.jsp>

The concentration of hydroxide ( $\text{OH}^-$ ) ions in soil is the main factor responsible for alkalinity. The hydroxide producing anions in the soil are usually carbonates and bicarbonates. Sometimes alkaline soils are associated with carbonate salts having a high content of exchangeable sodium, which on its hydrolysis elevates the soil pH, for example, following the hydrolysis of sodium carbonate ( $\text{Na}_2\text{CO}_3$ ) and sodium bicarbonate ( $\text{NaHCO}_3$ ). Plants growing on these soils not only suffer from sodium toxicity but also alkaline pH stress (Jin et al., 2006). Little research attention has been paid to assess the combined effects of sodium and alkaline pH on plant growth and development (Yang et al., 2008; Xu et al., 2012).

### 1.2.1 Aluminium toxicity in alkaline soils

After oxygen and silicon, aluminium is the third most abundant element that makes up 7% of the earth's crust. Aluminium ( $\text{Al}^{3+}$ ) toxicity is extensively studied in acidic soils because of the phototoxic  $\text{Al}^{3+}$  concentration increases when the soil pH drops below 5 (Delhaize and Ryan, 1995; Matsumoto, 2000; Kochian et al., 2005). When the pH is above 5, it is often assumed that aluminium is not toxic to plants. However, there is evidence suggesting that the aluminate ion [ $\text{Al}(\text{OH})_4^-$ ; the predominant species of aluminium under alkaline pH] (Kinraide, 1990; Ma et

al., 2003; Kopittke et al., 2005; Stass et al., 2006; Brautigam et al., 2012, 2014) can be toxic to plants when the pH is above 9.0. For example, anionic aluminate species reduced the root growth even at concentrations as low as 1 mg L<sup>-1</sup> (Ma et al., 2003), which is 12 micromolar as sodium aluminate. Hence, future research must focus on understanding aluminate toxicity and tolerance mechanisms under alkaline pH.

### 1.2.2 Healthy roots, healthy plants

Plants have a remarkable ability to change their growth and development continually in response to changing environmental signals. The root system is the main interface between a plant and soil environment that is responsible for a number of processes, such as nutrient and water absorption, and anchoring the plant to the ground. Root growth plasticity determines overall plant growth and survival under harsh environments (Gruber et al., 2013). Since, the roots are the first organ to sense and face rhizotoxicity of different metal ions and extreme pH stresses, studying their role in stress tolerance is very important.

### 1.2.3 Mechanism of root growth in alkaline soils

Under alkaline pH, primary root elongation is inhibited because of reduced meristematic cell division and ethylene modulates this inhibition by stimulating AUX1 expression resulting in increased auxin accumulation (Li et al., 2015). The plasma membrane H<sup>+</sup>-ATPase plays an important role in the adaptation of roots to alkaline stress by lowering rhizosphere pH through secretion of protons (Yang et al., 2010; Xu et al., 2012). For instance, a PKS5 type protein kinase can inhibit the activity of the plasma membrane H<sup>+</sup>-ATPase by preventing interaction with 14-3-3 proteins, accordingly, *pks5* knockout mutants of Arabidopsis were more tolerant to alkaline stress because of greater extrusion of protons to the extracellular space. Similarly, a chaperone DNAJ-HOMOLOG3 (J3) activated the plasma membrane H<sup>+</sup>-ATPase by repressing the protein kinase PKS5. Arabidopsis mutants lacking J3 were hypersensitive to alkaline pH stress and exhibited a decrease in plasma membrane H<sup>+</sup>-ATPase activity (Fuglsang et al., 2007; Yang et al., 2010). These studies show that both J3 and PKS5 regulate H<sup>+</sup> extrusion by controlling the interaction between plasma membrane H<sup>+</sup>-ATPase and 14-3-3 proteins during alkaline pH stress. It is also noteworthy that if there is H<sup>+</sup> efflux out of cells there needs to be an accompanying anion efflux, or cation influx into the cell to maintain charge balance and continuous operation H<sup>+</sup> -ATPase (Tyerman, 1992).

A number of other factors are also involved in regulation of plasma membrane H<sup>+</sup> -ATPase, which include hormones (like auxin and ABA), blue light, calcium and fungal elicitors (Kinoshita et al., 1995; Xing et al., 1997; Kim et al., 2001; Brault et al., 2004; Zhang et al., 2004). Interference with control of cytosolic Ca<sup>2+</sup> has been indicated to be an important

component in  $\text{Al}^{3+}$  toxicity at low pH (Rengel, 1992; Zhang and Rengel, 1999). Among plant hormones, auxin is the major hormone regulating the plasma membrane  $\text{H}^+$ -ATPase. For instance, auxin activates the  $\text{H}^+$ -ATPase, resulting in apoplastic acidification, a process leading to cell wall loosening, which is a primary determinant of root elongation (Baluška et al., 2010). Auxin transport in the root tip is driven by PIN2 (a member of the PIN-formed auxin efflux transporter family (PIN) transporters PIN1-4 and PIN 7) (Kleine-Vehn et al., 2008), which strongly influences the growth of the primary root (Grieneisen et al., 2007). Furthermore, Xu et al (2012) demonstrated a role of PIN2 (an auxin efflux transporter) in root tolerance to alkaline pH stress. They suggested that PIN2 is required for the acclimation of roots to alkaline pH stress by accumulating auxin in the root tip which appears to upregulate  $\text{H}^+$  efflux from these cells and maintain primary root growth.

Plasma membrane  $\text{H}^+$ -ATPases are encoded by a gene family of 12 members (AHA1 to AHA12) in *Arabidopsis thaliana* (Palmgren, 2001). These  $\text{H}^+$ -ATPases play the essential role in regulating membrane potential and pH control across cell membranes. Alteration in either of these two factors has an important regulatory role in signal transduction during processes such as cell growth and turgor regulation (Palmgren, 2001; Merlot et al., 2007; Yang et al., 2010). Anion efflux through anion permeable channels is an important component of controlling membrane potential in tandem with the  $\text{H}^+$ -ATPase (Tyerman, 1992). Without a concurrent efflux of anions, the membrane potential will hyperpolarise due to the continual activity of the  $\text{H}^+$ -ATPase, and so the inhibition or stimulation of anion efflux (and the resulting change in membrane potential) via the block or activation of anion channels is a common signal during growth, development or stress (Barbier-Brygoo et al., 2000; Marten et al., 2007). How these anion channels are regulated during alkaline pH stress is not addressed in the literature. Filling this knowledge gap is the main aim of my thesis.

### **1.3 Anion channels have multifarious and integrated roles in plants**

Anion channels in plant cells are transporters that allow the transport of anions across cell membranes. These transporters have a wide range of different functions including cell signalling, osmoregulation, metal tolerance, plant nutrition and compartmentalization of metabolites (Barbier-Brygoo et al., 2000). Plant cells have various major anions, for instance, sulphate, nitrate, phosphate and chloride as well as organic anions like citrate and malate (Barbier-Brygoo et al., 2011). Citrate and malate play an intermediary role in carbohydrate metabolism and pH regulation due to their weak acid characteristics (Barbier-Brygoo et al., 2011). Organic anions have multiple carboxyl groups, hence these anions can chelate with divalent and trivalent cations (e.g.  $\text{Al}^{3+}$ ; Figure 3). Early patch-clamp studies in guard cells of

*Vicia faba* showed that there are at least two types of anion channels: the Rapid-type (R-type) and Slow-type (S-type) anion channels. S-type and R-type anion channels (Hedrich et al. 1990; Linder and Raschke 1992; Schroeder and Keller 1992) are now known to be encoded by members of the Slowly activating anion channel family (SLAC) (Vahisalu et al., 2008) and quick anion channel or aluminium-activated malate transporter (QUAC1/ALMT) families, respectively (Meyer et al. 2010; Sasaki et al. 2010). R-type anion channels activate or deactivate within milliseconds and are voltage dependent and are involved in the transduction of multiple signals (Barbier-Brygoo et al., 2011).

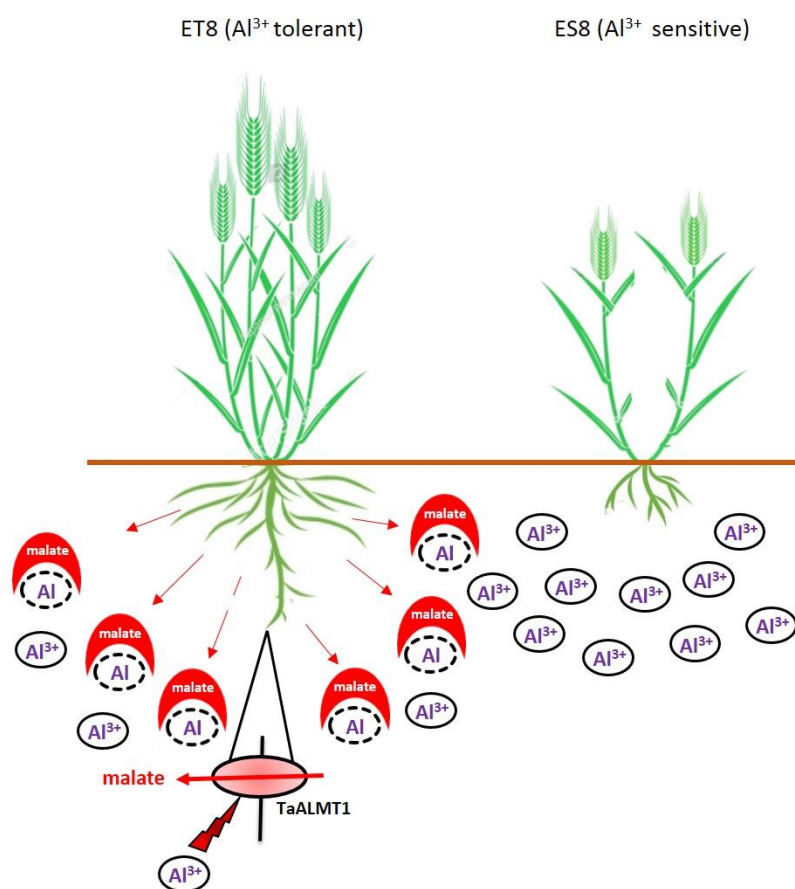


**Figure 3:** Mechanism of aluminium tolerance

### 1.3.1 R-type anion channels are encoded by ALMTs

The R-type anion channels are activated by ABA and malate in the guard cell (Hedrich and Marten, 1993; Roelfsema et al., 2004). The R-type anion channel activation stimulates a depolarisation of membrane potential and initiates the signal transduction that leads to stomatal closure. Two parallel studies by Sasaki et al (2009) and Meyer et al (2010) suggested that ALMT family members show the R-type anion conductance. For instance, the electrophysiological

analysis in guard cell protoplasts from *almt12* knockout plants and ALMT12 heterologously expressed in *Xenopus* oocytes were consistent with the hypothesis that ALMT12 facilitates R-type anion channel conductance (Meyer et al. 2010; Sasaki et al. 2010) (Figure 4). These studies also demonstrated that AtALMT12 is needed for plants to exhibit a normal rate of stomatal closure (similar to wildtype) stimulated by various environmental cues.

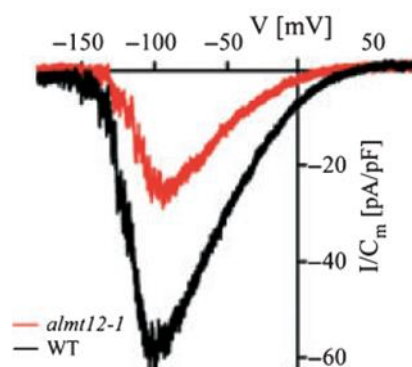


**Figure 4:** Activation of R-type currents (voltage dependent) from guard cell protoplast. The black colour represents Wild type (WT) and the red colour represents *atalmt12-1*. Current responses were obtained with a voltage ramp from +70 to -180 mV and holding voltage of -180 mV. Adapted from Meyer et al. (2010)

### 1.3.2 What are ALMTs?

Toxicity to  $\text{Al}^{3+}$  is a major selection pressure for adaptation, and a number of plant species have evolved mechanisms to alleviate  $\text{Al}^{3+}$  toxicity by triggering  $\text{Al}^{3+}$ -activated exudation of organic acid (OA) anions from root apices, e.g. malate and citrate (Figure 3). These OA anions chelate  $\text{Al}^{3+}$  in the rhizosphere (and/or the apoplast), resulting in the formation of non-toxic Al complexes that prevents  $\text{Al}^{3+}$  from entering the root (Ma et al., 2001; Ryan et al., 2001; Kochian et al., 2004) (Figure 3). Though it has recently been shown that Al complexed to malate may enter cells via an aquaporin (Wang et al., 2017). The stimulation of malate release by free  $\text{Al}^{3+}$  at low pH became the basis for the identification and characterization of the first member of the Aluminium-activated Malate Transporter proteins (ALMT) family. They were named after the first  $\text{Al}^{3+}$  resistance gene identified, *TaALMT1*, which is expressed in root tips of Al-tolerant varieties of wheat (Sasaki et al., 2004) (Figure 4). This gene, *TaALMT1* encodes an anion transporter protein found on the plasma membrane of root apex that facilitates the efflux of malate from root cells in acid soils and is unique to the plant kingdom (Dreyer et al., 2012). The same role for a homologous gene was confirmed in Arabidopsis (*AtALMT1*) and other plant species using mutational analysis (Hoekenga et al., 2006; Ligaba et al., 2006; Kobayashi et al., 2007) (Figure 5).

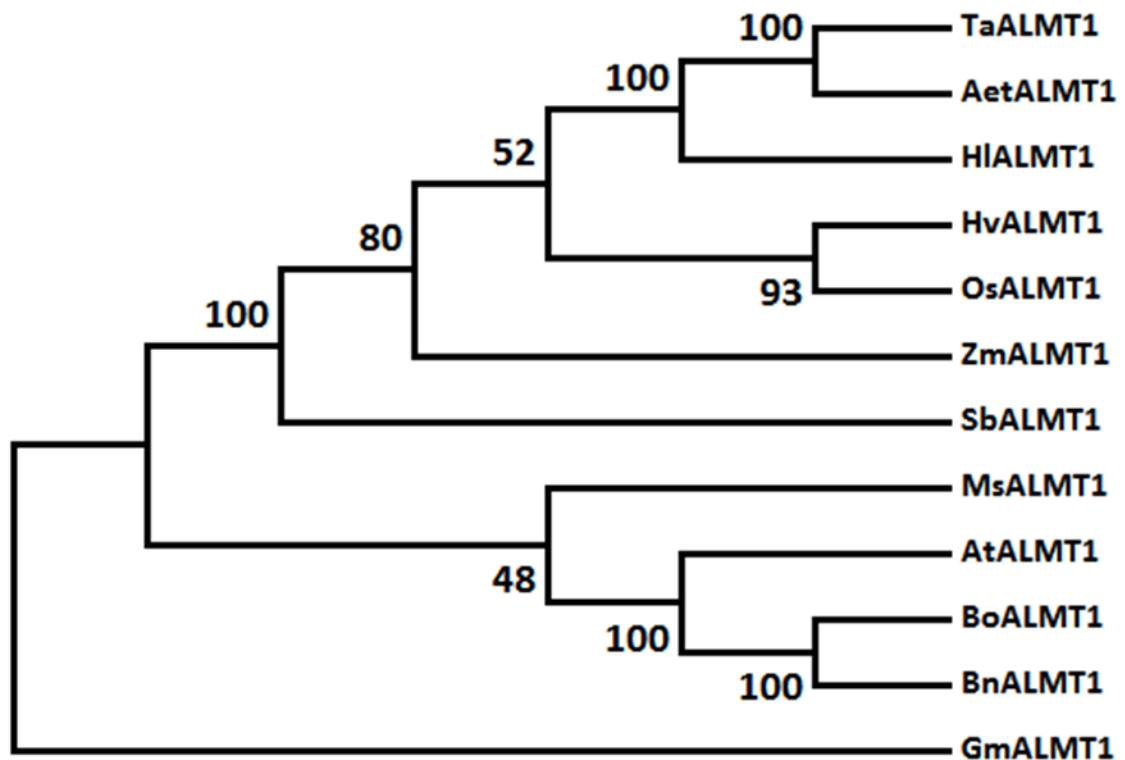


**Figure 5:** The Phylogenetic tree of ALMT1 family constructed from selected protein sequences. The aligned protein sequences through neighbour-joining method was used to analyse for phylogenetic relationship using Bootstrap method with 1000 replicates in Mega 7.0 (Kumar et al., 2016). The associated taxa that clustered together in the bootstrap are shown in terms of percentage of replicate trees and are shown next to the branches. The evolutionary distances were calculated by Poisson correction method and represented in units of number of amino acid substitutions per site. All the positions having gaps or missing data were removed.

### 1.3.3 The Role of ALMTs is diverse and not specific to Al resistance

ALMTs are a large anion channel family, found in a variety of plant species. For example, Arabidopsis has 14 members, grapevine has at least 13 members, soybean has 33 members, and there are 9 ALMTs in rice (Delhaize et al., 2007) (Table 1). Although TaALMT1 and AtALMT1 confer Al<sup>3+</sup>-activated malate efflux and resistance to Al<sup>3+</sup>, and reports have suggested that AtALMT1 is an Al<sup>3+</sup> sensor (Hoekenga et al., 2006), an increasing number of studies show that the roles of ALMTs extend beyond Al tolerance. The TaALMT1 can also transport other anions (e.g. sulfate, chloride, and nitrate), in addition to malate raising doubts over whether TaALMT1 is specifically involved in Al tolerance (Piñeros et al., 2008; Zhang et al., 2008). Another study suggested that the maize homolog ZmALMT1 is permeable to anions other than malate, and is neither activated by Al<sup>3+</sup> nor has a role in Al tolerance (Piñeros et al., 2008) (Table 1). Studies conducted by Koverman et al (2007) confirmed that another member of ALMT family AtALMT9 is located on the tonoplast and required for cytosolic malate homeostasis. Furthermore, AtALMT12 (as mentioned) and HvALMT1 regulate stomatal aperture (Sasaki et

al., 2010; Meyer et al., 2011). From above, it is becoming clear that most ALMTs are not involved in Al tolerance.

Microarray data suggested that AtALMT members are expressed in a range of tissues but individual members are often localised to discrete cell types. Initially ALMTs were identified in guard cells (*AtALMT6*, *AtALMT9* and *AtALMT12*)(Meyer et al., 2011; De Angeli et al., 2013) and roots (*TaALMT1*, *AtALMT1*, and *ZmALMT1,2*)(Sasaki et al., 2004; Hoekenga et al., 2006; Piñeros et al., 2008; Ligaba et al., 2012), but now they have been identified and characterized in other cell types, for instance in pericycle and seed coat (*AtALMT7*), pericycle and hypocotyls (*AtALMT10*), seed endosperm (*AtALMT11*), and in pollen tubes (*AtALMT12*) (Delhaize et al., 2007) (Table 1). *AtALMT* expression also responds to stress, e.g. *AtALMT5* and 9 are up-regulated by pathogens, and *AtALMT10* is up-regulated by iron deficiency, but is down-regulated by salt stress. This suggests unidentified roles of ALMT proteins in *planta*.

Transporter	AC number	Expression location	Subcellular localization	Function	Reference
GmALMT5	GLYMA_02G147900	roots	plasma membrane	enhances P efficiency in P limited condition	(Peng et al., 2017)
OsALMT4		root and shoot	plasma membrane	Altered expression disrupts mineral nutrition	(Liu et al., 2017)
SlALMT4	NP_001340701	fruit	endoplasmic reticulum	fruit development	(Sasaki et al., 2016)
SlALMT5	NP_001340702	fruit	endoplasmic reticulum	alters organic acid contents in seeds in tomato	(Sasaki et al., 2016)
LjALMT4		nodules		involved in transporting carbon source as well as inorganic anions to and from lotus nodule	(Takanashi et al., 2016)
MsALMT1	ADD71138	roots	plasma membrane	role in aluminium tolerance	(Chen et al., 2013)
VvALMT9		berries	vacuolar membrane	malate and tartrate accumulation in the vacuole of grape berries.	(De Angeli et al., 2013)
GmALMT1	GLYMA_01G083700	roots	plasma membrane	role in aluminium tolerance	(Liang et al., 2013)
ZmALMT2		roots	plasma membrane	mineral nutrient acquisition and transport	(Ligaba et al., 2012)
AtALMT6	AT2G17470	guard cells of leaves, stems and flower organs	vacuolar membrane	vacuolar malate transport system in guard cells	(Meyer et al., 2011)
HvALMT1	ABQ59605	guard cells and roots	plasma membrane	organic anion transport in stomatal function and expanding cells, role in stomatal closure	(Gruber et al., 2010; Xu et al., 2015)
AtALMT12	AT4G17970	guard cells	plasma membrane	role in stomatal closure	(Meyer et al., 2010; Sasaki et al., 2010)

ZmALMT1	NP_001105992	roots, leaves	plasma membrane	mineral nutrition and ion homeostasis	(Piñeros et al., 2008)
AtALMT9	AT3G18440	leaves	tonoplast	role in stomatal opening	(Kovermann et al., 2007; De Angeli et al., 2013)
BnALMT1		roots	plasma membrane	role in aluminium tolerance	(Ligaba et al., 2006)
BnALMT2		roots	plasma membrane	role in aluminium tolerance	(Ligaba et al., 2006)
AtALMT1	AT1G08430	roots	plasma membrane	role in aluminium tolerance	(Hoekenga et al., 2006)
TaALMT1	BAD10882	roots	plasma membrane	role in aluminium tolerance	(Sasaki et al., 2004)

**Table 1:** Characteristics of different ALMT transporters

#### 1.3.4 Are ALMTs involved in signalling?

R-type anion channels have been reported to play an important role in cell turgor regulation, nutrient transport and in signal transduction (Barbier-Brygoo et al., 2000). Colcombet et al (2000) suggested that the R-type channel may have a major role in signal transduction leading to Reactive Oxygen Species (ROS) production in response to pathogen-associated molecular patterns (PAMP) perception. In roots, R-type anion channels have been shown to be responsible for the efflux of organic anions and these channels have been specifically recognized when roots were in phosphate starvation (Diatloff et al., 2004). A separate R-type channel was shown electrophysiologically to be responsible for the efflux of inorganic ions such as sulphate, chloride and nitrate (Kiegle et al., 2000; Diatloff et al., 2004). In addition to the R-type anion channels present in guard cells, those that regulate hypocotyl growth shown by electrophysiology may also be encoded by ALMT proteins (Meyer et al., 2010). It is likely that all R-type anion channels in plants are encoded by ALMTs, and many of these have an important role in signalling. Though there is a substantial body of knowledge about R-type anion channels from a biophysical (electrophysiology) point of view, less is known about their molecular identity.

#### 1.3.5 Links between ALMTs and plant hormones

Phytohormones such as ethylene, auxin and jasmonate (JA) are reported to have a role in Al-induced root growth inhibition (Tian et al., 2014; Yang et al., 2017) and brassinosteroids are reported to be involved in interaction with sucrose transporter in the root (Bitterlich et al., 2014). It has been shown that ethylene gas and ACC pre-treatment of wheat roots suppressed aluminium induced malate efflux which is likely due to the inhibition of ALMT1-mediated malate efflux. A similar effect was also observed in tobacco BY2 cells expressing TaALMT1, suggesting that ethylene is a negative regulator of TaALMT1 (Tian et al., 2014). Recently, it has been reported that JA enhances Al-induced root growth inhibition by modulating ALMT1 mediated malate efflux (Yang et al., 2016). However, the mechanism of how jasmonic acid regulates TaALMT1 is still unknown. As a whole, it is also very important to understand and explore links between ALMTs and other known regulatory pathways such as auxin, jasmonic acid, salicylic acid, abscisic acid and brassinosteroids.

### 1.3.6 TaALMT1 is more active at pH 9 than pH 4.5

Recently, it has been found that TaALMT1 is more active in alkaline pH rather than in acidic pH (in the absence of Al<sup>3+</sup>) (Ramesh et al., 2015). By expressing TaALMT1 in tobacco BY2 cells, malate efflux was clearly stimulated by increasing pH (Figure 6A). Whilst Al was not required for the activation of malate efflux through TaALMT1 at alkaline pH, a trans-activating anion was required. A common feature of all ALMTs so far examined (for this property) is that presence of an anion on both sides of the membrane is required for the pore to transmit anionic currents (Sasaki et al., 2004; Hoekenga et al., 2006; Meyer et al., 2010). Alkaline pH activation of malate efflux through *TaALMT1* could also be replicated in *Xenopus laevis* oocytes by expressing *TaALMT1* (Ramesh et al., 2015). Another experiment was carried out to examine the physiological significance of pH regulation of TaALMT1 *in planta* (Ramesh et al. 2015). Near-isogenic lines (NIL) of wheat, which were originally used to clone TaALMT1 (Sasaki et al., 2004) (i.e. the tolerant line (ET8) and sensitive line (ES8)) were grown at pH 9 and significant malate efflux was observed (Figure 6B) (Ramesh et al., 2015). This correlated with the greater growth of ET8 in alkaline conditions compared to that of ES8. Malate efflux through TaALMT1 and other ALMTs was also found to be inhibited by micromolar concentrations of external gamma-aminobutyric acid (GABA) and its analogue muscimol, although in intact roots higher concentrations of GABA in the millimolar range were required for inhibition (Ramesh et al., 2015). Both root growth and malate exudation was inhibited by muscimol in ET8 at high pH to that of ES8 levels implicating TaALMT1 in the response (Figure 6).

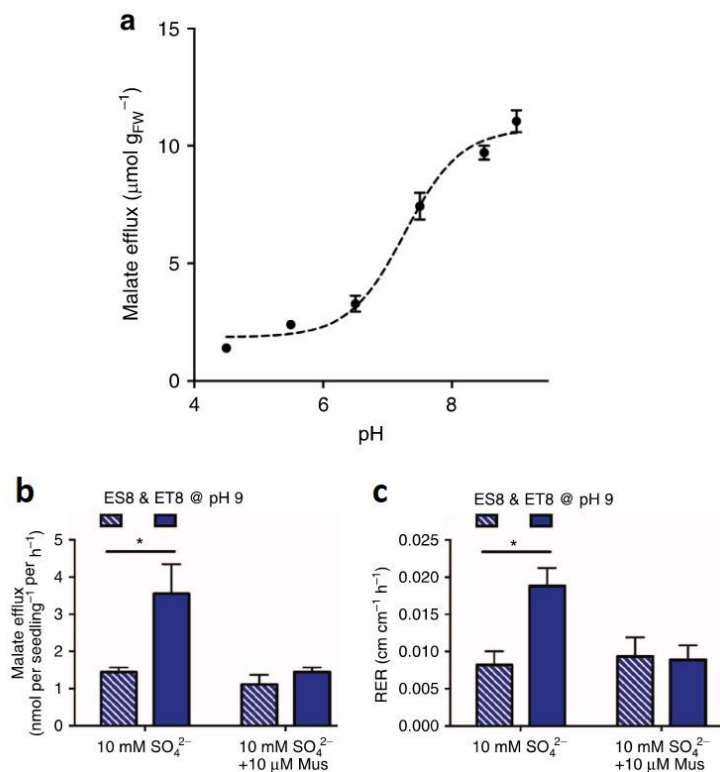


**Figure 6:** **a)** pH stimulated malate efflux from tobacco BY2 cells,  $n = 5$ . **b)** Comparative malate efflux of wheat near-isogenic lines (ET8 =  $\text{Al}^{3+}$ -tolerant, ES8 =  $\text{Al}^{3+}$ -sensitive) at alkaline pH, +/- muscimol and +/- trans-activator  $\text{SO}_4^{2-}$ . **c)** Corresponding effects on growth. Reproduced from Ramesh et al (2015)

#### 1.4 Organic anion efflux is linked to alkaline soil tolerance – is this due to acidification of apoplast and avoidance of phosphorus and iron deficiency?

In alkaline soils, plant roots can change the rhizosphere environment by effluxing protons and organic anions (carbon-containing compounds with at least one carboxyl group). Organic anions have important roles in plant nutrition, including absorption and adjustment of ionic species in the soil and buffering the pH of soil, apoplast and cytoplasm (Zhou et al., 2010). Organic anion exudation is often enhanced when plants are under stress, like Al toxicity, or iron (Fe) and phosphorus (P) deficiency (Hinsinger et al., 2003). It has been suggested that organic anion efflux could constitute an adaptive mechanism of plants in response to alkaline stress (Shi and Wang, 2005). However, it is not clear whether this increased organic anion efflux at alkaline pH is a response to P deficiency or Fe deficiency, or to the higher pH itself. The physiological mechanism involved in such responses and root growth under the alkaline condition is a question for further investigation. On the basis of recent research conducted by (Ramesh et al., 2015) on young wheat seedlings, it can be hypothesised that increased organic anion efflux via TaALMT1 and concurrent activation of the  $\text{H}^+$ -ATPase under alkaline pH is closely linked with root growth

via apoplast acidification. This is because the experiments of Ramesh et al (2015) were conducted with 3-5 day old seedlings that are unlikely to be suffering from Fe or P deficiency. It is also noteworthy that the alkaline pH-induced activation of TaALMT1 is noticeable when TaALMT1 is heterologously expressed in BY2 cells and *Xenopus* oocytes, so efflux of organic anions through TaALMT1 is likely to be an inherent property of the protein and does not need to be stimulated by P or Fe deficiency. Ramesh et al (2015) only showed activation of TaALMT1 and malate efflux at alkaline pH, and did not consider the effect that this may have on proton efflux and acidification of the rhizosphere.

One way to further explore the link between root growth and malate efflux is to find factors that can inhibit either of these variables. In acidic conditions, in the absence of  $Al^{3+}$ ,  $H^+$  would not necessarily need to be extruded from cells to cause apoplastic acidification as the apoplast should already be acidic, as a consequence malate efflux through ALMT would not be required to short-circuit the  $H^+$ -ATPase to maintain a physiological membrane potential and the proton motive force. It was previously shown that charge balance was achieved by activation of outward rectifying  $K^+$  channels (Zhang et al., 2001). At low pH, it is known that  $\gamma$ -aminobutyric acid (GABA) concentration rapidly increases in plant tissues as a likely means to regulate cytosolic pH, since synthesis of GABA from glutamate (via glutamate decarboxylase, GAD) results in the absorption of a proton (Shelp et al., 1999). The effect of GABA, and the GABA analogue muscimol, on malate efflux through TaALMT1 expressed in tobacco BY2 cells was explored at different pHs and both were found to block malate efflux at alkaline pH (Ramesh et al., 2015). GABA and muscimol did not alter the magnitude of malate efflux at pH 4.5, as the levels of anion-activated efflux were already very low in the absence of Al. Furthermore, the malate efflux from ET8 and ES8 wheat NILs in alkaline conditions was inhibited by muscimol (Figure 6 B), and this inhibition of malate efflux again correlated with a reduction in root growth (Ramesh et al., 2015). Exogenous application of a compound that blocks an *in planta* process is not definitive proof that this compound plays the same role endogenously. To examine whether GABA is likely to be an endogenous signal the link between GABA and plant stress responses is reviewed below.

### **1.5 GABA is a ubiquitous molecule**

The four carbon  $\gamma$ -aminobutyric acid (GABA) is a non-protein amino acid commonly found in bacteria, animals and plants. Though GABA was first discovered in potato tubers in 1949 (Steward et al. 1949) it has been well-researched in animals because of its key role as a neurotransmitter (Owens and Kriegstein, 2002), but its role in plants is less well defined. GABA is considered to be an ancient agent for cellular communication (Planamente et al., 2010).

GABA rapidly accumulates in plants in response to many environmental stresses like hypoxia, acidosis, mechanical stress, cold stress (Kinnersley and Turano, 2000). Recent studies have revealed a role of GABA in regulating important physiological processes such as pollen tube growth (Palanivelu et al., 2003; Yu et al., 2014), root and hypocotyl elongation (Renault et al., 2011), and pathogen defence (Park et al., 2010). GABA has a central role in C/N metabolism through the GABA shunt: the pathway that converts glutamate to succinate (Renault et al., 2011). It is important to note that substrates for the ALMTs are compounds associated with the GABA shunt and the associated tricarboxylic acid (TCA) cycle (i.e. malate, fumarate and succinate).

### 1.5.1 GABA metabolism

GABA is metabolized through the GABA shunt pathway, composed of three enzymes; namely, Glutamate decarboxylase (GAD) a cytosolic enzyme, and the mitochondrial enzymes GABA transaminase (GABA-T) and Succinic Semialdehyde Dehydrogenase (SSADH) (Bouché and Fromm, 2004) (Figure 7). GABA metabolism bypasses two steps of the tricarboxylic acid (TCA) cycle (Figure 8) and takes place in two cellular compartments, the cytosol and mitochondria. GABA is irreversibly synthesized from glutamate (Glu) via glutamate decarboxylase (GAD) in the cytosol; this releases CO<sub>2</sub> and absorbs one proton. The GABA is then transferred to mitochondria and is reversibly converted to succinic semialdehyde (SSA) by GABA transaminase (GABA-T) (Van Cauwenberghe et al., 2002). SSA is subsequently oxidized by succinate semialdehyde dehydrogenase (SSADH) to produce succinate and this finally flows into the TCA cycle (Busch and Fromm, 1999). The regulation of this conserved metabolic pathway seems to have special properties in plants. The GABA shunt has been associated with various physiological responses, including carbon fluxes into the TCA cycle, deterrence of insects, nitrogen metabolism, osmoregulation, protection against oxidative stress, signalling and regulation of cytosolic pH (Bouché and Fromm, 2004).

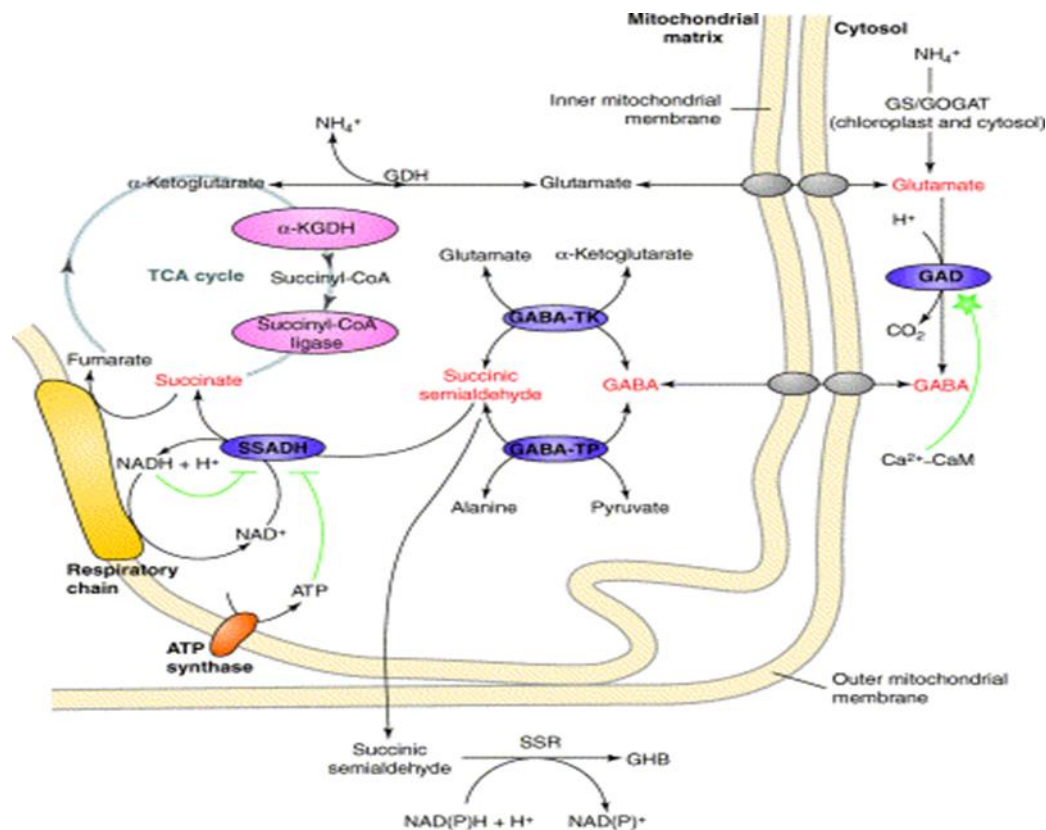


**Figure 7:** GABA shunt, the pathway through which GABA is metabolized. Reproduced from Bouché and Fromm (2004)

### 1.5.2 The transcriptional link between GABA and ALMT1

In plants, GABA accumulates in response to cytosolic acidification (Shelp et al., 1999). GAD is activated by acidic pH and calcium ( $\text{Ca}^{2+}$ )/calmodulin (CaM) (Snedden et al., 1995). In the GABA shunt, GAD uses cytosolic protons ( $\text{H}^+$ ) to convert glutamate to GABA through a decarboxylation reaction. Because GAD activity consumes  $\text{H}^+$ , it has been proposed that stress-induced GABA synthesis can contribute to pH regulation (Crawford et al., 1994). The zinc-finger protein (STOP1, sensitive to proton in rhizosphere 1) has many common characteristics of plant transcription factors that regulate tolerance to abiotic stresses (Iuchi et al., 2007). In *Arabidopsis*, activation of AtALMT1 by  $\text{Al}^{3+}$  occurs at both the transcriptional and the protein level and involves various genes that are ultimately controlled by AtSTOP1 (Iuchi et al., 2007; Sawaki et al., 2009). It has been shown in *Arabidopsis thaliana* that STOP1 co-regulates ALMT1 and GAD (*GAD1* and *GAD4*), which controls the accumulation of GABA. Further glutamate dehydrogenase (*AtGDH1* and 2), glutamate decarboxylase (*AtGAD*) and GABA amino transferase (*AtGABA-T*), which constitute components of the GABA shunt are transcriptionally regulated by STOP1 (Sawaki et al., 2009).

Based on the profile of metabolites and transcripts in the *Atstop1* knockout mutant, Sawaki et al (2009) also revealed that expression of *AtALMT1* is also down-regulated in addition to the pH-

regulating metabolic pathways of the GABA shunt at low pH, demonstrating a clear link between AtALMT1 and cytosolic pH regulation.

### 1.5.3 Is GABA a stress signal?

In animals, GABA regulates ion flow across nerve cell membranes via two classes of receptor, the GABA<sub>A</sub> and GABA<sub>B</sub>. The GABA<sub>A</sub> receptors are chloride (Cl<sup>-</sup>)-channels, and the GABA<sub>B</sub> are G-protein coupled receptors that ultimately regulate cation channels (Barnard et al., 1998). As a neurotransmitter in animals, GABA has a clearly defined role in signalling. The interests of GABA signalling shifted to plants when GABA rapidly accumulated in response to biotic/abiotic stresses (Roberts, 2007). GABA also has been shown to act as a signalling molecule for nitrate uptake modulation (Beuve et al., 2004), 14-3-3 gene regulation (Lancien and Roberts, 2006) and pollen tube growth and guidance (Palanivelu et al., 2003). In addition, GABA binding sites have been detected on pollen tube and mesophyll cell membranes (Yu et al., 2006). This has led to speculation that GABA signalling also occurs in plant cells but the mechanisms by which this signalling occurs has not been determined.

In animals, GABA exerts its effects on neuromuscular signalling through GABA-gated ion channels (GABA<sub>A</sub> and GABA<sub>B</sub> receptors) (Pinal and Tobin, 1998). GABA<sub>A</sub> receptor is a macromolecular protein composed of a chloride ion- selective channel with binding sites for picrotoxin, barbiturates, benzodiazepines and GABA (Macdonald and Twyman, 1991). GABA binds to GABA<sub>A</sub> receptors to open the channel and allows Cl<sup>-</sup> ion to move into neurons (Macdonald and Twyman, 1991). Ramesh et al (2015) showed that a region of ALMT proteins has amino acid residues similar to the GABA binding domain of mammalian GABA<sub>A</sub>  $\alpha$  subunits (Figure 8). Further, GABA or GABA analogue (muscimol) negatively regulated anion currents through several members of ALMTs at high affinity when ALMTs were expressed in *Xenopus* oocytes (Figure 8). Mutation of a key residue in TaALMT1 within this site (F231C) rendered the protein insensitive to GABA and muscimol (Ramesh et al. 2015). From above it appears that GABA could participate in plant stress signalling and adaptation by modulating anion currents through ALMTs.

		(EC <sub>50</sub> μM)	(E <sub>max</sub> %)
GABA <sub>A</sub>	DVEFRQTWKDERL	≈8.0	≈80
TaALMT1	TVFLFPVWAGEDV	3.4	64.5
AtALMT13	SLLFFPIWSGDDL	6.8	40.7
AtALMT14	SLLVFPIWSGEDL	1.1	23.8
OsALMT9	SLFVLPNWSGEDL	1.2	100
OsALMT5	TIFVMPVWAGEDL	1.0	100
HvALMT1	TIFVFPVWAGEDL	0.6	62.0
AtALMT1	SIFVCPVWAGQDL	1.3	66.4
VvALMT9	NICIYPIWAGEDL	6.0	48.9

**Figure 8:** Residues closest in similarity between GABA<sub>A</sub> (α subunits that are associated with GABA efficacy) and ALMT proteins (spanning 13 amino acids of different ALMTs from Arabidopsis, wheat, rice, barley, and grapevine); black = identical, grey = 80% similar and <60% similar (unshaded); EC<sub>50</sub> and E<sub>max</sub> for GABA efficacy. Reproduced from Ramesh et al. (2015).

#### 1.5.4 TaALMT1 is regulated by external GABA, but its activation also changes endogenous GABA levels.

Among all amino acids exuded from wheat roots, GABA showed the highest efflux as well as influx (Warren, 2015) and such carbon loss was proposed to be only justified energetically if GABA was involved in cell to cell communication (Gilliham and Tyerman 2016). A model proposed by Gilliham and Tyerman (2016) (Figure 9) suggested that an ALMT in a cell can sense and signal metabolic status leading to the conversion of this signal into physiological responses related to membrane voltage. It is well-established that AtGAT1 is an influx transporter that can transport GABA into the cells (Meyer et al., 2006), however, to date, no transporter has been identified that can transport GABA from the cytoplasm into the apoplast where its mode of action on ALMTs was proposed. Increased malate efflux through TaALMT1 always coincided with low endogenous GABA levels (Ramesh et al., 2015) suggesting either that GABA was effluxed into the rhizosphere and/or GABA catabolism was enhanced in response to activation of TaALMT1. Both these possibilities must be addressed to shed light on how TaALMT1 is regulated by GABA and how GABA may be linked to alkaline pH tolerance, given that endogenous GABA concentrations are linked to pH regulation.

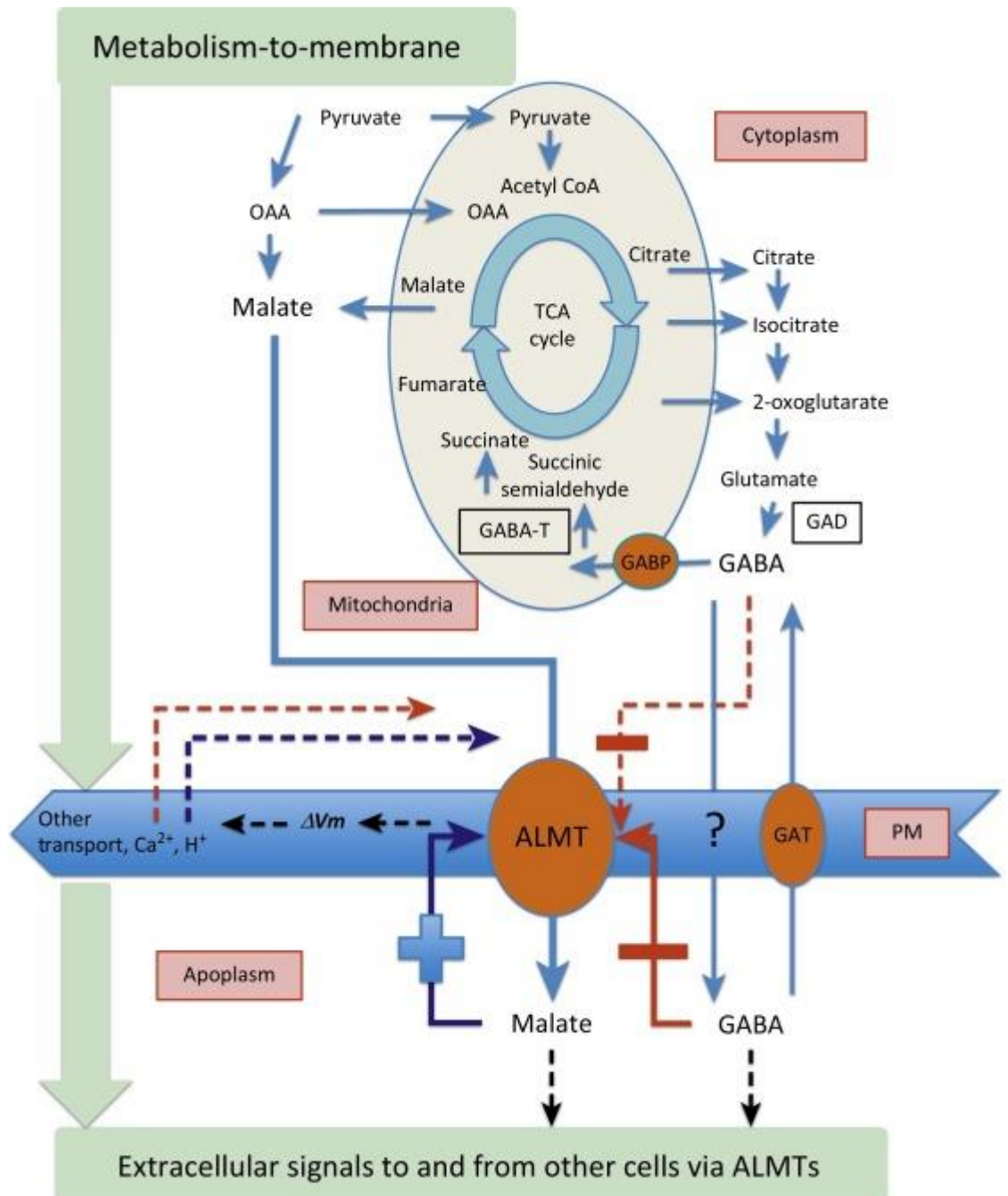


**Figure 9:** Proposed model which shows how the Aluminum-Activated Malate Transporter (ALMT) may communicate metabolic status in plants. The ALMT regulation activity on the plasma membrane (PM) by malate (blue arrow with plus sign) and GABA (red arrow with minus sign) describes a mechanism through which changes in cell metabolism could lead to voltage changes ( $\Delta V_m$ ); which can possibly convey cell metabolic status to nearby cells. The ALMT channel is inhibited with high affinity (1  $\mu M$ ) by GABA from the apoplast side, and on the other hand activated by malate with lower affinity (1 mM); these properties may lead to transient activation of ALMTs. It is unclear how GABA is released to the apoplast (indicated by?). Reproduced from Gilliham and Tyerman (2016)

## 1.6 Research questions

This literature review has uncovered a number of research gaps with respect to the mechanisms of root growth in alkaline soils, the regulation of malate efflux from roots and the role of GABA in this process. Following are the key research questions that I attempted to address during my PhD.

1. Alkaline pH stimulates TaALMT1-mediated malate efflux. What is the role of TaALMT1 in alkaline pH tolerance?
2. Among the amino acids exuded into rhizosphere of wheat roots, GABA is the highest. If this is true, which transport mechanism facilitates GABA exudation into the rhizosphere and what role(s) does GABA play in the rhizosphere?
3. How does exogenous GABA regulate root and shoot growth in alkaline soils?
4. Aluminate ions are prevalent in alkaline soils. Do aluminate ions regulate ALMT1 function in alkaline pH?
5. What are the links between ALMT1 signalling and other known plant hormones eg. jasmonic acid and brassinosteroids?

## 1.7 Aims and objective

The aim of my thesis was to investigate the role TaALMT1 in alkaline soil tolerance. Specifically, the research described in this thesis explored if TaALMT1-mediated regulation of root growth underlies a novel mechanism through which plants can tolerate alkaline stress. The aims were to:

- Investigate why endogenous GABA levels decrease when TaALMT1 is activated, either by Al at low pH or by anions at high pH.
- investigate the mechanism of wheat root tolerance to high pH
- identify the role of GABA efflux in alkaline soil tolerance
- find the link between malate efflux, GABA efflux and wheat root growth in alkaline conditions
- examine candidate genes involved in alkaline stress resistance using qPCR
- Identify the events downstream of GABA perception and how these lead to a physiological response (specifically under alkaline conditions).
- To identify the TaALMT1 signalling role including links with known growth regulatory pathways eg. jasmonic acid and brassinosteroids
- To find links between malate efflux and proton efflux and their role in tolerating alkaline conditions.

## 1.8 References

- Baluška F, Mancuso S, Volkmann D, Barlow PW** (2010) Root apex transition zone: a signalling–response nexus in the root. *Trends in Plant Science* **15**: 402-408
- Barbier-Brygoo H, De Angeli A, Filleur S, Frachisse J-M, Gambale F, Thomine S, Wege S** (2011) Anion Channels/Transporters in Plants: From Molecular Bases to Regulatory Networks. *Annual Review of Plant Biology* **62**: 25-51
- Barbier-Brygoo H, Vinauger M, Colcombet J, Ephritikhine G, Frachisse J-M, Maurel C** (2000) Anion channels in higher plants: functional characterization, molecular structure and physiological role. *Biochimica et Biophysica Acta (BBA) - Biomembranes* **1465**: 199-218
- Barnard EA, Skolnick P, Olsen RW, Mohler H, Sieghart W, Biggio G, Braestrup C, Bateson AN, Langer SZ** (1998) International Union of Pharmacology. XV. Subtypes of  $\gamma$ -Aminobutyric AcidA Receptors: Classification on the Basis of Subunit Structure and Receptor Function. *Pharmacological Reviews* **50**: 291-314
- Beuve N, Rispaill N, Laine P, Cliquet JB, Ourry A, Le Deunff E** (2004) Putative role of  $\gamma$  -aminobutyric acid (GABA) as a long-distance signal in up-regulation of nitrate uptake in *Brassica napus* L. *Plant, Cell & Environment* **27**: 1035-1046
- Bitterlich M, Krügel U, Boldt-Burisch K, Franken P, Kühn C** (2014) The sucrose transporter SISUT2 from tomato interacts with brassinosteroid functioning and affects arbuscular mycorrhiza formation. *The Plant Journal* **78**: 877-889
- Bouché N, Fromm H** (2004) GABA in plants: just a metabolite? *Trends in Plant Science* **9**: 110-115
- Braut M, Amiar Z, Pennarun A-M, Monestiez M, Zhang Z, Cornel D, Dellis O, Knight H, Bouteau F, Rona J-P** (2004) Plasma Membrane Depolarization Induced by Abscisic Acid in Arabidopsis Suspension Cells Involves Reduction of Proton Pumping in Addition to Anion Channel Activation, Which Are Both  $\text{Ca}^{2+}$  Dependent. *Plant Physiology* **135**: 231-243
- Brautigan DJ, Rengasamy P, Chittleborough DJ** (2012) Aluminium speciation and phytotoxicity in alkaline soils. *Plant and Soil* **360**: 187-196
- Brautigan DJ, Rengasamy P, Chittleborough DJ** (2014) Amelioration of alkaline phytotoxicity by lowering soil pH. *Crop and Pasture Science* **65**: 1278-1287
- Busch KB, Fromm H** (1999) Plant Succinic Semialdehyde Dehydrogenase. Cloning, Purification, Localization in Mitochondria, and Regulation by Adenine Nucleotides. *Plant Physiology* **121**: 589-598

- Chen Q, Wu K-H, Wang P, Yi J, Li K-Z, Yu Y-X, Chen L-M** (2013) Overexpression of MsALMT1, from the Aluminum-Sensitive *Medicago sativa*, Enhances Malate Exudation and Aluminum Resistance in Tobacco. *Plant Molecular Biology Reporter* **31**: 769-774
- Colcombet J, Mathieu Y, Peyronnet R, Agier N, Lelièvre F, Barbier-Brygoo H, Frachisse J-M** (2009) R-type anion channel activation is an essential step for ROS-dependent innate immune response in *Arabidopsis* suspension cells. *Functional Plant Biology* **36**: 832-843
- Crawford LA, Bown AW, Breitkreuz KE, Guinel FC** (1994) The Synthesis of [ $\gamma$ ]-Aminobutyric Acid in Response to Treatments Reducing Cytosolic pH. *Plant Physiology* **104**: 865-871
- De Angeli A, Baetz U, Francisco R, Zhang J, Chaves MM, Regalado A** (2013) The vacuolar channel VvALMT9 mediates malate and tartrate accumulation in berries of *Vitis vinifera*. *Planta* **238**: 283-291
- De Angeli A, Zhang J, Meyer S, Martinoia E** (2013) AtALMT9 is a malate-activated vacuolar chloride channel required for stomatal opening in *Arabidopsis*. *Nature Communications* **4**: 1804
- De Caritat P, Cooper M, Wilford J** (2011) The pH of Australian soils: field results from a national survey. *Soil Research* **49**: 173-182
- Delhaize E, Gruber BD, Ryan PR** (2007) The roles of organic anion permeases in aluminium resistance and mineral nutrition. *FEBS Letters* **581**: 2255-2262
- Delhaize E, Ryan PR** (1995) Aluminum Toxicity and Tolerance in Plants. *Plant Physiology* **107**: 315-321
- Diatloff E, Roberts M, Sanders D, Roberts SK** (2004) Characterization of Anion Channels in the Plasma Membrane of *Arabidopsis* Epidermal Root Cells and the Identification of a Citrate-Permeable Channel Induced by Phosphate Starvation. *Plant Physiology* **136**: 4136-4149
- Eagles HA, Cane K, Trevaskis B, Vallance N, Eastwood RF, Gororo NN, Kuchel H, Martin PJ** (2014) *Ppd1*, *Vrn1*, *ALMT1* and *Rht* genes and their effects on grain yield in lower rainfall environments in southern Australia. *Crop and Pasture Science* **65**: 159-170
- Fuglsang AT, Guo Y, Cuin TA, Qiu Q, Song C, Kristiansen KA, Bych K, Schulz A, Shabala S, Schumaker KS** (2007) *Arabidopsis* protein kinase PKS5 inhibits the plasma membrane H<sup>+</sup>-ATPase by preventing interaction with 14-3-3 protein. *The Plant Cell* **19**: 1617-1634

- Gilliham M, Tyerman SD** (2016) Linking Metabolism to Membrane Signaling: The GABA–Malate Connection. *Trends in Plant Science* **21**: 295-301
- Grieneisen VA, Xu J, Maree AFM, Hogeweg P, Scheres B** (2007) Auxin transport is sufficient to generate a maximum and gradient guiding root growth. *Nature* **449**: 1008-1013
- Gruber BD, Giehl RF, Friedel S, von Wirén N** (2013) Plasticity of the Arabidopsis root system under nutrient deficiencies. *Plant Physiology* **163**: 161-179
- Gruber BD, Ryan PR, Richardson AE, Tyerman SD, Ramesh S, Hebb DM, Howitt SM, Delhaize E** (2010) HvALMT1 from barley is involved in the transport of organic anions. *Journal of Experimental Botany* **61**: 1455-1467
- Guerinot ML** (2007) It's elementary: Enhancing Fe<sup>3+</sup> reduction improves rice yields. *Proceedings of the National Academy of Sciences* **104**: 7311-7312
- Guo M, Wang R, Wang J, Hua K, Wang Y, Liu X, Yao S** (2014) ALT1, a Snf2 Family Chromatin Remodeling ATPase, Negatively Regulates Alkaline Tolerance through Enhanced Defense against Oxidative Stress in Rice. *PLOS ONE* **9**: e112515
- Hinsinger P, Plassard C, Tang C, Jaillard B** (2003) Origins of root-mediated pH changes in the rhizosphere and their responses to environmental constraints: A review. *Plant and Soil* **248**: 43-59
- Hoekenga OA, Maron LG, Piñeros MA, Cançado GM, Shaff J, Kobayashi Y, Ryan PR, Dong B, Delhaize E, Sasaki T** (2006) AtALMT1, which encodes a malate transporter, is identified as one of several genes critical for aluminum tolerance in Arabidopsis. *Proceedings of the National Academy of Sciences* **103**: 9738-9743
- Iuchi S, Koyama H, Iuchi A, Kobayashi Y, Kitabayashi S, Kobayashi Y, Ikka T, Hirayama T, Shinozaki K, Kobayashi M** (2007) Zinc finger protein STOP1 is critical for proton tolerance in Arabidopsis and coregulates a key gene in aluminum tolerance. *Proceedings of the National Academy of Sciences* **104**: 9900-9905
- Jin H, Plaha P, Park JY, Hong CP, Lee IS, Yang ZH, Jiang GB, Kwak SS, Liu SK, Lee JS, Kim YA, Lim YP** (2006) Comparative EST profiles of leaf and root of *Leymus chinensis*, a xerophilous grass adapted to high pH sodic soil. *Plant Science* **170**: 1081-1086
- Kiegle E, Gilliham M, Haseloff J, Tester M** (2000) Hyperpolarisation-activated calcium currents found only in cells from the elongation zone of Arabidopsis thaliana roots. *The Plant Journal* **21**: 225-229
- Kim Y-S, Min J-K, Kim D, Jung J** (2001) A Soluble Auxin-binding Protein, ABP57 : Purification with anti-bovine serum albumin antibody and characterization of its

- mechanistic role in the auxin effect on plant plasma membrane H<sup>+</sup>-ATPase. *Journal of Biological Chemistry* **276**: 10730-10736
- Kinnersley AM, Turano FJ** (2000) Gamma aminobutyric acid (GABA) and plant responses to stress. *Critical Reviews in Plant Sciences* **19**: 479-509
- Kinoshita T, Nishimura M, Shimazaki K** (1995) Cytosolic Concentration of Ca<sup>2+</sup> Regulates the Plasma Membrane H<sup>+</sup>-ATPase in Guard Cells of Fava Bean. *The Plant Cell Online* **7**: 1333-1342
- Kinraide TB** (1990) Assessing the rhizotoxicity of the aluminate ion, Al (OH)<sub>4</sub><sup>-</sup>. *Plant Physiology* **93**: 1620-1625
- Kleine-Vehn J, Leitner J, Zwiewka M, Sauer M, Abas L, Luschig C, Friml J** (2008) Differential degradation of PIN2 auxin efflux carrier by retromer-dependent vacuolar targeting. *Proceedings of the National Academy of Sciences* **105**: 17812-17817
- Kobayashi Y, Hoekenga OA, Itoh H, Nakashima M, Saito S, Shaff JE, Maron LG, Piñeros MA, Kochian LV, Koyama H** (2007) Characterization of AtALMT1 Expression in Aluminum-Inducible Malate Release and Its Role for Rhizotoxic Stress Tolerance in Arabidopsis. *Plant Physiology* **145**: 843-852
- Kochian LV, Hoekenga OA, Piñeros MA** (2004) How do crop plants tolerate acid soils? mechanisms of aluminum tolerance and phosphorous efficiency. *Annual Review of Plant Biology* **55**: 459-493
- Kochian LV, Piñeros MA, Hoekenga OA** (2005) The Physiology, Genetics and Molecular Biology of Plant Aluminum Resistance and Toxicity. *Plant and Soil* **274**: 175-195
- Kopittke PM, Menzies N, Blamey F** (2005) Rhizotoxicity of aluminate and polycationic aluminium at high pH. *Plant and Soil* **266**: 177-186
- Kovermann P, Meyer S, Hörtensteiner S, Picco C, Scholz-Starke J, Ravera S, Lee Y, Martinoia E** (2007) The Arabidopsis vacuolar malate channel is a member of the ALMT family. *The Plant Journal* **52**: 1169-1180
- Kumar S, Stecher G, Tamura K** (2016) MEGA7: Molecular Evolutionary Genetics Analysis Version 7.0 for Bigger Datasets. *Molecular Biology and Evolution* **33**: 1870-1874
- Lancien M, Roberts MR** (2006) Regulation of Arabidopsis thaliana 14-3-3 gene expression by  $\gamma$ -aminobutyric acid. *Plant, Cell & Environment* **29**: 1430-1436
- Li J, Xu H-H, Liu W-C, Zhang X-W, Lu Y-T** (2015) Ethylene Inhibits Root Elongation during Alkaline Stress through AUXIN1 and Associated Changes in Auxin Accumulation. *Plant Physiology* **168**: 1777-1791
- Liang C, Piñeros MA, Tian J, Yao Z, Sun L, Liu J, Shaff J, Coluccio A, Kochian LV, Liao H** (2013) Low pH, Aluminum, and Phosphorus Coordinately Regulate Malate Exudation

- through *GmALMT1* to Improve Soybean Adaptation to Acid Soils. *Plant Physiology* **161**: 1347-1361
- Ligaba A, Katsuhara M, Ryan PR, Shibasaka M, Matsumoto H** (2006) The BnALMT1 and BnALMT2 Genes from Rape Encode Aluminum-Activated Malate Transporters That Enhance the Aluminum Resistance of Plant Cells. *Plant Physiology* **142**: 1294-1303
- Ligaba A, Maron L, Shaff JON, Kochian L, Piñeros M** (2012) Maize ZmALMT2 is a root anion transporter that mediates constitutive root malate efflux. *Plant, Cell & Environment* **35**: 1185-1200
- Liu J, Guo Y** (2011) The alkaline tolerance in Arabidopsis requires stabilizing microfilament partially through inactivation of PKS5 kinase. *Journal of Genetics and Genomics* **38**: 307-313
- Liu J, Zhou M, Delhaize E, Ryan PR** (2017) Altered expression of a malate-permeable anion channel, OsALMT4, disrupts mineral nutrition. *Plant Physiology* **75**:1745-1759
- Ma G, Rengasamy P, Rathjen A** (2003) Phytotoxicity of aluminium to wheat plants in high-pH solutions. *Australian Journal of Experimental Agriculture* **43**: 497-501
- Ma JF, Ryan PR, Delhaize E** (2001) Aluminium tolerance in plants and the complexing role of organic acids. *Trends in Plant Science* **6**: 273-278
- Macdonald RL, Twyman RE** (1991) Biophysical properties and regulation of GABAA receptor channels. *Seminars in Neuroscience* **3**: 219-230
- Marten H, Hedrich R, Roelfsema MRG** (2007) Blue light inhibits guard cell plasma membrane anion channels in a phototropin-dependent manner. *The Plant Journal* **50**: 29-39
- Matsumoto H** (2000) Cell biology of aluminum toxicity and tolerance in higher plants. *In International Review of Cytology*: **200**: Academic Press, pp 1-46
- McDonald GK, Taylor JD, Verbyla A, Kuchel H** (2013) Assessing the importance of subsoil constraints to yield of wheat and its implications for yield improvement. *Crop and Pasture Science* **63**: 1043-1065
- Meng C, Quan TY, Li ZY, Cui KL, Yan L, Liang Y, Dai JL, Xia GM, Liu SW** (2017) Transcriptome profiling reveals the genetic basis of alkalinity tolerance in wheat. *BMC Genomics* **18**: 14
- Merlot S, Leonhardt N, Fenzi F, Valon C, Costa M, Piette L, Vavasseur A, Genty B, Boivin K, Müller A, Giraudat J, Leung J** (2007) Constitutive activation of a plasma membrane H<sup>+</sup>-ATPase prevents abscisic acid-mediated stomatal closure. *The EMBO Journal* **26**: 3216-3226

- Meyer A, Eskandari S, Grallath S, Rentsch D** (2006) AtGAT1, a high affinity transporter for gamma-aminobutyric acid in *Arabidopsis thaliana*. *Journal of Biological Chemistry* **281**: 7197-7204
- Meyer S, Mumm P, Imes D, Endler A, Weder B, Al-Rasheid KAS, Geiger D, Marten I, Martinoia E, Hedrich R** (2010) AtALMT12 represents an R-type anion channel required for stomatal movement in *Arabidopsis* guard cells. *The Plant Journal* **63**: 1054-1062
- Meyer S, Scholz-Starke J, De Angeli A, Kovermann P, Burla B, Gambale F, Martinoia E** (2011) Malate transport by the vacuolar AtALMT6 channel in guard cells is subject to multiple regulation. *The Plant Journal* **67**: 247-257
- Owens DF, Kriegstein AR** (2002) Is there more to gaba than synaptic inhibition? *Nat Rev Neurosci* **3**: 715-727
- Palacios JM, Wamsley JK, Kuhar MJ** (1981) High affinity GABA receptors — Autoradiographic localization. *Brain Research* **222**: 285-307
- Palanivelu R, Brass L, Edlund AF, Preuss D** (2003) Pollen tube growth and guidance is regulated by POP2, an *Arabidopsis* gene that controls GABA levels. *Cell* **114**: 47-59
- Palmgren MG** (2001) Plant Plasma Membrane H<sup>+</sup>-ATPases: Powerhouses for Nutrient Uptake. *Annual Review of Plant Physiology and Plant Molecular Biology* **52**: 817-845
- Park DH, Mirabella R, Bronstein PA, Preston GM, Haring MA, Lim CK, Collmer A, Schuurink RC** (2010) Mutations in  $\gamma$ -aminobutyric acid (GABA) transaminase genes in plants or *Pseudomonas syringae* reduce bacterial virulence. *The Plant Journal* **64**: 318-330
- Peng W, Wu W, Peng J, Li J, Lin Y, Wang Y, Tian J, Sun L, Liang C, Liao H** (2017) Characterization of the soybean GmALMT family genes and the function of GmALMT5 in response to phosphate starvation. *Journal of Integrative Plant Biology* **60**: 216-31
- Pinal C, Tobin T** (1998) Uniqueness and redundancy in GABA production. *Perspectives on Developmental Neurobiology* **5**: 109-118
- Piñeros MA, Cançado GMA, Maron LG, Lyi SM, Menossi M, Kochian LV** (2008) Not all ALMT1-type transporters mediate aluminum-activated organic acid responses: the case of ZmALMT1 – an anion-selective transporter. *The Plant Journal* **53**: 352-367
- Planamente S, Vigouroux A, Mondy S, Nicaise M, Faure D, Moréra S** (2010) A Conserved Mechanism of GABA Binding and Antagonism Is Revealed by Structure-Function Analysis of the Periplasmic Binding Protein Atu2422 in *Agrobacterium tumefaciens*. *Journal of Biological Chemistry* **285**: 30294-30303

- Raman H, Zhang KR, Cakir M, Appels R, Garvin DF, Maron LG, Kochian LV, Moroni JS, Raman R, Imtiaz M, Drake-Brockman F, Waters I, Martin P, Sasaki T, Yamamoto Y, Matsumoto H, Hebb DM, Delhaize E, Ryan PR** (2005) Molecular characterization and mapping of ALMT1, the aluminium-tolerance gene of bread wheat (*Triticum aestivum* L.). *Genome* **48**: 781-791
- Ramesh SA, Tyerman SD, Xu B, Bose J, Kaur S, Conn V, Domingos P, Ullah S, Wege S, Shabala S, Feijo JA, Ryan PR, Gilliam M** (2015) GABA signalling modulates plant growth by directly regulating the activity of plant-specific anion transporters. *Nature Communications* **6**: 7879
- Renault H, El Amrani A, Palanivelu R, Updegraff EP, Yu A, Renou J-P, Preuss D, Bouchereau A, Deleu C** (2011) GABA Accumulation Causes Cell Elongation Defects and a Decrease in Expression of Genes Encoding Secreted and Cell Wall-Related Proteins in *Arabidopsis thaliana*. *Plant and Cell Physiology* **52**: 894-908
- Rengasamy P, Olsson K** (1991) Sodicity and soil structure. *Soil Research* **29**: 935-952
- Rengel Z** (1992) Role of calcium in aluminum toxicity. *New Phytologist* **121**: 499-513
- Roberts MR** (2007) Does GABA Act as a Signal in Plants? Hints from Molecular Studies: Hints from Molecular Studies. *Plant Signaling & Behavior* **2**: 408-409
- Ryan PR, Delhaize E, Randall PJ** (1995) Characterization of Al-stimulated efflux of malate from the apices of al-tolerant wheat roots. *Planta* **196**: 103-110
- Ryan PR, Raman H, Gupta S, Sasaki T, Yamamoto Y, Delhaize E** (2010) The multiple origins of aluminium resistance in hexaploid wheat include *Aegilops tauschii* and more recent cis mutations to TaALMT1. *Plant Journal* **64**: 446-455
- Ryan P, Delhaize E, Jones D** (2001) Function and mechanism of organic anion exudation from plant roots. *Annual Review of Plant Biology* **52**: 527-560
- Ryan PR, Tyerman SD, Sasaki T, Furuichi T, Yamamoto Y, Zhang W, Delhaize E** (2011) The identification of aluminium-resistance genes provides opportunities for enhancing crop production on acid soils. *Journal of Experimental Botany* **62**: 9-20
- Sasaki T, Mori IC, Furuichi T, Munemasa S, Toyooka K, Matsuoka K, Murata Y, Yamamoto Y** (2010) Closing Plant Stomata Requires a Homolog of an Aluminum-Activated Malate Transporter. *Plant and Cell Physiology* **51**: 354-365
- Sasaki T, Tsuchiya Y, Ariyoshi M, Nakano R, Ushijima K, Kubo Y, Mori IC, Higashiizumi E, Galis I, Yamamoto Y** (2016) Two Members of the Aluminum-Activated Malate Transporter Family, SIALMT4 and SIALMT5, are Expressed during Fruit Development, and the Overexpression of SIALMT5 Alters Organic Acid Contents in Seeds in Tomato (*Solanum lycopersicum*). *Plant and Cell Physiology* **57**: 2367-2379

- Sasaki T, Yamamoto Y, Ezaki B, Katsuhara M, Ahn SJ, Ryan PR, Delhaize E, Matsumoto H** (2004) A wheat gene encoding an aluminum-activated malate transporter. *The Plant Journal* **37**: 645-653
- Sawaki Y, Iuchi S, Kobayashi Y, Kobayashi Y, Ikka T, Sakurai N, Fujita M, Shinozaki K, Shibata D, Kobayashi M, Koyama H** (2009) STOP1 Regulates Multiple Genes That Protect Arabidopsis from Proton and Aluminum Toxicities. *Plant Physiology* **150**: 281-294
- Shelp BJ, Bown AW, McLean MD** (1999) Metabolism and functions of gamma-aminobutyric acid. *Trends in Plant Science* **4**: 446-452
- Shelp BJ, Bozzo GG, Trobacher CP, Zarei A, Deyman KL, Brikis CJ** (2012) Hypothesis/review: Contribution of putrescine to 4-aminobutyrate (GABA) production in response to abiotic stress. *Plant Science* **194**: 130-135
- Shi D, Sheng Y** (2005) Effect of various salt–alkaline mixed stress conditions on sunflower seedlings and analysis of their stress factors. *Environmental and Experimental Botany* **54**: 8-21
- Shi D, Wang D** (2005) Effects of various salt-alkaline mixed stresses on *Aneurolepidium chinense* (Trin.) Kitag. *Plant and Soil* **271**: 15-26
- Silva CMS, Zhang CY, Habermann G, Delhaize E, Ryan PR** (2018) Does the major aluminium-resistance gene in wheat, TaALMT1, also confer tolerance to alkaline soils? *Plant and Soil* **424**: 451-462
- Snedden WA, Arazi T, Fromm H, Shelp BJ** (1995) Calcium/calmodulin activation of soybean glutamate decarboxylase. *Plant Physiology* **108**: 543-549
- Stass A, Wang Y, Eticha D, Horst WJ** (2006) Aluminium rhizotoxicity in maize grown in solutions with Al<sup>3+</sup> or Al(OH)<sub>4</sub><sup>-</sup> as predominant solution Al species. *Journal of Experimental Botany* **57**: 4033-4042
- Takanashi K, Sasaki T, Kan T, Saida Y, Sugiyama A, Yamamoto Y, Yazaki K** (2016) A Dicarboxylate Transporter, LjALMT4, Mainly Expressed in Nodules of *Lotus japonicus*. *Molecular Plant-Microbe Interactions* **29**: 584-592
- Tian Q, Zhang X, Ramesh S, Gilliam M, Tyerman SD, Zhang W-H** (2014) Ethylene negatively regulates aluminium-induced malate efflux from wheat roots and tobacco cells transformed with TaALMT1. *Journal of Experimental Botany* **65**: 2415-2426
- Tyerman SD** (1992) Anion Channels in Plants. *Annual Review of Plant Physiology and Plant Molecular Biology* **43**: 351-373
- Vahisalu T, Kollist H, Wang Y-F, Nishimura N, Chan W-Y, Valerio G, Lamminmaki A, Brosche M, Moldau H, Desikan R, Schroeder JI, Kangasjarvi J** (2008) SLAC1 is

- required for plant guard cell S-type anion channel function in stomatal signalling. *Nature* **452**: 487-491
- Van Cauwenberghe OR, Makhmoudova A, McLean MD, Clark SM, Shelp BJ** (2002) Plant pyruvate-dependent gamma-aminobutyrate transaminase: identification of an *Arabidopsis* cDNA and its expression in *Escherichia coli*. *Canadian Journal of Botany* **80**: 933-941
- Wang YQ, Li RH, Li DM, Jia XM, Zhou DW, Li JY, Lyi SM, Hou SY, Huang YL, Kochian LV, Liu JP** (2017) NIP1; 2 is a plasma membrane-localized transporter mediating aluminum uptake, translocation, and tolerance in *Arabidopsis*. *Proceedings of the National Academy of Sciences of the United States of America* **114**: 5047-5052
- Warren CR** (2015) Wheat roots efflux a diverse array of organic N compounds and are highly proficient at their recapture. *Plant and Soil* **397**: 147-162
- Wong VN, Dalal RC, Greene RS** (2008) Salinity and sodicity effects on respiration and microbial biomass of soil. *Biology and Fertility of Soils* **44**: 943-953
- Xing T, Higgins VJ, Blumwald E** (1997) Identification of G proteins mediating fungal elicitor-induced dephosphorylation of host plasma membrane H<sup>+</sup>-ATPase. *Journal of Experimental Botany* **48**: 229-237
- Xu M, Gruber BD, Delhaize E, White RG, James RA, You J, Yang Z, Ryan PR** (2015) The barley anion channel, HvALMT1, has multiple roles in guard cell physiology and grain metabolism. *Physiologia Plantarum* **153**: 183-193
- Xu W, Jia L, Baluška F, Ding G, Shi W, Ye N, Zhang J** (2012) PIN2 is required for the adaptation of *Arabidopsis* roots to alkaline stress by modulating proton secretion. *Journal of Experimental Botany* **63**: 6105-6114
- Xu W, Jia L, Shi W, Baluška F, Kronzucker HJ, Liang J, Zhang J** (2013) The tomato 14-3-3 protein TFT4 modulates H<sup>+</sup> efflux, basipetal auxin transport, and the PKS5-J3 pathway in the root growth response to alkaline stress. *Plant Physiology* **163**: 1817-1828
- Yang C, Chong J, Li C, Kim C, Shi D, Wang D** (2007) Osmotic adjustment and ion balance traits of an alkali resistant halophyte *Kochia sieversiana* during adaptation to salt and alkali conditions. *Plant and Soil* **294**: 263-276
- Yang C, Wang P, Li C, Shi D, Wang D** (2008) Comparison of effects of salt and alkali stresses on the growth and photosynthesis of wheat. *Photosynthetica* **46**: 107-114
- Yang Y, Qin Y, Xie C, Zhao F, Zhao J, Liu D, Chen S, Fuglsang AT, Palmgren MG, Schumaker KS** (2010) The *Arabidopsis* chaperone J3 regulates the plasma membrane H<sup>+</sup>-ATPase through interaction with the PKS5 kinase. *The Plant Cell* **22**: 1313-1332

- Yang ZB, He CM, Ma YQ, Herde M, Ding ZJ** (2017) Jasmonic Acid Enhances Al-Induced Root Growth Inhibition. *Plant Physiology* **173**: 1420-1433
- Yu G-H, Zou J, Feng J, Peng X-B, Wu J-Y, Wu Y-L, Palanivelu R, Sun M-X** (2014) Exogenous  $\gamma$ -aminobutyric acid affects pollen tube growth via modulating putative  $\text{Ca}^{2+}$ -permeable membrane channels and is coupled to negative regulation on glutamate decarboxylase. *Journal of Experimental Botany* **65**: 3235–3248
- Yu G, Liang J, He Z, Sun M** (2006) Quantum Dot-Mediated Detection of  $\gamma$ -Aminobutyric Acid Binding Sites on the Surface of Living Pollen Protoplasts in Tobacco. *Chemistry & Biology* **13**: 723-731
- Zhang H, Liu XL, Zhang RX, Yuan HY, Wang MM, Yang HY, Ma HY, Liu D, Jiang CJ, Liang ZW** (2017) Root Damage under Alkaline Stress Is Associated with Reactive Oxygen Species Accumulation in Rice (*Oryza sativa* L.). *Frontiers in Plant Science* **8**: 12
- Zhang JR, Wei J, Li DX, Kong XY, Rengel Z, Chen LM, Yang Y, Cui XM, Chen Q** (2017) The Role of the Plasma Membrane  $\text{H}^+$ -ATPase in Plant Responses to Aluminum Toxicity. *Frontiers in Plant Science* **8**: 9
- Zhang JT, Mu CS** (2009) Effects of saline and alkaline stresses on the germination, growth, photosynthesis, ionic balance and anti-oxidant system in an alkali-tolerant leguminous forage *Lathyrus quinquenervius*. *Soil Science & Plant Nutrition* **55**: 685-697
- Zhang WH, Rengel Z** (1999) Aluminium induces an increase in cytoplasmic calcium in intact wheat root apical cells. *Australian Journal of Plant Physiology* **26**: 401-409
- Zhang WH, Ryan PR, Sasaki T, Yamamoto Y, Sullivan W, Tyerman SD** (2008) Characterization of the TaALMT1 protein as an  $\text{Al}^{(3+)}$ -activated anion channel in transformed tobacco (*Nicotiana tabacum* L.) cells. *Plant and Cell Physiology* **49**: 1316-1330
- Zhang WH, Ryan PR, Tyerman SD** (2001) Malate-permeable channels and cation channels activated by aluminum in the apical cells of wheat roots. *Plant Physiology* **125**: 1459-1472
- Zhang X, Wang H, Takemiya A, Song C-p, Kinoshita T, Shimazaki K-i** (2004) Inhibition of Blue Light-Dependent  $\text{H}^+$  Pumping by Abscisic Acid through Hydrogen Peroxide-Induced Dephosphorylation of the Plasma Membrane  $\text{H}^+$ -ATPase in Guard Cell Protoplasts. *Plant Physiology* **136**: 4150-4158
- Zhou Y, Yang Z, Guo G, Guo Y** (2010) Microfilament dynamics is required for root growth under alkaline stress in *Arabidopsis*. *Journal of Integrative Plant Biology* **52**: 952-958

## **Chapter 2: RESEARCH ARTICLE**

### **Aluminium-Activated Malate Transporters Can Facilitate GABA Transport**

# Statement of Authorship

Title of Paper	Aluminum-Activated Malate Transporters Can Facilitate GABA Transport
Publication Status	<input checked="" type="checkbox"/> Published <input type="checkbox"/> Accepted for Publication <input type="checkbox"/> Submitted for Publication <input type="checkbox"/> Unpublished and Unsubmitted work written in manuscript style
Publication Details	Sunita A. Ramesh, Muhammad Kamran, Wendy Sullivan, Larissa Chirkova, Mamoru Okamoto, Fien Degryse, Michael McLaughlin, Matthew Gilliam, Stephen D. Tyerman (2018) Aluminum-Activated Malate Transporters Can Facilitate GABA Transport. <i>The Plant Cell</i> May 2018, 30 (5) 1147-1164; DOI: 10.1105/tpc.17.00864

## Principal Author

Name of Principal Author (Candidate)	Muhammad Kamran
Contribution to the Paper	Designed and executed some plant experiments and analysed the data. Commented on and edited the manuscript.
Overall percentage (%)	20%
Certification:	This paper reports on original research I conducted during the period of my Higher Degree by Research candidature and is not subject to any obligations or contractual agreements with a third party that would constrain its inclusion in this thesis. I am the primary author of this paper.
Signature	
Date	14-06-18

## Co-Author Contributions

By signing the Statement of Authorship, each author certifies that:

- i. the candidate's stated contribution to the publication is accurate (as detailed above);
- ii. permission is granted for the candidate to include the publication in the thesis; and
- iii. the sum of all co-author contributions is equal to 100% less the candidate's stated contribution.

Name of Co-Author	Sunita Ramesh
Contribution to the Paper	Planned, designed and performed experiments; analyzed the data and drafted the paper with edits from all authors.
Signature	
Date	13/6/18

Name of Co-Author	Wendy Sullivan		
Contribution to the Paper	Assisted in plant, oocyte, and tobacco cell experiments; commented on the manuscript.		
Signature		Date	14.6.18

Name of Co-Author	Larissa Chirkova		
Contribution to the Paper	Optimised and carried out UPLC measurements; commented and edited the manuscript.		
Signature		Date	12 <sup>th</sup> June 2018

Name of Co-Author	Mamoru Okamoto		
Contribution to the Paper	Facilitated and optimised UPLC measurements; commented and edited the manuscript.		
Signature		Date	13/06/2018

Name of Co-Author	Fien Degryse		
Contribution to the Paper	Optimised and carried GABA-AI <sup>9+</sup> binding assays; drafted components of the MS and edited and commented on the manuscript.		
Signature		Date	12 <sup>th</sup> June 2018

Name of Co-Author	Michael McLaughlin		
Contribution to the Paper	Facilitated and supervised GABA-AI <sup>9+</sup> binding assays; commented on the manuscript.		
Signature		Date	11 <sup>th</sup> June 2018

Name of Co-Author	Matthew Gilliam		
Contribution to the Paper	Co- conceived the project; planned and designed experiments; edited and commented on the manuscript.		
Signature		Date	13/6/2018

Name of Co-Author	Stephen Tyerman		
Contribution to the Paper	Co- conceived the project; supervised the research; planned and designed experiments; analysed the data and edited the paper.		
Signature		Date	13/6/2018



# Aluminum-Activated Malate Transporters Can Facilitate GABA Transport<sup>[OPEN]</sup>

Sunita A. Ramesh,<sup>a</sup> Muhammad Kamran,<sup>a</sup> Wendy Sullivan,<sup>a</sup> Larissa Chirkova,<sup>b</sup> Mamoru Okamoto,<sup>b</sup> Fien Degryse,<sup>c</sup> Michael McLaughlin,<sup>c</sup> Matthew Gilliam,<sup>a</sup> and Stephen D. Tyerman<sup>a,1</sup>

<sup>a</sup>ARC Centre of Excellence in Plant Energy Biology, Department of Plant Science, School of Agriculture, Food, and Wine, Waite Research Institute, University of Adelaide, Glen Osmond SA 5064, Australia

<sup>b</sup>ARC Industrial Transformation Research Hub for Wheat in a Hot and Dry Climate, Department of Plant Science, Waite Research Institute, School of Agriculture, Food, and Wine, University of Adelaide, Glen Osmond SA 5064, Australia

<sup>c</sup>Fertilizer Technology Research Centre, School of Agriculture, Food, and Wine, Waite Research Institute, University of Adelaide, Glen Osmond SA 5064, Australia

ORCID IDs: 0000-0003-2230-4737 (S.A.R.); 0000-0003-4511-7766 (M.K.); 0000-0002-3666-4947 (W.S.); 0000-0002-2989-607X (M.O.); 0000-0002-4875-2944 (F.D.); 0000-0003-0666-3078 (M.G.); 0000-0003-2455-1643 (S.D.T.)

**Plant aluminum-activated malate transporters (ALMTs) are currently classified as anion channels; they are also known to be regulated by diverse signals, leading to a range of physiological responses. Gamma-aminobutyric acid (GABA) regulation of anion flux through ALMT proteins requires a specific amino acid motif in ALMTs that shares similarity with a GABA binding site in mammalian GABA<sub>A</sub> receptors. Here, we explore why TaALMT1 activation leads to a negative correlation between malate efflux and endogenous GABA concentrations ([GABA]<sub>i</sub>) in both wheat (*Triticum aestivum*) root tips and in heterologous expression systems. We show that TaALMT1 activation reduces [GABA]<sub>i</sub> because TaALMT1 facilitates GABA efflux but GABA does not complex Al<sup>3+</sup>. TaALMT1 also leads to GABA transport into cells, demonstrated by a yeast complementation assay and via <sup>14</sup>C-GABA uptake into *TaALMT1*-expressing *Xenopus laevis* oocytes; this was found to be a general feature of all ALMTs we examined. Mutation of the GABA motif (TaALMT1<sup>F213C</sup>) prevented both GABA influx and efflux, and resulted in no correlation between malate efflux and [GABA]<sub>i</sub>. We conclude that ALMTs are likely to act as both GABA and anion transporters in planta. GABA and malate appear to interact with ALMTs in a complex manner to regulate each other's transport, suggestive of a role for ALMTs in communicating metabolic status.**

## INTRODUCTION

Gamma-aminobutyric acid (GABA) is a four-carbon nonproteinogenic amino acid that was first discovered in potato tubers (Steward et al., 1949) but has mainly been studied in mammals as an inhibitory neurotransmitter (Sigel and Steinmann, 2012). When plants encounter stress—whether abiotic (e.g., hypoxia, heat, cold, salt, drought) or biotic (e.g., herbivory, pathogen infection)—they rapidly accumulate GABA (Shelp et al., 2012). This accumulation has been shown to play an important role in the regulation of C:N balance (Fait et al., 2008, 2011), cytosolic pH (Carroll et al., 1994; Shelp et al., 1999), salt tolerance (Renault et al., 2010), and oxidative stress tolerance (Bouché et al., 2003b; Bouché and Fromm, 2004). GABA has also been proposed to be an endogenous plant-signaling molecule (Kinnersley and Turano, 2000; Palanivelu et al., 2003; Roberts, 2007). More recently, it was shown that GABA at low micromolar concentrations regulates anion currents through aluminum-activated malate transporter (ALMT) proteins from various species. While the wheat (*Triticum aestivum*) TaALMT1 can be activated by aluminum (Al<sup>3+</sup>), this is not a general feature of ALMTs,

despite their name. Some ALMTs can facilitate anion efflux when activated by external anions such as sulfate (SO<sub>4</sub><sup>2-</sup>) or malate<sup>2-</sup> in alkaline solutions (Ramesh et al., 2015). Such activation by an ion from the same side as the direction of current is referred to in the literature as transactivation. A putative GABA binding motif was discovered in ALMTs with homology to the one found in mammalian GABA<sub>A</sub> receptors, and treatment with micromolar concentrations of muscimol (an analog of GABA) resulted in inhibition of anion flux (Ramesh et al., 2015). Addition of bicuculline (a GABA receptor antagonist) attenuated the effect of both muscimol and GABA (Ramesh et al., 2015). These results suggest that there are distinct classes of anion channels in plant and animal cells that have comparable modes of GABA regulation (Žárský, 2015; Gilliam and Tyerman, 2016; Ramesh et al., 2017).

It is well established that in acidic soils TaALMT1 confers Al<sup>3+</sup> tolerance in wheat through exuding malate from the root tips and chelating toxic Al<sup>3+</sup> (Delhaize and Ryan, 1995; Ma et al., 2001; Sasaki et al., 2004). Exogenous application of GABA or muscimol to the roots of wheat seedlings with high TaALMT1 expression inhibited malate efflux and impaired root growth in the presence of Al<sup>3+</sup>, which phenocopied a near isogenic line with less expression of TaALMT1 and less Al<sup>3+</sup> tolerance (Ramesh et al., 2015). Interestingly, in these conditions, it was observed that when root efflux of malate was high, endogenous GABA concentrations ([GABA]<sub>i</sub>) in the cells were low and vice versa (Ramesh et al., 2015). This reciprocal relationship remained unexplained and may indicate either TaALMT1 activation caused

<sup>1</sup> Address correspondence to [steve.tyerman@adelaide.edu.au](mailto:steve.tyerman@adelaide.edu.au).

The author responsible for distribution of materials integral to the findings presented in this article in accordance with the policy described in the Instructions for Authors ([www.plantcell.org](http://www.plantcell.org)) is: Stephen D. Tyerman ([steve.tyerman@adelaide.edu.au](mailto:steve.tyerman@adelaide.edu.au)).

<sup>[OPEN]</sup> Articles can be viewed without a subscription.

[www.plantcell.org/cgi/doi/10.1105/tpc.17.00864](http://www.plantcell.org/cgi/doi/10.1105/tpc.17.00864)

## IN A NUTSHELL

**Background:** Gamma-aminobutyric acid (GABA) is a signaling molecule in mammalian nervous systems where it regulates specific channels that conduct chloride ions in the brain controlling mood. Plants rapidly accumulate GABA under several adverse conditions, and a signaling role has been suggested. Certain proteins embedded in plant cell membranes conduct negatively charged ions like chloride, and one family of these anion channels, the ALMTs, previously was shown to be sensitive to GABA. In acid soils with aluminum, roots of some wheat varieties exude the negatively charged compound malate via ALMT1, which confers aluminum tolerance. Interestingly, GABA levels in these roots decrease in parallel with malate exudation.

**Question:** We wanted to know why and how GABA in wheat roots changed when the ALMT1 protein was activated. It was previously hypothesized that ALMT1 was regulated by GABA. We tested this by using compounds known to alter internal GABA levels in cells (some of which are used to treat human brain disorders).

**Findings:** We used wheat and barley seedlings, tobacco suspension cells, yeast cells, and *Xenopus laevis* (frog) oocytes expressing the wheat ALMT1 protein as well as other ALMTs. Expression of wheat ALMT1 reduced internal GABA levels by allowing GABA to come out of the cells along with malate. GABA could also be transported into yeast cells expressing ALMT1. A version of ALMT1 with mutations in the GABA binding site abolished the relationship between malate and GABA and prevented GABA transport by the protein. We concluded that the wheat ALMT1 protein is a malate-GABA transporter. The activation of ALMT1, and possibly others in the ALMT family, changes cellular GABA concentrations. Because GABA plays a central role in nitrogen and carbon metabolism as well as regulation of pH, the ALMT proteins may provide a means of communicating metabolic status between and within cells.

**Next steps:** We want to understand the role of GABA and malate exudation in signalling and how the signal is propagated within and between cells. We also want to know why some drugs that influence GABA receptors in humans also work on plant ALMTs, despite very little similarity in protein structure.

changes in  $[GABA]_i$  or that  $[GABA]_i$  is altered in some way that then regulates TaALMT1.

Identification of a putative GABA binding motif in ALMTs provided a possible mechanism by which plant GABA may act as a signal (Ramesh et al., 2015; Žárský, 2015), but we are yet to fully understand the molecular and physiological basis of how this occurs and the relationship between anion flux and GABA regulation in plant cells. A number of pharmacological agents have been used to characterize animal GABA receptors, some of which are plant or fungal derived, either as agonists, i.e., muscimol, or as regulators of GABA synthesis or catabolism i.e., amino-oxyacetate (AOA) and vigabatrin, respectively (Wood and Peesker, 1973; Jackson et al., 1982; Grant and Heel, 1991). Using these inhibitors to manipulate  $[GABA]_i$  in plant cells may increase our understanding of how ALMT-mediated anion efflux is regulated.

It was previously hypothesized that ALMT might sense and signal metabolic status via regulation by GABA and malate, which alters membrane voltage and transduces the signal into a physiological response (Gilliham and Tyerman, 2016). Cellular efflux of GABA has been well documented (Bown and Shelp, 1989; Chung et al., 1992). Micromolar concentrations of GABA are found in root exudates and the apoplast, and among all amino acids exuded from wheat roots, GABA shows the highest efflux (Warren, 2015). It was envisaged that such carbon and nitrogen loss might only be justified energetically if GABA was involved in signaling (Gilliham and Tyerman, 2016). While a high affinity GABA influx transporter (AtGAT1) has been characterized and is expressed in *Arabidopsis thaliana* roots (Meyer et al., 2006), no transporter that can efflux GABA from the cytoplasm into the apoplast has been identified. This raises an interesting question as to how GABA exits the cytoplasm and enters the apoplast.

In this study, we used two GABA analogs to manipulate  $[GABA]_i$  in cells expressing TaALMT1: vigabatrin, a GABA transaminase

(GABA-T) inhibitor used as an antiepileptic in humans (Livingston et al., 1989; Nanavati and Silverman, 1991), and AOA, an inhibitor of both GABA-T and glutamate decarboxylase (GAD) (John and Charteris, 1978; Miller et al., 1991; Snedden et al., 1992). We demonstrate that exogenous application of AOA and vigabatrin had an effect on both anion efflux via TaALMT1 and  $[GABA]_i$ , resulting in negative correlations between  $[GABA]_i$  and anion efflux, which were also evident following  $Al^{3+}$  application. Interestingly, these negative correlations were abolished when the site-directed mutant *TaALMT1*<sup>F213C</sup>—impaired in its GABA regulation of malate transport—was expressed instead of *TaALMT1*. Although vigabatrin and AOA can affect  $[GABA]_i$  via inhibition of GABA-T and glutamate decarboxylase, respectively, their primary effect appeared to be via TaALMT1 (vigabatrin blocks and AOA activates). We propose that the reduction in  $[GABA]_i$  upon  $Al^{3+}$  treatment at low pH is due to efflux of GABA via TaALMT1. ALMT activity strongly affects  $[GABA]_i$ , likely resulting in changes in metabolic flux through the GABA shunt. In the case of the wheat root, this may provide a signaling mechanism by which TaALMT1 can regulate root growth in acidic and alkaline conditions.

## RESULTS

### Validating Measurement of Intracellular GABA Concentration

GABA concentrations are routinely measured using the GABase enzyme assay. GABase is a commercially available enzyme mixture composed of  $\gamma$ -aminobutyric acid aminotransferase and succinic semialdehyde dehydrogenase from *Pseudomonas fluorescens*. The coupled enzyme reaction results in GABA conversion to succinate with the stoichiometric reduction of  $NADP^+$

(Zhang and Bown, 1997). While examining the effects of inhibitors on cell and tissue GABA concentrations ( $[GABA]_i$ ) we found that this assay was inhibited by AOA when added directly to the enzyme mix (Supplemental Figure 1C). We therefore tested if the GABase assay was compromised when it was used on extracts of tissues that had been treated with AOA,  $Al^{3+}$ , or vigabatrin by performing GABA spike and recovery experiments (Supplemental Figures 1A to 1L). After 22-h treatment with 1 mM AOA, the recovery of spiked GABA from wheat seedling root extract was 97% (Supplemental Figures 1A to 1C);  $Al^{3+}$  treatment also did not compromise measurement of  $[GABA]_i$  (Supplemental Figures 1D to 1F). Vigabatrin-treated wheat root tips also yielded full recovery of spiked GABA (Supplemental Figures 1G to 1I). *Xenopus laevis* oocytes treated with these compounds were also examined and similarly full recovery of GABA was obtained (Supplemental Figures 1J to 1L). We further used ultra-high-performance liquid chromatography (UPLC) to measure  $[GABA]_i$  on the same wheat root tip tissue extracts, after treatment with  $Al^{3+}$  and AOA, validating the results obtained by the enzyme assay (Supplemental Figure 1M). Thus, we expect the GABase assay to faithfully measure  $[GABA]_i$  following  $Al^{3+}$ , AOA, or vigabatrin treatments.

### Wheat Root Malate Efflux and $[GABA]_i$

External  $Al^{3+}$  at low pH was previously shown to reduce  $[GABA]_i$  while stimulating malate efflux from roots of wheat seedlings (Ramesh et al., 2015). The  $Al^{3+}$ -tolerant wheat line ET8 has higher expression of *TaALMT1* compared with ES8, its near isogenic line (NIL) (Yamaguchi et al., 2005); we found that *TaALMT1* expression was further increased in ET8 by external  $Al^{3+}$  treatment (Supplemental Figure 2). We confirmed that ET8 exhibited  $Al^{3+}$  (100  $\mu$ M) induced malate efflux from roots of 3-d-old wheat seedlings and that this coincided with a reduction in root tip  $[GABA]_i$  (Figure 1). We also confirmed that line ET8 had higher  $[GABA]_i$  than ES8 in pH 4.5 and that ES8  $[GABA]_i$  did not respond to  $Al^{3+}$  treatment (Supplemental Figure 1N) (Ramesh et al., 2015). When the corresponding values of  $Al^{3+}$ -stimulated malate efflux and root tip  $[GABA]_i$  from the same plants were plotted against each other, we observed that they were negatively correlated (Figure 1A). Delhaize et al. (1993) and others have shown through the use of excised root tips that they are the major site for malate efflux in response to  $Al^{3+}$ . We used this system to confirm, over a shorter time period, that  $Al^{3+}$  stimulates both malate efflux (Figure 1B) and a reduction in root tip  $[GABA]_i$  (Figure 1C). We also observed that treatment with the GAD/GABA-T inhibitor AOA (1 mM) at pH 4.5 also stimulated malate efflux (Figure 1B) and reduced  $[GABA]_i$  in excised root tips of ET8 seedlings (Figure 1C) to the same degree as 100  $\mu$ M  $Al^{3+}$ .

We treated roots of intact ET8 wheat seedlings with either a basal solution at pH 4.5 or pH 7.5  $\pm$  10 mM  $Na_2SO_4$  (to add an activating external anion),  $\pm$  1 mM AOA, or  $\pm$  100  $\mu$ M vigabatrin (Figure 2). We used vigabatrin, as an inhibitor of GABA-T, as this should increase  $[GABA]_i$  and, as such, would be expected to inhibit malate efflux via *TaALMT1*. Both in the presence and absence of external  $SO_4^{2-}$ , AOA significantly stimulated malate efflux at pH 4.5 (Figure 2A), confirming the results we observed for excised root tips (Figure 1). The corresponding  $[GABA]_i$  of root tips was lower in the presence of AOA (Figure 2B). The presence of  $SO_4^{2-}$  at pH 4.5

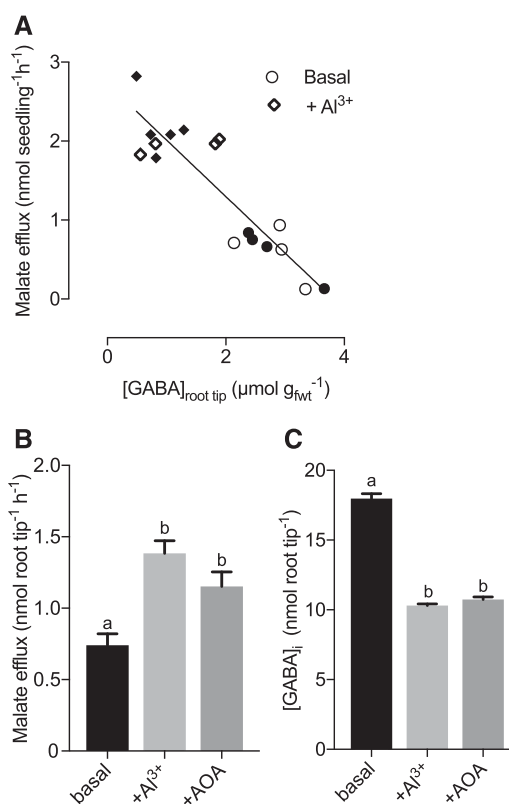


**Figure 1.** Aluminum and AOA Stimulate Efflux of Malate from Roots and Root Tips of ET8 Wheat Seedlings at pH 4.5 and Decrease  $[GABA]_i$  in Root Tips.

**(A)** Malate efflux over 22 h from intact seedling root tips correlates with  $[GABA]_i$  in root tips of ET8 in response to  $Al^{3+}$  at pH 4.5. Linear regression ( $y = -0.715 \cdot X + 2.73$ ,  $R^2 = 0.82$ ,  $P < 0.0001$ ). Each point is a single biological replicate consisting of root tips from a single seedling. **(B)** Malate efflux from excised root tips of wheat seedlings (NIL line ET8) after 6 h in basal solution (pH 4.5) and addition of  $Al^{3+}$  (100  $\mu$ M) or AOA (1 mM). **(C)**  $[GABA]_i$  in excised root tips in response to the same treatments at 6 h. Replicates from two experiments and different letter combinations indicate significant difference ( $P < 0.05$ ). For **(B)** and **(C)**,  $n = 10$  biological replicates each consisting of three excised root tips from one seedling.

made no difference to root tip  $[GABA]_i$  and vigabatrin did not elevate  $[GABA]_i$ . A significant negative correlation was observed between malate efflux and root tip  $[GABA]_i$  at pH 4.5 (Figure 2C) when all the individual replicates were plotted for two independent experiments. At pH 7.5, malate efflux was significantly higher in the presence of  $SO_4^{2-}$ , and vigabatrin inhibited the  $SO_4^{2-}$ -stimulated efflux (Figure 2D). Root tip  $[GABA]_i$  at pH 7.5 was slightly lower but not significantly so than at pH 4.5 (Figures 2B and 2E); however, it was significantly decreased by the addition of  $SO_4^{2-}$ , contrasting with the lack of effect seen at pH 4.5. At pH 7.5, treatment with  $SO_4^{2-}$  plus vigabatrin significantly increased  $[GABA]_i$  compared with  $SO_4^{2-}$  treatment alone (Figure 2E). At pH 4.5, vigabatrin elevated  $[GABA]_i$  when applied on its own, but this did not occur at pH 7.5 (Figures 2B and 2E); furthermore, AOA did not significantly affect malate efflux or  $[GABA]_i$  at pH 7.5 (Figure 2B,E). Again, there was a significant negative correlation between root tip  $[GABA]_i$  and

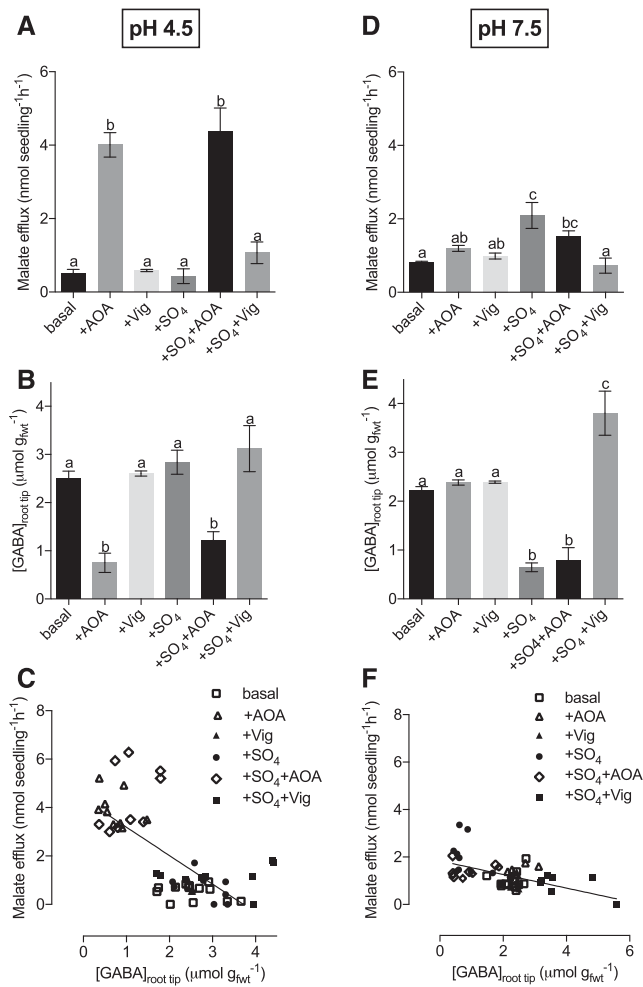


**Figure 2.** Malate Efflux Activation and Inhibition at pH 4.5 and 7.5 by AOA and Vigabatrin Is Correlated to Root Tip  $[GABA]_i$  in Intact Roots of ET8 Wheat Seedlings.

**(A)** Malate efflux measured over 22 h at pH 4.5 in basal solution plus AOA (1 mM), vigabatrin (Vig; 100  $\mu$ M),  $SO_4^{2-}$  (10 mM  $Na_2SO_4$ ),  $SO_4^{2-}$  + AOA, and  $SO_4^{2-}$  + Vig.

**(B)** Root tip  $[GABA]_i$  measured at the end of the flux period (22 h) with the same treatments above.

**(C)** Negative linear correlation between malate efflux and root tip  $[GABA]_i$  for the individual replicates for the treatments at pH 4.5. Linear regression ( $Y = -1.17 \cdot X + 4.36$ ),  $R^2 = 0.51$ ,  $P < 0.0001$ .

**(D)** Malate efflux measured over 22 h at pH 7.5 in basal solution plus AOA (1 mM), Vig (100  $\mu$ M),  $SO_4^{2-}$  (10 mM  $Na_2SO_4$ ),  $SO_4^{2-}$  + AOA, and  $SO_4^{2-}$  + Vig.

**(E)** Root tip  $[GABA]_i$  measured at the end of the flux period (22 h) with the same treatments above.

**(F)** Negative linear correlation between malate efflux and root tip  $[GABA]_i$  for the individual replicates for the treatments at pH 7.5. Linear regression ( $Y = -0.286 \cdot X + 1.84$ ),  $R^2 = 0.29$ ,  $P < 0.0001$ .

Different letter combination indicates significant difference ( $P < 0.05$ ). For **(A)**, **(B)**, **(D)**, and **(E)**,  $n = 5$  to 20 biological replicates where each replicate consists of root tips from one seedling. For **(C)** and **(F)**, each point is a single biological replicate consisting of root tips from one seedling.

malate efflux (Figure 2F), though the slope was lower than that observed at pH 4.5 ( $P < 0.001$ ). Taken together, these results show that in roots of intact wheat seedlings, there exists a consistent negative correlation between malate efflux and  $[GABA]_i$  in root tips that is common across the treatments that were used to alter malate flux.

### Malate Efflux and $[GABA]_i$ in Tobacco BY2 Expressing *TaALMT1*

Tobacco BY2 (*Nicotiana tabacum* cv *Bright Yellow-2*) cells were used to test whether heterologous expression of *TaALMT1* was sufficient to induce the negative linear relationship between malate efflux and  $[GABA]_i$  that was observed in wheat roots. Both  $Al^{3+}$  and AOA stimulated malate efflux in *TaALMT1*-expressing BY2 cells (Figure 3A); the effect of AOA was greatest at pH 4.5 compared with higher pHs (Supplemental Figure 3). At pH 4.5, the stimulated malate efflux corresponded to a lowered  $[GABA]_i$  at the end of the efflux period (Figure 3B). There was no effect of  $SO_4^{2-}$  by itself on either parameter at pH 4.5 (Supplemental Figures 4A and 4B). Neither malate efflux nor  $[GABA]_i$  varied at pH 4.5 in BY2 cells transformed with the empty vector when treated with AOA or  $Al^{3+}$  (Figures 3A and 3B). As observed for wheat roots, BY2 cells expressing *TaALMT1* exhibited a significant negative linear correlation between malate efflux and  $[GABA]_i$  across individual replicates and treatments at pH 4.5 (Figure 3C; Supplemental Figure 4).

In contrast to its effect at pH 4.5,  $SO_4^{2-}$  at pH 7.5 significantly stimulated malate efflux from BY2 cells expressing *TaALMT1* (Figure 3E), as it did in ET8 wheat roots. The addition of vigabatrin inhibited  $SO_4^{2-}$ -stimulated malate efflux in a dose-dependent manner, with complete block observed at 100  $\mu$ M (Supplemental Figure 5), but had little effect on controls expressing the empty vector (Figure 3E). In BY2 cells expressing *TaALMT1*, the reduction of malate efflux correlated with an increase in  $[GABA]_i$  (Figure 3E).  $[GABA]_i$  in BY2 cells was elevated by vigabatrin as expected from its proposed action on GABA-T in both *TaALMT1* and empty vector-expressing cells. Following both AOA and vigabatrin treatment, the significant relationships between malate efflux and  $[GABA]_i$  (Figures 3C and 3G) were dependent upon the expression of *TaALMT1* since empty vector controls did not show a significant correlation (Supplemental Figure 6).

### The F213C Mutation in *TaALMT1* Abolishes the Relationship between $[GABA]_i$ and Malate Efflux

A phenylalanine residue (F) has been shown to be important for GABA sensitivity in  $GABA_A$  receptors and *TaALMT1* (Boileau et al., 1999; Ramesh et al., 2015). Substitution of this residue by cysteine (C) impairs GABA sensitivity of *TaALMT1* but did not abolish activation of the malate efflux by  $Al^{3+}$  or external anions (Ramesh et al., 2015). Therefore, we tested whether the exogenous application of  $Al^{3+}$  or AOA affected the relationship between malate efflux and  $[GABA]_i$  in tobacco BY2 cells expressing site-directed mutant *TaALMT1*<sup>F213C</sup>. In the presence of  $Al^{3+}$  or AOA at low pH, malate efflux and  $[GABA]_i$  in the *TaALMT1*-expressing cells were significantly negatively correlated (Figure 3C), but these were not correlated in cells expressing the *TaALMT1*<sup>F213C</sup> mutant at pH 4.5

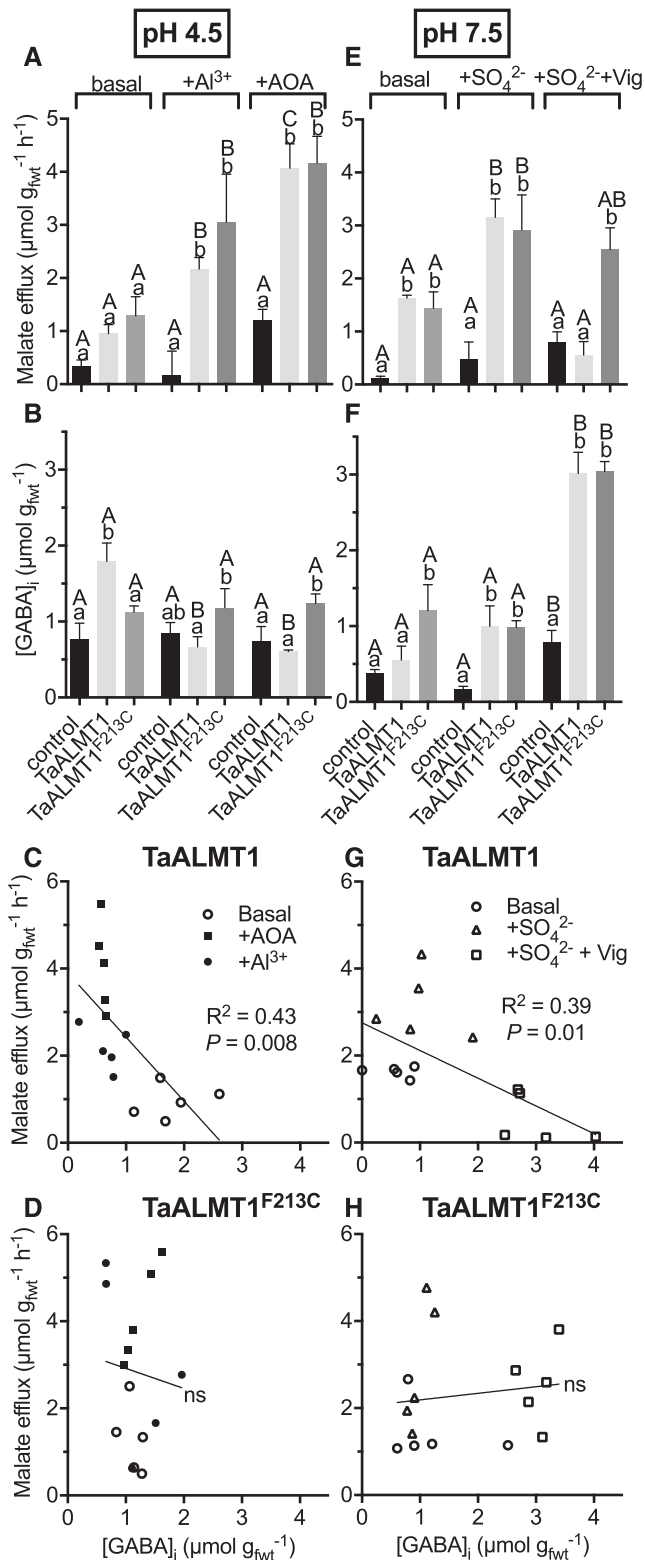


**Figure 3.** Tobacco BY2 Cells Expressing *TaALMT1* Show the Same Negative Correlation between Malate Efflux and Endogenous GABA Concentration as Intact ET8 Roots in Response to  $\text{Al}^{3+}$  and AOA at pH 4.5 and  $\text{SO}_4^{2-}$  and Vigabatrin at pH 7.5.

(Figure 3D). Malate efflux increased with exogenous application of  $\text{Al}^{3+}$  or AOA in cells expressing *TaALMT1*<sup>F213C</sup> similarly to cells expressing *TaALMT1* (Figure 3A), but unlike for *TaALMT1*-expressing cells,  $[\text{GABA}]_i$  was not significantly reduced by these treatments (Figure 3B). At pH 7.5, malate efflux from *TaALMT1*<sup>F213C</sup>-expressing cells was stimulated by  $\text{SO}_4^{2-}$  to a similar degree as for those expressing *TaALMT1* (Figure 3E). However, vigabatrin did not inhibit efflux from cells expressing *TaALMT1*<sup>F213C</sup>, and this contrasts with cells expressing *TaALMT1*, even though  $[\text{GABA}]_i$  was elevated in both (Figure 3F). Thus, the relationship between malate efflux and  $[\text{GABA}]_i$  was also abolished in cells expressing the *TaALMT1*<sup>F213C</sup> mutant at pH 7.5 (Figure 3H).

### Activation of *TaALMT1* Results in GABA Efflux

To determine if the reduction in  $[\text{GABA}]_i$  was due to transport of GABA through *TaALMT1*, we tested if  $\text{Al}^{3+}$  not only activated malate efflux but also GABA efflux from the wheat NILs ET8 and ES8 (Figure 4). We observed that ET8 showed not only significantly higher malate efflux (Figure 4A) but also higher GABA efflux from intact seedling roots over 22 h when compared with ES8 (Figure 4C). This higher efflux could be detected from excised ET8 root tips even after 2 h (Figure 4D), corresponding to a stimulated malate efflux (Figure 2B). Similarly, transgenic barley (*Hordeum vulgare*) expressing *TaALMT1* (OE) (Delhaize et al., 2004; Ramesh et al., 2015) when exposed to  $\text{Al}^{3+}$  at low pH showed significantly increased malate efflux (Figure 4E) as well as higher GABA efflux (Figure 4F) when compared with the Golden Promise background alone. It is also interesting to note that the efflux of GABA was

**(A)**  $\text{Al}^{3+}$  (100  $\mu\text{M}$ ) and AOA (1 mM) activate malate efflux from BY2 cells expressing *TaALMT1* and *TaALMT1*<sup>F213C</sup> at pH 4.5 in standard (basal) solution over 22 h.

**(B)**  $[\text{GABA}]_i$  in BY2 cells expressing *TaALMT1* and *TaALMT1*<sup>F213C</sup> at the end of the efflux period.

**(C)** Wild-type *TaALMT1* malate efflux versus  $[\text{GABA}]_i$  in the cells at the end of the efflux period (22 h) at pH 4.5 after treatment with 100  $\mu\text{M}$   $\text{Al}^{3+}$  or 1 mM AOA addition to basal solution. Linear regression ( $Y = -1.47 \times X + 3.90$ ),  $R^2 = 0.43$ ,  $P = 0.008$ .

**(D)** Site-directed mutant *TaALMT1*<sup>F213C</sup> at pH 4.5; treatments as in **(C)**. ns, regression not significant.

**(E)**  $\text{SO}_4^{2-}$  (10 mM  $\text{Na}_2\text{SO}_4$ ) activates malate efflux from BY2 cells expressing *TaALMT1* and *TaALMT1*<sup>F213C</sup> at pH 7.5 in standard (basal) solution over 22 h but vigabatrin (100  $\mu\text{M}$ ) only inhibits *TaALMT1* malate efflux.

**(F)**  $[\text{GABA}]_i$  in BY2 cells expressing *TaALMT1* and *TaALMT1*<sup>F213C</sup> at the end of the efflux period.

**(G)** Wild-type *TaALMT1* malate efflux versus  $[\text{GABA}]_i$  in the cells at the end of the efflux period (22 h) at pH 7.5 after treatment with  $\text{SO}_4^{2-}$  or  $\text{SO}_4^{2-}$  + vigabatrin addition to basal solution. Linear regression ( $Y = -0.64 \times X + 2.75$ ),  $R^2 = 0.39$ ,  $P = 0.01$ .

**(H)** Site-directed mutant *TaALMT1*<sup>F213C</sup> at pH 7.5; treatments as in **(G)**. Different lowercase letters indicate significant differences within a treatment group between genotypes; different uppercase letters indicate significant differences between treatments at a particular pH for each genotype ( $P < 0.05$ ). For **(A)**, **(B)**, **(D)**, and **(F)**,  $n = 5$  replicates each consisting of subculture of BY2 suspension culture. For **(C)**, **(D)**, **(G)**, and **(H)**, each point is a single biological replicate. No significant relationship exists between malate efflux and endogenous GABA concentrations in cells expressing empty vector at pH 4.5 or 7.5 (Supplemental Figure 6).

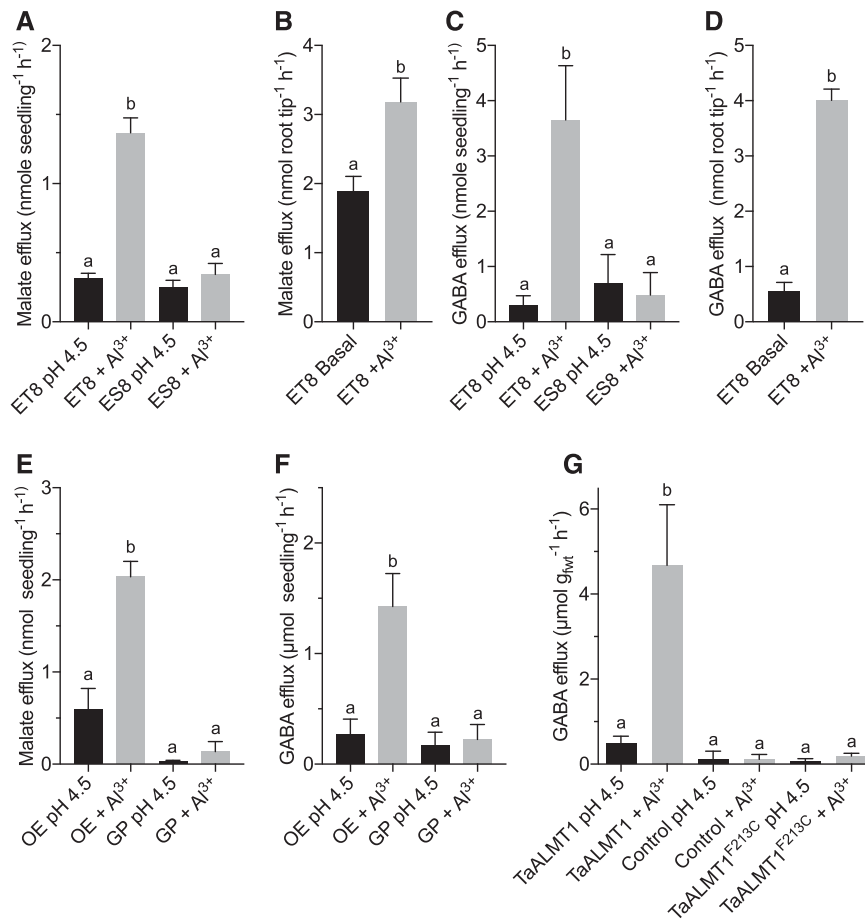


**Figure 4.** A Large GABA Efflux Occurs from Roots and BY2 Cells Expressing *TaALMT1* together with Malate Efflux in Response to Al<sup>3+</sup> at pH 4.5.

(A) Malate efflux from intact seedling roots of NIL ET8 and ES8 wheat after treatment with 100 μM Al<sup>3+</sup> over 22 h.

(B) Malate efflux from excised root tips of ET8 wheat measured over 2 h in response to 100 μM Al<sup>3+</sup>.

(C) GABA efflux from roots of ET8 and ES8 in response to Al<sup>3+</sup> measured over 22 h (same experiment as in [A]).

(D) GABA efflux from excised root tips of ET8 in response to Al<sup>3+</sup> measured over 2 h (same experiment as in [B]).

(E) Malate efflux from intact seedling roots of transgenic barley (Golden Promise) expressing *TaALMT1* (OE) compared with Golden Promise (GP) background after treatment with 100 μM Al<sup>3+</sup> over 22 h.

(F) GABA efflux from barley roots *TaALMT1* OE and GP as above.

(G) GABA efflux from tobacco BY2 cells over 22 h in response to Al<sup>3+</sup> at pH 4.5 for empty vector (Control), cells expressing *TaALMT1*, or site-directed mutant *TaALMT1*<sup>F213C</sup>. Only *TaALMT1* + Al<sup>3+</sup> showed a significant increase in GABA efflux ( $P < 0.0001$ ). For malate efflux, see Figure 3.

For all data,  $n = 5$  to 12 replicates where each replicate consists of one seedling ([A], [C], [E], and [F]) or root tips from one seedling ([B] and [D]) or one subculture of BY2 suspension cells ([D]). Different letter combinations indicate significant differences between treatments ( $P < 0.05$ ).

higher than that of malate on a molar basis by 3-fold in ET8 wheat and over 500-fold in *TaALMT1*-expressing barley roots. GABA efflux was also examined in tobacco BY2 cells expressing *TaALMT1* and the *TaALMT1*<sup>F213C</sup> mutant, where at low pH we observed very large GABA efflux with Al<sup>3+</sup> treatment only for cells expressing *TaALMT1* (Figure 4G). GABA efflux in response to Al<sup>3+</sup> from BY2 cells expressing *TaALMT1* was also higher than malate efflux (compare Figures 3A and 4G).

Given that Al<sup>3+</sup> activates GABA efflux through *TaALMT1* in addition to malate, we tested the possibility that GABA may also complex Al<sup>3+</sup>, since there was no data in the literature on possible interactions between GABA and Al<sup>3+</sup>. Using a fluoride competitive ligand method and comparing GABA with the organic anions citrate,

oxalate, malate, and salicylate, we found that GABA had very low affinity for Al<sup>3+</sup> compared with these other compounds, with the strength of complexation following the order: citrate>oxalate>malate>salicylate>>GABA (detailed in Supplemental Methods). We also found no synergistic or antagonistic interaction between GABA and malate in Al<sup>3+</sup> complexation.

#### Al<sup>3+</sup>, AOA, and Vigabatrin Have Direct Effects on *TaALMT1* Correlating with Rapid Changes in [GABA]<sub>i</sub> in *X. laevis* Oocytes

Since AOA had similar effects to Al<sup>3+</sup> in activation of malate efflux and on reducing [GABA]<sub>i</sub>, it prompted us to examine if the GABA

analogs AOA and vigabatrin may have direct effects on TaALMT1 that may then alter  $[GABA]_i$  (Figure 5). Using two-electrode voltage clamp electrophysiology (TEVC) on *X. laevis* oocytes expressing TaALMT1 and TaALMT1<sup>F213C</sup>, we perfused the bath with 1 mM AOA or 100  $\mu$ M Al<sup>3+</sup> to compare the inward current activation corresponding to activation of malate efflux (Figures 5A and 5B). AOA activates TaALMT1 and the TaALMT1<sup>F213C</sup> mutant rapidly and with similar kinetics to Al<sup>3+</sup>. Vigabatrin was also examined for its effect on anion-activated currents at pH 7.5 (Figure 5C; Supplemental Figure 7). Vigabatrin acted rapidly on the SO<sub>4</sub><sup>2-</sup> and malate-activated inward current giving close to 100% inhibition at the applied concentration of 100  $\mu$ M. Furthermore, this inhibition was consistent for repeated applications indicating no enduring effect that would be expected if  $[GABA]_i$  were increased by inhibition of GABA-T. Water injected control oocytes showed no responses to these treatments (Figure 5D).

Oocyte  $[GABA]_i$  and GABA efflux were examined in separate batches of oocytes after 10-min treatment with Al<sup>3+</sup>, AOA, and vigabatrin and compared with water-injected controls (Figures 5E to 5G). Both Al<sup>3+</sup> and AOA resulted in reduced  $[GABA]_i$ , but only in TaALMT1-expressing oocytes. The reduction in  $[GABA]_i$  was almost fully accounted for by the amount of GABA effluxed from the oocytes in 10 min (Figures 5E and 5F). The effect of vigabatrin was examined at pH 7.5. Vigabatrin increased  $[GABA]_i$  compared with Na<sub>2</sub>SO<sub>4</sub>-treated oocytes only in TaALMT1-expressing oocytes. All these data are consistent with rapid effects of Al<sup>3+</sup> and vigabatrin on TaALMT1, which appears to alter  $[GABA]_i$  by activation of GABA efflux through TaALMT1 (Al<sup>3+</sup>) or inhibition (vigabatrin). In the case of AOA, although AOA rapidly activated the anion currents and rapidly reduced  $[GABA]_i$  within 10 min (Figure 5G), we could not confirm that this occurred via GABA efflux due to the GABA enzyme assay being inhibited by 1 mM AOA in the external medium.

### TaALMT1 and Other ALMTs Also Facilitate GABA Influx

To test if TaALMT1 also facilitated GABA influx, we expressed TaALMT1 and TaALMT1<sup>F213C</sup> in *X. laevis* oocytes and tested their ability to influx <sup>14</sup>C-GABA. The GABA transporter AtGAT1 from Arabidopsis was used as a positive control in these uptake experiments (Figure 6). At pH 4.5, TaALMT1-expressing oocytes showed significantly higher GABA uptake from an external concentration of 1 mM compared with both control and mutant TaALMT1<sup>F213C</sup>-expressing oocytes and similar to that facilitated by AtGAT1 (Figure 6A). At pH 7.5, TaALMT1-expressing oocytes (without an external activating anion) did not show significant GABA influx compared with control oocytes, with the rate being significantly lower than AtGAT1-expressing oocytes (Figure 6B). AtGAT1-expressing oocytes had significantly reduced influx at pH 7.5 compared with that at pH 4.5, consistent with the hypothesis that this transporter uses the proton motive force to drive transport (Meyer et al., 2006). Activation of TaALMT1 at pH 7.5 with 10 mM Na<sub>2</sub>SO<sub>4</sub> increased GABA uptake significantly into the TaALMT1-expressing oocytes when compared with either the controls or TaALMT1<sup>F213C</sup>-expressing oocytes (Figure 6B).

Wheat ALMT1 is the founding member of the ALMT family (Sasaki et al., 2004). A large number of these genes are present in

Arabidopsis, barley, and rice (*Oryza sativa*) as well as other plants. Not all ALMTs are activated by Al<sup>3+</sup> but can be (trans-)activated by millimolar concentrations of external anions (Ramesh et al., 2015) and play diverse roles in plant physiology (Roelfsema et al., 2012; Sharma et al., 2016). Thus, we tested ALMTs from Arabidopsis, barley, and rice that had previously been shown to exhibit GABA-inhibited malate currents, for their ability to transport GABA into *X. laevis* oocytes. All the ALMTs tested (HvALMT1, AtALMT1, OsALMT5, and OsALMT9) facilitated transport of GABA into the respective cRNA-injected oocytes at pH 4.5 (Figure 6C). In all cases, 100  $\mu$ M Al<sup>3+</sup> reduced this uptake to control levels. However, the presence of Al<sup>3+</sup> did not affect the uptake of GABA by AtGAT1. These results demonstrate that transport of GABA is a general feature of the ALMT family and that extracellular Al<sup>3+</sup> is a common inhibitor for GABA uptake despite differences between the family in Al<sup>3+</sup>-activated malate currents.

### TaALMT1 Complements Growth of a Yeast Mutant Deficient in the Transport of GABA

To further explore GABA transport by TaALMT1, we tested if GABA could be used as a nitrogen source for yeast growth, where TaALMT1 and site-directed mutant TaALMT1<sup>F213C</sup> were transformed into a yeast triple mutant strain 22754d (MAT $\alpha$  ura3-1, gap1-1, put4-1, uga4-1) (Figure 7). This yeast strain carries mutations in general amino acid permease (gap1), proline (put4), and GABA (uga4) and is unable to grow on proline, citrulline, or GABA as the sole nitrogen source; it was used to characterize high affinity GABA transport (Meyer et al., 2006). The efflux of malate was observed to be higher in each of the transformants expressing TaALMT1 and the mutant when grown on galactose, which induces expression of the transgene via the GAL1 promoter (Figure 7A). This is consistent with TaALMT1 and its mutant being located on the plasma membrane and able to efflux malate, as previously shown in *X. laevis* and tobacco BY2 cells (Ramesh et al., 2015). All the yeast strains were capable of growth on selective drop out medium (SC-ura) supplemented with 2% glucose or galactose as carbon source and ammonium sulfate as nitrogen source (Supplemental Figures 8A and 8B). When the yeast strains were starved of nitrogen by growth in nitrogen-free medium and transferred to medium with no GABA, there were no significant differences in growth of the yeast strains (Supplemental Figure 8C). However, in medium supplemented with 1 mM GABA as the sole nitrogen source, yeast cells expressing TaALMT1 showed significantly higher relative growth rate compared with control (empty vector) or mutant TaALMT1<sup>F213C</sup> (Figure 7B; Supplemental Figure 8E). On medium supplemented with GABA at a concentration of 20 or 37.83 mM, which corresponds to SC medium with GABA at the concentration equivalent to that of ammonium sulfate, all the yeast strains showed similar growth (Supplemental Figure 8D), indicating that the stimulation of growth by 1 mM GABA was already saturating. Therefore, we examined the GABA dose-response of yeast growth (Figure 7C). The apparent  $K_d$  for growth stimulation by GABA was 0.56 mM, indicating at least moderate affinity for GABA transport by TaALMT1. This growth stimulation was completely inhibited by the addition of 2 mM malate to the medium for TaALMT1 (Figure 7D).

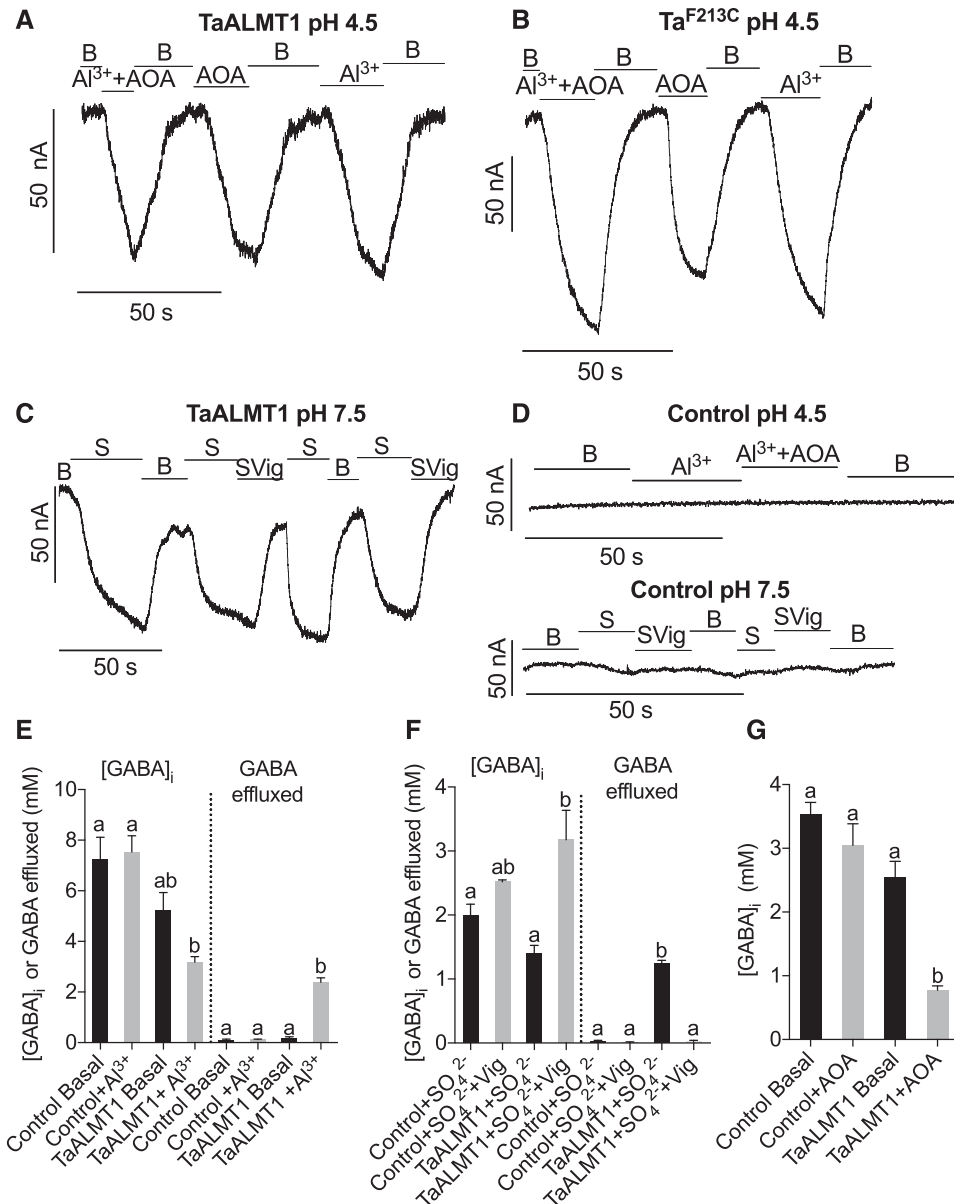


**Figure 5.** Rapid Activation of Inward Currents (Anion Efflux) by Al<sup>3+</sup>, AOA, Sulfate, and Inhibition by Vigabatrin for *TaALMT1* Expressed in *X. laevis* Oocytes and Changes in [GABA]<sub>i</sub> and GABA Efflux over 10 min.

**(A)** *TaALMT1*-expressing oocytes under TEVC showing inward current activation (at  $-80$  mV) in response to  $100 \mu\text{M}$  Al<sup>3+</sup> and  $1 \text{ mM}$  AOA addition to the bath (pH 4.5) (continuous perfusion). Rates of activation of the inward current by Al<sup>3+</sup> and AOA were similar.

**(B)** Current responses of *TaALMT1*<sup>F213C</sup> mutant-expressing oocytes under TEVC as in **(A)**. Rates of activation of the inward current by Al<sup>3+</sup> and AOA were similar. Currents were consistently larger for *TaALMT1*<sup>F213C</sup> and less cRNA was injected for these oocytes ( $16 \text{ ng}$  compared with  $32 \text{ ng}$  in **(A)**).

**(C)** Vigabatrin ( $100 \mu\text{M}$ ) effect on sulfate-activated inward currents at pH 7.5.

**(D)** Water-injected control oocytes treated with Al<sup>3+</sup>, AOA, or vigabatrin.

**(E)** Effect of Al<sup>3+</sup> ( $100 \mu\text{M}$ ) treatment over 10 min on [GABA]<sub>i</sub> (volume basis) and GABA efflux into the external medium (right plots, external GABA normalized to oocyte volume).

**(F)** Effect of vigabatrin ( $100 \mu\text{M}$ ) in the presence of SO<sub>4</sub><sup>2-</sup> (as  $10 \text{ mM}$  Na<sub>2</sub>SO<sub>4</sub>) at pH 7.5 on [GABA]<sub>i</sub> (volume basis) and GABA efflux into the external medium (right plots, external GABA normalized to oocyte volume).

**(G)** Effect of AOA ( $1 \text{ mM}$ ) treatment (10 min) on [GABA]<sub>i</sub> (volume basis). Different letter indicates significance ( $P < 0.05$ ).

For **(E)** to **(G)**, data are  $n = 4$  to 5 replicates each consisting of four oocytes. For **(A)** to **(D)**, individual oocyte examples are shown from repeated experiments on at least two harvests of oocytes.

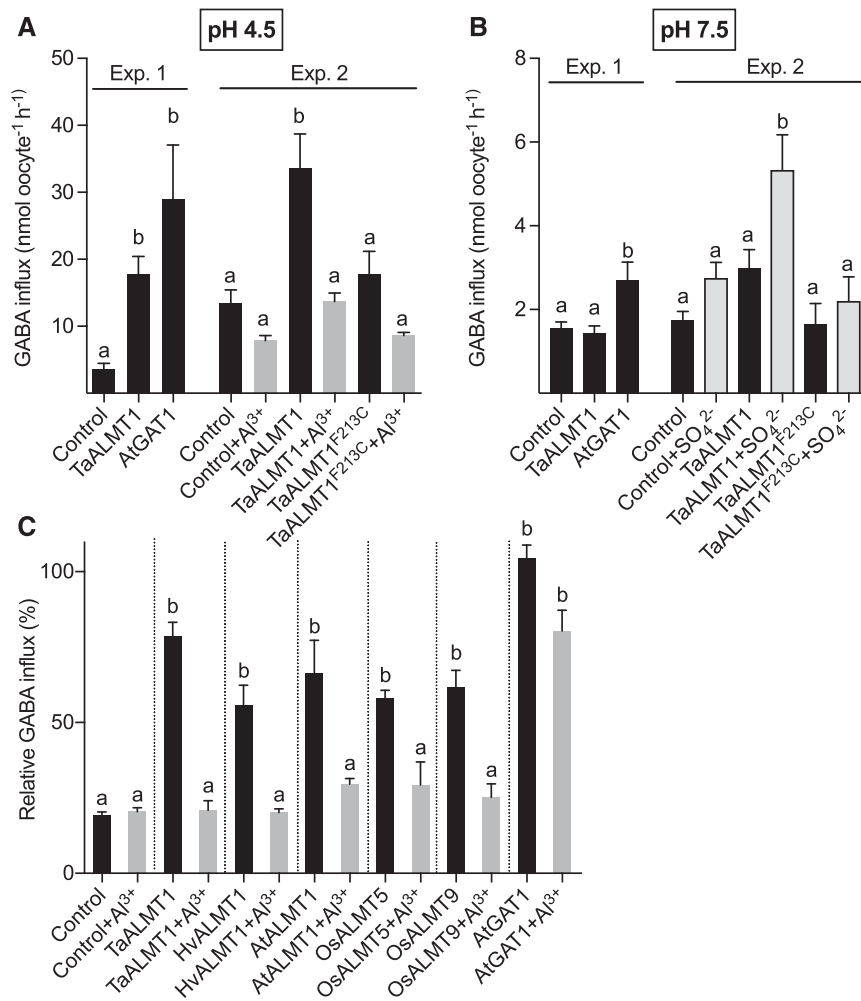


**Figure 6.** ALMTs but Not TaALMT1<sup>F213C</sup> Facilitate pH-Dependent GABA Influx from 1 mM External GABA When Expressed in *X. laevis* Oocytes and Are Blocked by 100  $\mu\text{M}$  Al<sup>3+</sup>.

**(A)** Comparison of <sup>14</sup>C-GABA uptake into *X. laevis* oocytes expressing TaALMT1 and AtGAT1 high-affinity GABA transporter at pH 4.5 (Exp. 1). Exp. 2: Comparison of <sup>14</sup>C-GABA uptake between control, TaALMT1, and TaALMT1<sup>F213C</sup>-expressing oocytes and the effect of 100  $\mu\text{M}$  Al<sup>3+</sup>.

**(B)** Comparison of <sup>14</sup>C-GABA uptake for TaALMT1 and AtGAT1 at pH 7.5 (Exp. 1). Exp. 2: Effect of 10 mM Na<sub>2</sub>SO<sub>4</sub> on <sup>14</sup>C-GABA uptake comparing control, TaALMT1, and TaALMT1<sup>F213C</sup>-expressing oocytes.

**(C)** Comparison of <sup>14</sup>C-GABA uptake and the effect of 100  $\mu\text{M}$  Al<sup>3+</sup> for oocytes expressing ALMTs from wheat (TaALMT1), barley (HvALMT1), Arabidopsis (AtALMT1), rice (OsALMT5 and OsALMT9), and Arabidopsis GABA transporter (AtGAT1) at pH 4.5. Fluxes were normalized to the median of AtGAT1. Different letters denote significant difference ( $P < 0.05$ ) within each experiment. For all data,  $n = 7$  to 10 biological replicates each consisting of eight oocytes from three oocyte harvests.

## DISCUSSION

### GABA Transport by TaALMT1 Is Demonstrated across a Wide Range of Expression Systems and May Be a General Feature of ALMTs

Anion transport via ALMTs is an important and well-accepted mechanism for signaling (Bouché et al., 2003a; Roberts, 2007; Piñeros et al., 2008; Dreyer et al., 2012; Ligaba et al., 2013; Ramesh et al., 2015), stomatal pore regulation (Meyer et al., 2010; Roelfsema et al., 2012; De Angeli et al., 2013; Kollist et al., 2014; Palmer et al., 2016), phosphorous nutrition (Liang et al., 2013;

Balzerque et al., 2017), and for providing tolerance to Al<sup>3+</sup> at low pH (Delhaize and Ryan, 1995; Sasaki et al., 2004; Zhang et al., 2008; Ryan et al., 2011). We have demonstrated that TaALMT1 is also able to facilitate GABA efflux (Figures 4 and 5) and influx (Figure 6) at very high rates. This mostly accounts for the negative linear relationship observed between malate efflux and endogenous GABA concentrations in cells expressing TaALMT1.

We have shown GABA transport by TaALMT1 using NILs of wheat that differ in the expression of TaALMT1 (Figure 4C), transgenic barley expressing TaALMT1 (Figure 4F), tobacco BY2 cells expressing TaALMT1 (Figure 4G), *X. laevis* oocytes expressing TaALMT1 (Figures 5E, 5F, and 6), and complementation by

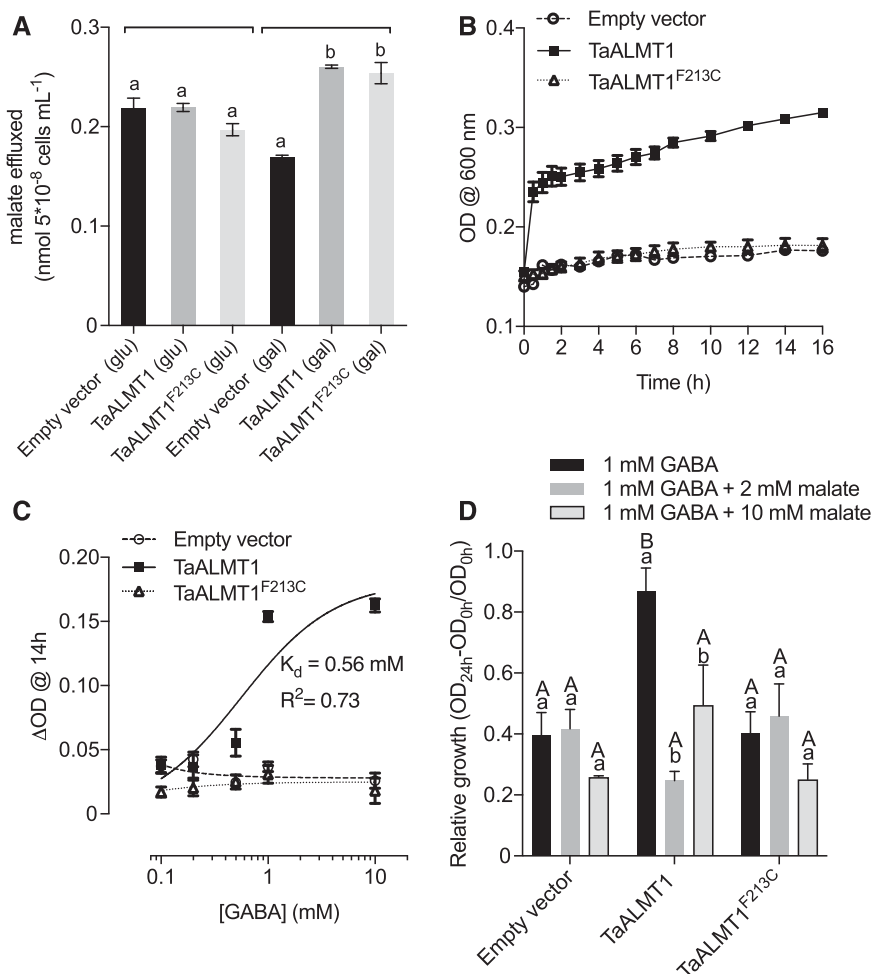


**Figure 7.** TaALMT1, but Not TaALMT1<sup>F213C</sup> Mutant, Can Complement a Yeast Mutant Strain Deficient in GABA Transport for Growth on GABA as Sole Source of Nitrogen.

**(A)** Malate efflux over 16 h from yeast mutant strain 22574d expressing TaALMT1 or TaALMT1<sup>F213C</sup> mutant and empty vector control grown on glucose and galactose. With galactose, TaALMT1 and TaALMT1<sup>F213C</sup> showed increased malate efflux consistent with expression of TaALMT1 and TaALMT1<sup>F213C</sup> in the plasma membrane. Significance is indicated by different letter combinations for within glucose (glu) or galactose (gal) (indicated by brackets above).

**(B)** Growth of yeast mutant strain 22574d expressing TaALMT1 or site-directed mutant TaALMT1<sup>F213C</sup> in medium with 1 mM GABA and galactose for 16 h.

**(C)** GABA concentration dependence of yeast growth. The fitted curve is the hyperbolic  $Y = B_{\text{max}} * [\text{GABA}] / (K_d + [\text{GABA}])$  with best fit  $K_d$  of 0.56 mM ( $n = 6$ ).

**(D)** Comparison of the effect of 1 mM GABA and addition of malate on growth for empty vector controls and TaALMT1- and TaALMT1<sup>F213C</sup>-expressing 22574d yeast strain. Lowercase letters comparison within genotype between treatments; uppercase letters comparison between genotypes within treatment ( $P < 0.05$ ).

For all data,  $n = 3$  biological replications each consisting of separate yeast subcultures.

TaALMT1 of a yeast mutant deficient in GABA transport (Figure 7). The yeast mutant 22574d that we used to characterize GABA transport and nitrogen utilization in yeast cells (Grenson et al., 1970; Breitreuz et al., 1999; Meyer et al., 2006) will likely be a very useful system in which to characterize other ALMTs for interactions with GABA and to further explore the pharmacology of the transporter.

Uptake studies with *X. laevis* oocytes showed that GABA uptake via ALMTs is not unique to TaALMT1, but ALMTs from barley, rice, and Arabidopsis also transported significantly more GABA into the cells than controls (Figure 6). Interestingly, the addition of  $\text{Al}^{3+}$  reduced the uptake in each case. We applied  $\text{Al}^{3+}$  since this activates TaALMT1 to efflux both malate and GABA at low pH. The

block of GABA influx by  $\text{Al}^{3+}$  indicates that influx is mutually exclusive of efflux. In contrast, the uptake of GABA by AtGAT1 was not reduced in response to  $\text{Al}^{3+}$  (Figure 6C). It is interesting to note that there is evidence for interactions of  $\text{Al}^{3+}$  with GABA<sub>A</sub> receptors (Trombley, 1998) and GABA transporters in animals (Albrecht and Norenberg, 1991; Cordeiro et al., 2003).

#### Reconciling GABA Efflux via TaALMT1 and GABA Block of Malate Efflux

External GABA inhibits malate efflux and inward membrane currents through ALMTs with high affinity ( $\text{IC}_{50}$  1 to 7  $\mu\text{M}$ ) dependent

on the presence of a motif containing phenylalanine (F213 in TaALMT1), which has similarities to a region in GABA<sub>A</sub> receptors (Smith and Olsen, 1995; Boileau et al., 1999; Ramesh et al., 2015). This external GABA block highlights the question of how GABA is exported from the cell to the apoplast to regulate TaALMT1. As far as we are aware, no transport system has been identified that is able to account for GABA efflux across the plasma membrane into the apoplast (Shelp and Zarei, 2017). This is despite numerous examples of relatively high extracellular concentrations of GABA being measured (Chung et al., 1992; Snedden et al., 1992; Crawford et al., 1994) and particularly the case for wheat roots where GABA is by far the most exported amino acid from roots (Warren, 2015). We propose that GABA efflux through TaALMT1 could account for this pathway and that the resulting GABA accumulation in the apoplast then inhibits malate transport via TaALMT1.

We note that there is some controversy regarding the membrane topology of ALMT proteins (Sharma et al., 2016), and this is important in the context of the location of F213 within the GABA motif of TaALMT1 and the rapidity of effect of externally applied GABA (Ramesh et al., 2015). Most recent algorithms (e.g., MEMSAT-SVM, TOPCONS; Nugent and Jones, 2012; Tsirigos et al., 2015) predict six to seven transmembrane domains for the more hydrophobic N terminus half of the protein and with the hydrophilic C terminus located in the cytosol. This is consistent with the model proposed by Zhang et al. (2013) in their study of the putative pore-forming domains of the vacuolar anion channel, AtALMT9. A similar model was also presented by Ramesh et al. (2017), who computed from evolutionary sequence variation over 3688 alignments using the EvFold web portal (Marks et al., 2012). Notably, the GABA motif previously characterized is located toward the end of TMD 6 (or 7) just before the long C terminus, which in most predictions is oriented toward the cytoplasm. It was suggested that this was oriented toward the apoplast to account for the rapid effect of GABA (Ramesh et al., 2015) and corresponding with immunocytochemical evidence for the C terminus to be located on the apoplast side (Motoda et al., 2007). Another model formulated from extensive sequence alignments across the family and secondary structure predictions also indicates that the GABA motif may be oriented toward the apoplast, but with a further two TMDs within the C terminus (Dreyer et al., 2012). If the GABA motif (beginning at F213 in TaALMT1) does orient toward the cytosolic side, the transport of GABA that we demonstrate here may reconcile the rapid action of GABA on malate currents, which presumably also applies to some GABA analogs that block depending on F213, such as muscimol and vigabatrin. Equally, the apoplastic localization of the motif is still consistent with our data. Clearly, a crystal structure will resolve this issue.

### Inhibitors That Target GABA Metabolism and Catabolism Directly Interact with TaALMT1

Manipulating [GABA]<sub>i</sub> in cells and studying the effects of this perturbation on anion transport may provide information on the role of GABA in ALMT regulation for signaling and growth. Arabidopsis mutants deficient in GABA metabolism and catabolism have been previously used to demonstrate the role of altered [GABA]<sub>i</sub> in directing pollen tube growth, guard cell closure under

drought, and systemic signaling upon wounding (Palanivelu et al., 2003; Mekonnen et al., 2016; Scholz et al., 2017). In this study, we used inhibitors assumed to disturb key steps in the GABA shunt pathway because of the rapidity of their effects, albeit compromised by possible lack of target specificity. Inhibition of GAD enzyme activity by AOA has been indicated for isolated mesophyll cells of asparagus (*Asparagus officinalis*; Snedden et al., 1992). Vigabatrin, by contrast, is a known inhibitor of GABA-T in animal cells that catalyzes the breakdown of GABA into succinate (Ben-Menachem, 2011). Both of these agents superficially appeared to have the desired effects in that AOA reduced [GABA]<sub>i</sub> and activated malate efflux when *TaALMT1* was expressed, while vigabatrin increased [GABA]<sub>i</sub> and inhibited malate efflux.

Apart from the expected associations with the inhibitors described above, we observed that activation of the TaALMT1-mediated malate efflux by external Al<sup>3+</sup> at low pH (Figures 1C and 3B) and by SO<sub>4</sub><sup>2-</sup> at pH 7.5 (Figure 2E) also reduced [GABA]<sub>i</sub>. Based on the prevailing view that both these treatments activate malate efflux through TaALMT1 directly, these observations could be explained by [GABA]<sub>i</sub> being depleted in order to support malate synthesis, since internal malate concentrations remain stable when malate efflux is stimulated by Al<sup>3+</sup> in wheat root apices (Delhaize et al., 1993). If GABA is required for malate synthesis and the demand from increased malate efflux through TaALMT1 results in depletion of [GABA]<sub>i</sub>, we would have expected to observe a reduction in [GABA]<sub>i</sub> when the TaALMT1<sup>F213C</sup> mutant channel was activated. This was not observed in BY2 cells, where [GABA]<sub>i</sub> remained at similar levels to controls when malate efflux was activated resulting in no relationship between [GABA]<sub>i</sub> and malate efflux (Figure 3). Therefore, we conclude that the reduction in [GABA]<sub>i</sub> in response to Al<sup>3+</sup> at low pH, and anions at high pH, is due to the large GABA efflux through the activated TaALMT1.

A direct effect of Al<sup>3+</sup> and anions on TaALMT1 and some other ALMTs has been demonstrated by the rapid activation observed through continuous current recording of voltage-clamped *X. laevis* oocytes (Figure 5A) (Sasaki et al., 2004; Hoekenga et al., 2006; Kobayashi et al., 2007; Kovermann et al., 2007; Piñeros et al., 2008; Meyer et al., 2011; De Angeli et al., 2013; Ramesh et al., 2015). Similarly, GABA and muscimol inhibition of the currents was as rapid as could be expected for solution change kinetics (Ramesh et al., 2015). AOA at pH 4.5 rapidly activated inward current in *TaALMT1*-expressing *X. laevis* oocytes consistent with malate anion efflux. The activation occurs with the same velocity (initial current rise) as that induced by Al<sup>3+</sup> (Figure 5A). Within 10 min, [GABA]<sub>i</sub> in the oocytes was significantly reduced by AOA, exactly as was observed when TaALMT1 was activated by Al<sup>3+</sup> (Figures 5E and 5G). The fact that neither of these treatments changed [GABA]<sub>i</sub> in control water-injected oocytes indicates that the change in [GABA]<sub>i</sub> was due to activation of TaALMT1. The mutant TaALMT1<sup>F213C</sup> that is not responsive to GABA was also activated by AOA both in *X. laevis* oocytes (Figure 5B) and tobacco BY2 cells (Figure 3A). Thus, AOA is interacting with a site/s on TaALMT1 independently from the GABA binding motif.

Vigabatrin also inhibits the TaALMT1 inward current carried by anions rather rapidly (Figure 5C), which is not consistent with increasing [GABA]<sub>i</sub>. Though vigabatrin did increase [GABA]<sub>i</sub> in tobacco BY2 cells not expressing *TaALMT1* (Figure 3F), the effect of vigabatrin was greater when *TaALMT1* or *TaALMT1*<sup>F213C</sup> was

expressed in BY2 (Figure 3F) and when activated by  $\text{SO}_4$  at pH 7.5 in wheat root (Figure 2E) and in *X. laevis* oocytes (Figure 5F). Thus, we conclude that both AOA and vigabatrin not only alter  $[\text{GABA}]_i$  by their known target enzymes, but also directly target TaALMT1 to change GABA efflux. The negative correlations observed between malate efflux and  $[\text{GABA}]_i$  in both wheat roots and tobacco BY2 cells is mainly indicative of altered GABA efflux through TaALMT1. Notwithstanding this conclusion, higher expression of *TaALMT1* appeared to elevate  $[\text{GABA}]_i$  independently of any treatments as was initially observed when comparing ET8 with ES8 wheat NILs (Figure 1 in Ramesh et al., 2015; Supplemental Figure 1N). This was observed with tobacco BY2 cells expressing *TaALMT1* (Figure 3B) at pH 4.5 and *TaALMT1*<sup>F213C</sup> at pH 7.5 (Figure 3F), but not in *X. laevis* oocytes (Figure 5E). Interestingly TaALMT1<sup>F213C</sup> does not transport GABA (Figures 4G, 6A, and 6B), yet its expression is able to influence  $[\text{GABA}]_i$  depending on pH. Currently we have no explanation for these observations, and further research is needed on the interaction between TaALMT1 and GABA metabolism related to the GABA interaction motif.

It may not be surprising that both AOA and vigabatrin interact with TaALMT1 since both are structural analogs of GABA. In the case of AOA, it inhibits GAD and GABA-T via interaction with the pyridoxal phosphate cofactor binding site (Wallach, 1961; John and Charteris, 1978; Löscher et al., 1989; Miller et al., 1991). It is interesting that AOA strongly activates TaALMT1, so far the only known external organic compound besides transported anions that has this effect. AOA is one atom shorter than GABA and is also a zwitterion that has no net charge at neutral pH. The possibility that ALMTs also have a pyridoxal phosphate binding site needs to

be explored, though there is no clear pyridoxal phosphate (vitamin B6) binding motif (InterPro IPR021115, Prosite entry Ps00392) evident in TaALMT1. GABA-T is also a pyridoxal phosphate-dependent enzyme and is reported to be inhibited by AOA (Storici et al., 2004). Vigabatrin has a similar structure to GABA; therefore, it may inhibit TaALMT1 as does the GABA analog muscimol. We conclude that the effect of vigabatrin and AOA on  $[\text{GABA}]_i$  is mainly via interactions with TaALMT1.

### Potential Roles for GABA Transport via ALMTs

Until now, the identity of a GABA efflux transporter across the plasma membrane was not known. Our studies show that TaALMT1 in addition to mediating efflux of organic anions also mediates GABA efflux from cells when activated (Figures 4 and 5). Its transport capacity for GABA is very high as indicated by its activation being able to significantly reduce  $[\text{GABA}]_i$  in root tips and other cells expressing TaALMT1. In fact, we have shown higher capacity for GABA efflux relative to malate efflux on a molar basis (Figure 4). This is quite novel as changes in  $[\text{GABA}]_i$  are likely to have broad effects on carbon metabolism and signaling. We have shown that GABA does not significantly complex  $\text{Al}^{3+}$  (Supplemental Methods); therefore, we can exclude the hypothesis that GABA efflux with malate may provide additional protection against  $\text{Al}^{3+}$ . Although it is not clear why high GABA efflux may be an advantage when TaALMT1 is activated by  $\text{Al}^{3+}$  at low pH, or activated at high pH, we may speculate along the following lines.

First, GABA may act as an extracellular pH buffer. GABA addition to solutions at both low and high pH tends to bring the pH

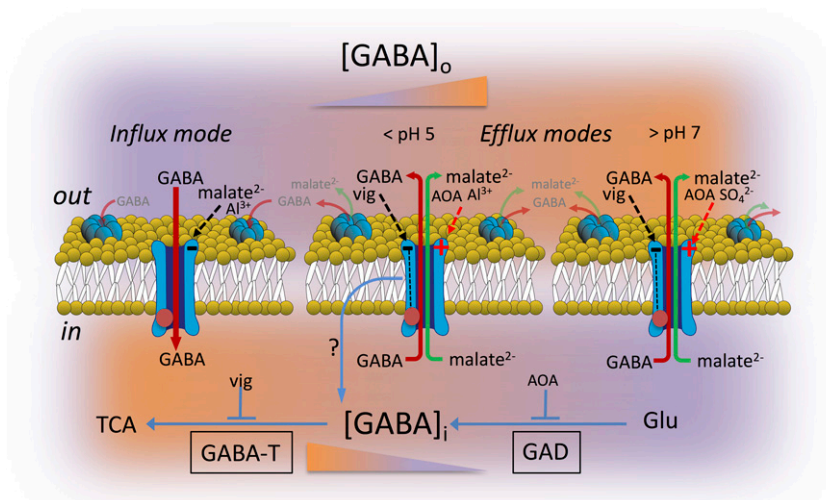


**Figure 8.** Summary of GABA and Malate Transport Interactions through TaALMT1 and the Effects on Internal and External GABA Concentrations.

Influx mode (left) occurs when GABA blocks malate transport (–) through TaALMT1 both outwards and inwards, based on TEVC and fluxes (Ramesh et al., 2015), but GABA transport can proceed inwards more so at low pH. This influx is blocked by external malate and  $\text{Al}^{3+}$ . Influx mode will tend to reduce  $[\text{GABA}]_o$  and increase  $[\text{GABA}]_i$  (orange = high  $[\text{GABA}]_i$ ; purple = low  $[\text{GABA}]_i$ ). Efflux modes (center and right) occur when TaALMT1 is activated (+) by  $\text{Al}^{3+}$  at low pH (center), AOA, or the presence of anions ( $\text{malate}^{2-}$ ,  $\text{SO}_4^{2-}$ ) on the outside at high pH (>7) (right). This will tend to increase  $[\text{GABA}]_o$  and reduce  $[\text{GABA}]_i$ . Vigabatrin (vig) and AOA can also affect  $[\text{GABA}]_i$  via inhibition of GABA-T and glutamate decarboxylase (GAD), respectively, though their primary effect appears to be via direct action on TaALMT1 (vigabatrin blocks and AOA activates). The F213 residue is shown oriented to the cytoplasm (red ball), which is critical for GABA transport and GABA block of anion flux. Light-blue arrow with a question mark from TaALMT1 (center) to  $[\text{GABA}]_i$  indicates that the expression of TaALMT1 at low pH increases  $[\text{GABA}]_i$  via an unknown mechanism. TCA, tricarboxylic acid (Krebs) cycle.

toward neutrality. Thus, at low pH where GABA synthesis by GAD acts to regulate pH (Snedden et al., 1992; Crawford et al., 1994; Shelp et al., 1999; Snedden and Fromm, 1999), its efflux to the external medium will also tend to increase the external pH. It has been reported that exogenously supplied GABA (10  $\mu$ M) significantly improved root growth of barley seedlings at pH 4.5 and when exposed to 20  $\mu$ M Al<sup>3+</sup> at pH 5.0 (Song et al., 2010). This was considered to be via alleviation of oxidative damage.

Second, AtALMT1 has been implicated as the key regulator in the attraction of the beneficial *Bacillus subtilis* strain FB17 to the Arabidopsis root (Lakshmanan et al., 2013), in addition to its role in Al<sup>3+</sup> tolerance. Pseudomonads are known for their specific GABA receptors and positive chemotactic response to GABA (Reyes-Darias et al., 2015) and *B. subtilis* has positive chemotaxis to Arabidopsis roots with chemoreceptors that recognize a range of amino acids.

Third, GABA transported by TaALMT1 also provides feedback regulation on the cotransport of organic anions. As GABA builds up in the apoplast, this will tend to reduce malate efflux. Apoplastic GABA may also signal to adjacent cells via its effect on TaALMT1. Malate has the opposite effect since it activates TaALMT1 from the *trans* side of TaALMT1 particularly at higher pH. Thus, the two transported substrates have opposite effects on the *trans* (apoplastic) side of the transporter (Figure 8). ALMTs in general have rather complex regulation via anions, for example, the activation of AtALMT9 on the tonoplast membrane by cytosolic malate to efflux Cl<sup>-</sup> into the vacuole of guard cells during stomatal opening (De Angeli et al., 2013).

### The Transport Mechanism for GABA and Its Interaction with Malate

Considering the transport of GABA via TaALMT1, it is necessary to account for the likely ionic charge on GABA. GABA is a zwitterion at neutral pH and is thus uncharged in the cytosol. Only at very high pH (above pK<sub>a</sub> 10.43) or at low pH (below pK<sub>a</sub> 4.23) does either a negative or positive charge become >50% of the total concentration. At pH 4.5, we calculate that there would be 35% of GABA in the external medium that has a net positive charge due to a proportion of molecules not deprotonated at the carboxyl end, while the amino terminal will remain positively charged. Efflux from the cytoplasm (slightly alkaline pH) would not be detectable as an electrical current, but influx at pH 4.5 could be detected as an inward current if the cationic form of GABA is transported, particularly if there is a high affinity of transport as suggested by the IC<sub>50</sub> of block by GABA of the anion current, and from the high influx measured relative to that of AtGAT1 at pH 4.5. It is also possible that GABA fluxes may be coupled to the movement of protons in the same direction, similar to GABA transport via AtGAT1 (Meyer et al., 2006), which would be detectable as an electrogenic current. GABA influx into *X. laevis* oocytes was substantially higher at pH 4.5 than pH 7.5 (10-fold), and the flux at pH 7.5 was similar to that of control water-injected oocytes. However, GABA influx was activated at pH 7.5 by the addition of Na<sub>2</sub>SO<sub>4</sub> to the bathing medium, which also stimulates malate efflux.

The ALMTs we tested that facilitated GABA influx (Figure 6) also showed external GABA inhibition of the malate efflux current at pH 7.5 (Ramesh et al., 2015). However, GABA on the inside of the cell

clearly allows efflux of malate and GABA together, since in the heterologous expression systems used here and in the wheat NIL lines both GABA and malate efflux occur simultaneously. In the case of the *X. laevis* oocyte, the [GABA]<sub>i</sub> is well above the concentrations that block malate efflux from the external (*trans*) side. The F213C mutation in TaALMT1 greatly reduces the external GABA sensitivity of anion efflux currents (Ramesh et al., 2015). We have shown here that this mutation also effectively abolishes GABA influx and GABA efflux via TaALMT1, but still allows activation by external anions and external Al<sup>3+</sup>, further confirming the importance of this site in GABA interactions. The F213C mutation also shows extremely high malate efflux when expressed in *X. laevis* oocytes compared with the unmutated TaALMT1, suggesting that “cotransport” of malate and GABA has been uncoupled. A summary of the observed interactions between GABA and malate transport via TaALMT1 and how this is expected to affect internal and external GABA concentrations is presented in Figure 8. Although Figure 8 depicts the ALMT as a channel, as this is the consensus in the literature, it is possible that the mechanism of transport may also be carrier-like.

To fully understand the transport mechanism in ALMTs, more detailed kinetic studies will be required wherein GABA and malate concentrations are varied on both *cis* and *trans* faces, most probably best achieved via patch-clamp studies. Our work reported here indicates that ALMTs are more complicated than a relatively simple ligand-gated anion channel, and we suggest that at least some (e.g., TaALMT1) could be considered as GABA transporters with anion channel activity. Why this has not been revealed from the many previous studies is probably related to several factors including the focus upon Al<sup>3+</sup> tolerance resulting from the malate transport through TaALMT1 and the probable lack of or low electrogenic activity associated with GABA transport.

The dual function of TaALMT1 and other ALMTs is analogous to some transporters that display channel activity such as the excitatory amino acid transporters from animals that function as both glutamate transporters and chloride channels (Cater et al., 2016). There is also a precedent for GABA transport in that the mammalian GAT1 transporter displays sodium channel activity (Risso et al., 1996). In the context of the biological link between GABA and anion transport and particularly that of malate, the regulation of efflux of both substrates is titrated finely by apoplastic concentrations of both substrates, making them uniquely positioned to provide intercellular and intracellular communication of metabolic status (Figure 8).

## METHODS

### Chemicals

All chemicals were purchased from Sigma-Aldrich. <sup>14</sup>C-GABA was obtained from American Radiolabeled Chemicals.

### cRNA Synthesis

Plasmid DNA from ALMT and site-directed mutants (Nugent and Jones, 2012; Ramesh et al., 2015) was extracted using the Mini Prep kit from Sigma-Aldrich, and 1  $\mu$ g of plasmid DNA was linearized with the restriction enzyme *Nhe*I. Capped cRNA was synthesized using the MESSAGE Mmachine T7 Kit (Ambion) as per the manufacturer's instructions.

### Voltage-Clamp Electrophysiology

Electrophysiology was performed on *Xenopus laevis* oocytes 2 d after injection with water/cRNA (Preuss et al., 2010; Ramesh et al., 2015). Oocytes were injected with 46 nL of RNase-free water using a microinjector (Nanoject II, automatic nanoliter injector; Drummond Scientific)  $\pm$  16 to 32 ng cRNA. Sodium malate (10 mM, pH 7.5) was injected into oocytes 1 to 4 h before measurement. Aluminum activation was performed in ND88 solution at pH 4.5 (Sasaki et al., 2004; Hoekenga et al., 2006)  $\pm$  aluminum chloride ( $\text{AlCl}_3$  100  $\mu\text{M}$ ). Basal external solutions for anion activation contained 0.5 mM  $\text{CaCl}_2$  (pH 4.5) or 0.7 mM  $\text{CaCl}_2$  (pH 7.5) and mannitol to 220 mOsm  $\text{kg}^{-1}$ ,  $\pm$  10 mM sodium sulfate or 10 mM malate buffered with 5 mM BTP/MES from pH 4.5 to 7.5. Vigabatrin and AOA were added at 100  $\mu\text{M}$  and 1 mM, respectively, in the experiments. In all *X. laevis* oocyte experiments, solutions were applied to gene-injected oocytes in the same order as controls (water injected). Randomly selected oocytes were alternated between control and gene injected to limit any bias caused by time-dependent changes after gene injection or malate injection. The University of Adelaide Animal Ethics Committee approved the *X. laevis* oocyte experiments (project number S-2014-192).

### Root Assays

NILs of wheat (*Triticum aestivum*) ET8 and ES8 (Sasaki et al., 2004) and barley (*Hordeum vulgare*) transgenic line overexpressing TaALMT1 (a gift from Peter Ryan, CSIRO, Canberra; Delhaize et al., 2004) were surface sterilized in 1% bleach for 1 min, rinsed three times in water, and germinated on moist filter paper in the dark on the bench. The 3-d-old seedlings were placed in a microcentrifuge tube with roots immersed for 22 h in 3 mM  $\text{CaCl}_2$  and 5 mM MES/BTP to pH 4.5 to 7.5  $\pm$  treatments. For root flux assays, experiments were performed wherein the identity of the treatment solutions was unknown to the person performing the experiments to remove any bias. Malate concentrations were measured on an OMEGA plate-reading spectrophotometer (BMG) following the K-LMALR/K-LMALL assay11 (Megazyme). One hundred microliters of the treatment solution collected from roots was added to a master mix containing the various components of the K-LMALR/K-LMALL assay11 kit (Megazyme) as per the manufacturer's instructions. The change in absorbance at 340 nm was used to calculate the concentration of malate in the samples.

### Endogenous GABA Concentrations and GABA Efflux

GABA concentrations were measured on an OMEGA plate-reading spectrophotometer following the GABase enzyme assay (Zhang and Bown, 1997). Briefly, 5 mm of root tips was excised and snap frozen in liquid nitrogen after seedlings were subjected to treatment solutions for 22 h unless otherwise stated. The root tips (three per seedling/replicate) were ground in liquid nitrogen and a known weight (10–15 mg) was added to methanol and incubated at 25°C for 10 min. The samples were vacuum dried, resuspended in 70 mM  $\text{LaCl}_3$ , pelleted at 500g in a desktop microcentrifuge, and precipitated with 1 M KOH. These samples were re-centrifuged at 500g, and 45.2  $\mu\text{L}$  of supernatant was assayed for GABA concentrations using the GABase enzyme from Sigma-Aldrich as per the manufacturer's instructions. For oocyte GABA measurements, *X. laevis* oocytes injected with TaALMT1 cRNA or water (controls) were imaged in groups of four to five using a stereo zoom microscope (SMZ800) with a Nikon (cDSS230) camera 48 h after injection. The oocytes were incubated in treatment solutions indicated in the figure legends for 10 min. After 10 min, treatment solution was removed, and oocytes were snap frozen in liquid nitrogen and stored at  $-80^\circ\text{C}$  until further use. Oocytes were extracted with same protocol used for root tips and assayed as mentioned above. Samples from root flux assays or tobacco (*Nicotiana tabacum*) BY2 suspension cell assays were used to measure external GABA using the GABase enzyme as described above.

GABA concentrations were also analyzed with UPLC. As described above, the same GABA extracts from root tips, oocytes, and tobacco BY2 cells were centrifuged at 16,000g in a tabletop centrifuge for 10 min, and the supernatant was filtered with a 0.2- $\mu\text{m}$  syringe filter. For GABA efflux, 1 mL of efflux solution was concentrated by drying down and reconstituted with 200 to 250  $\mu\text{L}$  of water, followed by the filtering step as mentioned above. GABA in the samples was derivatized with the AccQ Tag Ultra Derivatization Kit (Waters) according to the manufacturer's protocol. Chromatographic analysis of GABA was performed on an Acquity UPLC System (Waters) using a Cortecs UPLC  $\text{C}_{18}$  column (1.6  $\mu\text{m}$ ,  $2.1 \times 100$  mm). The gradient protocol for amino acids analysis was used to measure GABA with mobile solvents AccQ Tag Ultra Eluents A and B (Waters). Calibration range for GABA was 0 to 500  $\mu\text{M}$ . The results were analyzed with Empower 3 chromatography software by Waters.

### Tobacco BY2 Transgenic Lines

Tobacco suspension cells (*Nicotiana tabacum* cv Bright Yellow-2) were transformed with TaALMT1, site-directed mutants, or the empty vector pTOOL37 (Supplemental Table 1) using a slightly modified protocol (An, 1985). Briefly, fresh suspension cells in Murashige and Skoog (MS) medium were cocultivated with agrobacterium strains carrying the binary vectors with genes of interest for 48 h with 20  $\mu\text{M}$  acetosyringone at 25°C. The cells were washed four times in MS medium, with a final wash in MS medium with carbenicillin (500  $\mu\text{g}/\text{mL}$ ). Cells were then plated on selective plates with MS medium, carbenicillin, and hygromycin (50  $\mu\text{g}/\text{mL}$ ) and incubated at 25°C for 14 d. Microcalli visible on plates were transferred to fresh selective plates for further growth. The transformed calli were used to extract DNA to confirm the presence of transgenes by PCR and maintained by subculturing every 3 weeks. The transgenic BY2 cell lines were used in further experiments.

### Tobacco BY2 Malate Efflux and GABA Concentrations

Tobacco suspension cells were grown in MS medium on a rotary shaker (~100 rpm) until the logarithmic phase. Aliquots of suspension cells containing ~1 g of cells were centrifuged and gently resuspended in a basal BY2 solution (Zhang et al., 2008). TaALMT1 and site-directed mutants expressing or vector control tobacco BY2 suspension cells (0.15 g) were placed in 3 mL of 3 mM  $\text{CaCl}_2$ , 3 mM sucrose, and 5 mM MES/BTP to pH 4.5 to 7.5  $\pm$  treatments as shown in the figure legends, in 50-mL tubes on a rotary shaker for 22 h, unless otherwise stated. Malate fluxes were measured as stated above. Cells were harvested after treatments by centrifugation at 5000g in a desktop microcentrifuge and snap frozen in liquid nitrogen. Frozen cells were subjected to extraction and GABA concentrations measured as described above using GABase enzyme (Sigma-Aldrich).

### $^{14}\text{C}$ -GABA Tracer Flux Experiments

*X. laevis* oocytes expressing ALMTs, site-directed mutant, controls, and AtGAT1 (At1g08230) were incubated in uptake buffer containing 0.5 mM  $\text{CaCl}_2$  (pH 4.5) or 0.7 mM  $\text{CaCl}_2$  (pH 7.5), buffered with 5 mM MES/BTP  $\pm$   $\text{AlCl}_3$  (100  $\mu\text{M}$ )/sodium sulfate (10 mM), mannitol to 220 mOsm  $\text{kg}^{-1}$  and 1.018 mM GABA for 2 h. The oocytes were washed twice with ice-cold uptake buffer and placed in 0.1 N nitric acid before addition of scintillation fluid (4 mL) and radioactivity measured in a Beckman and Coulter multi-purpose scintillation counter (LS6500). The AtGAT1 used as a positive control was a gift from Doris Rentsch, University of Bern, Switzerland.

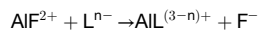
### Yeast Experiments

*Saccharomyces cerevisiae* strain 22574d (*MAT $\alpha$  ura3-1, gap1-1, put4-1, uga4-1*) (Jauniaux et al., 1987) was transformed with TaALMT1 and

site-directed mutants cloned (Supplemental Table 1) into yeast transformation vector pDEST52, which carries the promoter and enhancer sequences from the *GAL1* gene for galactose-regulated expression according to Schiestl and Gietz (1989), and the transformants were selected on minimal medium supplemented with 2% glucose. Selected transformants were grown in Grenson's medium (Grenson et al., 1970) lacking nitrogen supplemented with 2% galactose for 16 to 18 h before transfer to medium supplemented with either 1 mM GABA as the sole nitrogen source for growth studies or different concentrations of GABA (0–1 mM) for dose-response curves. The yeast strain used was a gift from Doris Rentsch.

#### Ligand Complexation Method for Testing Al<sup>3+</sup>-GABA Complexation

A competitive ligand method was developed (Supplemental Methods) and tested wherein the ligand of interest, L (e.g., GABA), is added to a solution containing Al<sup>3+</sup> and fluoride (F). Depending on the strength of Al<sup>3+</sup> complexation with the ligand of interest, F will be displaced from the AlF<sup>2+</sup> complex, resulting in higher free F concentration, which can be detected with a fluoride ion selective electrode (ISE).



Five organic ligands were used in the measurements: citric acid, oxalic acid, malic acid, salicylic acid, and GABA. Stock solutions of 0.05 and 0.005 M were made and adjusted to pH 4.5 using NaOH. A solution containing 10 mM NaCl, 60 μM Al<sup>3+</sup> (as AlCl<sub>3</sub>), 60 μM F (as Na<sub>2</sub>SiF<sub>6</sub>), and 10 mM MES, adjusted to pH 4.5 was made. Ten milliliters of this solution was titrated with organic ligand, and the free F concentration was determined using a fluoride ion selective electrode (Orion 9609BNWP), allowing several minutes between each titration step until the reading stabilized. The ISE was calibrated using solutions with 10 mM NaCl, 10 mM MES (pH 4.5), and 1 to 100 μM F. All ISE measurements were made in aluminum foil-covered beakers while stirring the solution. The pH of the solution was checked at the end of each titration run and was always between 4.45 and 4.55.

#### Statistics

All graphs and data analysis were performed in GraphPad Prism 7 (version 7.02). All data shown are mean ± SE. Where appropriate, one-way and two-way ANOVA were performed with post tests to determine significance between individual treatments (Supplemental Table 2).

#### Accession Numbers

Sequence data from this article can be found in the EMBL/GenBank data libraries under the following accession numbers: TaALMT1 (DQ072260), HvALMT1 (EF424084), OsALMT5 (Os04g0417000), OsALMT9 (Os10g0572100), AtALMT1 (AT1G08430), AtGAT1 (At1g08230), Actin (KC775782), Tubb4 (U76895.1), Cyclophilin (EU035525.1), and GAPDH (EF592180.1).

#### Supplemental Data

**Supplemental Figure 1.** GABA spike and recovery experiments with root tips of 3-d-old wheat seedlings (ET8) and *X. laevis* oocytes (control and TaALMT1 injected) to test the impact of AOA, Al<sup>3+</sup>, and vigabatrin treatment on the enzyme assay of GABA and UPLC versus GABase measurements.

**Supplemental Figure 2.** Expression of TaALMT1 relative to three housekeeping genes (*GAPDH*, *Cyclophilin*, and *Actin*) in seedling roots of plants treated with 100 μM AlCl<sub>3</sub> pH 4.5 or basal solution for 22 h.

**Supplemental Figure 3.** Malate efflux via TaALMT1 expressed in tobacco BY2 cells as a function of external pH and the effect of AOA.

**Supplemental Figure 4.** Further evidence of a negative linear correlation between malate efflux and [GABA]<sub>i</sub> in tobacco BY2 cells expressing TaALMT1 showing that sulfate does not activate malate efflux at low pH.

**Supplemental Figure 5.** Vigabatrin, an inhibitor of GABA transaminase, inhibits malate efflux activated by 10 mM Na<sub>2</sub>SO<sub>4</sub> while elevating endogenous GABA concentrations in BY2 cells expressing TaALMT1 at pH 7.5.

**Supplemental Figure 6.** Tobacco BY2 empty vector controls show no significant correlation (P > 0.05) between malate efflux and endogenous GABA concentrations at pH 4.5 when treated with Al<sup>3+</sup>, AOA, or at pH 7.5 when treated with Na<sub>2</sub>SO<sub>4</sub> or vigabatrin.

**Supplemental Figure 7.** Malate-activated inward currents in TaALMT1-expressing *Xenopus laevis* oocytes at pH 7.5 (−80 mV) are also rapidly inhibited by 100 μM vigabatrin.

**Supplemental Figure 8.** Details of complementation of yeast strain 22754d (MAT<sub>α</sub> ura3-1, gap1-1, put4-1, uga4-1) expressing TaALMT, TaALMT<sup>F213C</sup>.

**Supplemental Table 1.** Primers used for cloning and site directed mutagenesis.

**Supplemental Table 2.** ANOVA tables.

**Supplemental Methods.** Details of measurement of possible complexation of Al<sup>3+</sup> by GABA.

#### ACKNOWLEDGMENTS

We thank Doris Rentsch for providing the yeast strain and Peter Ryan for providing transgenic barley seeds. We thank Muyun Xu for cloning the cDNAs of *OsALMT5* and *OsALMT9*. We thank Sue Tyerman for professional editing of the manuscript. The Australian Research Council has supported this research through CE140100008 and IH130200027, and DP130104205 awarded to S.D.T. and M.G., who is also supported by FT130100709. M.O. and L.C. were supported by IH130200027.

#### AUTHOR CONTRIBUTIONS

S.D.T. supervised the research. S.A.R., S.D.T., and M.G. planned and designed experiments. S.A.R. performed experiments with oocytes and tobacco BY2 cells, as well as yeast and plant experiments. M.K. performed additional plant experiments. W.S. assisted in plant, oocyte, and tobacco cell experiments. M.O. and L.C. optimized and carried out UPLC measurements. M.M. and F.D. optimized and carried out GABA-Al<sup>3+</sup> binding assays. S.A.R. and S.D.T. analyzed the data and wrote the article with edits from M.G. All authors had intellectual input into the project and commented on the manuscript.

Received November 7, 2017; revised February 27, 2018; accepted April 2, 2018; published April 4, 2018.

#### REFERENCES

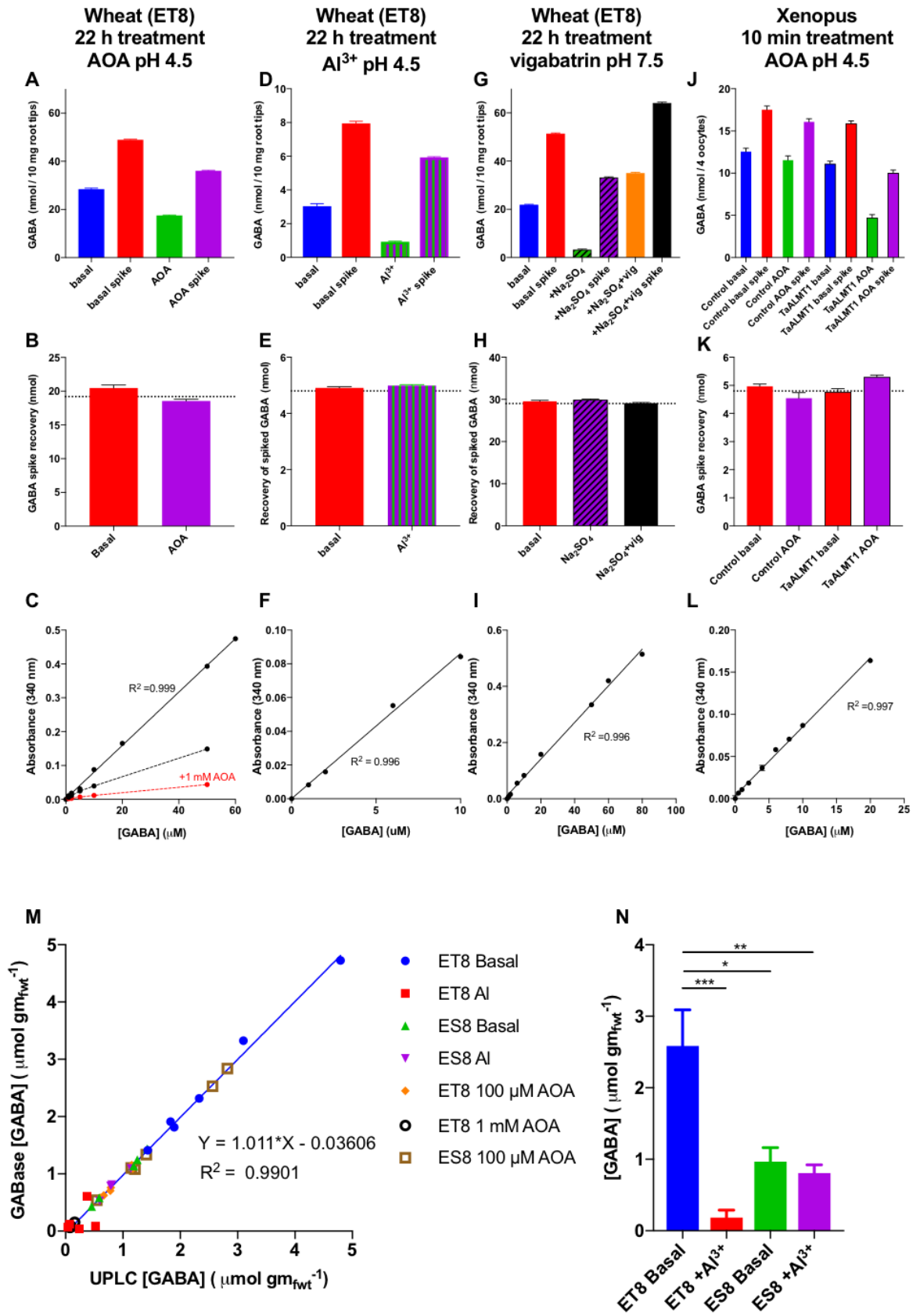
- Albrecht, J., and Norenberg, M.D.** (1991). Aluminum chloride stimulates NACl-dependent release of taurine and γ-aminobutyric acid in rat cortical astrocytes. *Neurochem. Int.* **18**: 125–129.
- An, G.** (1985). High efficiency transformation of cultured tobacco cells. *Plant Physiol.* **79**: 568–570.
- Balzerque, C., et al.** (2017). Low phosphate activates STOP1-ALMT1 to rapidly inhibit root cell elongation. *Nat. Commun.* **8**: 15300.

- Ben-Menachem, E.** (2011). Mechanism of action of vigabatrin: correcting misperceptions. *Acta Neurol. Scand. Suppl.* **124**: 5–15.
- Boileau, A.J., Evers, A.R., Davis, A.F., and Czajkowski, C.** (1999). Mapping the agonist binding site of the GABAA receptor: evidence for a beta-strand. *J. Neurosci.* **19**: 4847–4854.
- Bouché, N., and Fromm, H.** (2004). GABA in plants: just a metabolite? *Trends Plant Sci.* **9**: 110–115.
- Bouché, N., Fait, A., Bouchez, D., Møller, S.G., and Fromm, H.** (2003b). Mitochondrial succinic-semialdehyde dehydrogenase of the gamma-aminobutyrate shunt is required to restrict levels of reactive oxygen intermediates in plants. *Proc. Natl. Acad. Sci. USA* **100**: 6843–6848.
- Bouché, N., Lacombe, B., and Fromm, H.** (2003a). GABA signaling: a conserved and ubiquitous mechanism. *Trends Cell Biol.* **13**: 607–610.
- Bown, A., and Shelp, B.** (1989). The metabolism and physiological roles of 4-aminobutyric acid. *Biochemistry* **8**: 21–25.
- Breitkreuz, K.E., Shelp, B.J., Fischer, W.N., Schwacke, R., and Rentsch, D.** (1999). Identification and characterization of GABA, proline and quaternary ammonium compound transporters from *Arabidopsis thaliana*. *FEBS Lett.* **450**: 280–284.
- Carroll, A.D., Fox, G.G., Laurie, S., Phillips, R., Ratcliffe, R.G., and Stewart, G.R.** (1994). Ammonium assimilation and the role of gamma-aminobutyric-acid in pH homeostasis in carrot cell-suspensions. *Plant Physiol.* **106**: 513–520.
- Cater, R.J., Ryan, R.M., and Vandenberg, R.J.** (2016). The split personality of glutamate transporters: A chloride channel and a transporter. *Neurochem. Res.* **41**: 593–599.
- Chung, I., Bown, A.W., and Shelp, B.J.** (1992). The production and efflux of 4-aminobutyrate in isolated mesophyll cells. *Plant Physiol.* **99**: 659–664.
- Cordeiro, J.M., Silva, V.S., Oliveira, C.R., and Gonçalves, P.P.** (2003). Aluminium-induced impairment of Ca<sup>2+</sup> modulatory action on GABA transport in brain cortex nerve terminals. *J. Inorg. Biochem.* **97**: 132–142.
- Crawford, L.A., Bown, A.W., Breitkreuz, K.E., and Guinel, F.C.** (1994). The synthesis of [gamma]-aminobutyric acid in response to treatments reducing cytosolic pH. *Plant Physiol.* **104**: 865–871.
- De Angeli, A., Zhang, J., Meyer, S., and Martinoia, E.** (2013). AtALMT9 is a malate-activated vacuolar chloride channel required for stomatal opening in *Arabidopsis*. *Nat. Commun.* **4**: 1804.
- Delhaize, E., and Ryan, P.R.** (1995). Aluminum toxicity and tolerance in plants. *Plant Physiol.* **107**: 315–321.
- Delhaize, E., Ryan, P.R., and Randall, P.J.** (1993). Aluminum tolerance in wheat (*Triticum aestivum* L) 2. Aluminum-stimulated excretion of malic-acid from root apices. *Plant Physiol.* **103**: 695–702.
- Delhaize, E., Ryan, P.R., Hebb, D.M., Yamamoto, Y., Sasaki, T., and Matsumoto, H.** (2004). Engineering high-level aluminum tolerance in barley with the ALMT1 gene. *Proc. Natl. Acad. Sci. USA* **101**: 15249–15254.
- Dreyer, I., Gomez-Porras, J.L., Riaño-Pachón, D.M., Hedrich, R., and Geiger, D.** (2012). Molecular evolution of slow and quick anion channels (SLACs and QUACs/ALMTs). *Front. Plant Sci.* **3**: 263.
- Fait, A., Fromm, H., Walter, D., Galili, G., and Fernie, A.R.** (2008). Highway or byway: the metabolic role of the GABA shunt in plants. *Trends Plant Sci.* **13**: 14–19.
- Fait, A., Nesi, A.N., Angelovici, R., Lehmann, M., Pham, P.A., Song, L., Haslam, R.P., Napier, J.A., Galili, G., and Fernie, A.R.** (2011). Targeted enhancement of glutamate-to-γ-aminobutyrate conversion in *Arabidopsis* seeds affects carbon-nitrogen balance and storage reserves in a development-dependent manner. *Plant Physiol.* **157**: 1026–1042.
- Gilliham, M., and Tyerman, S.D.** (2016). Linking metabolism to membrane signaling: the GABA-malate connection. *Trends Plant Sci.* **21**: 295–301.
- Grant, S.M., and Heel, R.C.** (1991). Vigabatrin. A review of its pharmacodynamic and pharmacokinetic properties, and therapeutic potential in epilepsy and disorders of motor control. *Drugs* **41**: 889–926.
- Grenson, M., Hou, C., and Crabeel, M.** (1970). Multiplicity of the amino acid permeases in *Saccharomyces cerevisiae*. IV. Evidence for a general amino acid permease. *J. Bacteriol.* **103**: 770–777.
- Hoekenga, O.A., et al.** (2006). AtALMT1, which encodes a malate transporter, is identified as one of several genes critical for aluminum tolerance in *Arabidopsis*. *Proc. Natl. Acad. Sci. USA* **103**: 9738–9743.
- Jackson, M.B., Lecar, H., Mathers, D.A., and Barker, J.L.** (1982). Single channel currents activated by gamma-aminobutyric acid, muscimol, and (-)-pentobarbital in cultured mouse spinal neurons. *J. Neurosci.* **2**: 889–894.
- Jauniaux, J.C., Vandenbol, M., Vissers, S., Broman, K., and Grenson, M.** (1987). Nitrogen catabolite regulation of proline permease in *Saccharomyces cerevisiae*. Cloning of the PUT4 gene and study of PUT4 RNA levels in wild-type and mutant strains. *Eur. J. Biochem.* **164**: 601–606.
- John, R.A., and Charteris, A.** (1978). The reaction of amino-oxyacetate with pyridoxal phosphate-dependent enzymes. *Biochem. J.* **171**: 771–779.
- Kinnersley, A.M., and Turano, F.J.** (2000). Gamma aminobutyric acid (GABA) and plant responses to stress. *Crit. Rev. Plant Sci.* **19**: 479–509.
- Kobayashi, Y., Hoekenga, O.A., Itoh, H., Nakashima, M., Saito, S., Shaff, J.E., Maron, L.G., Piñeros, M.A., Kochian, L.V., and Koyama, H.** (2007). Characterization of AtALMT1 expression in aluminum-inducible malate release and its role for rhizotoxic stress tolerance in *Arabidopsis*. *Plant Physiol.* **145**: 843–852.
- Kollist, H., Nuhkat, M., and Roelfsema, M.R.G.** (2014). Closing gaps: linking elements that control stomatal movement. *New Phytol.* **203**: 44–62.
- Kovermann, P., Meyer, S., Hörtensteiner, S., Picco, C., Scholz-Starke, J., Ravera, S., Lee, Y., and Martinoia, E.** (2007). The *Arabidopsis* vacuolar malate channel is a member of the ALMT family. *Plant J.* **52**: 1169–1180.
- Lakshmanan, V., Castaneda, R., Rudrappa, T., and Bais, H.P.** (2013). Root transcriptome analysis of *Arabidopsis thaliana* exposed to beneficial *Bacillus subtilis* FB17 rhizobacteria revealed genes for bacterial recruitment and plant defense independent of malate efflux. *Planta* **238**: 657–668.
- Liang, C., Piñeros, M.A., Tian, J., Yao, Z., Sun, L., Liu, J., Shaff, J., Coluccio, A., Kochian, L.V., and Liao, H.** (2013). Low pH, aluminum, and phosphorus coordinately regulate malate exudation through GmALMT1 to improve soybean adaptation to acid soils. *Plant Physiol.* **161**: 1347–1361.
- Ligaba, A., Dreyer, I., Margaryan, A., Schneider, D.J., Kochian, L., and Piñeros, M.** (2013). Functional, structural and phylogenetic analysis of domains underlying the Al sensitivity of the aluminum-activated malate/anion transporter, TaALMT1. *Plant J.* **76**: 766–780.
- Livingston, J.H., Beaumont, D., Arzimanoglou, A., and Aicardi, J.** (1989). Vigabatrin in the treatment of epilepsy in children. *Br. J. Clin. Pharmacol.* **27** (suppl 1): 109S–112S.
- Löscher, W., Hönack, D., and Gramer, M.** (1989). Use of inhibitors of γ-aminobutyric acid (GABA) transaminase for the estimation of GABA turnover in various brain regions of rats: a reevaluation of aminooxyacetic acid. *J. Neurochem.* **53**: 1737–1750.
- Ma, J.F., Ryan, P.R., and Delhaize, E.** (2001). Aluminum tolerance in plants and the complexing role of organic acids. *Trends Plant Sci.* **6**: 273–278.
- Marks, D.S., Hopf, T.A., and Sander, C.** (2012). Protein structure prediction from sequence variation. *Nat. Biotechnol.* **30**: 1072–1080.
- Mekonnen, D.W., Flügge, U.I., and Ludewig, F.** (2016). Gamma-aminobutyric acid depletion affects stomata closure and drought tolerance of *Arabidopsis thaliana*. *Plant Sci.* **245**: 25–34.

- Meyer, A., Eskandari, S., Grallath, S., and Rentsch, D.** (2006). AtGAT1, a high affinity transporter for gamma-aminobutyric acid in *Arabidopsis thaliana*. *J. Biol. Chem.* **281**: 7197–7204.
- Meyer, S., Mumm, P., Imes, D., Endler, A., Weder, B., Al-Rasheid, K.A., Geiger, D., Marten, I., Martinoia, E., and Hedrich, R.** (2010). AtALMT12 represents an R-type anion channel required for stomatal movement in *Arabidopsis* guard cells. *Plant J.* **63**: 1054–1062.
- Meyer, S., Scholz-Starke, J., De Angeli, A., Kovermann, P., Burla, B., Gambale, F., and Martinoia, E.** (2011). Malate transport by the vacuolar AtALMT6 channel in guard cells is subject to multiple regulation. *Plant J.* **67**: 247–257.
- Miller, R., McRae, D., and Joy, K.** (1991). Glutamate and  $\gamma$ -aminobutyrate metabolism. *Mol. Plant Microbe Interact.* **4**: 37–45.
- Motoda, H., Sasaki, T., Kano, Y., Ryan, P.R., Delhaize, E., Matsumoto, H., and Yamamoto, Y.** (2007). The membrane topology of ALMT1, an aluminum-activated malate transport protein in wheat (*Triticum aestivum*). *Plant Signal. Behav.* **2**: 467–472.
- Nanavati, S.M., and Silverman, R.B.** (1991). Mechanisms of inactivation of gamma-aminobutyric acid aminotransferase by the antiepilepsy drug, gamma-vinyl GABA (vigabatrin). *J. Am. Chem. Soc.* **113**: 9341–9349.
- Nugent, T., and Jones, D.T.** (2012). Detecting pore-lining regions in transmembrane protein sequences. *BMC Bioinformatics* **13**: 169.
- Palanivelu, R., Brass, L., Edlund, A.F., and Preuss, D.** (2003). Pollen tube growth and guidance is regulated by POP2, an *Arabidopsis* gene that controls GABA levels. *Cell* **114**: 47–59.
- Palmer, A.J., Baker, A., and Muench, S.P.** (2016). The varied functions of aluminium-activated malate transporters—much more than aluminium resistance. *Biochem. Soc. Trans.* **44**: 856–862.
- Piñeros, M.A., Cañado, G.M., and Kochian, L.V.** (2008). Novel properties of the wheat aluminum tolerance organic acid transporter (TaALMT1) revealed by electrophysiological characterization in *Xenopus* oocytes: functional and structural implications. *Plant Physiol.* **147**: 2131–2146.
- Preuss, C.P., Huang, C.Y., Gilliham, M., and Tyerman, S.D.** (2010). Channel-like characteristics of the low-affinity barley phosphate transporter PHT1;6 when expressed in *Xenopus* oocytes. *Plant Physiol.* **152**: 1431–1441.
- Ramesh, S.A., et al.** (2015). GABA signalling modulates plant growth by directly regulating the activity of plant-specific anion transporters. *Nat. Commun.* **6**: 7879.
- Ramesh, S.A., Tyerman, S.D., Gilliham, M., and Xu, B.** (2017).  $\gamma$ -Aminobutyric acid (GABA) signalling in plants. *Cell. Mol. Life Sci.* **74**: 1577–1603.
- Renault, H., Roussel, V., El Amrani, A., Arzel, M., Renault, D., Bouchereau, A., and Deleu, C.** (2010). The *Arabidopsis* pop2-1 mutant reveals the involvement of GABA transaminase in salt stress tolerance. *BMC Plant Biol.* **10**: 20.
- Reyes-Darias, J.A., García, V., Rico-Jiménez, M., Corral-Lugo, A., Lesouhaitier, O., Juárez-Hernández, D., Yang, Y., Bi, S., Feuilloley, M., Muñoz-Rojas, J., Sourjik, V., and Krell, T.** (2015). Specific gamma-aminobutyrate chemotaxis in pseudomonads with different lifestyle. *Mol. Microbiol.* **97**: 488–501.
- Risso, S., DeFelice, L.J., and Blakely, R.D.** (1996). Sodium-dependent GABA-induced currents in GAT1-transfected HeLa cells. *J. Physiol.* **490**: 691–702.
- Roberts, M.R.** (2007). Does GABA act as a signal in plants?: Hints from molecular studies. *Plant Signal. Behav.* **2**: 408–409.
- Roelfsema, M.R.G., Hedrich, R., and Geiger, D.** (2012). Anion channels: master switches of stress responses. *Trends Plant Sci.* **17**: 221–229.
- Ryan, P.R., Tyerman, S.D., Sasaki, T., Furuichi, T., Yamamoto, Y., Zhang, W.H., and Delhaize, E.** (2011). The identification of aluminium-resistance genes provides opportunities for enhancing crop production on acid soils. *J. Exp. Bot.* **62**: 9–20.
- Sasaki, T., Yamamoto, Y., Ezaki, B., Katsuhara, M., Ahn, S.J., Ryan, P.R., Delhaize, E., and Matsumoto, H.** (2004). A wheat gene encoding an aluminum-activated malate transporter. *Plant J.* **37**: 645–653.
- Schiestl, R.H., and Gietz, R.D.** (1989). High efficiency transformation of intact yeast cells using single stranded nucleic acids as a carrier. *Curr. Genet.* **16**: 339–346.
- Scholz, S.S., Malabarba, J., Reichelt, M., Heyer, M., Ludewig, F., and Mithöfer, A.** (2017). Evidence for GABA-induced systemic GABA accumulation in *Arabidopsis* upon wounding. *Front. Plant Sci.* **8**: 388.
- Sharma, T., Dreyer, I., Kochian, L., and Piñeros, M.A.** (2016). The ALMT family of organic acid transporters in plants and their involvement in detoxification and nutrient security. *Front. Plant Sci.* **7**: 1488.
- Shelp, B.J., and Zarei, A.** (2017). Subcellular compartmentation of 4-aminobutyrate (GABA) metabolism in *Arabidopsis*: An update. *Plant Signal. Behav.* **12**: e1322244.
- Shelp, B.J., Bown, A.W., and McLean, M.D.** (1999). Metabolism and functions of gamma-aminobutyric acid. *Trends Plant Sci.* **4**: 446–452.
- Shelp, B.J., Bozzo, G.G., Zarei, A., Simpson, J.P., Trobacher, C.P., and Allan, W.L.** (2012). Strategies and tools for studying the metabolism and function of  $\gamma$ -aminobutyrate in plants. II. Integrated analysis. *Botany* **90**: 781–793.
- Sigel, E., and Steinmann, M.E.** (2012). Structure, function, and modulation of GABA(A) receptors. *J. Biol. Chem.* **287**: 40224–40231.
- Smith, G.B., and Olsen, R.W.** (1995). Functional domains of GABAA receptors. *Trends Pharmacol. Sci.* **16**: 162–168.
- Snedden, W., and Fromm, H.** (1999). Regulation of the  $\gamma$ -aminobutyrate-synthesizing enzyme, glutamate decarboxylase, by calcium-calmodulin: a mechanism for rapid activation in response to stress. In *Plant Responses to Environmental Stresses: From Phytohormones to Genome Reorganization*, H.R. Lerner, ed (New York: Marcel Dekker), pp. 549–574.
- Snedden, W.A., Chung, I., Pauls, R.H., and Bown, A.W.** (1992). Proton/L-glutamate symport and the regulation of intracellular pH in isolated mesophyll cells. *Plant Physiol.* **99**: 665–671.
- Song, H., Xu, X., Wang, H., Wang, H., and Tao, Y.** (2010). Exogenous gamma-aminobutyric acid alleviates oxidative damage caused by aluminium and proton stresses on barley seedlings. *J. Sci. Food Agric.* **90**: 1410–1416.
- Steward, F.C., Thompson, J.F., and Dent, C.E.** (1949).  $\gamma$ -Aminobutyric acid, a constituent of the potato tuber. *Science* **110**: 439–440.
- Storici, P., De Biase, D., Bossa, F., Bruno, S., Mozzarelli, A., Peneff, C., Silverman, R.B., and Schirmer, T.** (2004). Structures of  $\gamma$ -aminobutyric acid (GABA) aminotransferase, a pyridoxal 5'-phosphate, and [2Fe-2S] cluster-containing enzyme, complexed with  $\gamma$ -ethynyl-GABA and with the antiepilepsy drug vigabatrin. *J. Biol. Chem.* **279**: 363–373.
- Trombley, P.Q.** (1998). Selective modulation of GABAA receptors by aluminum. *J. Neurophysiol.* **80**: 755–761.
- Tsirigos, K.D., Peters, C., Shu, N., Käll, L., and Elofsson, A.** (2015). The TOPCONS web server for consensus prediction of membrane protein topology and signal peptides. *Nucleic Acids Res.* **43**: W401–W407.
- Wallach, D.P.** (1961). Studies on the GABA pathway. I. The inhibition of gamma-aminobutyric acid-alpha-ketoglutaric acid transaminase

- in vitro and in vivo by U-7524 (amino-oxyacetic acid). *Biochem. Pharmacol.* **5**: 323–331.
- Warren, C.** (2015). Wheat roots efflux a diverse array of organic N compounds and are highly proficient at their recapture. *Plant Soil* **397**: 147–162.
- Wood, J.D., and Peesker, S.J.** (1973). The role of GABA metabolism in the convulsant and anticonvulsant actions of aminooxyacetic acid. *J. Neurochem.* **20**: 379–387.
- Yamaguchi, M., Sasaki, T., Sivaguru, M., Yamamoto, Y., Osawa, H., Ahn, S.J., and Matsumoto, H.** (2005). Evidence for the plasma membrane localization of Al-activated malate transporter (ALMT1). *Plant Cell Physiol.* **46**: 812–816.
- Žárský, V.** (2015). Signal transduction: GABA receptor found in plants. *Nat. Plants* **1**: 15115.
- Zhang, G., and Bown, A.W.** (1997). The rapid determination of  $\gamma$ -aminobutyric acid. *Phytochemistry* **44**: 1007–1009.
- Zhang, J., Baetz, U., Krügel, U., Martinoia, E., and De Angeli, A.** (2013). Identification of a probable pore-forming domain in the multimeric vacuolar anion channel AtALMT9. *Plant Physiol.* **163**: 830–843.
- Zhang, W.H., Ryan, P.R., Sasaki, T., Yamamoto, Y., Sullivan, W., and Tyerman, S.D.** (2008). Characterization of the TaALMT1 protein as an Al<sup>3+</sup>-activated anion channel in transformed tobacco (*Nicotiana tabacum* L.) cells. *Plant Cell Physiol.* **49**: 1316–1330.

## 2.2 SUPPLEMENTAL MATERIAL



**Supplemental Figure 1. (A-L) GABA spike and recovery experiments with root tips of 3-day-old wheat seedlings (ET8) and *Xenopus* oocytes (control and TaALMT1 injected) to test the impact of AOA, Al<sup>3+</sup> and vigabatrin treatment on the enzyme assay of GABA. (M) UPLC vs GABase measurements. (Supports Figures 1,2,3,4,5.)**

**(A)** GABA measured in the extract (960  $\mu$ L) of 10 mg of wheat root tips which had been treated in either basal medium or basal medium plus 1 mM AOA for 22 h. The extract was spiked with an additional 19.2 nmol of GABA for basal and AOA-treated roots.

**(B)** GABA recovery in the extract. Horizontal dotted line indicates the spiked amount of GABA (19.2 nmol).

**(C)** Enzyme assay standard curve used for A and B (solid black line) and the effect of AOA added directly to the assay. For direct effect of 1 mM AOA compare dashed black line (without AOA) with red dashed line (+AOA). Note there was variation in total absorbance between different assays (compare dashed black line with solid black line).

**(D)** GABA measured in the extract (960  $\mu$ L) of 10 mg of wheat root tips which had been treated in either basal medium, or basal medium plus 100  $\mu$ M Al<sup>3+</sup> for 22 h. The extract was spiked with an additional 4.8 nmol of GABA for each of the treatments.

**(E)** GABA recovery in the extract. Horizontal dotted line indicates the spiked amount of GABA (4.8 nmol).

**(F)** Enzyme assay standard curve used for D and E.

**(G)** GABA measured in the extract (960  $\mu$ L) of 10 mg of wheat root tips which had been treated in either basal medium plus 10 mM Na<sub>2</sub>SO<sub>4</sub> or basal medium plus 10 mM Na<sub>2</sub>SO<sub>4</sub> and 100  $\mu$ M vigabatrin for 22 h. The extract was spiked with an additional 29 nmol of GABA for each of the treatments.

**(H)** GABA recovery in the extract. Horizontal dotted line indicates the spiked amount of GABA (29 nmol).

**(I)** Enzyme assay standard curve used for G and H.

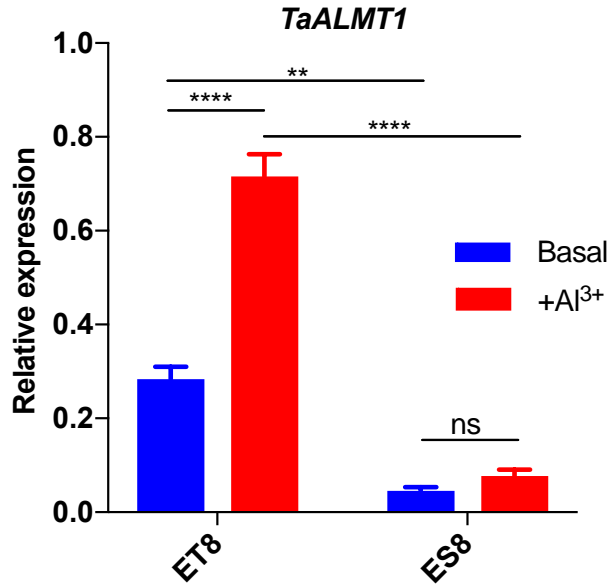
**(J)** GABA measured in the extract (960  $\mu$ L) of 4 oocytes which had been treated in either basal medium or basal medium plus 1 mM AOA for 10 min. Both control (water injected) and TaALMT1 injected oocytes were measured. The extract was spiked with an additional 4.8 nmol of GABA for basal and AOA treated eggs.

**(K)** GABA recovery in the extract. Horizontal dotted line indicates the spiked amount of GABA (4.8 nmol).

**(L)** Enzyme assay standard curve used for J and K.

**(M)** Measurements of GABA concentrations done by GABase enzyme and UPLC are highly similar for wheat root tips from NIL lines ET8 and ES8 treated with 100  $\mu$  Al<sup>3+</sup> pH 4.5 or 1 mM and 100  $\mu$ M AOA pH 4.5 for 22 hours.

**(N)** Measurements of GABA concentrations done by GABase enzyme for wheat root tips comparing ET8 with ES8 treated with 100  $\mu$  Al<sup>3+</sup> pH 4.5 for 22 hours.

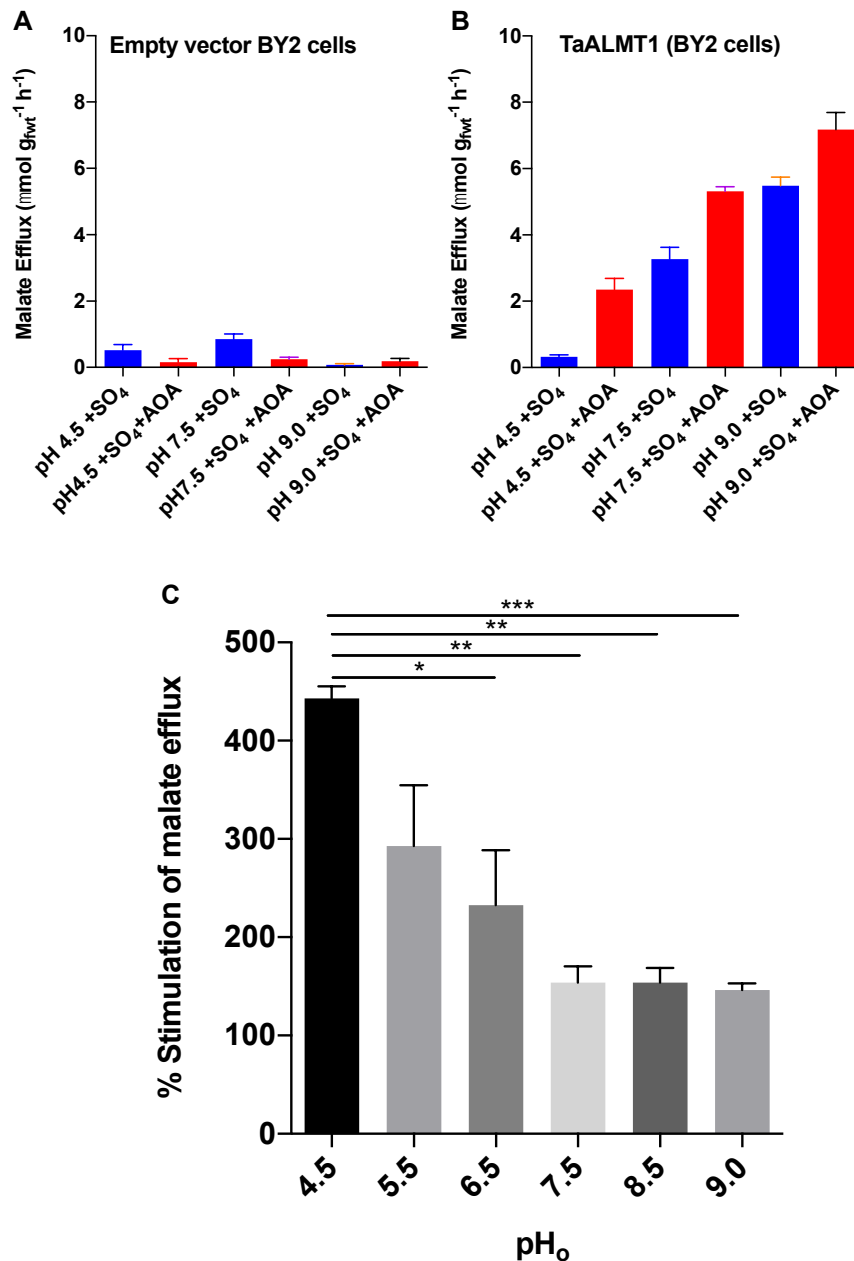


**Supplemental Figure 2. Expression of *TaALMT1* relative to three housekeeping genes (*GAPDH*, *Cyclophilin* and *Actin*) in seedling roots of plants treated with 100  $\mu$ M  $AlCl_3$  pH 4.5 or basal solution for 22 hours. (Supports Figure 1 and confirms previously shown difference between wheat NILs ET8 and ES8.)** Housekeeping genes were not affected by the treatment. Primers used and genbank accession numbers are listed in the Table below. All data n= 3; experiments repeated at least twice; all error bars  $\pm$  SE. \*, \*\*, \*\*\* and \*\*\*\* indicate significant differences between treatments at P< 0.05, 0.01, 0.001 and 0.0001 respectively, using a one-way ANOVA.

**Table Primers used for Supplemental Figure 2**

Gene	Primer (5' – 3')
<i>Cyclophilin_F</i>	CAAGCCGCTGCACTACAAGG
<i>Cyclophilin_R</i>	AGGGGACGGTGCAGATGAA
<i>GAPDH_F</i>	TTCAACATCATTCCAAGCAGCA
<i>GAPDH_R</i>	CGTAACCCAAAATGCCCTTG
<i>Tubb4_F</i>	AGTTCACGGCCATGTTCA
<i>Tubb4_R</i>	ACGAGGTCGTTTCATGTTGCT
<i>Actin_F</i>	TCACACCTTCTACAATGAGCTCCGTGT
<i>Actin_R</i>	ATCCAGACACTGTACTTCCTT
<i>TaALMT1_F</i>	AAATCGCGGAATGTGTTGAT
<i>TaALMT1_R</i>	ATAACCACGTCAGGCAAAGG

Genbank accession numbers for the housekeeping genes and *TaALMT1* listed in Table above are: *Actin* KC775782; *Tubb4* U76895.1; *Cyclophilin* EU035525.1; *GAPDH* EF592180.1; *TaALMT1* DQ072260.1 respectively.



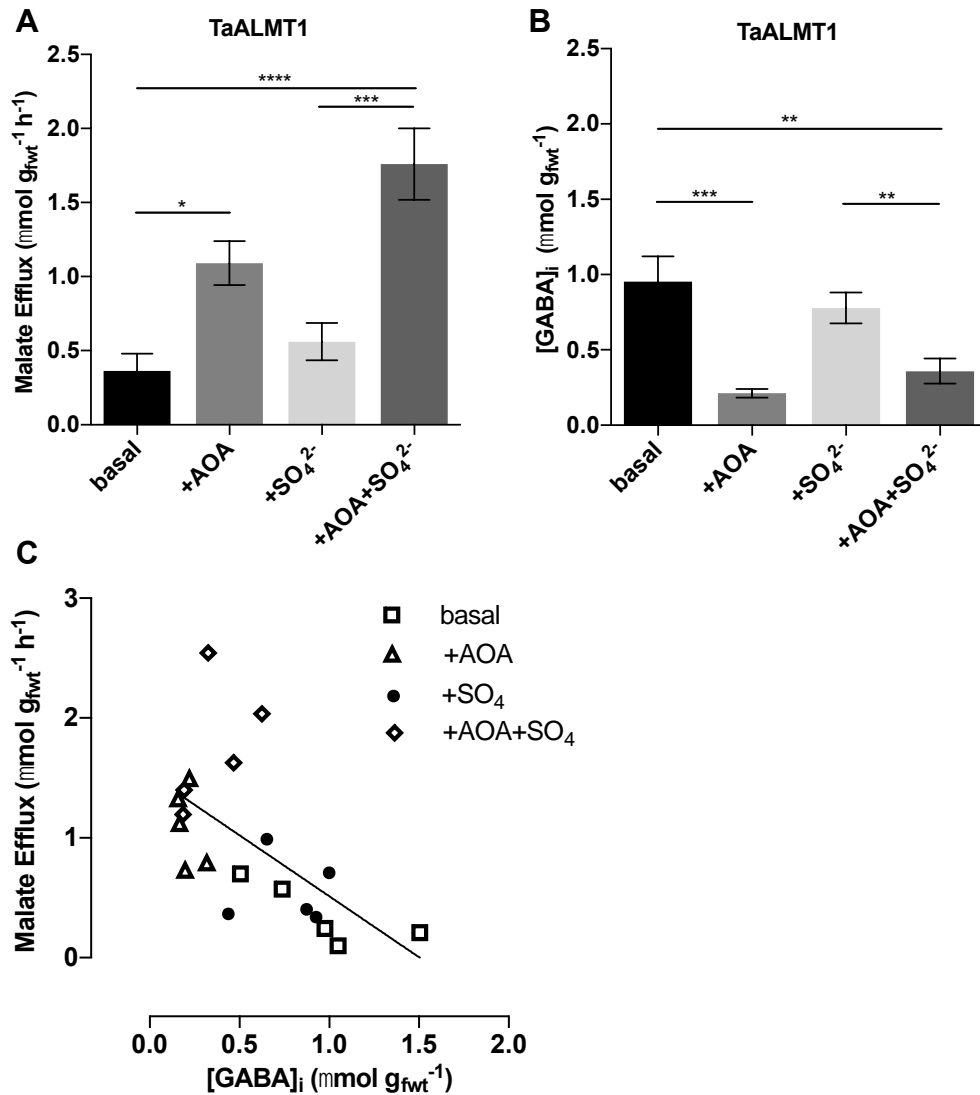
**Supplemental Figure 3. Malate efflux via TaALMT1 expressed in tobacco BY2 cells as a function of external pH and the effect of AOA. (Supports Figure 3.)**

**(A)** Empty vector controls do not show a response and have low malate efflux rates.

**(B)** Increasing pH in the presence of Na<sub>2</sub>SO<sub>4</sub> (10 mM) increases malate efflux measured over 22 h.

**(C)** Stimulation by AOA (1 mM) of malate efflux is highest at pH 4.5. \*, \*\* and \*\*\* indicate significant differences between treatments at P<0.05, 0.01 and 0.001 respectively, using a one-way ANOVA.

All data *n*=5 replicates and error bars are ± SE.



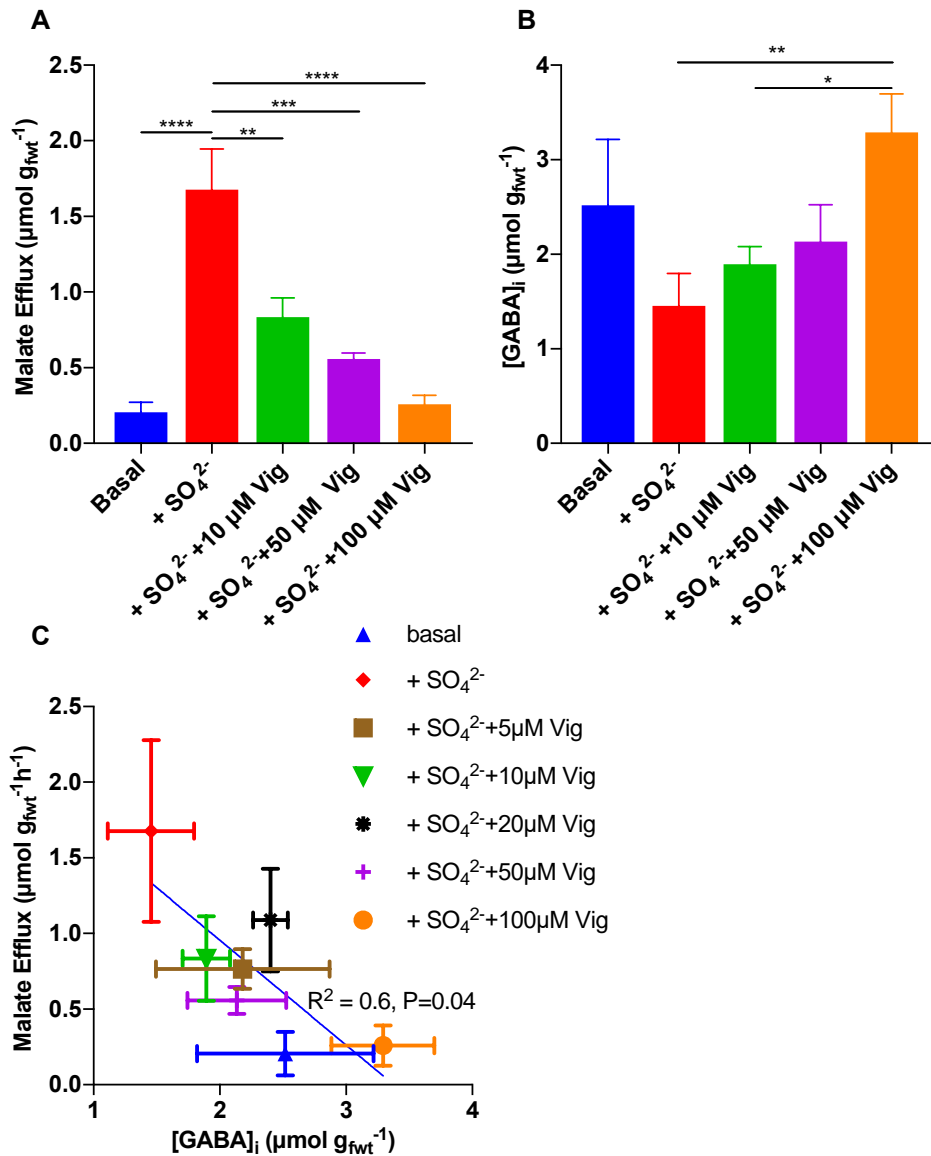
**Supplemental Figure 4. Further evidence of negative linear correlation between malate efflux and cell GABA concentration in tobacco BY2 cells expressing TaALMT1 showing that sulphate does not activate malate efflux at low pH. (Supports Figure 3.)**

(A) Malate efflux over 22 h activated by AOA (1 mM) at pH 4.5 plus and minus 10 mM Na<sub>2</sub>SO<sub>4</sub>. Error bars are ± SE.

(B) [GABA]<sub>i</sub> in the cells at the end of the efflux period. \*, \*\* and \*\*\* indicate significant differences between treatments at P<0.05, 0.01 and 0.001 respectively, using a one-way ANOVA.

Error bars are ± SE.

(C) Negative linear correlation between malate efflux and [GABA]<sub>i</sub>. Linear regression ( $Y = -1.018 \cdot X + 1.531$ ),  $R^2 = 0.35$ ,  $P = 0.006$ .



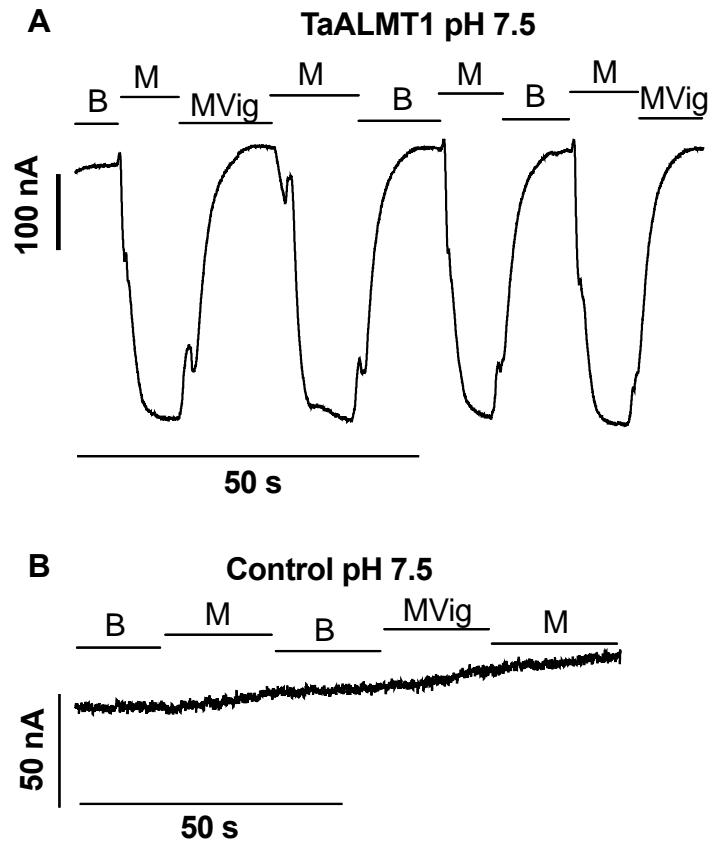
**Supplemental Figure 5. Vigabatrin, an inhibitor of GABA transaminase, inhibits malate efflux activated by 10 mM Na<sub>2</sub>SO<sub>4</sub> while elevating endogenous GABA concentrations in BY2 cells expressing TaALMT1 at pH 7.5. (Supports Figure 3.)**

**(A)** Vigabatrin (10 to 100 µM) effectively inhibits malate efflux pH 7.5 over 22h.

**(B)** Vigabatrin elevates [GABA]<sub>i</sub> in a dose dependent manner.

**(C)** Malate efflux is negatively correlated to final concentration of GABA in cells. Linear regression ( $Y = -0.6936X + 2.343$ ),  $R^2 = 0.60$ ,  $P = 0.04$ . All data  $n=5$  replicates; error bars are SE of the mean; \*, \*\*, \*\*\*, \*\*\*\* indicate significant differences between treatments at  $P < 0.05$ ,  $0.01$ ,  $0.001$ ,  $0.0001$  respectively, using a one-way ANOVA.

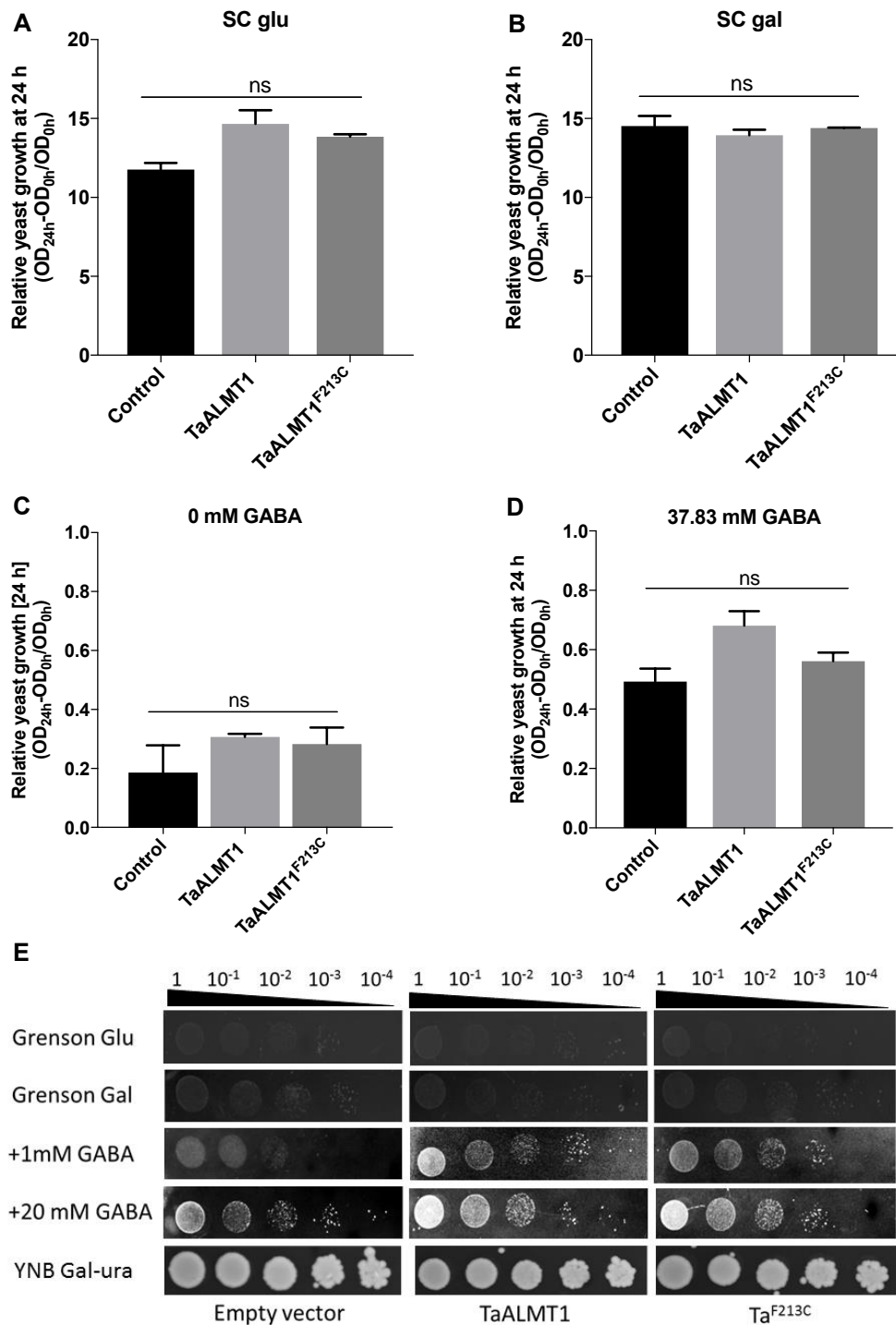




**Supplemental Figure 7. Malate (M) activated inward currents in TaALMT1 expressing *Xenopus laevis* oocytes at pH 7.5 (-80 mV) are also rapidly inhibited by 100  $\mu$ M vigabatrin (Vig). Same conditions as in Figure 5C. (Supports Figure 5.)**

(A) TaALMT1 expressing oocyte voltage clamped at -80 mV.

(B) Water injected (control) oocyte voltage clamped at -80 mV.



**Supplemental Figure 8. Details of complementation of yeast strain 22754d (MAT $\alpha$  ura3-1, gap1-1, put4-1, uga4-1) expressing TaALMT and TaALMT<sup>F213C</sup>. (Supports Figure 7.)** Each were capable of growth on selective drop out medium (SC-ura) supplemented with 2% glucose or galactose as carbon source and ammonium sulphate as nitrogen source (A,B). (C) Growth in nitrogen-free medium and subsequent transfer to medium with no GABA. There were no significant differences in growth. (D) On medium supplemented with 37.83 mM GABA (corresponds to SC medium with ammonium sulphate), each construct showed similar growth. (E) Spot growth assays of yeast at serial dilutions demonstrating enhanced growth of TaALMT1-transformed yeast on nitrogen-free media supplemented with 1 mM GABA compared to empty vector and TaALMT1<sup>F213C</sup>. Top rows are on nitrogen-free media with glucose or galactose as carbon source.

## Supplemental Table 1

### Primers used for cloning and site directed mutagenesis

Primer number	Primer name	Primer Sequence (5' to 3')
1	TaALMT1_pENTR_F	CACCATGGATATTGATCACGGCAGAG
2	TaALMT1_R	TTACAAAATAACCACGTCAGGCAAAGG
3	TaALMT1_Mut_F213C_F	TGCACCACCGTgTgCCTCTTCCCCG
4	TaALMT1_Mut_F213C_R	CGGGGAAGAGGcAcACGGTGGTGCA

The primers 1 and 2 were used to clone TaALMT1 into pENTR D TOPO (ThermoFisher Scientific). This entry vector was used to construct the site directed mutants using Polymerase Chain Reaction. These entry vectors were used to generate the destination vectors (pTOOL37 for tobacco BY2 cells; pDEST52 for *S. cerevisiae*) using the Gateway system.

## Supplemental ANOVA Tables

Sum Sq = Sum of squares; df = degrees of freedom; Mean Sq = Mean Squares

### Figure 1B

	Sum Sq	df	Mean Sq	F-value	P-value
Treatment	2.112	2	1.056	12.99	P=0.0001
Residual	2.196	27	0.08134		
Total	4.308	29			

### Figure 1C

	Sum Sq	df	Mean Sq	F-value	P-value
Treatment	370.5	2	185.3	336.6	P<0.0001
Residual	14.86	27	0.5504		
Total	385.4	29			

### Figure 2A

	Sum Sq	df	Mean Sq	F-value	P-value
Treatment	93.94	6	15.66	36.07	P<0.0001
Residual	14.32	33	0.434		
Total	108.3	39			

### Figure 2B

	Sum Sq	df	Mean Sq	F-value	P-value
Treatment	23.97	5	4.794	15.08	P<0.0001
Residual	11.76	37	0.3179		
Total	35.73	42			

### Figure 2D

	Sum Sq	df	Mean Sq	F-value	P-value
Treatment	7.381	5	1.476	10.67	P<0.0001
Residual	4.706	34	0.1384		
Total	12.09	39			

### Figure 2E

	Sum Sq	df	Mean Sq	F-value	P-value
Treatment	35.7	5	7.141	48.82	P<0.0001
Residual	7.898	54	0.1463		
Total	43.6	59			

### Figure 3A

	Sum Sq	df	Mean Sq	F-value	P-value
Interaction	8.684	4	2.171	2.308	P=0.0767
Treatment	39.39	2	19.7	20.94	P<0.0001
Genotype	40.71	2	20.35	21.64	P<0.0001
Residual	33.85	36	0.9404		

### Figure 3B

	Sum Sq	df	Mean Sq	F-value	P-value
Interaction	3.32	4	0.83	5.639	P=0.0012
Treatment	1.218	2	0.6089	4.137	P=0.0241
Genotype	1.191	2	0.5956	4.047	P=0.0260
Residual	5.299	36	0.1472		

### Figure 3E

	Sum Sq	df	Mean Sq	F-value (	P-value
Interaction	13.65	4	3.412	5.962	P=0.0009
Treatment	10.42	2	5.211	9.105	P=0.0006
Genotype	26.78	2	13.39	23.39	P<0.0001
Residual	20.6	36	0.5723		

### Figure 3F

	Sum Sq	df	Mean Sq	F-value	P-value
Interaction	6.412	4	1.603	8.204	P<0.0001
Treatment	24.54	2	12.27	62.81	P<0.0001
Genotype	14.54	2	7.271	37.21	P<0.0001
Residual	7.034	36	0.1954		

### Figure 4A

	Sum Sq	df	Mean Sq	F-value	P-value
Interaction	2.487	1	2.487	41.85	P<0.0001
Treatment	3.544	1	3.544	59.65	P<0.0001
Genotype	3.168	1	3.168	53.32	P<0.0001
Residual	2.317	39	0.05942		

### Figure 4B

Unpaired t test	
P-value	0.0054
P-value summary	**
Significantly different (P < 0.05)?	Yes
One- or two-tailed P-value?	Two-tailed
t, df	t=3.161 df=18

### Figure 4C

	Sum Sq	df	Mean Sq	F-value	P-value
Interaction	30.08	1	30.08	7.071	P=0.0115
Treatment	23.25	1	23.25	5.467	P=0.0249
Genotype	17.95	1	17.95	4.221	P=0.0470
Residual	157.4	37	4.253		

### Figure 4D

Unpaired t test	
P-value	<0.0001
P-value summary	****
Significantly different (P < 0.05)?	Yes
One- or two-tailed P-value?	Two-tailed
t, df	t=13.48 df=18

### Figure 4E

	Sum Sq	df	Mean Sq	F-value	P-value
Interaction	2.229	1	2.229	19.13	P=0.0005
Treatment	2.995	1	2.995	25.7	P=0.0001
Genoptype	7.543	1	7.543	64.72	P<0.0001
Residual	1.865	16	0.1165		

### Figure 4F

	Sum Sq	df	Mean Sq	F-value	P-value
Interaction	1.524	1	1.524	8.716	P=0.0094
Treatment	1.818	1	1.818	10.4	P=0.0053
Genoptype	2.117	1	2.117	12.11	P=0.0031
Residual	2.798	16	0.1749		

### Figure 4G

	Sum Sq	df	Mean Sq	F-value	P-value
Interaction	28.27	2	14.13	8.028	P=0.0021
Treatment	15.6	1	15.6	8.862	P=0.0066
Genotype	40.56	2	20.28	11.52	P=0.0003
Residual	42.25	24	1.76		

### Figure 5E Left

	Sum Sq	df	Mean Sq	F-value	P-value
Interaction	74.3	1	74.3	2.696	P=0.1350
Treatment	115.1	1	115.1	4.177	P=0.0713
Genotype	761.9	1	761.9	27.65	P=0.0005
Residual	248	9	27.56		

### Figure 5E Right

	Sum Sq	df	Mean Sq	F-value	P-value
Interaction	4.69	1	4.69	134.9	P<0.0001
Treatment	4.815	1	4.815	138.4	P<0.0001
Genotype	5.638	1	5.638	162.1	P<0.0001
Residual	0.4174	12	0.03478		

### Figure 5F Left

	Sum Sq	df	Mean Sq	F-value	P-value
Interaction	1.719	1	1.719	4.997	P=0.0422
Treatment	5.827	1	5.827	16.94	P=0.0010
Genotype	0.005266	1	0.005266	0.01531	P=0.9033
Residual	4.815	14	0.344		

### Figure 5F Right

	Sum Sq	df	Mean Sq	F-value	P-value
Interaction	1.605	1	1.605	443.8	P<0.0001
Treatment	1.66	1	1.66	459.1	P<0.0001
Genotype	1.687	1	1.687	466.6	P<0.0001
Residual	0.05063	14	0.003617		

### Figure 5G

	Sum Sq	df	Mean Sq	F-value	P-value
Interaction	1.718	1	1.718	8.67	P=0.0114
Treatment	5.44	1	5.44	27.46	P=0.0002
Genotype	11.25	1	11.25	56.8	P<0.0001
Residual	2.575	13	0.1981		

### Figure 6A Left

	Sum Sq	df	Mean Sq	F-value	P-value
Treatment	0.002576	2	0.001288	6.58	P=0.0060
Residual	0.004111	21	0.0001957		
Total	0.006686	23			

### Figure 6A Right

	Sum Sq	df	Mean Sq	F-value	P-value
Interaction	0.0005627	2	0.0002814	3.817	P=0.0281
Treatment	0.001999	1	0.001999	27.12	P<0.0001
Genotype	0.001914	2	0.0009571	12.99	P<0.0001
Residual	0.00398	54	0.00007371		

### Figure 6 B Left

	Sum Sq	df	Mean Sq	F-value	P-value
Treatment	0.000007809	2	0.000003904	5.886	P=0.0093
Residual	0.00001393	21	6.634E-07		
Total	0.00002174	23			

### Figure 6B Right

	Sum Sq	df	Mean Sq	F-value	P-value
Interaction	0.000007876	2	0.000003938	1.528	P=0.2273
Treatment	0.00002251	1	0.00002251	8.734	P=0.0048
Genotype	0.00005296	2	0.00002648	10.27	P=0.0002
Residual	0.0001237	48	0.000002577		

### Figure 6C

	Sum Sq	df	Mean Sq	F-value	P-value
Interaction	9473	6	1579	5.734	P<0.0001
Treatment	34238	1	34238	124.3	P<0.0001
Genotype	58033	6	9672	35.13	P<0.0001
Residual	34694	126	275.3		

### Figure 7A Left

	Sum Sq	df	Mean Sq	F-value	P-value
Treatment	0.0009616	2	0.0004808	2.998	P=0.1251
Residual	0.0009623	6	0.0001604		
Total	0.001924	8			

### Figure 7A Right

	Sum Sq	df	Mean Sq	F-value	P-value
Treatment	0.01549	2	0.007746	64.5	P<0.0001
Residual	0.0007206	6	0.0001201		
Total	0.01621	8			

### Figure 7D

	Sum Sq	df	Mean Sq	F-value	P-value
Interaction	0.4505	4	0.1126	6.418	P=0.0022
Genotype	0.1789	2	0.08945	5.097	P=0.0176
Treatment	0.2473	2	0.1236	7.045	P=0.0055
Residual	0.3159	18	0.01755		

## Supplemental Methods

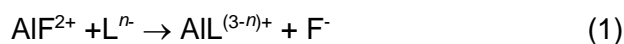
### Test of possible complexation of Al by GABA

#### Summary

A method was developed to determine Al complexation strength of a ligand, by titrating a solution containing Al and F with the ligand of interest and determining the free F<sup>-</sup> concentration. This method was used to determine the extent of Al complexation by GABA and various organic acids at pH 4.5. The order of complexation was: citric > oxalic > malic > salicylic >> GABA. It was found that the complexation of Al by GABA was very weak, with an estimated effective complexation constant of logK 1.4.

#### Principle

The ligand of interest, L, is added to a solution containing Al and F. Depending on the strength of Al complexation with the ligand of interest, F is displaced from the AlF<sup>2+</sup> complex, resulting in higher free F<sup>-</sup> concentration, which can be detected with a fluoride ion selective electrode (ISE).



The higher concentration of the added ligand or the higher the stability of the AlL complex, the more F<sup>-</sup> is liberated from the AlF complex.

Calculations were carried out with Visual Minteq to assess how the free F<sup>-</sup> concentration changes as a function of the concentration of competitive ligand and the stability of the complex (Figure A1). The stability of the complex is expressed by the complexation constant:

$$K_{\text{AIL}} = \frac{(\text{AIL}^{3-n})}{(\text{Al}^{3+})(\text{L}^{n-})}$$

with the round brackets representing activities. Note that these calculations were carried out for a simple ligand that does not undergo any other reactions. In reality, many ligands are organic acids that undergo pH-dependent protonation reactions. Since the metal usually is complexed by the deprotonated ligand, the complexation constant relates to the activity of deprotonated ligand. Hence, meaningful comparisons of metal-ligand binding cannot be done by simply examining the complexation constants. Effective or conditional constants can be derived that take into account the solution conditions (Parker et al, 2005). For instance, in case of organic monoprotic acids (HL) and only 1:1 complexation ( $\text{M}^{n+} + \text{L}^- \rightarrow \text{ML}^{(n-1)}$ ), a comparison in complexation strength can be made by using following effective constant:

$$K_{\text{eff}} = \frac{K_{\text{ML}}}{1 + 10^{\text{pK}_a - \text{pH}}}$$

However, because also other complexes may be formed (e.g. 1:2 complexes) and the metals themselves may undergo hydrolysis reactions, the derivation of effective or conditional

constants quickly becomes complicated. The easiest way in that case to assess complexation strength is through the use of a comprehensive geochemical modelling program (e.g. GEOCHEM or Visual Minteq), provided reliable thermodynamic constants are available.

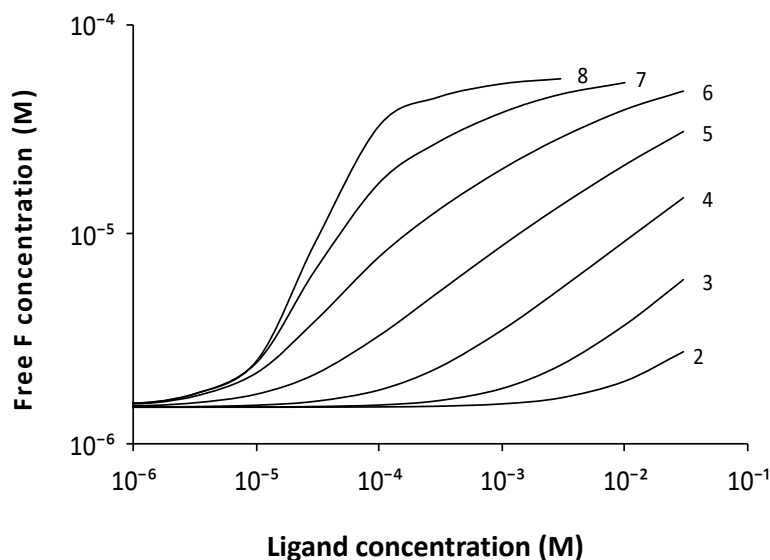


**Figure A1.** Predicted change in free fluoride concentration as a function of the concentration of competitive ligand, in a solution of 10 mM NaCl at pH 4.5 with 60  $\mu$ M Al and 60  $\mu$ M F, for various complexation constants of the AIL complex ( $\log K$  value indicated by the number next to the curve, only 1:1 complexation considered; calculated using the AIF complexation constants of Corbillon et al., 2008).

### Experimental methods

Five organic ligands were used in the measurements: citric acid, oxalic acid, malic acid, salicylic acid and GABA. Stock solutions of 0.05 and 0.005 M were made and adjusted to pH 4.5 using NaOH. A solution containing 10 mM NaCl, 60  $\mu$ M Al (as  $\text{AlCl}_3$ ), 60  $\mu$ M F (as  $\text{Na}_2\text{SiF}_6$ ) and 10 mM MES, adjusted to pH 4.5 was made. Ten ml of this solution was titrated with organic ligand and the free F concentration was determined using a fluoride ISE (Orion 9609BNWP), allowing several minutes between each titration step until the reading stabilized. The ISE was calibrated using solutions with 10 mM NaCl, 10 mM MES (pH 4.5) and F concentrations ranging from 1 to 100  $\mu$ M. All ISE measurements were made in Al-foil covered beakers while stirring the solution. The pH of the solution was checked at the end of each titration run and was always between 4.45 and 4.55.

## Results

Figure A2 shows the change in electrode potential and free F concentration as a function of the added concentration of the organic acid. A faster drop in electrode potential indicates stronger complexation of Al by the organic acid (F displaced from the AlF complex), hence the strength of complexation followed the order: citric > oxalic > malic > salicylic >> GABA. This order agrees with the order found by Hue et al. (1986) in root elongation experiments (with the exception of GABA which was not included in their experiments). We also included a titration run in which both malic acid and GABA were added at a concentration of 60  $\mu\text{M}$  (data not shown), and the results were identical to those for malic acid alone, confirming the low affinity of GABA for Al and indicating there was no interaction effect.

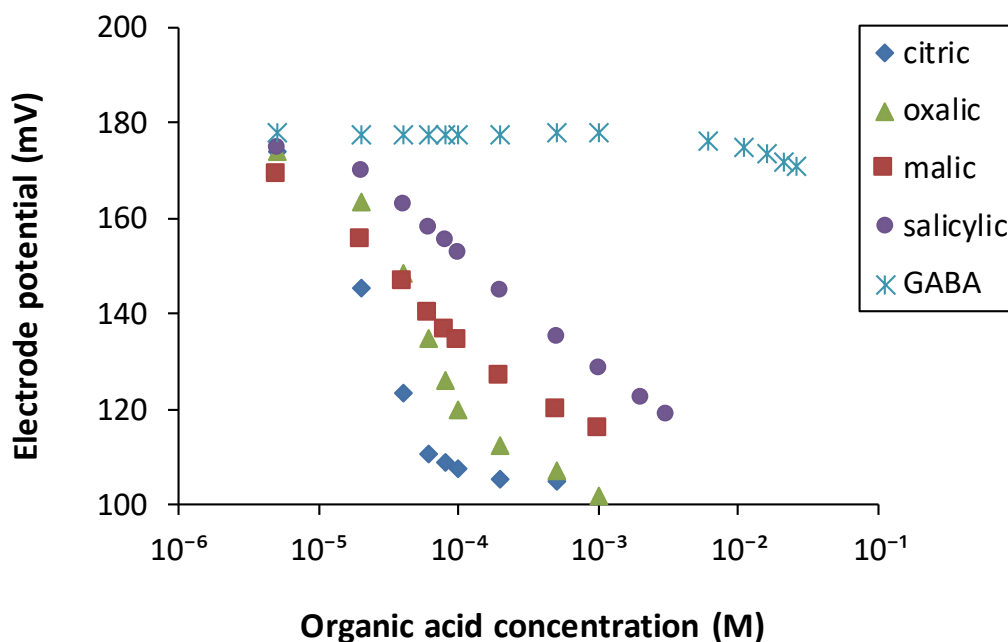


**Figure A2.** Change in electrode potential as a function of the organic acid concentration. (Solution composition: 10 mM NaCl, 10 mM MES, 60  $\mu\text{M}$  Al, 60  $\mu\text{M}$  F, pH 4.5).

From the electrode potential, the free F concentration was determined using the calibration curve (Figure A3). The measured change in free F concentration was compared to the predictions made with Visual Minteq using published complexation constants (Table A1). For GABA, no complexation constants are available in literature; it was found that the complexation agreed with that for a 1:1 complex ( $M + L \rightarrow ML$ ) with  $\log K$  1.4.

The observed and predicted order of the complexation strength of the various acids were in agreement. However, the Al complexation by malate and salicylate was underestimated, suggesting that relevant complexes were not included or that the complexation strength of the considered complexes was underestimated. For salicylate, we excluded the MLOH complexes from the default Minteq database, since the complexation of Al was strongly overestimated when including these complexes and these complexation constants are not included in the GEOCHEM database, casting doubt on their reliability. However, the underestimation of the Al complexation by salicylate suggests that these complexes may have contributed to some extent.

Overall, our results indicate the complexation of Al by GABA is very weak, and GABA-Al complexation is hence not likely to play an important biological role.

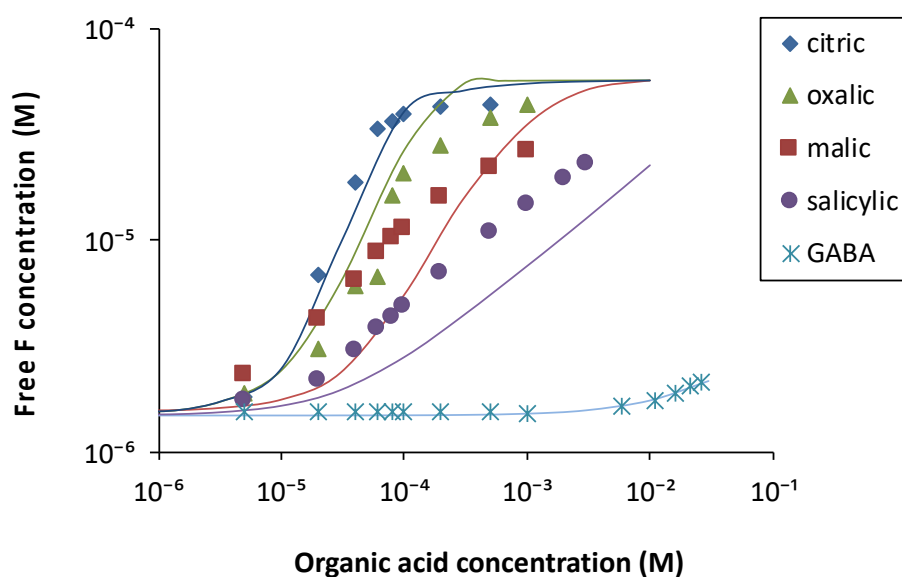


**Figure A3.** Change in free F concentration as a function of the organic acid concentration. The lines show the predicted change using the complexation constants given in Table A1 or for GABA using a  $\log K$  value of 1.4 assuming a simple 1:1 complex formation. (Solution composition: 10 mM NaCl, 10 mM MES, 60  $\mu$ M Al, 60  $\mu$ M F, pH 4.5).

**Table A1.** Relevant Al complexation constants used to calculate the titration results for the various acids in Figure A3. (Note: complexation constants for complexes that had negligible contribution (<0.3%) in the overall Al speciation are not included)

Acid	$\log K$	Complex	Reference
Citrate	9.98	$\text{Al}^{3+} + \text{Citr}^{-3} \rightarrow \text{AlCitr}$	NIST 46.6
	14.83	$\text{Al}^{3+} + 2 \text{Citr}^{-3} \rightarrow \text{AlCitr}_2$	NIST 46.6
	6.4	$\text{Al}^{3+} + \text{Citr}^{-3} - \text{H}^+ \rightarrow \text{AlOHCitr}^-$	Motekaitis and Martell (1984)
Oxalate	7.73	$\text{Al}^{3+} + \text{Oxal}^{-2} \rightarrow \text{AlOxal}^+$	NIST 46.6
	13.41	$\text{Al}^{3+} + 2 \text{Oxal}^{-2} \rightarrow \text{AlOxal}_2^-$	NIST 46.6
	17.09	$\text{Al}^{3+} + 3 \text{Oxal}^{-2} \rightarrow \text{AlOxal}_3^{-3}$	NIST 46.6
	2.57	$\text{Al}^{3+} + \text{Oxal}^{-2} - \text{H}^+ \rightarrow \text{AlOHOxal}$	NIST 46.6
Malate	5.54	$\text{Al}^{3+} + \text{Mal}^{-2} \rightarrow \text{AlMal}^+$	Pellet et al. (1996)
	11.3	$\text{Al}^{3+} + 2 \text{Mal}^{-2} \rightarrow \text{AlMal}_2^-$	Pellet et al. (1996)
Salicylate <sup>a</sup>	14.37	$\text{Al}^{3+} + \text{Sal}^{-2} \rightarrow \text{AlSal}^+$	NIST 46.6
	25.18	$\text{Al}^{3+} + 2 \text{Sal}^{-2} \rightarrow \text{AlSal}_2^-$	NIST 46.6
Fluoride	6.72	$\text{Al}^{3+} + \text{F}^- \rightarrow \text{AlF}^{2+}$	Corbillon et al. (2008)
	12.08	$\text{Al}^{3+} + 2 \text{F}^- \rightarrow \text{AlF}_2^+$	Corbillon et al. (2008)
	16.09	$\text{Al}^{3+} + 3 \text{F}^- \rightarrow \text{AlF}_3^0$	Corbillon et al. (2008)

<sup>a</sup> MLOH complexes omitted from default Visual Minteq database

## References

- Corbillon, M.S., Olazabal, M.A. and Madariaga, J.M., 2008. Potentiometric study of aluminium-fluoride complexation equilibria and definition of the thermodynamic model. *Journal of Solution Chemistry*, 37, 567-579.
- Hue, N.V., Craddock, G.R. and Adams, F., 1986. Effect of organic acids on aluminum toxicity in subsoils. *Soil Science Society of America Journal*, 50, 28-34.
- Motekaitis, R.J. and Martell, A.E., 1984. Complexes of aluminum (III) with hydroxy carboxylic acids. *Inorganic Chemistry*, 23, 18-23.
- Parker DR, Reichman SM, Crowley DE (2005) Metal chelation in the rhizosphere. *In: Wright SF, Zabeab RW (eds) Root and soil management: interactions between roots and the soil. American Society of Agronomy Monograph, Soil Sci Soc Am: Madison, WI, 57–93.*
- Pellet, D.M., Papernik, L.A. and Kochian, L.V., 1996. Multiple aluminum-resistance mechanisms in wheat (roles of root apical phosphate and malate exudation). *Plant Physiology*, 112, 591-597.

### **Chapter 3: RESEARCH ARTICLE**

#### **Role of TaALMT1 malate-GABA transporter in alkaline pH tolerance of wheat.**

*Short title:* TaALMT1 confers high pH tolerance to wheat roots.

*Corresponding author:*

*Name:* Stephen D. Tyerman

*Address:* School of Agriculture, Food and Wine, University of Adelaide, Waite Research Institute, Glen Osmond, SA 5064, Australia

*Telephone:* +61 (0) 83136663

*Email:* steve.tyerman@adelaide.edu.au

*Article title:*

**Role of TaALMT1 malate-GABA transporter in alkaline pH tolerance of wheat.**

*Authors:* Muhammad Kamran<sup>1</sup>, Sunita A. Ramesh<sup>1</sup>, Matthew Gilliam<sup>1</sup> Jayakumar Bose<sup>1</sup> and Stephen D. Tyerman<sup>1\*</sup>

*Authors affiliations:*

<sup>1</sup>Plant Transport and Signalling Lab, ARC Centre of Excellence in Plant Energy Biology and School of Agriculture, Food and Wine, University of Adelaide, Waite Research Institute, Glen Osmond, SA 5064, Australia

# Statement of Authorship

Title of Paper	Role of TaALMT1 malate-GABA transporter in alkaline pH tolerance of wheat.
Publication Status	<input type="checkbox"/> Published <input type="checkbox"/> Accepted for Publication <input checked="" type="checkbox"/> Submitted for Publication <input type="checkbox"/> Unpublished and Unsubmitted work written in manuscript style
Publication Details	Submitted 17 <sup>th</sup> May 2018 to Plant Physiology, manuscript ID MSID#: PP2018-RA-00609

## Principal Author

Name of Principal Author (Candidate)	Muhammad Kamran
Contribution to the Paper	Designed and performed most of the experiments, analysed the data and drafted the article.
Overall percentage (%)	80%
Certification:	This paper reports on original research I conducted during the period of my Higher Degree by Research candidature and is not subject to any obligations or contractual agreements with a third party that would constrain its inclusion in this thesis. I am the primary author of this paper.
Signature	Date 14-06-18

## Co-Author Contributions

By signing the Statement of Authorship, each author certifies that:

- i. the candidate's stated contribution to the publication is accurate (as detailed above);
- ii. permission is granted for the candidate to include the publication in the thesis; and
- iii. the sum of all co-author contributions is equal to 100% less the candidate's stated contribution.

Name of Co-Author	Sunita Ramesh
Contribution to the Paper	Supervised experiments and provided technical assistance. Edited and commented on the manuscript.
Signature	Date 13.06.18

Name of Co-Author	Jay Bose		
Contribution to the Paper	Supervised experiments and provided technical assistance and analysis. Edited and commented on the manuscript.		
Signature		Date	13/06/18

Name of Co-Author	Matthew Gillham		
Contribution to the Paper	Co-conceived the project and research plans. Edited and commented on the manuscript.		
Signature		Date	13/6/2018

Name of Co-Author	Stephen Tyerman		
Contribution to the Paper	Co- conceived the project and research plans. Designed and supervised the experiments and analysed data. Edited and commented on the manuscript.		
Signature		Date	

***One sentence summary:***

The malate and GABA transporter TaALMT1, is activated by high pH to release GABA and malate, which facilitates rhizosphere acidification and tolerance to high pH.

***Footnotes:***

List of author contributions

MG and SDT conceived the project and research plans; SDT, JB and SR supervised the experiments; MK performed most of the experiments; SR and JB provided technical assistance to MK; MK, SDT and JB designed the experiments and analysed the data; MK drafted the article with contributions from all the authors.

Funding

This research was supported by the Australian Research Council Centre of Excellence in Plant Energy Biology (CE140100008)

Corresponding Author Email

steve.tyerman@adelaide.edu.au

## 2.1 ABSTRACT

Little is known about the mechanisms of plant alkaline soil tolerance. Malate exudation through Aluminum-activated Malate Transporter 1 (TaALMT1) confers  $\text{Al}^{3+}$  tolerance upon *Triticum aestivum* L (wheat) at low pH, but TaALMT1 is also activated by external anions at alkaline pH and is regulated by, and shows significant transport of gamma-aminobutyric acid (GABA, a zwitterionic buffer). Therefore TaALMT1 may facilitate acidification of an alkaline rhizosphere by exuding both malate and GABA. We compared wheat NILs, ET8 ( $\text{Al}^{3+}$ -tolerant, high *TaALMT1* expression) and ES8 ( $\text{Al}^{3+}$ -sensitive, low *TaALMT1* expression). Comparing pH 6 and pH 9 nutrient solutions, root growth (5-weeks) was higher for ET8 than ES8. Shoot gas exchange also differed between NILs. Continuous GABA application to roots interfered with growth and shoot gas exchange but did not inhibit malate exudation at high pH. Root apices and whole seedling roots with high *TaALMT1* expression exuded more malate and GABA at high pH and rhizosphere acidification was more rapid in ET8 than ES8. *Xenopus laevis* oocytes expressing *TaALMT1* also acidified an alkaline media more rapidly than controls corresponding to higher GABA efflux. *TaALMT1* expression did not change under alkaline conditions but key genes involved in GABA turnover changed in accord with a high rate of GABA synthesis in ET8. We conclude that TaALMT1 plays a role in alkaline soil tolerance by exuding malate and GABA, possibly coupled to proton efflux, facilitating rhizosphere acidification.

### 3.2 INTRODUCTION

Soil alkalinity is a major environmental factor limiting agricultural production throughout the world by affecting crop growth through poor soil structure, ion toxicities and nutrient (e.g. iron, phosphorus) deficiencies (Wong et al., 2008). About 434 million ha of cultivable land in the world is affected by soil alkalinity (Jin et al., 2006; Xu et al., 2013). Soil alkalisation has increasingly become an important problem for some crops in Australia with about 30% of Australian soils classified as sodic and 86% of these classified as alkaline (Rengasamy and Olsson, 1991). Improving alkaline tolerance of plants through molecular breeding is an attractive option to maintain crop productivity on alkaline soils and to achieve this goal, alkaline tolerance mechanisms as well as their respective genes in plants must be identified. In this respect, previous research has focused on the ability of plants to acidify the rhizosphere through enhanced activity of plasma membrane localised H<sup>+</sup>-ATPase (Fuglsang et al., 2007; Yang et al., 2010; Xu et al., 2012; Xu et al., 2013; Li et al., 2015), linked to auxin regulation in roots (Yu et al., 2017), as well as the ability to reduce excess ROS under alkali stress in rice (Guo et al., 2014; Zhang et al., 2017) and wheat (Meng et al., 2017). The presence of other tolerance mechanisms has not been fully explored and addressing this knowledge gap is the main objective of this study.

Plant roots exude organic compounds to keep the rhizosphere environment favourable for plant growth and development. In acid soils (pH < 4.5), Al<sup>3+</sup> toxicity reduces root growth, and to alleviate Al<sup>3+</sup> toxicity several plant species exude organic anions (OA, e.g. malate and citrate) from root apices (Ryan et al., 2011). These OA chelate Al<sup>3+</sup> in the rhizosphere (and/or the apoplast), resulting in the formation of non-toxic Al complexes that prevent phytotoxic Al<sup>3+</sup> entering the root (Ma et al., 2001; Ryan et al., 2001; Kochian et al., 2004). This mechanism, first demonstrated in the root tips of Al<sup>3+</sup>-tolerant varieties of wheat (Delhaize and Ryan, 1995; Ryan et al., 1995; Ryan et al., 1997), became the basis for the identification and characterization of the first member of the Aluminium-activated Malate Transporter (ALMT) family, TaALMT1 (Sasaki et al., 2004). Transgenic barley overexpressing *TaALMT1* enhanced Al<sup>3+</sup> tolerance in acid soils by exuding malate (Delhaize et al., 2004). The expression of *TaALMT1* in barley was also shown to improve phosphate nutrition on acid soils and not to impose a yield penalty or difference in shoot biomass in the absence of Al<sup>3+</sup> (Delhaize et al., 2009). Interestingly, bread wheat genotypes with the *ALMT1* allele have been shown to have a slight but significant yield advantage in alkaline soils which may also be associated with boron tolerance (McDonald et al., 2013). Also the presence of the Al<sup>3+</sup> tolerance allele *ALMT1* in wheat was shown to be advantageous in alkaline soils with low rainfall across southern Australia, and suggested to be linked to tolerance to the aluminate anion or through the efflux of malate to aid the uptake of

other nutrients at high pH (Eagles et al., 2014). Calcicoles (plants well adapted to grow in alkaline soils) also release several-fold higher organic acids in alkaline soils than in acid soils (Lee, 1999; Lopez-Bucio et al., 2000).

Recently two near isogenic lines (NILs) of wheat that have different expression and alleles for *TaALMT1* (ET8 Al<sup>3+</sup> tolerant and ES8 Al<sup>3+</sup> sensitive) were compared for tolerance to alkaline soils and alkaline hydroponic solutions (Silva et al., 2018). The ET8 NIL has the Type V allele of *TaALMT1* (TaALMT1-V) associated with high expression of *TaALMT1* in root apices and greater malate and GABA efflux, while ES8 NIL possesses the Type I allele of *TaALMT1* (TaALMT1-I) associated with low expression of *TaALMT1* and low malate and GABA efflux (Ryan et al., 1995; Sasaki et al., 2004; Raman et al., 2005; Ryan et al., 2010; Ramesh et al., 2018; Silva et al., 2018). These two NILs have been extensively compared in respect of malate efflux and the channels accounting for this efflux (Ryan et al., 1997; Zhang et al., 2001) as well as the newly discovered role of *TaALMT1* as a GABA transporter (Ramesh et al., 2018). Silva et al. (2018) found no consistent tolerance for alkaline conditions of ET8 over ES8. However further investigation is warranted in the light of the recent discovery that *TaALMT1* and other ALMTs are efficient GABA transporters and that external anion activation at pH 7.5 results in large GABA efflux via *TaALMT1* (Ramesh et al., 2018).

Alkaline pH in the absence of Al<sup>3+</sup> stimulated malate efflux through *TaALMT1* expressed in tobacco BY2 cells, reaching a maximum above pH 8 (Ramesh et al., 2015). A similar response was observed in *Xenopus laevis* oocytes for the ionic current attributed to malate efflux (*ibid*). Malate efflux through *TaALMT1* and other ALMTs was also found to be inhibited by micromolar concentrations of external gamma-aminobutyric acid (GABA) and its analogue muscimol, although in intact roots higher concentrations of GABA in the millimolar range were required for inhibition (Ramesh et al., 2015). Comparing the ET8 and ES8 NILs it was found that ET8 seedlings exuded more malate at pH 9 and that root growth of 3-4 day old seedlings was higher in ET8 than ES8 at pH 9 (Ramesh et al., 2015). Furthermore both root growth and malate exudation was inhibited by muscimol in ET8 at high pH to that of ES8 levels implicating *TaALMT1* in the response.

The findings above lead to the following hypotheses regarding the possible role of *TaALMT1* in alkaline pH tolerance: 1) Higher expression of *TaALMT1* imparts an advantage for plant growth under alkaline conditions. 2) *TaALMT1* malate-GABA transporter enables acidification of the rhizosphere at alkaline pH. To test these hypotheses we have performed experiments using the ET8 and ES8 wheat NILs as well as *Xenopus laevis* oocytes expressing *TaALMT1*. The following specific questions were addressed to test the two hypotheses: 1) Can

the difference in root growth and malate efflux at pH 9 observed between ET8 and ES8 in young seedlings (Ramesh et al., 2015) be observed in older plants grown at high pH, and is this reflected also in shoot characteristics, notwithstanding the negative results observed by Silva et al., (2018) on younger plants? 2) Is there increased exudation of malate and GABA at high alkaline pH in wheat associated with the expression of *TaALMT1*? 3) Are there higher order effects on plant growth through modified leaf gas exchange given that GABA is transported by TaALMT1, and that GABA has been linked to stomatal regulation under drought stress (Mekonnen et al., 2016). 4) Does expression of *TaALMT1* and genes associated with GABA metabolism in root apices change in response to growth at high pH? 5) What is the role of GABA and malate exudation via TaALMT1 in alkaline pH tolerance? Our findings indicate that under alkaline pH, TaALMT1 mediates efflux of malate and GABA and possibly protons to acidify the rhizosphere pH. By doing so TaALMT1 is able to improve overall alkaline pH tolerance in wheat.

### 3.3 RESULTS

#### **Comparisons of growth and shoot gas exchange between ET8 and ES8 wheat NILs at acid and alkaline pH and the interaction with applied GABA**

To examine the effect of rhizosphere pH on growth characteristics and shoot gas exchange of wheat NILs (ET8 and ES8), plants were grown in washed sand with nutrient solution pH set at 6 and 9 over 5 weeks. A subset of these plants were also treated with 10 mM GABA at each pH. We used 10 mM GABA since Ramesh et al (2015) had shown that this concentration could inhibit root growth and malate efflux in ET8 to phenocopy ES8 in the presence of  $Al^{3+}$  at pH 4.5. After 5 weeks growth significant differences were observed in shoot and root growth characteristics between the genotypes at each pH (Fig. 1A,B). Comparing shoot fresh mass of genotypes at the same pH showed a significantly higher mass for ES8 at pH 6 and pH 9 (Fig. 1A) while there was a significantly higher root mass for ET8 at pH 9 (Fig. 1B). For both genotypes, GABA treatment significantly decreased shoot and root biomass to between 30-60% of controls at the same pH, but with no differences between ET8 and ES8 at each pH (Supplemental Fig. S1A,B). There was a tendency for ET8 to show greater differences between pHs with GABA treatment (Supplemental Fig. S1B) relative to that without GABA treatment (Fig. 1B). Analysis of root morphology showed a significantly higher root length and root surface area for ET8 at pH 9.0 compared to ES8 (Fig. 1C,D). GABA treatment reduced both root length and root surface area for both genotypes and for each pH. There were no significant differences between genotypes when treated with GABA (Supplemental Fig. S1C,D). Fig. 1E shows root images illustrating the typical differences between genotypes at each pH.

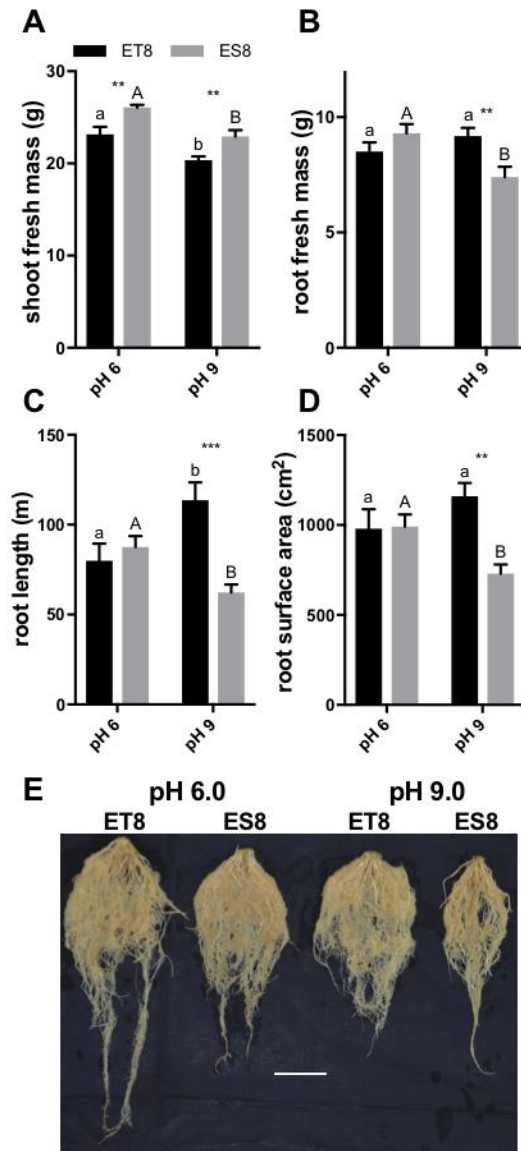


**Figure 1.** Effect of nutrient solution pH on root and shoot growth of ET8 and ES8 wheat plants. Near-isogenic wheat lines ET8 ( $Al^{3+}$  tolerant, black bars) and ES8 ( $Al^{3+}$  sensitive, grey bars) were grown in pots for 5 weeks (see methods). Nutrient solution at pH 6 and pH 9 were applied to each pot 3-4 times a week. A, Shoot fresh mass (n=10), B, Root fresh mass (n=10), C, Root length (n=5), D, Root surface area (n=5). E, Examples of root systems harvested at 5 weeks growth for both genotypes at each pH (scale bar = 5 cm). \*\* and \*\*\* indicate significant difference between genotypes at a given pH where  $P < 0.01$  and  $0.001$  respectively. Different letter combination for a genotype indicate significant difference ( $P < 0.05$ ) between pHs (lower case = ET8, upper case = ES8) using two-way ANOVA and post-tests.

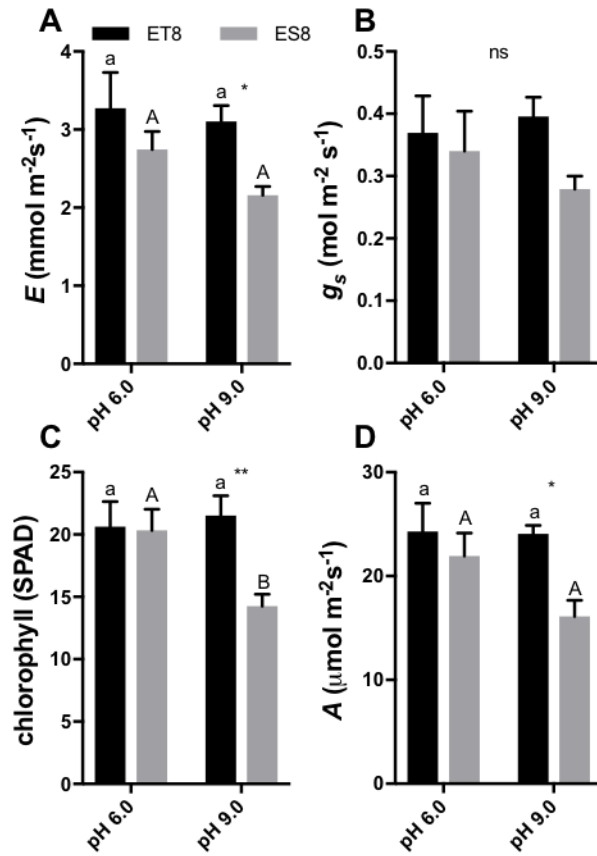


**Figure 2.** Effect of nutrient solution pH on leaf gas exchange of ET8 and ES8 plants. A, Transpiration rate ( $E$ ) (n=5), B, Stomatal conductance ( $g_s$ ) (n=5), C, Relative chlorophyll concentration measured using SPAD (n=10), D, Net assimilation rate ( $A$ ) (n=5). All parameters were measured after 5 weeks. \* and \*\* indicates significant difference between genotypes at a particular pH,  $P < 0.05$  and  $P < 0.01$  respectively. Different letter combination for a genotype indicate significant difference ( $P < 0.05$ ) between pHs (lower case = ET8, upper case = ES8) using two-way ANOVA and post-tests. ns = no significant differences.

Transpiration rate ( $E$ ), stomatal conductance ( $g_s$ ), chlorophyll content (SPAD values), and net assimilation rate ( $A$ ) after 5 weeks of treatments are shown in Fig. 2. There were no significant differences between genotypes and pH for  $g_s$  (Fig. 2B), but  $E$  was significantly higher in ET8 than ES8 at pH 9. Relative chlorophyll concentration was significantly reduced in ES8 leaves at pH 9 compared to ET8 (Fig. 2C). Net assimilation was significantly reduced in ES8 compared to ET8 at pH 9 (Fig. 2D). GABA treatment significantly reduced leaf chlorophyll concentration for both genotypes to between 40 and 60% of controls independent of pH (Supplemental Fig. S2C), while  $A$  was unaffected in both genotypes (Supplemental Fig. S2D). Both  $E$  and  $g_s$  showed interesting responses to GABA treatment; with stimulation by up to 50% at pH 6 and pH 9 (Supplemental Fig. S2A,B), but with no differences between genotypes.

### **Estimates of rhizosphere malate and GABA concentrations for ET8 and ES8 wheat NILs.**

Pots with rooted plants used in the experiments described above were flushed with a constant volume of treatment solution and allowed to drain to capture a root-wash eluate. GABA and malate concentrations of the eluate were measured and an estimate was made of the rhizosphere malate and GABA concentrations on a root fresh mass basis (Fig. 3). Rhizosphere malate concentration was significantly higher from ET8 compared to ES8 at pH 9 (Fig. 3A). GABA treatment tended to enhance malate concentration but with no significant difference between genotypes and pH (Fig. 3B).

Rhizosphere GABA estimations were also made for the non-GABA treated plants (Fig. 3C). Rhizosphere GABA was higher from ET8 roots than for ES8 roots at pH 9 but not significantly different at pH 6.

### **Efflux of malate and GABA from root apices and intact seedling roots at high pH**

To elaborate on the results shown in Figure 3 we measured the efflux of malate and GABA from excised root apices from 3-day old seedling roots of ET8 and ES8 exposed to solutions at pH 6 and pH 9 (Fig. 4). This was performed over a short a time as possible (1h) (see Fig. 6). Malate efflux was significantly higher for ET8 root tips at pH 9 in both unbuffered and buffered media and there was a significant elevation in malate efflux comparing pH 6 and pH 9 for ET8 (Fig. 4A). There was no significant effect of pH on malate efflux from ES8 apices. There was also a large increase in GABA efflux from ET8 apices at pH 9 compared to pH 6

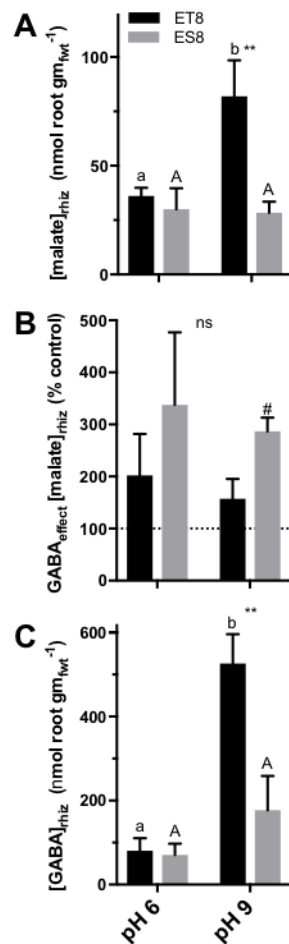


**Figure 3.** Estimates of rhizosphere malate and GABA for ET8 and ES8 plants in response to nutrient solution pH and the effect of 10 mM GABA on malate concentration. A, Malate concentration. B, Effect of 10 mM GABA on the estimated rhizosphere malate concentration (% of the control without GABA). C, GABA concentration. Root washes were measured for plants *in situ* after five weeks of growth. For (A) and (C) values are normalised to the root fresh mass of each replicate plant. In each case different letter combination for a genotype indicates significant difference ( $P < 0.05$ ) between pHs (lower case = ET8, upper case = ES8) and \*\* indicates significant difference between genotypes at a given pH  $P < 0.01$  (two-way ANOVA with post-tests). ns = no significant differences. # = significantly different from 100% (one-tailed t-test). All  $n=5$ .

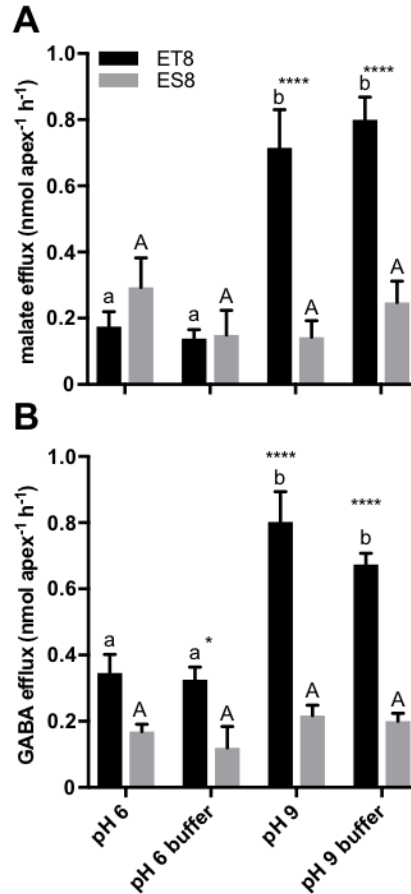


**Figure 4.** Root apex exudation of malate (A) and GABA (B) at pH 6 and 9 (+/- buffer) comparing wheat ET8 and ES8. Net flux was measured over 1 h after placing excised root apices (5 mm) in different pH +/- buffer (all 3 mM CaCl<sub>2</sub>, 10 mM Na<sub>2</sub>SO<sub>4</sub>): pH 6, 0.01 mM NaOH; pH 6 buffer, 5 mM MES, 2.6 mM NaOH; pH 9: 0.05 mM NaOH, pH 9 + buffer, 5 mM BTP, 2 mM MES. In each case different letter combination for a genotype indicates significant difference ( $P < 0.05$ ) between pHs (lower case = ET8, upper case = ES8) and \*, \*\*\*\* indicate significant difference between genotypes at a given pH  $P < 0.05$ , 0.0001 respectively (two-way ANOVA and post-tests),  $n=5$ .

(with or without buffer) that was significantly higher in ET8 compared to ES8 (Fig. 4B). There was no significant effect of pH on GABA efflux from ES8 apices.

A comparison was made for ET8 and ES8 between short term malate efflux (1 h) from root apices (Fig. 5A) and longer term (21 h) efflux (Fig. 5B) from intact 3-day old seedlings. In this experiment the response to  $\text{Al}^{3+}$  at low pH was added as a positive control, since this has been previously shown for apices and intact seedlings of ET8, ES8 (Ryan et al., 1995; Ramesh et al., 2018; Silva et al., 2018). For root apices the results confirmed those in Fig. 4A, but also showed that the increased malate efflux from ET8 apices at high pH over the short term was similar to that triggered by  $\text{Al}^{3+}$  at low pH, and at high pH, the response of ET8 apices was independent of buffer or the presence of  $\text{Na}_2\text{SO}_4$  (Fig. 5A). There was no significant difference between treatments for ES8. For longer term (21h) efflux of malate from intact seedling roots (Fig. 5B) the situation changed dramatically, in that the presence of buffer and  $\text{Na}_2\text{SO}_4$  made a large difference to the response. Only with buffer present was there a significant increase in net malate efflux from ET8 roots at high pH and this was also lower than that observed for  $\text{Al}^{3+}$  activation.

### **Kinetics of changes in solution pH and the release of malate and GABA from ET8 and ES8 seedling roots at high pH.**

To test the hypothesis that release of malate and/or GABA at high pH may be associated with a reduction in external pH, we treated the wheat ET8 and ES8 NILs with a slightly (carbonate) buffered alkaline pH and monitored changes in external concentrations of malate and GABA as well as the external pH (Fig. 6). Solution concentrations of malate and GABA were normalised to the root fresh mass. Two independent experiments are shown in Fig. 6, which although showing some large quantitative differences, also show qualitative similarities. The external malate concentration arising from ET8 seedling roots was initially (at 2-3h) higher compared to that for ES8 and then remained either stable with time (Fig. 6A) or decreased (Fig. 6B). Note that where there was a decrease in external malate, this indicates that malate was first released then taken up from the solution. In both experiments the external malate concentration converged to similar values for ET8 and ES8 seedlings after 22 hours. Over this time the solution pH reduced from about 9.2-9.3 to 7.5 with ET8 showing significantly greater acidification than ES8 (Fig. 6E,F). Control aerated solutions of the same volume and in the same conditions but without plants showed a much smaller drop in external pH. The initial and final malate concentrations in the solution are also shown on the right side of each graph in Fig. 6A,B and settled at between 5-8  $\mu\text{M}$  with no differences between genotypes.

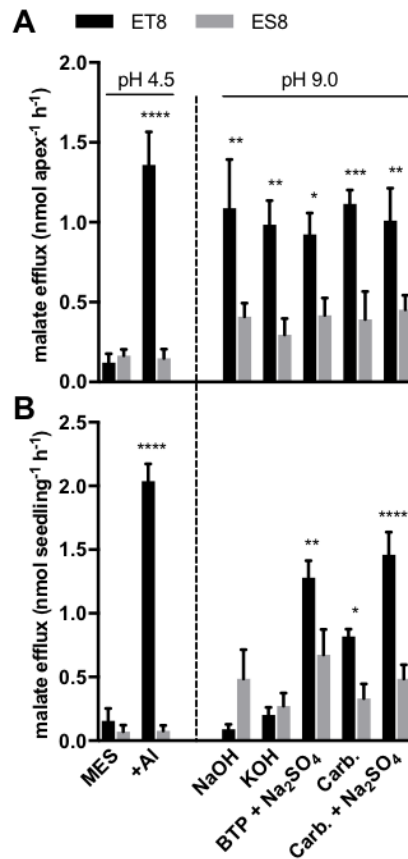


**Figure 5.** Exudation of malate comparing low pH and effect of Al<sup>3+</sup>, and high pH with +/- buffer for excised root apices and intact seedling roots measured over different time scales. A, Net flux from excised root apices measured over 1 h after placing apices in the respective pH solution (n=8). B, Net flux measured over 21 h from intact seedlings roots in the respective pH solution (n=5). Solutions (all 3 mM CaCl<sub>2</sub>) from left to right were: pH 4.5, 5 mM MES; pH 4.5, 5 mM MES, 0.1 mM AlCl<sub>3</sub>; pH 9, 0.12 mM NaOH; pH 9, 0.2 mM, KOH; pH 9, 20 mM BTP, 10 mM Na<sub>2</sub>SO<sub>4</sub>, 9 mM MES; pH 9, 18 mM NaHCO<sub>3</sub>, 2 mM Na<sub>2</sub>CO<sub>3</sub>; pH 9, 18 mM NaHCO<sub>3</sub>, 2 mM Na<sub>2</sub>CO<sub>3</sub>, 10 mM Na<sub>2</sub>SO<sub>4</sub>. \*, \*\*, \*\*\*, \*\*\*\* indicate significant difference between genotypes at a given pH  $P < 0.05, 0.01, 0.001, 0.0001$ , respectively (two-way ANOVA and post-tests).

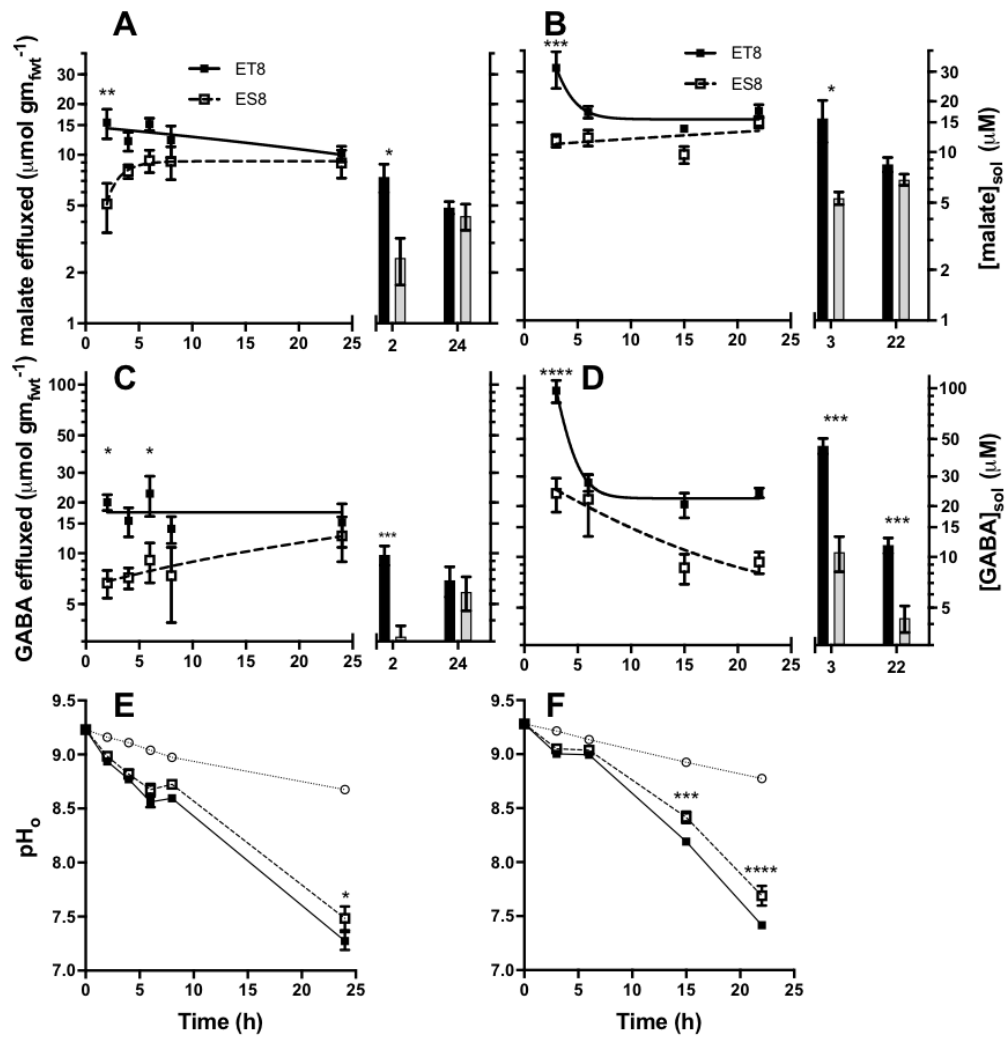


**Figure 6.** Kinetics of malate and GABA release from roots and change in external pH for ET8 and ES8 seedlings in hydroponic solution during the first 24 hours of alkaline pH treatment. Four days old seedlings were bathed in aerated basal nutrient solution (pH 6) for 3 days then transferred to aerated nutrient solution (200 ml) initially at pH 9.2-9.3 for 24 hours. Two independent experiments are shown. A, B, Time course of malate concentration in solution normalised to root fresh mass (left) and initial and final solution concentrations (right). C, D, Time course of GABA concentration in solution normalised to root fresh mass (left) and initial and final solution concentrations (right). Concentrations are given on a log scale to compare across experiments due to large differences. E, F, pH measured in the external medium. Open circles (dotted line) shows the change in pH for aerated solution without plants over the same time. For (A), (B), (C), (D) Fitted lines were significantly different (Extra Sum of Squares F-Test). \*, \*\*, \*\*\*, and \*\*\*\* indicate significant difference between genotypes at a given time point  $P < 0.05$ , 0.01, 0.001 and 0.0001 (2-way repeated measures ANOVA with post-test). All data  $n=5$  biological replicates consisting of approximately 7-8 seedlings per replicate 0.36-0.55  $\text{g}_{\text{fw}}$  of roots.

External GABA concentration was also initially much higher from ET8 than ES8 roots and converged to similar values in one of the experiments (Fig. 6C) but differed at 22 hours in the other experiment (Fig. 6D). Final solution concentrations of GABA ranged between 5 and 12  $\mu\text{M}$ . There were larger GABA and malate concentrations initially recorded for the second experiment (right side of Fig. 6) (note log scale to compare experiments), corresponding to a slightly higher initial pH, though final malate and GABA concentrations were similar.

### **Rhizosphere acidification by root apices of intact ET8 and ES8 seedlings.**

In order to examine more closely the greater capacity of ET8 roots to acidify alkaline solutions we used the micro-electrode ion flux estimation (MIFE) technique to compare ET8 and ES8 wheat NILs (Fig. 7). The external pH and apparent proton flux were examined near the root apex since *TaALMT1* is mainly expressed in root apices of ET8 correlating with the high malate and GABA release in response to high pH (Fig. 4). Also it was previously shown that TaALMT1 was activated by anions at alkaline pH (Ramesh et al 2015), therefore we applied  $\text{SO}_4^{2-}$  (as 10 mM  $\text{Na}_2\text{SO}_4$ ) in the external solution 5 minutes after the alkaline solution was applied. Fig. 7A shows the external pH near the root apex over time after the roots were bathed in alkaline solution. ET8 was able to acidify the immediate rhizosphere (50  $\mu\text{m}$  from the root surface) to a greater extent than ES8 settling to an external pH that was 0.2 units lower than that for ES8. However, both genotypes showed a greater rate of acidification in response to  $\text{Na}_2\text{SO}_4$ . The greater degree of acidification by ET8 apices correlated with a larger apparent  $\text{H}^+$  efflux (larger negative flux) that was sustained over time (Fig. 7B). The apparent  $\text{H}^+$  effluxed is shown in Fig. 7C calculated from the integration of the  $\text{H}^+$  flux.

### **GABA release and acidification at high pH associated with the expression of *TaALMT1* in *Xenopus laevis* oocytes.**

To confirm that TaALMT1 actually released GABA at high pH and that this may be associated with medium acidification we heterologously expressed *TaALMT1* in *Xenopus laevis* oocytes then exposed the oocytes to alkaline pH with  $\text{Na}_2\text{SO}_4$  (Fig. 8). The *TaALMT1* cRNA-injected oocytes were compared to water injected controls. The changes in external pH and  $\text{H}^+$  fluxes were monitored using MIFE (Fig. 8A,B,C), while GABA efflux over a similar time frame (10 minutes) was estimated by measuring GABA in the oocyte and in the external solution for separate batches of oocytes (Fig. 8D). These oocytes were not malate injected therefore we did not measure malate efflux. *TaALMT1* injected oocytes acidified the external medium much faster than the water injected controls (Fig. 8A). Interestingly, the *TaALMT1* injected oocytes

took only 3 minutes to reduce the external pH (100  $\mu\text{m}$  from the oocytes' membrane) from 9 to 7.5. The apparent  $\text{H}^+$  efflux from *TaALMT1* injected oocytes was four-to- five fold higher than water-injected oocytes at the peak efflux (4 min) (Fig. 8B). This large difference is more clearly indicated from the integral of the apparent proton flux shown in Fig. 8C. Concomitant with the acidification associated with the expression of *TaALMT1*, there was a large efflux of GABA to the external medium at pH 9 over 10 minutes. This resulted in a substantial loss of GABA from the oocytes (Fig. 8D).

### **Expression of *TaALMT1* and genes related to GABA metabolism in wheat root apices exposed to high pH and GABA**

It was previously shown that ET8 roots have higher expression of *TaALMT1* compared to ES8 (Yamaguchi et al., 2005) and that *TaALMT1* expression in root apices was further increased in ET8 by external  $\text{Al}^{3+}$  treatment at pH 4.5 (Ramesh et al., 2018). Therefore we measured the expression of *TaALMT1* in root apices after 5 weeks growth in pH 6 and pH 9 in the same conditions as those for Figure 1 plus and minus GABA treatment. Not surprisingly there was higher expression of *TaALMT1* in ET8 apices compared to that of ES8 (Fig. 9A); however, there was no change in expression at pH 9 compared to pH 6. Treatment with 10 mM GABA depressed expression of *TaALMT1* in ET8 significantly at pH 9, but there was no overall significance between pHs or genotypes (Fig. 9E). Since GABA efflux is stimulated at pH 9 in ET8 we measured genes involved in GABA metabolism: glutamate decarboxylase (*TaGAD* and *TaGAD1*) and GABA transaminase (*TaGABA-T*). Glutamate decarboxylase is the primary enzyme responsible for GABA synthesis, while GABA-T catalyses the conversion of GABA and 2-oxyglutarate in the mitochondria to succinate semialdehyde and glutamate. Of the two GAD genes (Fig. 9B & C) the more lowly expressed gene *TaGAD*, showed significantly higher expression in ET8 at pH 9 than ES8 (Fig. 9B) but there was no significant change with pH. The ET8 *TaGABA-T* showed significantly lower expression at pH 9 compared to pH 6 while ES8 showed no difference (Fig. 9D). Neither *TaGAD*, *TaGAD1* or *TaGABA-T* were significantly altered in expression by GABA treatment (Fig. 9F,G,H).

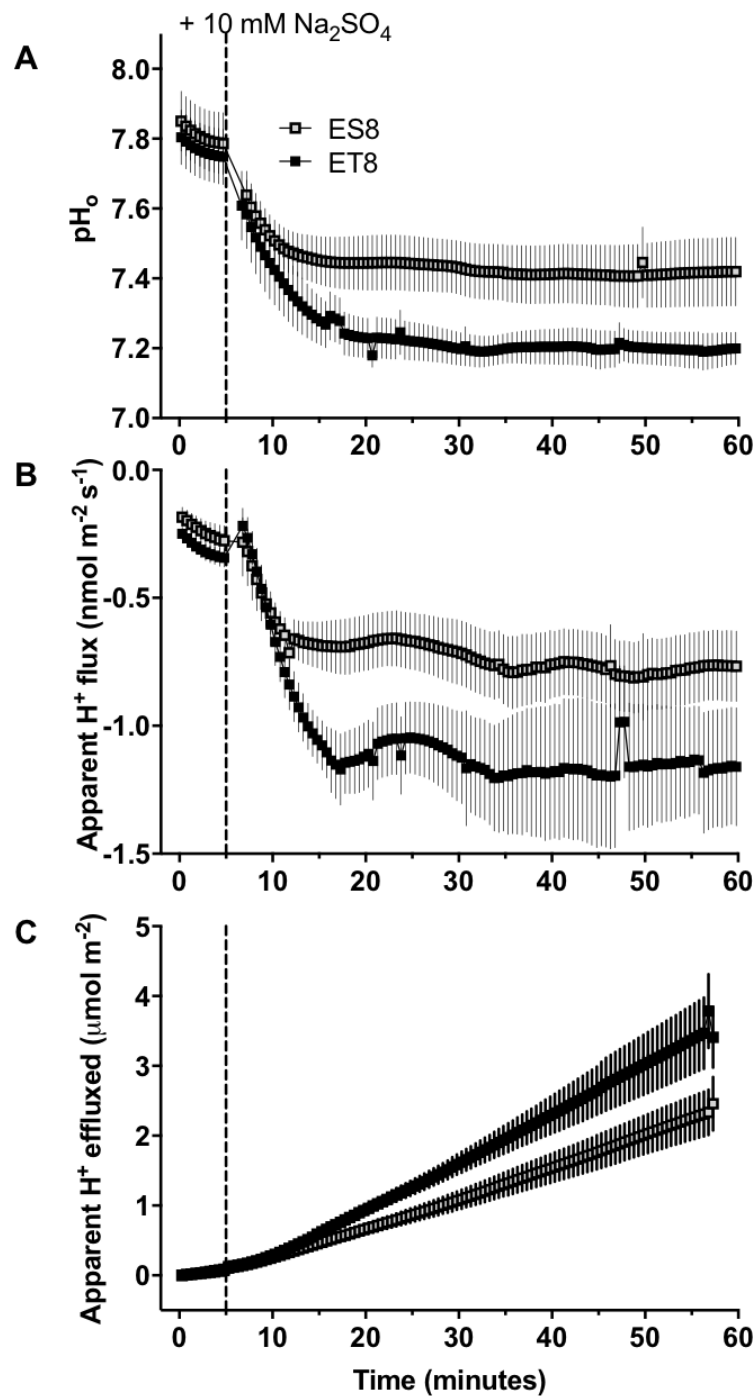


**Figure 7.** Comparison of ET8 and ES8 rhizosphere acidification in response to sodium sulphate (10 mM Na<sub>2</sub>SO<sub>4</sub>) at alkaline pH, using the Micro Electrode Ion Flux Estimation (MIFE). A, External pH (pH<sub>o</sub>) measured at the root apex ( $\approx$  1.5 mm from root cap) of three-to-four days old wheat seedlings. B, Apparent net H<sup>+</sup> flux. C, total H<sup>+</sup> effluxed (calculated as the integral of apparent H<sup>+</sup> fluxes). pH sensing micro-electrodes were used to measure changes in rhizosphere pH and proton fluxes 50  $\mu$ m from the root surface. The roots of intact seedlings were pre-conditioned in 0.2 mM KCl + 0.2 mM CaCl<sub>2</sub> + 3 mM MES + 4 mM TRIS, pH 7.87 for 30 minutes. After pre-conditioning, steady-state rhizosphere pH and proton fluxes were measured for 5 minutes then 10 mM Na<sub>2</sub>SO<sub>4</sub> was added (vertical dashed line) and the resulting changes were monitored over time. n=6 seedlings.

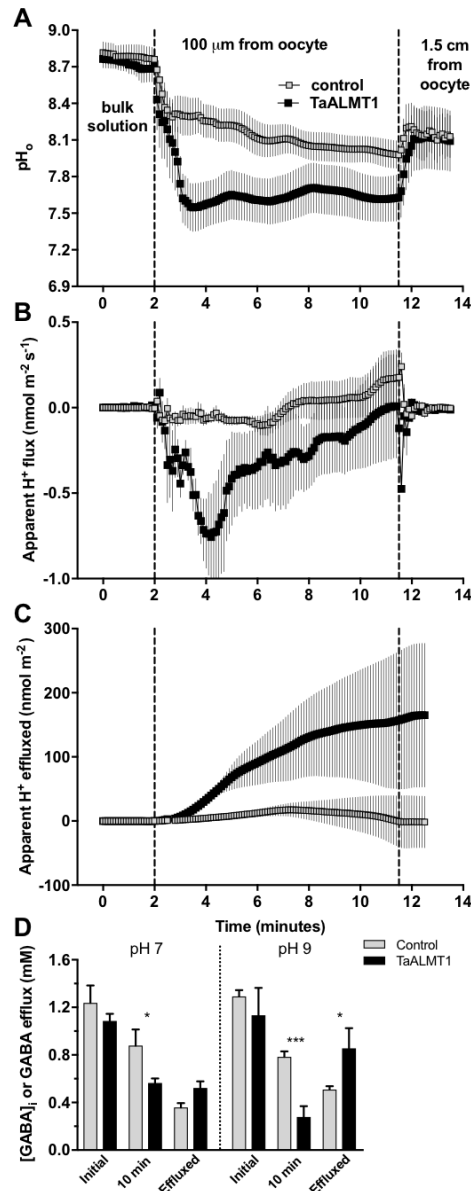


**Figure 8.** The effect of alkaline pH on efflux of protons and GABA from *Xenopus laevis* oocytes expressing TaALMT1. TaALMT1 and water injected (Control) *X. laevis* oocytes were used in these experiments. A, External pH ( $pH_o$ ), B, Apparent  $H^+$  fluxes, C, Total  $H^+$  effluxed (calculated as the integral of apparent  $H^+$  fluxes), were measured at 100  $\mu\text{m}$  from the oocyte membrane (or as indicated) using the Micro Electrode Ion Flux Estimation (MIFE) technique. D, The  $[GABA]_i$  of separate oocytes was measured after a 10 minute efflux period in either pH 7 or pH 9 and the GABA effluxed was measured from GABA concentrations in the external medium. The initial  $[GABA]_i$  for each replicate was calculated from the sum of that effluxed and 10 minute  $[GABA]_i$ . All values are normalised to the geometric volume of each oocyte. \*, \*\*\*, indicate significant difference between genotypes at the different times where  $P < 0.05$ , 0.001, respectively. For A,B,C  $n=6$  oocytes, for D  $n=5$  batches of 4-5 oocytes.

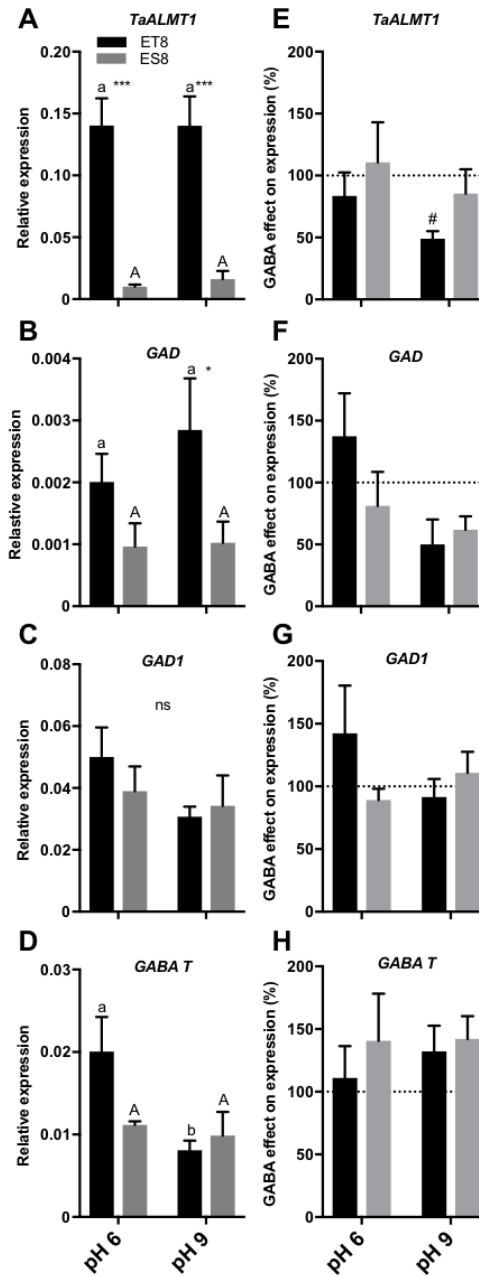


**Figure 9.** Expression of *TaALMT1* (A), *GAD* (B), *GAD1* (C) and *GABA T* (D) relative to three housekeeping genes (*GAPDH*, *Cyclophilin* and *Tubulin*) in root tips (see methods) and the effect of GABA treatment on expression (E,F,G,H respectively). Wheat NILs ET8 (black) and ES8 (grey) were grown in pots for 6 weeks. Nutrient solution (see material and methods) at pH 6 and pH 9  $\pm$  10 mM GABA were applied to each pot 2-3 times a week. Housekeeping genes were not affected by the treatments. Primers used and Genbank accession numbers are listed in Supplementary Table 1. In each case different letter combination for a genotype indicates significant difference ( $P < 0.05$ ) between pHs (lower case = ET8, upper case = ES8) and \*, \*\*\*, indicate significant difference between genotypes at a given pH  $P < 0.05$ , 0.001, (2-way ANOVA and post-tests),  $n = 3-4$ .

### 3.4 DISCUSSION

In alkaline soils, the capacity of plants to acidify the rhizosphere is critical for the uptake of nutrients such as iron (Takei et al., 2012) and phosphorus (Raghothama, 1999), as well as enabling a proton gradient into root cells for the uptake of anions such as nitrate and sulphate through proton coupled transporters (Wang et al., 2015). Here we have tested the hypotheses: 1) That the higher expression of *TaALMT1* imparts an advantage for plant growth under alkaline conditions. 2) That the *TaALMT1* malate-GABA transporter enables acidification of the rhizosphere at alkaline pH. We present evidence from the ET8/ES8 comparison in support of Hypothesis 1. Given the negative results of Silva et al. (2018) in respect of Hypothesis 1, which contrasts to our results for the ET8/ES8 comparison, we compare some elements of our experiments with those of Silva et al. (2018) below. Hypothesis 2 is supported by our results demonstrating that ET8 apices have enhanced malate and GABA efflux at high pH (Fig. 3,4,5,6) correlating with greater expression of *TaALMT1* (Fig. 9A), and that this efflux is associated with a greater capacity to acidify the external solution (Fig. 6, 7). A direct involvement of *TaALMT1* is demonstrated by the observed higher GABA efflux and greater acidification under alkaline conditions for *TaALMT1* expressing *X. laevis* oocytes (Fig. 8).

#### **Root growth over 5 weeks is enhanced at high pH by the presence of the *TaALMT1-V* allele in ET8 plants.**

Previously it was shown that root growth and malate efflux at pH 9 was higher in young seedlings of ET8 compared to ES8 (Ramesh et al., 2015). However, this result was not confirmed by Silva et al. (2018) using a variety of naturally alkaline soils and hydroponic solutions. Silva et al (2018) confirmed the advantage of the *TaALMT1-V* allele in acid soils, and in the presence of  $Al^{3+}$  in acidic hydroponic solution. The advantage of the *TaALMT1-V* allele in ET8 root growth at acid pH plus  $Al^{3+}$  was also shown by Ramesh et al (2015).

Comparing 5 weeks old ET8 and ES8 plants grown in washed sand supplied with nutrient solution at pH 6 and 9, we observed that root growth was enhanced in the ET8 plants at pH 9 (Fig. 1B). This was also evident in terms of total root length and root surface area (Fig. 1C,D). The parameters measured at pH 6 appeared to be typical for wheat of the same age from other studies (Narayanan et al., 2014). For the younger seedlings (less than 10 days old) used by Silva et al., (2018) these differences in root growth were not observed or there were variable responses in hydroponics at high pH depending on the buffer solution. In our longer-term growth experiments we used a bicarbonate buffer (as did Silva et al), but the roots were challenged with high pH, 3-4 times per week over 5 weeks. Considering the rapidity that roots acidify alkaline media over 24 hours (Fig. 6), it is possible that in experiments of a few days without

replenishment of the solution, the average pH is much less than the initial alkaline pH. The lack of difference observed by Silva et al (2018) may be due to the much higher buffering capacity of soils compared to that imposed in nutrient solutions used here.

Interestingly shoot growth of ET8 and ES8 in the different pHs did not reflect differences in root growth, with ES8 showing slightly higher but significant shoot biomass at pH 6 and pH 9 (Fig. 1A). A greater depression in root growth relative to that of the shoot was also observed in a comparison between alkali tolerant and intolerant rice cultivars (Wang et al., 2015). Silva et al (2018) did not observe differences in shoot biomass between ET8 and ES8 at high pH for younger seedlings. Our results may reflect a difference in shoot:root carbon allocation and in this respect it is relevant that ET8 had higher relative chlorophyll, higher transpiration and higher assimilation at pH 9 (Fig. 2). This is also similar to the results for rice cultivars differing in alkali tolerance (Wang et al., 2015).

Previously it was shown that GABA inhibited the efflux of malate at acid pH in the presence of  $\text{Al}^{3+}$  in ET8 seedlings, causing root growth of ET8 to phenocopy that of ES8 (Ramesh et al., 2015). Therefore we tested the effect of GABA at 10 mM in a subset of the wheat NILs at each of the pHs over 5 weeks of growth. GABA at 10 mM strongly inhibited both root and shoot growth over this period in both ET8 and ES8 plants and there was no differences observed between the two NILs at each pH in the degree of growth inhibition. However, there was a greater dependency of the inhibition on pH for ET8 (Supplemental Fig. S1A), which may be explained by GABA having a blocking action on malate exudation in the ET8 NIL. This however could not be confirmed from rhizosphere estimations of malate concentration in response to GABA after 5 weeks growth (Fig. 4C).

GABA treatment did have interesting effects on shoot gas exchange (Supplemental Fig. S2) where at both pH 6 and pH 9,  $E$  and  $g_s$  were increased significantly in the GABA treated plants, but with no differences between the two NILs. It should be noted that despite a significant decrease in chlorophyll concentration with GABA in both NILs at pH 6 and 9 there was no reduction in  $A$  corresponding to the enhanced  $g_s$ . This may indicate that reduced stomatal limitation on  $\text{CO}_2$  diffusion into leaves has compensated for reduced photosynthetic capacity. We did not measure GABA in the leaves of GABA treated plants so we cannot be certain if this effect is due to elevated GABA in the shoots.

## **Higher root exudation of malate and GABA occurs at alkaline pH in wheat associated with the expression of *TaALMT1*.**

Associated with the greater root growth observed for ET8 over ES8 at pH 9 there was also a greater apparent rhizosphere concentration of malate and GABA for ET8 root systems sampled after 5 weeks of growth compared to that for ES8 (Fig. 3). The concentrations of malate and GABA were also higher for ET8 at pH 9 than for pH 6, while ES8 showed no differences. The values obtained cannot be attributed to actual rhizosphere concentrations, which are likely to be higher, but can be used for comparison between the genotypes. Elevated concentrations of organic acids in roots including malate have been observed for alkali tolerant rice grown under alkaline hydroponic conditions (Wang et al., 2015), and especially malate for wheat in combination with mild salinity (Guo et al., 2010), but media/rhizosphere concentrations in these studies were not reported.

There was no inhibitory effect of GABA treatment on the concentration of malate sampled from root systems, which is contrary to the expected effect of GABA as a blocker of malate efflux through *TaALMT1* (Ramesh et al. 2015). Perhaps longer-term treatment by GABA has secondary effects as indicated by the alteration of leaf gas exchange. Interestingly for ES8, there was a significant increase in malate rhizosphere concentration in response to GABA that was not observed for ET8 (Fig. 3B). It was previously shown that the expression of *TaALMT1* increased endogenous GABA concentrations by an unknown mechanism (Ramesh et al., 2018). This may account for the difference in malate exudation in response to GABA associated with *TaALMT1* if GABA is a source for malate synthesis through the GABA shunt and tricarboxylate acid (TCA) cycle.

The efflux of malate and GABA from root apices were increased in the short term (1h) in response to pH 9 for the wheat ET8 (Fig. 4). This effect was not dependent on solution buffering. These results reflect the situation observed for whole root systems of ET8 and ES8 (Fig. 4). In contrast Silva et al (2018) did not observe a significant difference for root apex efflux of malate at pH 9 for the ET8/ES8 comparison using unbuffered solution. Although our malate effluxes for root apices of both ET8 and ES8 at pH 6 and for ES8 at pH 9 are very similar to those reported by Silva et al (2018) we differ substantially for malate efflux at pH 9. Our values at pH 9 are very similar to those of Silva et al for  $Al^{3+}$  activation at pH 4.5, and also to previous values reported from our laboratory for  $Al^{3+}$  activation (Ramesh et al. 2018). The following possibilities are explored in an attempt to explain this difference which may ultimately depend on solution buffering and the ratio of the mass of roots to the solution volume: Firstly the activation of *TaALMT1* by high pH is likely to be very different to the situation for  $Al^{3+}$

activation. At pH 9  $[\text{OH}^-]$  is initially at 10  $\mu\text{molar}$  compared to 100  $\mu\text{molar}$   $[\text{Al}^{3+}]$  normally used to activate TaALMT1. The roots rapidly reduce the external pH and this in turn would reduce the activation of TaALMT1 according to the data presented by Ramesh et al. (2015). The degree of this effect will depend on the proportion of root mass to solution volume in the efflux experiment. In our case we used the minimum mass of roots compared to solution volume that would still allow accurate estimations of malate and GABA concentrations. The presence of buffer, which would tend to maintain a high pH in the media for longer, would be expected to enhance the apparent malate and GABA efflux. This buffer effect is clearly evident when longer term efflux experiments are performed (Fig. 5,6). Another complication in these experiments is the accumulation of GABA in the external solution through the activation of TaALMT1. GABA can inhibit the efflux of malate and again this would depend on the ratio of mass of root apex to solution volume with a higher ratio potentially resulting in greater inhibition of malate efflux by the larger concentration of GABA. These effects of both external pH and GABA concentration are likely to partially account for the complicated kinetics of external malate and GABA concentrations observed in Fig. 6. This is evident in the final concentrations of malate and GABA observed after 22 h where there was no significant differences in malate effluxed between ET8 and ES8, though there was a larger difference at earlier times. Our previous results for GABA and malate efflux from 3 day old seedling roots showed significant differences after 22 h (Ramesh et al. 2018), but in this case there was a low ratio of root mass to solution volume. It is also evident in the results of Fig. 6 that there may have been re-uptake of initially released GABA and malate although there were differences between repeated experiments. It was previously shown that GABA released by wheat roots is recycled back into roots (Warren, 2015). Extending this discussion to the actual situation in the rhizosphere around a growing root would suggest that the amount of malate and GABA released could be quite small in response to high pH, relative to what happens in a large volume of solution in the experiments reported here.

### **GABA release and acidification at high pH associated with the expression of *TaALMT1***

ET8 roots and root apices showed a greater capacity to acidify alkaline media in comparison with ES8 (Fig. 6,7). This difference for whole root systems was evident after 6 h and after only 10 minutes for the rhizosphere within 50  $\mu\text{m}$  from the root apices. In parallel there was higher malate and GABA released from the root apices of ET8 (Fig. 6). GABA can act as an effective buffer at both low and high pH, and at high pH GABA released from the root cytosol (assumed to be near neutrality) would be detected as an apparent  $\text{H}^+$  efflux. GABA is a zwitterion with an amine group ( $\text{pK}_a = 10.43$ ) and a carboxyl group ( $\text{pK}_a = 4.23$ ) (Thwaites et al., 2000). At neutral pH the amine group is protonated and the carboxyl group is deprotonated

to give a net neutral charge. At high pH the amine group will lose its proton, thus GABA becomes an anion at alkaline pH. However, from the data shown in Figure 6 the final concentration of GABA measured in the nutrient solution after 22-24 h (7-12 micromolar) could not have resulted in the measured drop in pH or the difference in pH between ET8 and ES8. Simulations of change in pH with addition of GABA using the concentrations of nutrients that have buffering capacity (e.g.  $\text{NH}_4^+$ ,  $\text{H}_2\text{PO}_4^-$ ,  $\text{H}_3\text{BO}_3$ ,  $\text{HCO}_3^-$ ,  $\text{CO}_3^{2-}$ ) would indicate that millimolar concentrations of GABA are required to lower pH to near 7.5 (Gutz, 2018). Malate efflux on the other hand could allow the  $\text{H}^+$ -ATPase in roots to operate at higher rates by balancing charge across the plasma membrane (summarised in Fig. 10).

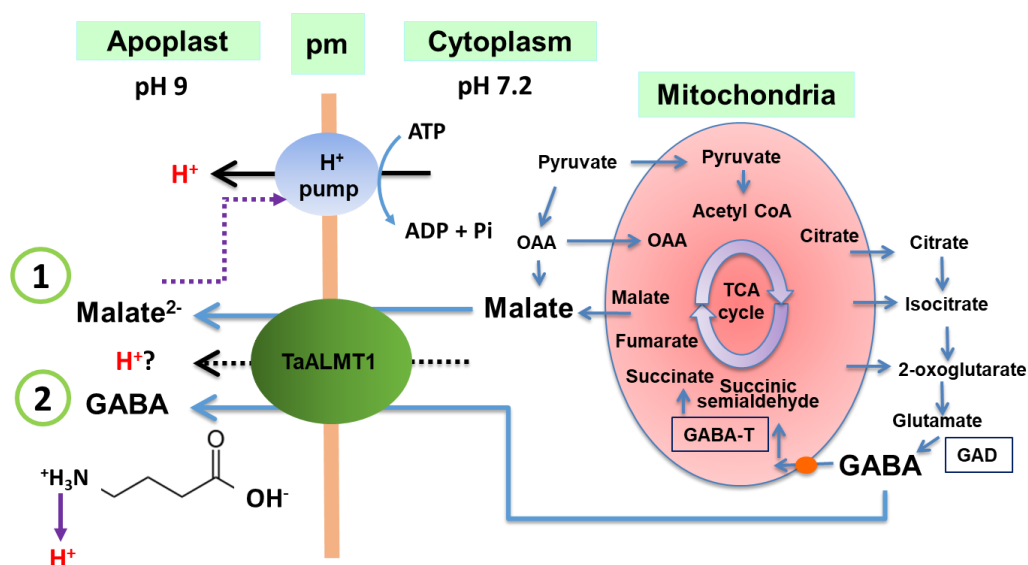


**Figure 10.** Diagram of the hypothesis of how TaALMT1 may reduce external pH under alkaline conditions. TaALMT1 allows the efflux of both malate anions and neutral GABA (zwitterion at pH 7.4) into the apoplast when activated by high external pH. (1) The release of malate anions can balance charge required for the operation of the  $\text{H}^+$ -ATPase. (2) The release of GABA will lower the external pH by virtue of its pKa of the ammonium group and possibly by the coupling to proton efflux. Mitochondria are central to the supply of malate and GABA and key enzymes in the GABA shunt that are involved include glutamate decarboxylase (GAD) and GABA transaminase (GABA-T).

The expression of *TaALMT1* in *X. laevis* oocytes demonstrated the strong effect of GABA release via TaALMT1 in lowering external pH (Fig. 8). Since *X. laevis* does not have an  $\text{H}^+$ -ATPase it is unlikely that anion release through TaALMT1 in this case could stimulate  $\text{H}^+$  release from oocytes. Potassium was previously shown to balance malate efflux at low pH in the presence of  $\text{Al}^{3+}$  (Zhang et al., 2001), however it is known that the  $\text{H}^+$ -ATPase is stimulated by alkaline pH (Fuglsang et al., 2007; Yang et al., 2010) and this would require simultaneous

release of an anion.. There was a large release of GABA over 10 minutes from the oocytes expressing *TaALMT1* resulting in a substantial reduction in internal GABA concentration (Fig. 8D). This corresponded to a rapid reduction in pH close to the oocyte membrane (Fig. 8A). The external pH (100  $\mu\text{m}$  from membrane) dropped to around 7.6 within a few minutes in *TaALMT1* expressing eggs after emersion in high pH (Fig. 8A). The concentration of GABA at a distance of 100  $\mu\text{m}$  from the oocyte surface required to reduce pH from 8.7 to 7.6 is approximately 5 mM. For the controls the pH dropped to about 8.1 after 10 minutes. This would require a GABA concentration at 100  $\mu\text{m}$  of about 1 mM, more slowly accumulated over 10 minutes. There are two issues arising from this simple calculation. First the measured concentration of GABA in the oocytes for controls and *TaALMT1* expressing eggs was approximately 1.2 mM (Fig. 8D), thus for the GABA concentration to be higher than this (5 mM) adjacent to the external surface requires that GABA be effluxed against a concentration gradient for *TaALMT1* expressing oocytes. Second is it even possible for the measured rate of GABA efflux to account for such high concentrations of GABA adjacent to the external face of the membrane? Taking the volume of a thin shell 200  $\mu\text{m}$  thick around the exterior of an oocyte we can calculate the time it would take for this shell to fill with GABA using the measured efflux rates. For *TaALMT1* expressing eggs the shell would fill in less than 100 ms based on the fluxes normalised to oocyte surface area (mean for *TaALMT1* = 293  $\text{nmol m}^{-2} \text{s}^{-1}$ ). For the controls a concentration of about 1 mM would be reached within about the same time (mean flux = 172  $\text{nmol m}^{-2} \text{s}^{-1}$ ), but if passively distributed it would not increase beyond the concentration of GABA within the oocyte. This approximate calculation serves to illustrate that it is likely that GABA efflux is against a concentration gradient in *TaALMT1* expressing oocytes, and that the fluxes measured are likely to be able to account for the concentration gradient adjacent to the egg membrane. A more complex mathematical model of diffusion and simultaneous reaction would be required to properly model this. It is possible that GABA efflux is coupled to the release of protons for which in the conditions of the experiment there would be an initial gradient of 1.5 pH units (pH of oocyte cytoplasm of 7.2, initial pH outside of 8.7) however, the gradient rapidly diminished. The net proton flux from the oocyte (Fig. 8B) may be a combination of the actual proton flux and the consequences of GABA dissociation. GABA influx through *TaALMT1* was also stimulated by low external pH (Ramesh et al., 2018) pointing to the possibility of reversible proton coupling of GABA transport. The possibility that GABA efflux is coupled to proton release is illustrated in Figure 10.

## **Expression of genes associated with GABA metabolism change in response to growth at high pH, but TaALMT1 expression is not altered.**

We confirmed that ET8 plants had higher root apex expression of *TaALMT1* than that of ES8, but unlike the increase in *TaALMT1* expression shown for ET8 in response to  $Al^{3+}$  at low pH (Ramesh et al., 2018) we did not observe a significant increase in expression in response to pH 9 (Fig. 9A). We observed that a *GAD-like* gene had increased expression at pH 9 in ET8 roots and that this was significantly higher than that for ES8 (Fig. 9B). This would correspond to the increase in GABA efflux that may require increased GAD to support GABA synthesis. However, the more highly expressed *GAD1* gene did not show a significant difference (Fig. 9C). In support of a “supply and demand” interpretation is the depression of *GABA-T* expression at pH 9 in ET8, but not in ES8 roots (Fig. 9D). GABA-T converts GABA to succinate semialdehyde so a reduced enzyme activity may result in higher GABA accumulation in ET8. These possibilities need confirmation from enzyme activity measurements.

GABA treatment of roots did not result in significant changes in expression, although the *GAD-like* transcript that showed a pH effect was depressed in both ET8 and ES8. There was a significant reduction in *TaALMT1* expression at pH 9 in response to GABA, which further supports the observations by Ramesh et al (2018) of a close link between *TaALMT1* expression and GABA concentrations in roots.

## **A new mechanism for rhizosphere control of pH via TaALMT1 under alkaline conditions**

Several studies have demonstrated the importance of  $H^+$  exudation as a mechanism of alkaline soil tolerance (Fuglsang et al., 2007; Yang et al., 2010; Xu et al., 2012; Xu et al., 2013; Li et al., 2015). Here we have shown how TaALMT1 can enhance rhizosphere acidification in alkaline soils. TaALMT1 and possibly other ALMTs in other plants associated with  $Al^{3+}$  tolerance are likely to have broader functions than the well-established  $Al^{3+}$  tolerance at low pH and may be associated with both acid and alkaline soil pH tolerance and metabolic signalling (Ramesh et al. 2018). Our results can explain previous associations between higher grain yield in alkaline soil and the presence of the TaALMT1 allele (McDonald et al., 2013; Eagles et al., 2014). Elevated malate exudation in alkaline soils, will improve root growth in two ways: (1) providing charge balance for enhanced  $H^+$  efflux mediated by the  $H^+$ -ATPase thereby lowering the apoplastic pH to a more conducive level to allow root elongation (Landsberg, 1981) and (2) improving iron and phosphorus availability (Landsberg, 1981; Lopez-Bucio et al., 2000; Delhaize et al., 2009). In addition the concomitant release of GABA by TaALMT1 and possibly protons at high pH would further enhance acidification of the rhizosphere (Fig. 10). GABA released into the rhizosphere is likely to be taken back up by roots either via a high affinity

GABA transporter (Meyer et al., 2006) or back through TaALMT1 once the pH has been lowered (Ramesh et al., 2018). The role of the enzymes GAD and GABA-T in regulating the supply of GABA for efflux via TaALMT1 and their possible interactions with GABA signalling and pH under alkaline conditions remain to be fully explored.

### 3.5 MATERIALS AND METHODS

#### Chemicals

All chemicals were purchased from Sigma Aldrich.

#### Plant material and growth

NILs of wheat (*Triticum aestivum* L) ET8 and ES8 (Sasaki et al., 2004) both a gift from Dr Peter Ryan, CSIRO, Canberra (Delhaize et al., 2004), were surface sterilised in 1% bleach for 1 min, rinsed 3X in water and germinated on moist filter paper in the dark on the bench. Three-day-old seedlings were transferred into pots filled with washed sand. The pots were placed on a bench in a growth room (randomly arranged), with average photosynthetic active radiation (PAR) at plant height of 300-350  $\mu\text{mol m}^{-2} \text{s}^{-1}$  on a 12 hour photoperiod (7am-7pm) and with day/night temperature of 21°C/16°C. The plants were supplied with a basal nutrient solution (BNS): 2 mM  $\text{NH}_4\text{NO}_3$ , 3 mM  $\text{KNO}_3$ , 0.1 mM  $\text{CaCl}_2$ , 2 mM  $\text{KCl}$ , 2 mM  $\text{Ca}(\text{NO}_3)_2 \cdot 4\text{H}_2\text{O}$ , 2 mM  $\text{MgSO}_4 \cdot 7\text{H}_2\text{O}$ , 0.6 mM  $\text{KH}_2\text{PO}_4$ , 50  $\mu\text{M}$   $\text{NaFe}(\text{III})\text{-EDTA}$ , 50  $\mu\text{M}$   $\text{H}_3\text{BO}_3$ , 5  $\mu\text{M}$   $\text{MnCl}_2 \cdot 4\text{H}_2\text{O}$ , 10  $\mu\text{M}$   $\text{ZnSO}_4 \cdot 7\text{H}_2\text{O}$ , 0.5  $\mu\text{M}$   $\text{CuSO}_4 \cdot 5\text{H}_2\text{O}$  and 0.1  $\mu\text{M}$   $\text{Na}_2\text{MoO}_4$  and pH adjusted to 6 with  $\text{NaOH}$ . For pH 9 treatment, the same nutrient solution was supplied with 1 mM  $\text{NaHCO}_3$ , 80  $\mu\text{M}$   $\text{Na}_2\text{CO}_3$  (Ma et al., 2003) and pH adjusted to 9 using  $\text{NaOH}$ . A subset of plants were also treated with the addition of 10 mM GABA to the BNS solution and the pH checked and adjusted to that of the treatment pH with  $\text{NaOH}$ . The treatment solutions were applied 3-4 times/week allowing pots to drain as their only water supply and the plants were treated for 5 weeks. At 5 weeks shoots and roots of the wheat ET8 and ES8 plants were harvested. Fresh mass was measured and then roots were scanned with an Epson digital scanner (Expression 10000XL, Epson Inc.). Scans were analysed with the WinRHIZO software (Regent Instruments Inc.). Dry mass was obtained after oven-drying at 75 °C for 3 days.

#### Relative chlorophyll content, and leaf gas exchange

Relative chlorophyll content (SPAD values) were measured using a portable chlorophyll content meter (CCM-200 plus, OPTI-SCIENCES). Transpiration ( $E$ ), stomatal conductance ( $g_s$ ) and assimilation rate ( $A$ ), were measured using a portable infrared data analysis system (LC-pro SD, ADC Bioscientific, Hoddesdon, England). PAR was set at 1000  $\mu\text{mol m}^{-2} \text{s}^{-1}$  using the internal chamber LED light system. The  $\text{CO}_2$  concentration of the measuring chamber was kept at ambient (between 370–400  $\mu\text{mol mol}^{-1}$ ). Measurements once stable for each replicate were made between 11:00 am and 2:00 pm on two fully expanded youngest leaves of each plant after 5 weeks growth under each of the treatments described above. A section of each leaf was placed

in the broad leaf chamber of the instrument while still attached to the plant and leaf area adjusted for internal calculations based on measured leaf width.

### **Estimates of rhizosphere malate and GABA**

A root wash was applied for plants *in situ* after five weeks of growth in the washed sand by adding 120 ml of the appropriate treatment solution over the surface of the sand and collecting the eluate from the base of the pot over 1 hour. The malate and GABA content was normalised on a root fresh mass basis. Malate and GABA concentrations were measured as described below.

### **Net fluxes of malate and GABA from excised root apices and intact seedlings**

Root apices (5 mm) were excised from three-day-old seedlings and washed three times in 3 mM CaCl<sub>2</sub>, pH 6 adjusted with NaOH. In one experiment five apices were incubated in 0.2 ml per replicate for one hour in treatment solutions at pH 6 and 9 with and without buffer (all with 3 mM CaCl<sub>2</sub>, 10 mM Na<sub>2</sub>SO<sub>4</sub>): *pH 6 solution*, 0.01 mM NaOH; *pH 6 + buffer*: 5 mM MES, 2.6 mM NaOH; *pH 9 solution*, 0.05 mM NaOH; *pH 9 + buffer*, 5 mM BTP, 2mM MES. In another experiment root apices were treated as above for 1 h in the following solutions (all 3 mM CaCl<sub>2</sub>): *pH 4.5*, 5 mM MES; *pH 4.5+Al*, 5 mM MES, 0.1 mM AlCl<sub>3</sub>; *pH 9 NaOH*, 0.12 mM NaOH; *pH 9 KOH*, 0.2 mM, KOH; *pH 9 BTP Na<sub>2</sub>SO<sub>4</sub>*, 20 mM BTP, 10 mM Na<sub>2</sub>SO<sub>4</sub>, 9 mM MES; *pH 9 Carbonate*, 18 mM NaHCO<sub>3</sub>, 2 mM Na<sub>2</sub>CO<sub>3</sub>; *pH 9 Carbonate Na<sub>2</sub>SO<sub>4</sub>*, 18 mM NaHCO<sub>3</sub>, 2 mM Na<sub>2</sub>CO<sub>3</sub>, 10 mM Na<sub>2</sub>SO<sub>4</sub>. The same solutions were used for intact seedling root experiments where intact roots of one 3-day old seedling per replicate were placed in to 1.8 mL and treated for 21 h (Ramesh et al., 2018).

### **Measurement of root medium malate and GABA concentrations and external solution pH for seedlings suddenly exposed to pH 9**

Wheat NILs ET8 and ES8 were surface sterilized, and germinated as described above. Three-day-old seedlings were placed in a microcentrifuge tube with roots immersed initially in a solution consisting of 3 mM CaCl<sub>2</sub> and 5 mM MES, pH 5 for 24 h after which 7-8 seedlings/replicate were selected. These were transferred so that their roots were bathed in 200 ml (per replicate) of aerated BNS solution at pH 9 (composition as described above). pH in the root bathing solution was monitored over time using a pH electrode (pH-HI2211, HANNA instruments). For malate and GABA concentration, samples of the solution were collected at various times after the seedlings were transferred to the pH 9 solution and measured as

described below. Root fresh mass (0.38 to 0.54 g) per replicate was measured at the end of the experiment after 22-24 hours.

### **Measurement of malate and GABA concentrations**

For malate a sample of solution (usually 0.1 ml) was added to a master mix containing the various components of the KLMAL- assay (Megazyme) kit as per the manufacturer's instructions. The conversion of L-malic acid to 2-oxoglutarate + L-aspartate using L-malate dehydrogenase and glutamate-oxaloacetate transaminase produces NADH from NAD<sup>+</sup>. The change in NADH was measured using an OMEGA plate-reading spectrophotometer (BMG) from the change in absorbance at 340 nm. Appropriate standard curves over the range of malate concentrations were obtained generally with triplicate technical replication. GABA concentrations were measured in treatment solutions following the GABase enzyme assay (Sigma-Aldrich) (Zhang and Bown, 1997), where the coupled enzyme mixture is composed of  $\gamma$ -aminobutyric acid aminotransferase and succinic semialdehyde dehydrogenase. The enzyme reaction results in GABA conversion to succinate with the stoichiometric production of NADPH measured by changes in absorbance at 340 nm in an Omega plate-reading spectrophotometer (BMG). This was previously validated for similar experiments by comparison with UPLC assays in Ramesh et al. (2018).

### **Gene expression in root apices**

Root apices (5 mm) were excised from 5 week old seedlings after gently removing the washed sand from around the seedling roots. Apices were frozen in liquid nitrogen and stored at -80 °C until further analysis by quantitative reverse transcription qPCR (RT-qPCR). Root apices were ground to a fine powder in liquid nitrogen using a mortar and pestle and total RNA was extracted using the Spectrum Plant Total RNA extraction Kit (Sigma-Aldrich, St. Louis, MO, USA). DNA contamination was avoided by digestion with the On-Column DNase I Digestion Set (Sigma-Aldrich, St. Louis, MO, USA) during RNA extraction according to manufacturer recommendations. Concentration and purity of total RNA were determined on a NanoDrop™ 1000 Spectrophotometer (Thermo Fisher Scientific Inc., MA, USA). Agarose gels electrophoresis (1.2 % agarose) was carried out to visualize the integrity of RNA. For cDNA synthesis, 1  $\mu$ g of total RNA was reverse transcribed using iScript™ cDNA Synthesis Kit (Bio-Rad, CA, USA) according to manufacturer instructions. Gene expression analysis was carried out by quantitative reverse transcription PCR (RT-PCR) (QuantStudio™ 12K Flex; ThermoFisher Scientific Inc., MA, USA). Gene specific primers (TaALMT1, GAD, GABA-T, tubulin and cyclophilin, Supplemental Table S1) were used to amplify products from control

cDNA and used for generation of standard curves. The amplified products were confirmed by sequencing. Briefly 1:10 serial dilutions of purified PCR products were made and used in RT-qPCR. The reaction volume was 10  $\mu$ l and contained 1  $\mu$ L of either the serial dilution or undiluted cDNA, 5  $\mu$ L KAPA SYBR® FAST Master Mix (2X) Universal (Kapa Biosystems Inc., MA, USA), 100 nM of gene-specific primers, and 0.2  $\mu$ L of ROX Reference Dye Low (50X). The thermal cycling conditions were: one cycle of 3 min at 95 °C followed by 40 cycles of 16 s at 95 °C and 20 s at 60 °C. Subsequently, melting curves were recorded from 60 to 95 °C at a ramp rate of 0.05°C/s. Normalized relative quantities (NRQ) of gene expression were calculated between the gene of interest and three reference genes taking differences in PCR efficiency into account (Pfaffl, 2001; Hellemans et al., 2007).

### **Ion-selective microelectrode measurements of pH and proton flux**

External pH and net H<sup>+</sup> flux from root apices of wheat ET8 and ES8 3-4 day old seedlings, or *Xenopus laevis* oocytes were measured using ion-selective microelectrodes (Newman, 2001). Microelectrode fabrication, conditioning and calibration were followed as detailed by Bose et al. (2013). Briefly, microelectrodes were pulled from borosilicate glass capillaries (GC 150-10, Harvard Apparatus Ltd, Kent, UK), oven dried at 230 °C overnight, and silanized using tributylchlorosilane (Fluka, catalogue no. 90796). Electrodes tips were broken back to obtain external tip diameter of 2–3  $\mu$ m. The electrodes were back-filled with 15 mM NaCl, 40 mM KH<sub>2</sub>PO<sub>4</sub> (pH adjusted to 6.0 with NaOH). The electrode tips were then front-filled with H<sup>+</sup> -selective ionophore II cocktail A (Fluka, catalogue no. 95297 for H<sup>+</sup>). Prepared electrodes were calibrated in buffers with pH 6, 7 and 9. The ion sensitive microelectrode was placed near the surface of the root apex or oocyte using a 3D-micromanipulator (MMT-5, Narishige, Tokyo, Japan). A computer-controlled stepper motor moved the electrode between two positions from the surface in 6 s cycles. The CHART software (Newman, 2001) recorded the potential difference between the two positions and converted these into electrochemical potential differences using the calibrated Nernst slope of the electrode. Net ion fluxes were calculated using the MIFEFLUX software for either spherical geometry (*X. laevis* oocytes) or cylindrical geometry (wheat ET8/ES8 roots) (Newman, 2001). For rhizosphere pH and net H<sup>+</sup> fluxes 3-4 day-old intact seedling roots were gently immobilized in the measuring chambers as described elsewhere (Bose et al. 2013) and pre-conditioned in 0.2 mM KCl + 0.2 mM CaCl<sub>2</sub> + 3 mM MES + 4 mM TRIS, pH 7.87 for about 30 minutes. After pre-conditioning, steady-state rhizosphere pH and proton fluxes were recorded at the root apex ( $\approx$  1.5 mm from root cap, 50  $\mu$ m from the surface) over a period of 5 minutes. Then, 10 mM Na<sub>2</sub>SO<sub>4</sub> was added and changes in rhizosphere pH and proton fluxes were measured for up to 60 minutes. External pH and

proton flux from *Xenopus laevis* oocytes expressing *TaALMT1* or water injected controls were also measured using the MIFE technique. An oocyte (one per replicate) was transferred from calcium Ringers solution (see below) to the test solution containing 0.7 mM CaCl<sub>2</sub>, 10 mM Na<sub>2</sub>SO<sub>4</sub>, pH adjusted to 9 using NaOH and the osmolality adjusted to 231 mosmol kg<sup>-1</sup> using D-mannitol. The electrode was positioned at different distances from the oocyte surface in order to monitor the changes in bulk solution pH and the pH and flux at 100 μm from the surface.

### **Heterologous expression of *TaALMT1* in *Xenopus laevis* oocytes**

ALMT1 from wheat was cloned using the listed primers (TaALMT1\_F 5' ATGGATATTGATCACGGCAGAG 3'; TaALMT1\_R 5' TTACAAAATAACCACGTCAGGCAAAGG 3' ) into GATEWAY enabled *Xenopus* expression vector pGEMHE-DEST (Ramesh et al., 2015). Plasmid DNA was extracted using a Sigma Genelute Plasmid Purification Kit and confirmed by sequencing. 1 μg of plasmid DNA was linearized with the restriction enzyme Nhe I (New England BioLabs). Capped RNA (cRNA) was synthesized *in vitro* with mMessage mMachine T7 kit (Ambion, Carlsbad, CA, USA) using linearised plasmid as template. Stage V and VI defolliculated oocytes surgically extracted from *Xenopus laevis* frogs were injected with 46 nl cRNA (32 ng cRNA), or sterile water. Injected oocytes were incubated in calcium Ringers solution (96 mM NaCl, 2 mM KCl, 5 mM MgCl<sub>2</sub>, 0.6 mM CaCl<sub>2</sub>, 5 mM HEPES, 5% (v/v) horse serum, 50 μg ml<sup>-1</sup> tetracycline and 1 x penicillin-streptomycin (Sigma P4333). The water and TaALMT1 cRNA injected oocytes were incubated for 48 h in Ringer's solution prior to experimentation. Randomly selected oocytes were alternated between control and gene injected to limit any bias caused by time-dependent changes after gene injection. The University of Adelaide Animal Ethics Committee approved the *Xenopus laevis* oocyte experiments; project number S-2014-192.

### **Endogenous GABA concentrations and GABA efflux from *Xenopus laevis* oocytes**

Oocyte GABA concentrations were measured as described in Ramesh et al (2018). For GABA efflux oocytes injected with TaALMT1 cRNA or water were imaged in groups of 4-5 to obtain cell volumes using a stereo zoom microscope (SMZ800) with a Nikon (cDSS230) camera at 48 h post-injection. The batches of oocytes were incubated in treatment solutions (pH 7: 0.7 mM CaCl<sub>2</sub>, 10 mM Na<sub>2</sub>SO<sub>4</sub>, mannitol to 220 mOsm kg<sup>-1</sup>. pH 9: 0.7 mM CaCl<sub>2</sub>, 10mM Na<sub>2</sub>SO<sub>4</sub>, mannitol to 220 mOsm kg<sup>-1</sup>, pH to 9 with NaOH) for 10 min. After 10 min, the solution was removed for the GABA assay and oocytes snap frozen in liquid nitrogen and stored at -80 °C. The frozen oocytes were ground in liquid nitrogen, added to methanol and incubated at 25 °C for 10 min. The samples were vacuum dried, resuspended in 70 mM LaCl<sub>3</sub>, pelleted at 500 x g

in a desktop microcentrifuge and precipitated with 1M KOH. These samples were re-centrifuged at 500 x g and 45.2 µl of supernatant was assayed for GABA concentrations using the GABase enzyme from Sigma as described above.

### **Statistical analysis**

All graphs and data analysis were performed in GraphPad Prism 7 (version 7.02). All data shown are mean + SE. Star symbols indicate significance ( $P < 0.05$ ) between values as determined by one-way or two-way analysis of variance. Post tests were performed taking account of total variation in the data.

### **ACCESSION NUMBERS**

Sequence data from this article can be found in the EMBL/GenBank data libraries under accession number(s) *TaALMT1* (DQ072260); *Tubb4* (U76895.1); *Cyclophilin* (EU035525.1); *GAPDH* (EF592180.1); *TaGABA-T* (AK333709.1); *TaGAD* (AK331230.1); *TaGAD1* (AK331897.1) respectively.

### **SUPPLEMENTAL DATA**

The following supplemental materials are available.

Supplemental Figure S1. Effect of GABA in the nutrient solution at each pH on root and shoot growth of ET8 and ES8 wheat plants.

Supplemental Figure S2. Effect of GABA in the nutrient solution at each pH on leaf gas exchange of ET8 and ES8 wheat plants.

Supplemental Table S1. Genbank accessions and primers used for Figure 7.

### **ACKNOWLEDGEMENTS**

We thank Wendy Sullivan for expert technical assistance. The Australian Research Council has supported this research through CE140100008.

### 3.6 LITERATURE CITED

- Bose J, Xie YJ, Shen WB, Shabala S (2013)** Haem oxygenase modifies salinity tolerance in *Arabidopsis* by controlling K<sup>+</sup> retention via regulation of the plasma membrane H<sup>+</sup>-ATPase and by altering SOS1 transcript levels in roots. *Journal of Experimental Botany* **64**: 471-481
- Delhaize E, Ryan PR (1995)** Aluminum Toxicity and Tolerance in Plants. *Plant Physiology* **107**: 35-321
- Delhaize E, Ryan PR, Hebb DM, Yamamoto Y, Sasaki T, Matsumoto H (2004)** Engineering high-level aluminum tolerance in barley with the ALMT1 gene. *Proceedings of the National Academy of Sciences of the United States of America* **101**: 15249-15254
- Delhaize E, Taylor P, Hocking PJ, Simpson RJ, Ryan PR, Richardson AE (2009)** Transgenic barley (*Hordeum vulgare* L.) expressing the wheat aluminium resistance gene (TaALMT1) shows enhanced phosphorus nutrition and grain production when grown on an acid soil. *Plant Biotechnology Journal* **7**: 391-400
- Eagles H, Cane K, Trevaskis B, Vallance N, Eastwood R, Gororo N, Kuchel H, Martin P (2014)** Ppd1, Vrn1, ALMT1 and Rht genes and their effects on grain yield in lower rainfall environments in southern Australia. *Crop and Pasture Science* **65**: 159-170
- Fuglsang AT, Guo Y, Cuin TA, Qiu Q, Song C, Kristiansen KA, Bych K, Schulz A, Shabala S, Schumaker KS (2007)** *Arabidopsis* protein kinase PKS5 inhibits the plasma membrane H<sup>+</sup>-ATPase by preventing interaction with 14-3-3 protein. *The Plant Cell* **19**: 1617-1634
- Guo M, Wang R, Wang J, Hua K, Wang Y, Liu X, Yao S (2014)** ALT1, a Snf2 Family Chromatin Remodeling ATPase, Negatively Regulates Alkaline Tolerance through Enhanced Defense against Oxidative Stress in Rice. *PLOS ONE* **9**: e112515
- Guo R, Shi LX, Ding XM, Hu YJ, Tian SY, Yan DF, Shao SA, Gao YA, Liu R, Yang YF (2010)** Effects of Saline and Alkaline Stress on Germination, Seedling Growth, and Ion Balance in Wheat. *Agronomy Journal* **102**: 1252-1260
- Gutz IGR (2018)** CurTiPot – pH and Acid–Base Titration Curves: Analysis and Simulation freeware, version 4.3 software for MS-Excel. URL: [http://www.iq.usp.br/gutz/Curtipot\\_.html](http://www.iq.usp.br/gutz/Curtipot_.html)
- Hellemans J, Mortier G, De Paepe A, Speleman F, Vandesomepele J (2007)** qBase relative quantification framework and software for management and automated analysis of real-time quantitative PCR data. *Genome Biology* **8**: R19

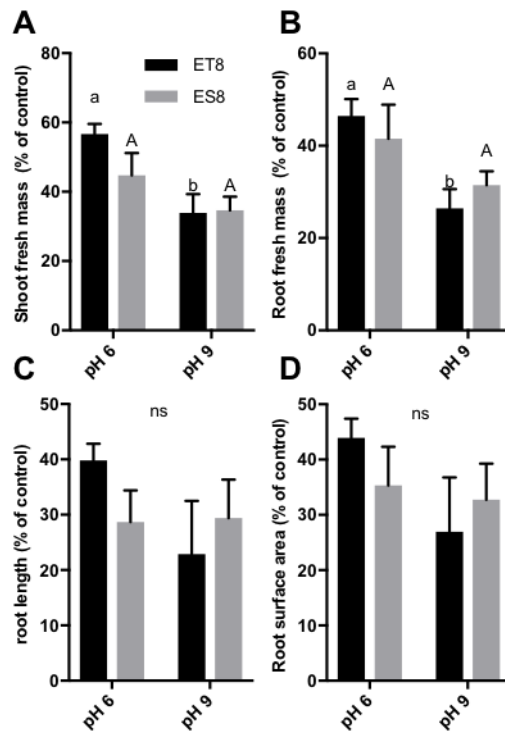
- Jin H, Plaha P, Park JY, Hong CP, Lee IS, Yang ZH, Jiang GB, Kwak SS, Liu SK, Lee JS, Kim YA, Lim YP** (2006) Comparative EST profiles of leaf and root of *Leymus chinensis*, a xerophilous grass adapted to high pH sodic soil. *Plant Science* **170**: 1081-1086
- Kakei Y, Ishimaru Y, Kobayashi T, Yamakawa T, Nakanishi H, Nishizawa NK** (2012) OsYSL16 plays a role in the allocation of iron. *Plant Molecular Biology* **79**: 583-594
- Kochian LV, Hoekenga OA, Piñeros MA** (2004) How do crop plants tolerate acid soils? Mechanisms of aluminum tolerance and phosphorous efficiency. *Annual Review of Plant Biology* **55**: 459-493
- Landsberg EC** (1981) Organic-acid synthesis and release of hydrogen-ions in response to Fe deficiency stress of mono-leonous and dicoty-leonous plant-species. *Journal of Plant Nutrition* **3**: 579-591
- Lee JA** (1999) The calcicole-calcifuge problem revisited. *In* JA Callow, ed, *Advances in Botanical Research Incorporating Advances in Plant Pathology*, Vol 29, Vol 29. Academic Press Ltd-Elsevier Science Ltd, London, pp 1-30
- Li J, Xu H-H, Liu W-C, Zhang X-W, Lu Y-T** (2015) Ethylene Inhibits Root Elongation during Alkaline Stress through AUXIN1 and Associated Changes in Auxin Accumulation. *Plant Physiology* **168**: 1777-1791
- Lopez-Bucio J, de la Vega OM, Guevara-Garcia A, Herrera-Estrella L** (2000) Enhanced phosphorus uptake in transgenic tobacco plants that overproduce citrate. *Nature Biotechnology* **18**: 450-453
- Lopez-Bucio J, Nieto-Jacobo MF, Ramirez-Rodriguez V, Herrera-Estrella L** (2000) Organic acid metabolism in plants: from adaptive physiology to transgenic varieties for cultivation in extreme soils. *Plant Science* **160**: 1-13
- Ma G, Rengasamy P, Rathjen AJ** (2003) Phytotoxicity of aluminium to wheat plants in high-pH solutions. *Australian Journal of Experimental Agriculture* **43**: 497-501
- Ma JF, Ryan PR, Delhaize E** (2001) Aluminium tolerance in plants and the complexing role of organic acids. *Trends in Plant Science* **6**: 273-278
- McDonald GK, Taylor J, Verbyla A, Kuchel H** (2013) Assessing the importance of subsoil constraints to yield of wheat and its implications for yield improvement. *Crop and Pasture Science* **63**: 1043-1065
- Mekonnen DW, Flugge UI, Ludewig F** (2016) Gamma-aminobutyric acid depletion affects stomata closure and drought tolerance of *Arabidopsis thaliana*. *Plant Science* **245**: 25-34

- Meng C, Quan TY, Li ZY, Cui KL, Yan L, Liang Y, Dai JL, Xia GM, Liu SW** (2017) Transcriptome profiling reveals the genetic basis of alkalinity tolerance in wheat. *BMC Genomics* **18**: 14
- Meyer A, Eskandari S, Grallath S, Rentsch D** (2006) AtGAT1, a high affinity transporter for gamma-aminobutyric acid in *Arabidopsis thaliana*. *Journal of Biological Chemistry* **281**: 7197-7204
- Narayanan S, Mohan A, Gill KS, Prasad PVV** (2014) Variability of Root Traits in Spring Wheat Germplasm. *Plos One* **9**: 15
- Newman I** (2001) Ion transport in roots: measurement of fluxes using ion-selective microelectrodes to characterize transporter function. *Plant, Cell & Environment* **24**: 1-14
- Pfaffl MW** (2001) A new mathematical model for relative quantification in real-time RT-PCR. *Nucleic Acids Research* **29**: 2002-2007
- Raghothama KG** (1999) Phosphate acquisition. *Annual Review of Plant Physiology and Plant Molecular Biology* **50**: 665-693
- Raman H, Zhang KR, Cakir M, Appels R, Garvin DF, Maron LG, Kochian LV, Moroni JS, Raman R, Imtiaz M, Drake-Brockman F, Waters I, Martin P, Sasaki T, Yamamoto Y, Matsumoto H, Hebb DM, Delhaize E, Ryan PR** (2005) Molecular characterization and mapping of ALMT1, the aluminium-tolerance gene of bread wheat (*Triticum aestivum* L.). *Genome* **48**: 781-791
- Ramesh SA, Kamran M, Sullivan W, Chirkova L, Okamoto M, Degryse F, McLauchlin M, Gilliam M, Tyerman SD** (2018) Aluminium-Activated Malate Transporters Can Facilitate GABA Transport. *The Plant Cell* DOI: <https://doi.org/10.1105/tpc.17.00864>
- Ramesh SA, Tyerman SD, Xu B, Bose J, Kaur S, Conn V, Domingos P, Ullah S, Wege S, Shabala S, Feijo JA, Ryan PR, Gilliam M** (2015) GABA signalling modulates plant growth by directly regulating the activity of plant-specific anion transporters. *Nature Communications* **6**: 7879-1-7879-9.
- Rengasamy P, Olsson K** (1991) Sodicity and soil structure. *Soil Research* **29**: 935-952
- Ryan P, Delhaize E, Jones D** (2001) Function and mechanism of organic anion exudation from plant roots. *Annual Review of Plant Biology* **52**: 527-560
- Ryan P, Delhaize E, Randall P** (1995) Characterisation of Al-stimulated efflux of malate from the apices of Al-tolerant wheat roots. *Planta* **196**: 103-110
- Ryan PR, Delhaize E, Randall PJ** (1995) Characterization of Al-stimulated efflux of malate from the apices of al-tolerant wheat roots. *Planta* **196**: 103-110

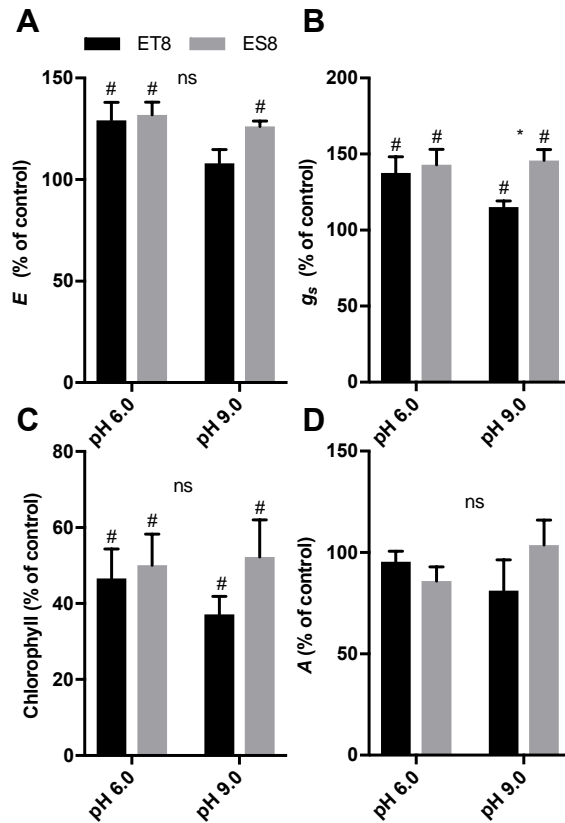
- Ryan PR, Raman H, Gupta S, Sasaki T, Yamamoto Y, Delhaize E** (2010) The multiple origins of aluminium resistance in hexaploid wheat include *Aegilops tauschii* and more recent cis mutations to TaALMT1. *Plant Journal* **64**: 446-455
- Ryan PR, Skerrett M, Findlay GP, Delhaize E, Tyerman SD** (1997) Aluminum activates an anion channel in the apical cells of wheat roots. *Proceedings of the National Academy of Sciences of the United States of America* **94**: 6547-6552
- Ryan PR, Tyerman SD, Sasaki T, Furuichi T, Yamamoto Y, Zhang WH, Delhaize E** (2011) The identification of aluminium-resistance genes provides opportunities for enhancing crop production on acid soils. *Journal of Experimental Botany* **62**: 9-20
- Sasaki T, Yamamoto Y, Ezaki B, Katsuhara M, Ahn SJ, Ryan PR, Delhaize E, Matsumoto H** (2004) A wheat gene encoding an aluminum-activated malate transporter. *The Plant Journal* **37**: 645-653
- Silva CMS, Zhang CY, Habermann G, Delhaize E, Ryan PR** (2018) Does the major aluminium-resistance gene in wheat, TaALMT1, also confer tolerance to alkaline soils? *Plant and Soil* **424**: 451-462
- Thwaites DT, Basterfield L, McCleave PMJ, Carter SM, Simmons NL** (2000) Gamma-aminobutyric acid (GABA) transport across human intestinal epithelial (Caco-2) cell monolayers. *British Journal of Pharmacology* **129**: 457-464
- Wang H, Lin X, Cao S, Wu Z** (2015) Alkali tolerance in rice (*Oryza sativa* L.): growth, photosynthesis, nitrogen metabolism, and ion homeostasis. *Photosynthetica* **53**: 55-65
- Warren CR** (2015) Wheat roots efflux a diverse array of organic N compounds and are highly proficient at their recapture. *Plant and Soil* **397**: 147-162
- Wong VN, Dalal RC, Greene RS** (2008) Salinity and sodicity effects on respiration and microbial biomass of soil. *Biology and Fertility of Soils* **44**: 943-953
- Xu W, Jia L, Baluška F, Ding G, Shi W, Ye N, Zhang J** (2012) PIN2 is required for the adaptation of Arabidopsis roots to alkaline stress by modulating proton secretion. *Journal of Experimental Botany* **63**: 6105-6114
- Xu W, Jia L, Shi W, Baluška F, Kronzucker HJ, Liang J, Zhang J** (2013) The tomato 14-3-3 protein TFT4 modulates H<sup>+</sup> efflux, basipetal auxin transport, and the PKS5-J3 pathway in the root growth response to alkaline stress. *Plant Physiology* **163**: 1817-1828
- Yang Y, Qin Y, Xie C, Zhao F, Zhao J, Liu D, Chen S, Fuglsang AT, Palmgren MG, Schumaker KS** (2010) The Arabidopsis chaperone J3 regulates the plasma membrane H<sup>+</sup>-ATPase through interaction with the PKS5 kinase. *The Plant Cell* **22**: 1313-1332

- Yu Y, Duan XB, Ding XD, Chen C, Zhu D, Yin KD, Cao L, Song XW, Zhu PH, Li Q, Nisa ZU, Yu JY, Du JY, Song Y, Li HQ, Liu BD, Zhu YM** (2017) A novel AP2/ERF family transcription factor from Glycine soja, GsERF71, is a DNA binding protein that positively regulates alkaline stress tolerance in Arabidopsis. *Plant Molecular Biology* **94**: 509-530
- Zhang G, Bown AW** (1997) The rapid determination of  $\gamma$ -aminobutyric acid. *Phytochemistry* **44**: 1007-1009
- Zhang H, Liu XL, Zhang RX, Yuan HY, Wang MM, Yang HY, Ma HY, Liu D, Jiang CJ, Liang ZW** (2017) Root Damage under Alkaline Stress Is Associated with Reactive Oxygen Species Accumulation in Rice (*Oryza sativa* L.). *Frontiers in Plant Science* **8**: 12
- Zhang WH, Ryan PR, Tyerman SD** (2001) Malate-permeable channels and cation channels activated by aluminum in the apical cells of wheat roots. *Plant Physiology* **125**: 1459-1472

### 3.7 SUPPLEMENTAL MATERIAL



**Supplemental Figure S1. Effect of GABA in the nutrient solution at each pH on root and shoot growth of ET8 and ES8 wheat plants.** Near-isogenic wheat lines ET8 (black bars) and ES8 (grey bars) were grown in pots for 5 weeks supplied with nutrient solution plus or minus 10 mM GABA at pH 6 and pH 9. All values are percentage of the control (without GABA): **(A)** Shoot fresh mass, **(B)** Root fresh mass, **(C)** Root length **(D)** Root surface area. Different letter combination for a genotype indicates significant difference ( $P < 0.05$ ) between pHs (lower case = ET8, upper case = ES8) using two-way ANOVA and post-tests. ns = no significant differences  $P > 0.05$ .



**Supplemental Figure S2. Effect of GABA in the nutrient solution at each pH on leaf gas exchange of ET8 and ES8 wheat plants.** Near-isogenic wheat lines ET8 (black bars) and ES8 (grey bars) were grown in pots for 5 weeks supplied with nutrient solution plus or minus 10 mM GABA at pH 6 and pH 9. All values are percentage of the control (without GABA): **(A)** Transpiration rate ( $E$ ), **(B)** Stomatal conductance ( $g_s$ ), **(C)** Chlorophyll content measured using SPAD, **(D)** Net assimilation rate ( $A$ ). \* indicates significant difference between genotypes at a particular pH,  $P < 0.05$ . Different letter combination for a genotype indicates significant difference ( $P < 0.05$ ) between pHs (lower case = ET8, upper case = ES8) using two-way ANOVA and post-tests. ns = no significant differences. # = significantly different to 100% ( $P < 0.05$ ).

## Supplemental Table S1

### Genbank accessions and primers used for Figure 7

Gene	Genbank		Primer (5' – 3')
Cyclophilin	EU035525.1	F	CAAGCCGCTGCACTACAAGG
		R	AGGGGACGGTGCAGATGAA
GAPDH	EF592180.1	F	TTCAACATCATTCCAAGCAGCA
		R	CGTAACCCAAAATGCCCTTG
Tubb4	U76895.1	F	AGTTCACGGCCATGTTCA
		R	ACGAGGTCGTTTCATGTTGCT
Actin	KC775782	F	TCACACCTTCTACAATGAGCTCCGTGT
		R	ATCCAGACACTGTACTTCCTT
TaALMT1	DQ072260.1	F	AAATCGCGGAATGTGTTGAT
		R	ATAACCACGTCAGGCAAAGG
GAD	AK331230.1	F	AAGGTCATGGTGGAGATGGA
		R	CAAACCAGGCTGTGCTTCTT
GAD1	AK331897.1	F	ACGCCATCAAGCTGTCCAA
		R	AGACTCCGGCCTTCTTGTC
GABA T	AK333709.1	F	TATTTGGTGCCGAGTGTGAG
		R	TTCAACTTCATCGGGAGTCA

Genbank accession numbers for the housekeeping genes and TaALMT1 listed in Table above are: Actin KC775782; Tubb4 U76895.1; Cyclophilin EU035525.1; GAPDH EF592180.1; TaALMT1 DQ072260.1.

### 3.8 APPENDIX TO CHAPTER 3

These results support some components of Chapter 3, but were not added to the submitted paper because either inappropriate controls were used (barley transgenics) or the experiments were only preliminary (hormone responses), and where time constraints prevented repetition or follow-on experiments. These issues will be identified in the following description of the Figures.

#### **Growth and shoot gas exchange of transgenic barley expressing TaALMT1 at alkaline pH.**

Five-week long growth experiments were performed similar to that for the wheat ET8-ES8 comparison but using golden promise barley expressing *TaALMT1* under a constitutive promoter (Delhaize et al., 2004) and Golden promise as the control. In this case it would have been more appropriate to have used the null transformant line as the control as in (Ramesh et al. 2015).

There was no significant effect of *TaALMT1* expression on shoot growth at both pHs (Figure A1A), however root fresh mass was more sensitive to pH for TaALMT1-GP (Figure A1B) with a significantly larger root fresh mass at pH 9 than at pH 6, but there was no difference between genotypes at either pH. GABA treatment significantly reduced both shoot fresh mass and root fresh mass independently of TaALMT1 expression and inhibition was greater for shoot fresh mass at pH 9 (Figure A2A, B).

Leaf gas exchange and photosynthesis was also compared for the 5-week old seedlings at the two pHs (Figure A1C,D,E,F) carried out as described in the Methods of Chapter 3. Transpiration ( $E$ ) and  $g_s$  were significantly higher at both pH 6 and pH 9 for TaALMT1-GP compared to GP. Relative chlorophyll concentration was also higher for TaALMT1-GP leaves compared to GP at pH 9 (Figure A1E) but there was no significant effects on  $A$  (Figure A1F). GABA treatment had little effect on  $E$  and  $g_s$  for both TaALMT1-GP and GP (Figure A2C,D) but the effect of GABA was more pH-dependent for TaALMT1-GP (Figure A2D). Relative chlorophyll concentration was significantly inhibited by GABA only in the TaALMT1-GP plants (Figure A2E). There was no significant differences in  $A$  between genotypes and pH though TaALMT1-GP had a significant inhibition at pH 6 (Figure A2F).

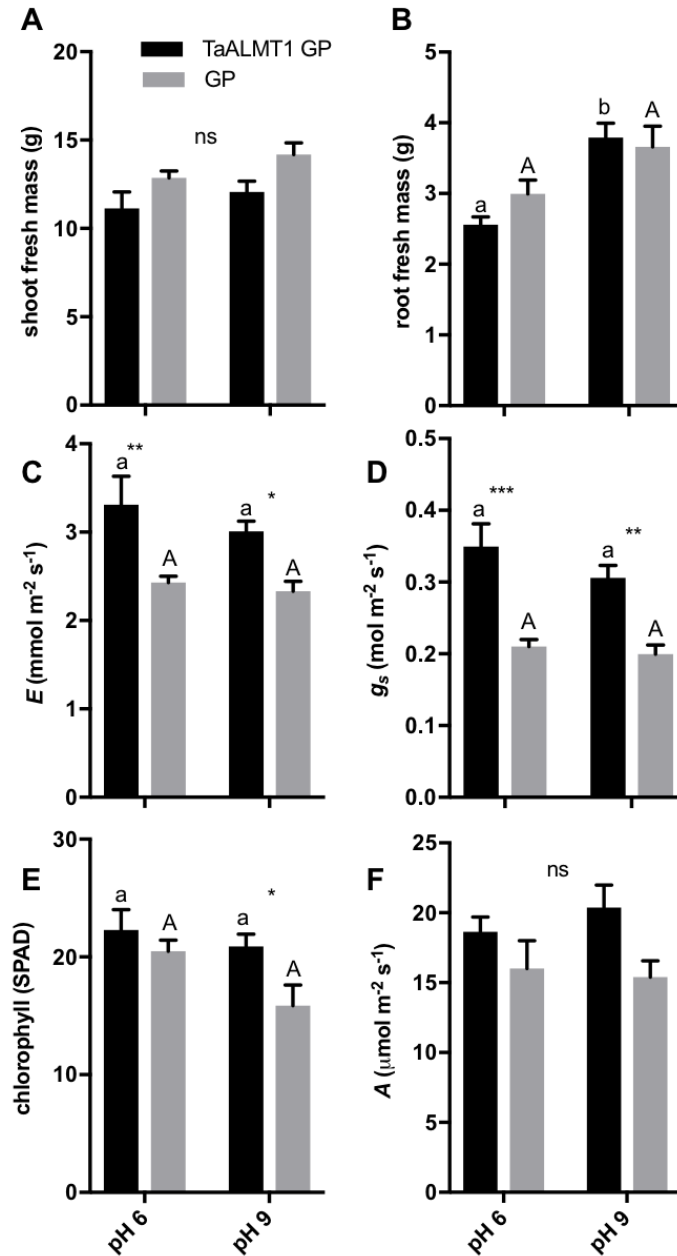


**Figure A1. The effect of alkaline pH on growth and leaf gas exchange of transgenic barley overexpressing TaALMT1 (TaALMT1 GP) and Golden Promise (GP) background.** Conditions were as in Figure 1 and 2. (A) Shoot fresh mass, (B) Root fresh mass, (C) Transpiration ( $E$ ), (D) Stomatal conductance ( $g_s$ ), (E) Chlorophyll content measured using SPAD, (F) Net assimilation rate ( $A$ ). \*, \*\*, \*\*\*, indicate significant difference between genotypes at a given pH  $P < 0.05$ ,  $0.01$ ,  $0.001$ , respectively. Different letter combination for a genotype indicates significant difference ( $P < 0.05$ ) between pHs (lower case = TaALMT1-GP, upper case = GP) using two-way ANOVA and post-tests. ns = no significant differences.

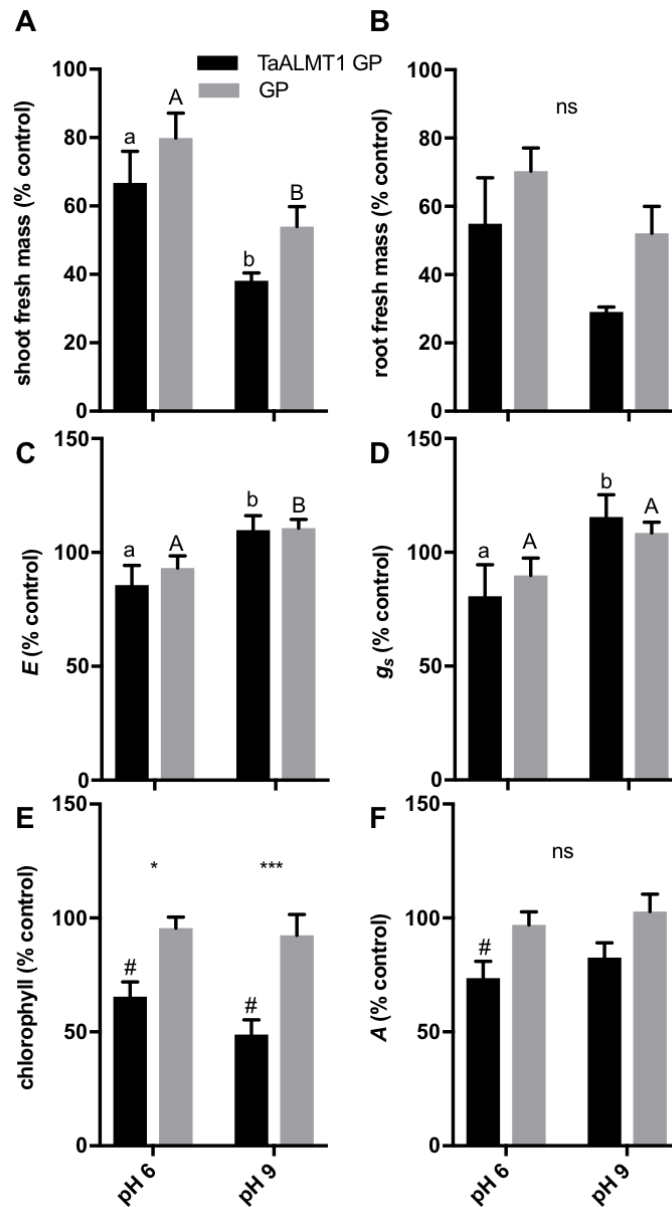


**Figure A2. The effect of GABA in the nutrient solution at pH 6 and pH 9 on plant growth of transgenic barley overexpressing TaALMT1 (TaALMT1 GP) and golden promise (GP) background.** TaALMT1 GP (black bars) and GP (grey bars) were grown in pots for 5 weeks supplied with nutrient solution plus or minus 10 mM GABA at pH 6 and pH 9. All values are percentage of the control (without GABA): (A) Shoot fresh mass, (B) Root fresh mass, (C) Transpiration ( $E$ ), (D) Stomatal conductance ( $g_s$ ), (E) Chlorophyll content measured using SPAD, (F) Net assimilation rate ( $A$ ). \*, \*\*\*, indicate significant difference between genotypes at a given pH  $P < 0.05$ ,  $0.001$ , respectively. Different letter combination for a genotype indicates significant difference ( $P < 0.05$ ) between pHs (lower case = TaALMT1 GP, upper case = GP) using two-way ANOVA and post-tests. ns = no significant differences.

### **Estimates of rhizosphere malate and GABA concentrations for TaALMT1-GP and GP barley and comparison with ET8 and ES8 wheat.**

Pots with rooted plants used in the experiments described above were flushed with a constant volume of treatment solution and allowed to drain to capture a root-wash eluate. GABA and malate concentrations of the eluate were measured and an estimate was made of the rhizosphere malate and GABA concentrations on a per root fresh mass basis (Figure A3). Rhizosphere malate estimates are shown comparing ET8 and ES8 plants in Figure A3A (also shown in Chapter 3, shown here for comparison with transgenic barley) and for TaALMT1-GP versus GP in Figure A3B. Similar to ET8 versus ES8, the TaALMT1-GP plants had higher rhizosphere malate at pH 9 than the GP plants, however the opposite was the case at pH 6 and furthermore there was no significant difference in rhizosphere malate for TaALMT1-GP plants between pH 6 to pH 9 (Figure A3B). There was a significantly lower rhizosphere malate at pH 9 compared to pH 6 for GP plants.

GABA treatment significantly affected rhizosphere malate for the TaALMT1-GP and GP plants with different effects between TaALMT-GP and GP (Figure A3D). While there was no significant effect of GABA treatment on rhizosphere malate for TaALMT1-GP plants, GABA treatment significantly increased malate at pH 9 for the GP plants and decreased malate at pH 6. This was similar to the effect of GABA on ES8 at pH 9 (Figure A3C)

Rhizosphere GABA estimations were also made for the non-GABA treated plants (Figure A3E,F). For the TaALMT1-GP and GP plants the results largely reflected those for malate, as was also the case for the ET8/ES8 comparison, with significantly higher rhizosphere GABA in TaALMT1-GP compared to GP at pH 9. The opposite occurred at pH 6 and no significant difference in GABA between pH 6 and 9 for the TaALMT1-GP plants (Figure A3F).

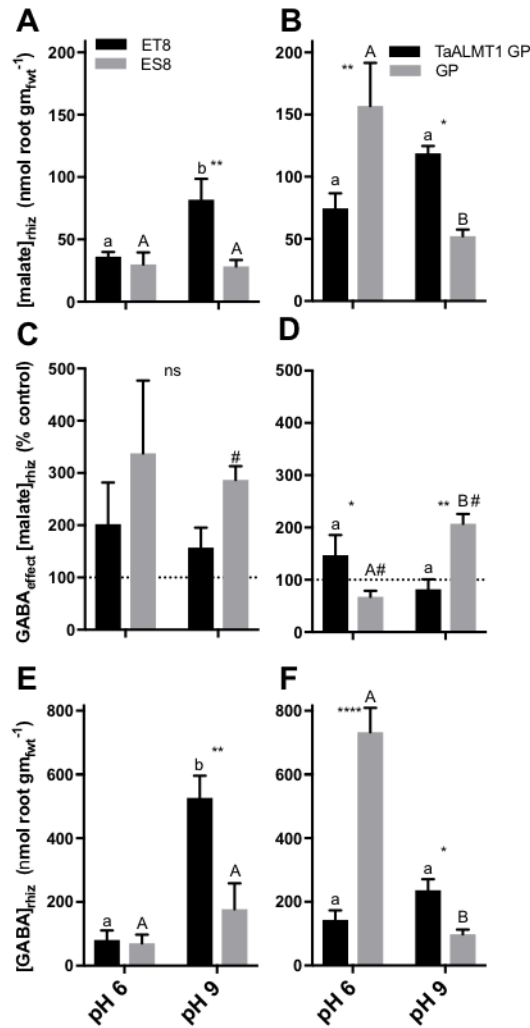


**Figure A3. Estimates of rhizosphere malate and GABA for ET8 and ES8 (A,C,E), TaALMT1-GP and GP (B,D,F) plants in response to nutrient solution pH and the effect of 10 mM GABA on malate concentration. (A,B)** Malate concentration estimated for the rhizosphere. **(C,D)** Effect of 10 mM GABA on the estimated rhizosphere malate concentration (% of the control without GABA). **(E,F)** GABA concentration estimated for the rhizosphere. Root washes were measured for plants *in situ* after five weeks of growth. For **A, B** and **E, F** values are normalised to the root fresh weight of each replicate plant. In each case different letter combination for a genotype indicates significant difference ( $P < 0.05$ ) between pHs (lower case = ET8 or TaALMT1 GP, upper case = ES8 or GP) and \*, \*\*, \*\*\*, \*\*\*\* indicate significant difference between genotypes at a given pH  $P < 0.05, 0.01, 0.01, 0.0001$ , respectively (two-way ANOVA with post-tests). ns = no significant differences, # = significantly different from 100%.

## Efflux of malate and GABA from root apices and intact seedling roots at high pH

The efflux of malate and GABA from excised root apices over 1 h was measured from 3-day old seedling roots of TaALMT1-GP and GP plants exposed to solutions at pH 6 and pH 9 (Figure A4). Again the ET8/ES8 comparison is reproduced from Chapter 3 for comparison with the transgenic barley. For malate efflux there was no significant genotype effect between TaALMT1-GP and GP with both genotypes increasing malate efflux at high pH (Figure A4B). In contrast there was a genotype effect for GABA efflux with higher GABA efflux for TaALMT1-GP than GP at pH 9 in buffered solution (Figure A4D). The results for the transgenic TaALMT1-GP barley were generally weaker in their response to high pH than was observed for ET8 (Figure A4C).

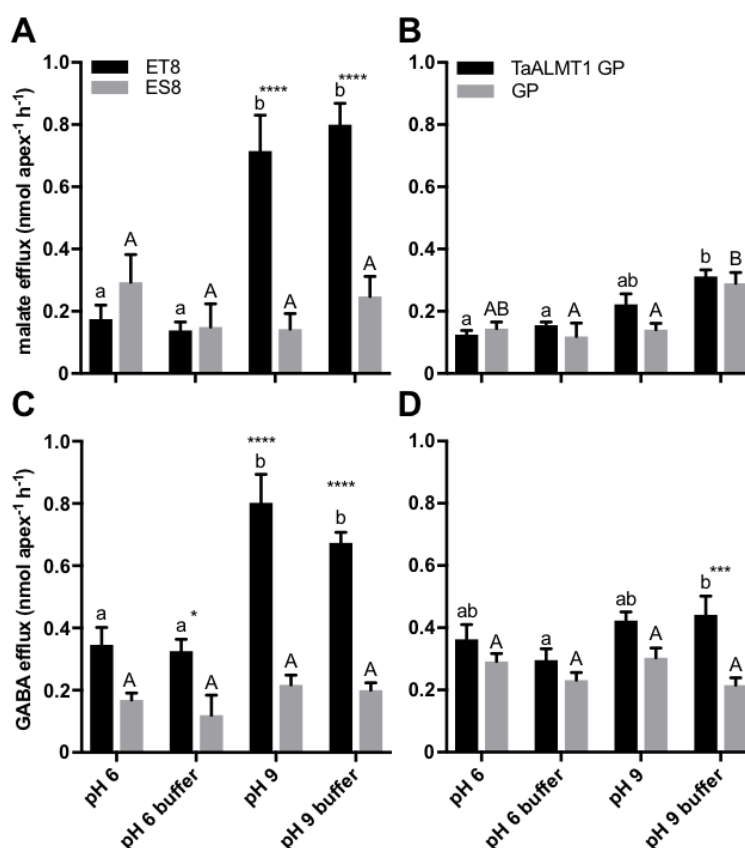


**Figure A4. Root tip exudation of malate (A,B) and GABA (C,D) at pH 6 and 9 (+/- buffer) comparing wheat ET8 and ES8 (A,C), and barley TaALMT1-GP and GP (B,D).** Net flux was measured over 1 h after placing excised root tips in different pH +/- buffer (all 3 mM CaCl<sub>2</sub>, 10 mM Na<sub>2</sub>SO<sub>4</sub>): **pH 6**, 0.01 mM NaOH; **pH 6 buffer**, 5 mM MES, 2.6 mM NaOH; **pH 9**: 0.05 mM NaOH, **pH 9 + buffer**, 5 mM BTP, 2 mM MES. In each case different letter combination for a genotype indicates significant difference ( $P < 0.05$ ) between pHs (lower case = ET8 or TaALMT1 GP, upper case = ES8 or GP) and \*, \*\*\*, \*\*\*\* indicate significant difference between genotypes at a given pH  $P < 0.05$ , 0.001, 0.0001, respectively (two-way ANOVA and post-tests).

### **Efflux of malate and GABA from intact seedling roots and root growth in response to sodium aluminate at high pH.**

To understand the possible role of TaALMT1 in aluminium tolerance under alkaline conditions, the effect of added aluminate at pH 9 was examined for the wheat NILs (ET8 & ES8) and transgenic barley overexpressing TaALMT1-GP. Three-days old seedlings were bathed in pH 9 basal solution composed of 3 mM CaCl<sub>2</sub> (pH with NaOH) and  $\pm$  100  $\mu$ M sodium aluminate for 22 hours. There was a significantly higher malate efflux from ET8 roots in both basal (pH 9) and plus sodium aluminate treatments when compared with ES8, and there was a significant elevation in malate efflux comparing pH 9 basal and pH 9 plus aluminate for ET8 (Figure A5A). There was no significant effect of pH 9 basal and plus aluminate on malate efflux from ES8 seedlings. There was also a large increase in GABA efflux from ET8 seedlings at pH 9 plus aluminate compared with pH 9 basal, and both were (with or without aluminate) significantly higher in ET8 compared to ES8 (Figure A5C). There was no significant effect of the addition of aluminate on GABA efflux from ES8 seedlings.

For malate efflux in barley, TaALMT1-GP showed a significantly higher malate efflux at pH 9 basal plus aluminate compared with GP, confirming results shown in Figure A3. However, there was no significant genotype effect between TaALMT1-GP and GP malate efflux at pH 9 basal (Figure A5B) confirming the results for root tip efflux in Figure A4D. On the other hand, aluminate had a large stimulatory effect on malate efflux from the TaALMT1-GP roots (Figure A5B). There was a significant genotype effect for GABA efflux with higher GABA efflux for TaALMT1-GP than GP at both pH 9 basal and pH 9 basal plus aluminate (Figure A5D). Again aluminate significantly stimulated the efflux of GABA.

Root growth over 22 hours was also measured in this experiment. There was a significantly higher root growth for ET8 compared with ES8 at both pH 9 basal and pH 9 basal plus aluminate (Figure A6A). There was no difference in ES8 root growth between the treatments. In contrast to ET8 and ES8, there was no significant genotype effect between TaALMT1-GP and GP for root growth in response to pH 9 basal condition, however, TaALMT1-GP showed a significantly higher root growth compared with GP at pH 9 plus aluminate (Figure A6B).

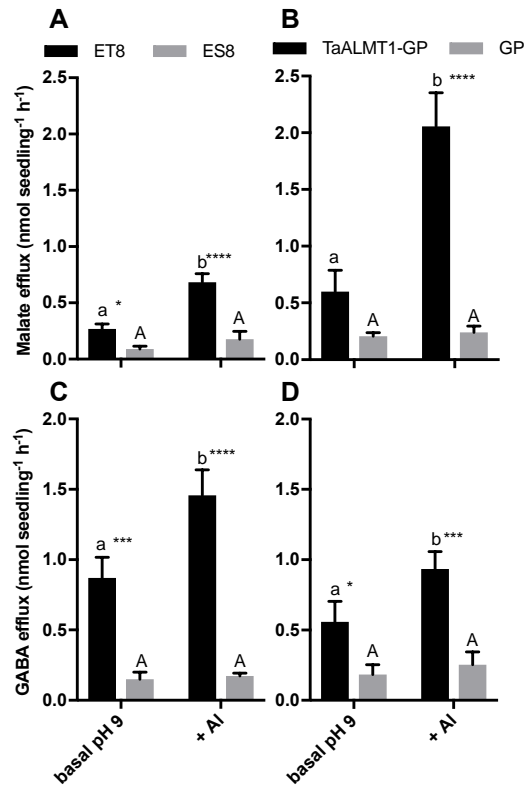


**Figure A5.** Efflux of malate (A,B) and GABA (C,D) in 3-day old seedlings of ET8 and ES8 wheat (A,C) and TaALMT1-GP and GP barley (B,D) in response to high pH (initially 9) and high pH plus 100 μM aluminate. The basal bathing solution was composed of 3 mM CaCl<sub>2</sub> pH 9 (NaOH). Fluxes were measured from individual seedlings (per replicate) over a 22 h incubation period (n=5). In each case different letter combination for a genotype indicates significant difference (P<0.05) between pHs (lower case = ET8 or TaALMT1-GP, upper case = ES8 or GP) \*, \*\*, \*\*\*, \*\*\*\* indicate significant difference between genotypes at a given pH P < 0.05, 0.01, 0.001, 0.0001, respectively (two-way ANOVA and post-tests).

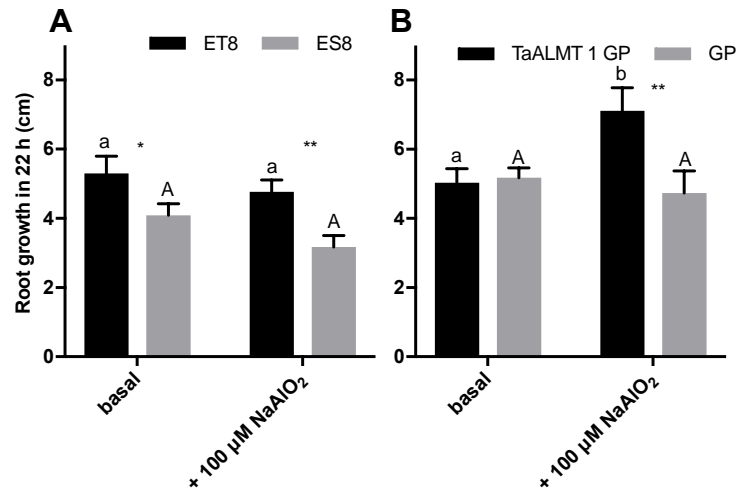


**Figure A6.** Root growth over 22 h in 3-day old seedlings of ET8 and ES8 wheat (A) and TaALMT1-GP and GP barley (B) in response to high pH (initially 9) and high pH plus 100  $\mu\text{M}$  aluminate. The basal bathing solution was composed of 3 mM CaCl<sub>2</sub> pH 9 (NaOH). Root growth of individual seedlings (per replicate) over a 22 h incubation period (n=8). In each case different letter combination for a genotype indicates significant difference ( $P < 0.05$ ) between pHs (lower case = ET8 or TaALMT1-GP, upper case = ES8 or GP) \*\* indicate significant difference between genotypes at a given pH  $P < 0.01$  (two-way ANOVA and post-tests).

### **Effect of pH on current -voltage curves of *Xenopus laevis* oocytes expressing TaALMT1 and controls**

Two-electrode voltage clamp (TEVC) was used to test if anion currents from *TaALMT1* expressing *Xenopus laevis* oocytes were transactivated by the addition of an external anion (as 10 mM Na<sub>2</sub>SO<sub>4</sub>) at pH 9 as shown previously for pH 7.5 (Ramesh et al 2015). Oocytes were injected with 32.2 ng of *TaALMT1* cRNA or water (controls) and incubated for 24h in Ca Ringers solution supplemented with tetracyclin and penicillin-streptomycin. The oocytes were incubated in Ca Ringers solution with 10 mM Na-malate overnight prior to TEVC experiments in order to pre-load the eggs with malate (Ramesh et al. 2015). The oocytes were perfused in either 0.7 mM CaCl<sub>2</sub>, mannitol to 220 mOsm kg<sup>-1</sup> and  $\pm$  10 mM sodium sulphate (Na<sub>2</sub>SO<sub>4</sub>) at pH 7 or pH 9 (NaOH was used to adjust the pH) and currents were recorded. Control oocytes did not respond to solutions at either pH (Figure A7A,B). *TaALMT1* oocytes showed greater variability, probably due to variations between replicates in degree of expression. *TaALMT1* expressing oocytes showed both increased inward and outward currents relative to controls in response to Na<sub>2</sub>SO<sub>4</sub>, however there was no significant effect of pH (Figure A7CD). These data are relevant to Figure 8 in Chapter 3 (MIFE experiments) on *Xenopus* oocytes, since it shows that the oocytes are quite tolerant of exposure to pH 9 (Control IV curves unchanged, Figure A7A,B). The data also shows that TaALMT1 was active but not so sensitive to increased pH in terms of the electrogenic (anion) current through the transporter, noting that GABA is a neutral molecule at cytosolic pH and therefore would not be registered as an ionic current when effluxed from the oocyte. The data in Figure 8 of Chapter 3 shows a stimulated GABA efflux from TaALMT1 expressing oocytes at high pH.

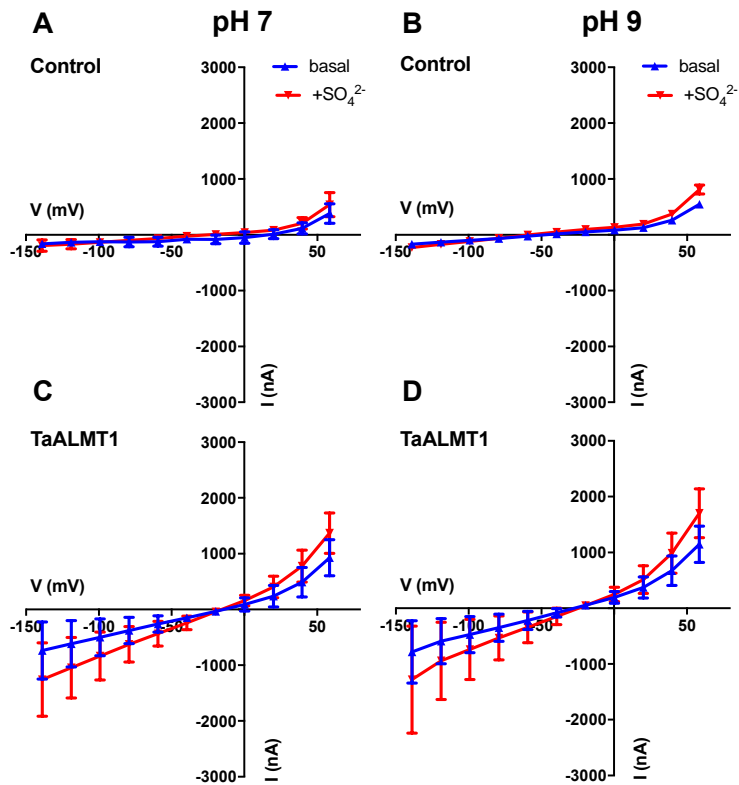


**Figure A7.** Effect of pH on current -voltage curves of *Xenopus laevis* oocytes expressing TaALMT1 and controls during two- electrode voltage clamp experiments. Control oocytes injected with water (A, B). TaALMT1 injected oocytes (C, D). Conductance in basal solution was higher in TaALMT1 oocytes compared to controls and were slightly activated by the addition of 10 mM Na<sub>2</sub>SO<sub>4</sub>. There was no significant effect of high pH on conductance for either water injected controls or TaALMT1 expressing oocytes. Data are mean SE of n=7-8 oocytes. . This data supports Figure 8 in Chapter 2, where proton fluxes were measured at high pH from oocytes. Importantly the high pH did not appear to compromise the integrity of the oocyte membrane.

### **Effect of exogenous GABA and muscimol application on malate efflux from intact seedling roots at low and high pH**

Previously, it had been shown by Ramesh et al (2015) that Al<sup>3+</sup> activates TaALMT1 to efflux malate in acidic (pH 4.5) conditions and that this efflux was blocked by GABA and muscimol (an analog of GABA). Ramesh et al (2015) also showed that the anion current was inhibited at pH 7.5 by these molecules. However, it was not known if TaALMT1 inhibition by GABA and muscimol occurred at more extreme alkaline pH. To confirm the previous findings by Ramesh et al (2015) and to test whether GABA and muscimol can block TaALMT1 mediate malate efflux at high pH, a series of experiments were performed using wheat Nil ET8 (Al<sup>3+</sup> tolerant) seedlings. Upon Al<sup>3+</sup> treatment (100 μM) at pH 4.5 a large malate efflux occurred over 22h, and this was inhibited by exogenous GABA (10 mM) and muscimol (10 μM) (Figure A8A, C). This

confirmed previous observations by Ramesh et al (2015). On the other hand, at pH 9 (buffered, with and without 10 mM Na<sub>2</sub>SO<sub>4</sub>) malate efflux was as high as the Al<sup>3+</sup>-activated efflux at pH 4.5, but this efflux was not inhibited by GABA or muscimol (Figure A8B,D). These data confirm the observation of no GABA effect on the rhizosphere malate concentration shown in Figure 3 (Chapter 3) in the 5 week seedling experiment at high pH.

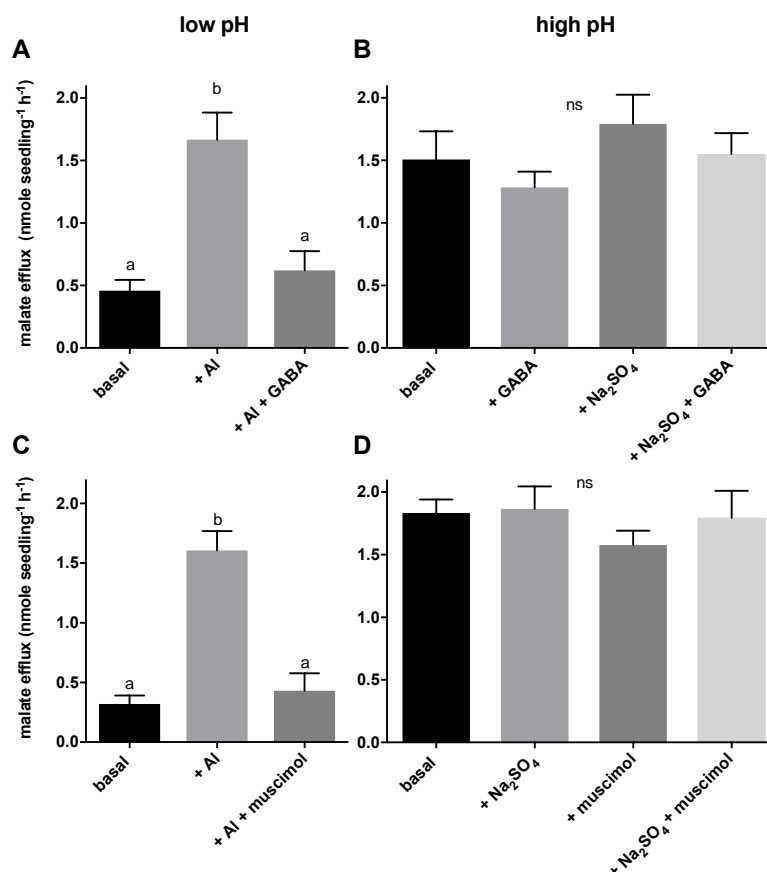


**Figure A8.** Muscimol and GABA do not block malate efflux from 3 day old wheat seedlings (ET8) over 22 h at high pH, but block occurs at low pH. Four separate experiments are shown (A, B, C, D). Each in a basal solution of 3 mM CaCl<sub>2</sub> with: 5 mM MES (pH 4.5) or 5 mM BTP (pH 9.0). GABA concentration was 10 mM, muscimol concentration was 10 μM. 10 mM Na<sub>2</sub>SO<sub>4</sub> was also added to some of the high pH treatments. Different letter combination indicates significant difference (P<0.05) (one way ANOVA and post-test). N=5-7 biological replicates each replicate being one seedling.

### **Effect of different concentrations of calcium on TaALMT1 mediated malate efflux.**

Previously, it had been demonstrated that aluminium toxicity was linked with the disturbance of cytoplasmic  $\text{Ca}^{2+}$  homeostasis in wheat, which may ultimately result in root growth inhibition (Zhang and Rengel, 1999). It is also well-established that TaALMT1 confers  $\text{Al}^{3+}$  tolerance by exuding malate to the rhizosphere that complexes the external  $\text{Al}^{3+}$  (Delhaize and Ryan, 1995; Sasaki et al., 2004; Ryan et al., 2011; Ramesh et al., 2015). Thus there may be a link between TaALMT1 activation and calcium. However, there appears to be no reports of the effect of exogenous calcium levels on TaALMT1-mediated malate efflux in the presence of  $\text{Al}^{3+}$ . To test the effect of external calcium on TaALMT1 mediated malate efflux, wheat near-isogenic lines (NILs) ET8 and ES8 were compared that differ in TaALMT1 expression levels (see Chapter 3, Figure 9) and sensitivity to  $\text{Al}^{3+}$  tolerance. A range of  $\text{CaCl}_2$  concentrations (0.1, 0.5, 1, 3 and 5mM)  $\pm$  100  $\mu\text{M}$   $\text{AlCl}_3$  were examined over a 22 hours incubation period. Except for 0.1 mM  $\text{CaCl}_2$ , all other  $\text{CaCl}_2$  concentrations (0.5, 1, 3 and 5mM) showed a significantly increased  $\text{Al}^{3+}$ -activated malate efflux in ET8 compared with ES8 (Figure A9). There was no significant effect of  $\text{CaCl}_2$  concentrations with and without aluminium on malate efflux from ES8 seedlings. The  $\text{CaCl}_2$  concentration that gave the largest response was 3 mM being significantly higher than the lower concentrations tested and also higher than that for 5 mM. There was no significant difference in malate efflux between ET8 and ES8 in all  $\text{CaCl}_2$  concentrations in the absence of aluminium.

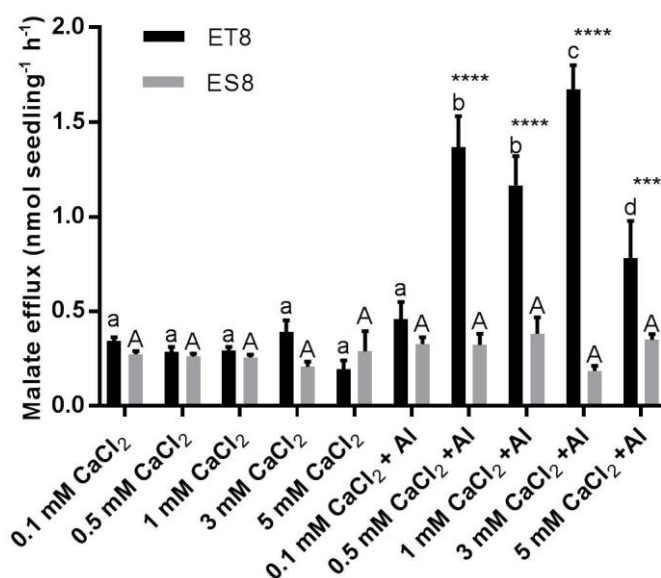


**Figure A9.** Apparent Ca<sup>2+</sup> sensitivity of malate efflux from 3-day old ET8 and ES8 wheat seedlings in response to 100 μM Al<sup>3+</sup> at pH 4.5. The CaCl<sub>2</sub> concentration that gave the largest response was 3 mM. Aluminium was added as 100 μM AlCl<sub>3</sub> at pH 4.6 with 5 mM MES. In each case different letter combination for a genotype indicates significant difference (P<0.05) between treatments (lower case = ET8, upper case = ES8) \*\*\*, \*\*\*\* indicate significant difference between genotypes at a given pH P < 0.001, 0.0001, respectively (two-way ANOVA and post-tests). N=5 biological replicates each replicate being one seedling.

### Effect of jasmonic acid and brassinosteroid on malate and GABA efflux and root growth in wheat.

Plant hormones such as ethylene, jasmonic acid (JA) and auxin have been reported to have a role in Al<sup>3+</sup> induced root growth inhibition (Tian et al., 2014; Yang et al., 2016). Another study demonstrated that brassinosteroid (BR) is involved in interaction with a root sucrose transporter (Bitterlich et al., 2014). Jasmonic acid was found to modulate ALMT1 mediated malate efflux and ultimately root growth inhibition in Arabidopsis (Yang et al., 2016) where it was proposed to be linked to ethylene production under Al<sup>3+</sup> stress. However, the mechanism of how JA regulates TaALMT1 is still unknown. Based on the above reports, it was hypothesized here that there might be links between TaALMT1 activity, root growth and regulatory pathways mediated by JA and BR. This is also relevant to the previous demonstration that ethylene inhibited TaALMT1 malate efflux induced by Al<sup>3+</sup> despite ethylene enhancing expression of TaALMT1 (Tian et al., 2014).

To test the hypothesis, 3 days old seedlings of wheat Nils ET8 and ES8 were used. Intact seedlings were bathed in treatment solutions for 22 hours and malate and GABA efflux were measured at the end of experiment as per previous experiments. Jasmonic acid at 1, 5 and 10 nM concentrations significantly increased Al<sup>3+</sup>-activated malate efflux in ET8 compared with

ES8 (Figure A10). However, malate efflux from ET8 seedling roots were not significantly different than ES8 in response to all three JA treatments without  $Al^{3+}$ . Jasmonic acid at 10 nM was found to give the largest response. As JA was dissolved in ethanol, an ethanol control was used but there was no significant difference between the ethanol control over basal solution for ET8 (ES8 was not examined in this respect). There was no significant effect of JA concentrations with and without  $Al^{3+}$  on malate efflux from ES8 seedlings (Figure A10 right).

Similarly, BR at 10 and 20 nM concentrations showed significantly higher  $Al^{3+}$ -activated malate efflux in ET8 compared with ES8 (Figure A11). However, malate efflux in response to 5 nM BR was not significantly different from that of the ET8  $Al^{3+}$  control. The ethanol control in this case resulted in a significant stimulation of malate efflux over basal solution in both genotypes. In ES8, 5 nM BR plus  $Al^{3+}$  resulted in significantly higher malate efflux over the  $Al^{3+}$  control (Figure A11 right).

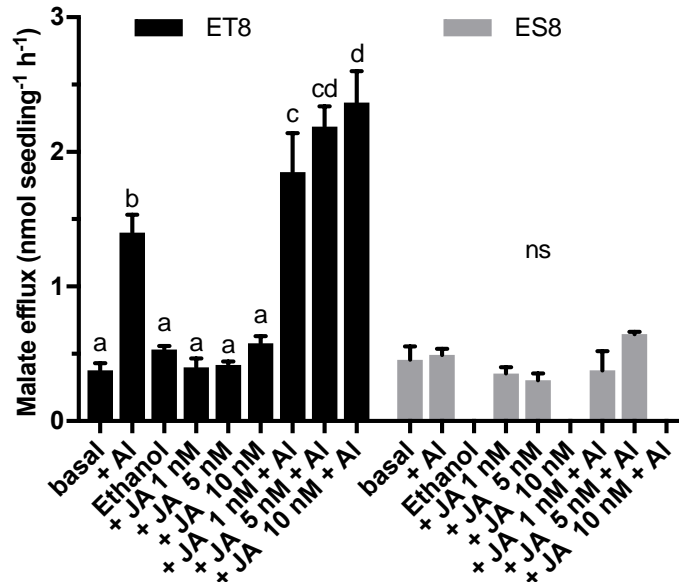


**Figure A10.** Potentiating effect of jasmonic acid (JA) on Al<sup>3+</sup> activated malate efflux from 3-day old ET8 wheat seedlings over 22 hours. Basal solution was 3 mM CaCl<sub>2</sub> 5 mM MES pH 4.5 and AlCl<sub>3</sub> was 100 μM. Jasmonic acid concentrations are shown and were added dissolved in an ethanol stock. An ethanol control was carried out with the same final ethanol concentration as the highest jasmonic acid concentration for ET8 seedlings. Different letter combination indicates significant difference (P<0.05) (one-way ANOVA with post-test) within a genotype. N=5 biological replicates each replicate being one seedling.

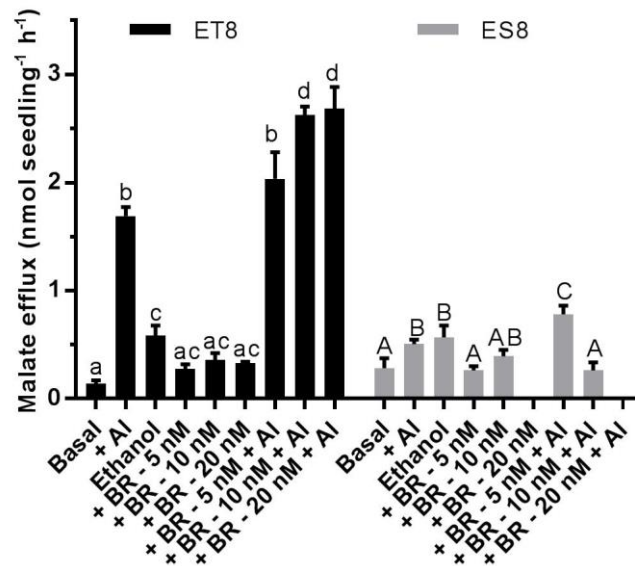


**Figure A11.** Effect of brassinosteroid (BR) on Al<sup>3+</sup> activated malate efflux from 3-day old ET8 and ES8 wheat seedlings over 22 hours. Ethanol control is also shown for each genotype, which gave a significant stimulation over the basal controls. Different letter combination indicates significant difference (P<0.05) (one-way ANOVA with post-test) within a genotype. N=5 biological replicates each replicate being one seedling.

The above experiments using JA and BR were repeated for ET8 seedlings (Figure A12), and the same responses to JA and BR were observed (Figure A12). An ethanol plus  $Al^{3+}$  control was also used but there was no significant difference in malate efflux between  $Al^{3+}$  control and  $Al^{3+}$  plus ethanol.

Interestingly, the response of  $Al^{3+}$ -activated GABA efflux to JA and BR were opposite to that of malate efflux (Figure A13). Both JA and BR treatment significantly reduced  $Al^{3+}$ -activated GABA efflux compared with the  $Al^{3+}$  treatment alone. There was no difference in GABA efflux between  $Al^{3+}$  control treatment and  $Al^{3+}$  plus ethanol control treatment. Jasmonic acid alone significantly stimulated GABA efflux compared with basal solution. In contrast, there was no significant difference in GABA efflux between BR and basal treatments (Figure A13).

Root growth of ET8 seedlings were measured after 22 hours of treatments in the same experiment reported in Figure 13. It was found that JA plus  $Al^{3+}$  significantly reduced root growth compared with  $Al^{3+}$  treatment alone (Figure A14) confirming the previous observation on Arabidopsis (Yang et al., 2016). On the other hand, interestingly, BR application plus  $Al^{3+}$  significantly enhanced root growth compared to  $Al^{3+}$  treatment alone (Figure A14). Brassinosteroid application alone also significantly enhanced root growth compared with basal treatment. Previously it was shown that BR stimulated root growth in Arabidopsis (Müssig et al., 2003). There was no difference in root growth between  $Al^{3+}$  control treatment and  $Al^{3+}$  plus ethanol treatment.

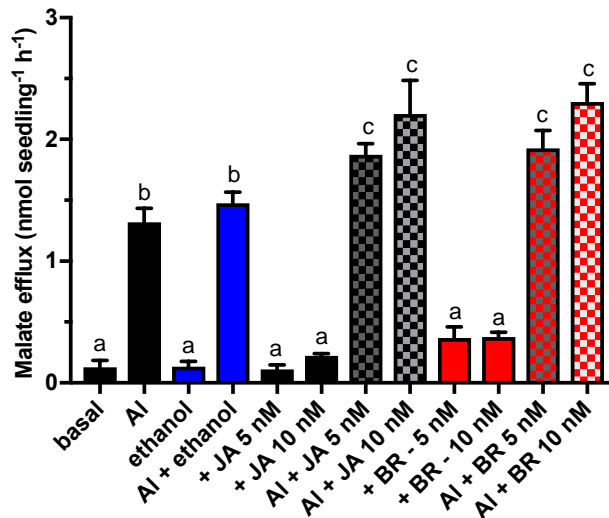


**Figure A12.** Repeated experiments of the effect of jasmonic acid (JA) and brassinosteroid (BR) on the Al<sup>3+</sup> activated malate efflux from 3-day old ET8 wheat seedlings measured over 22 h. Ethanol has no effect on the malate efflux in the presence of Al in this case and both jasmonic acid and brassinosteroid potentiated the Al response. Different letter combination indicates significant difference (P<0.05) (one-way ANOVA with post-test). N=5 biological replicates each replicate being one seedling.

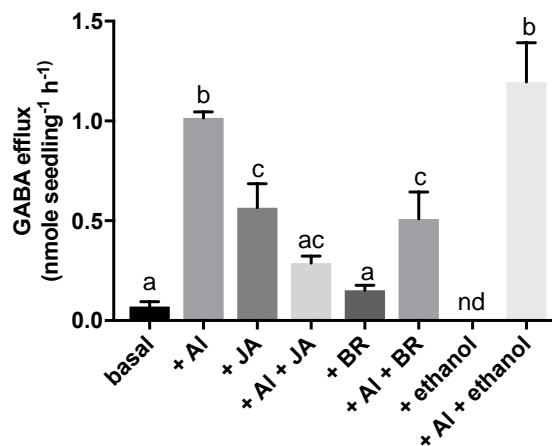


**Figure A13.** The effect of jasmonic acid (JA, 10 nM) and brassinosteroid (BR, 10 nM) on the Al<sup>3+</sup> (100 μM) activated GABA efflux from 3-day old ET8 wheat seedlings measured over 22 h. The effect on GABA efflux seemed to be opposite that on malate efflux, i.e. inhibition, though jasmonic acid by itself stimulated GABA efflux. Brassinosteroid also inhibited the GABA efflux. Different letter combination indicates significant difference (P<0.05) (one-way ANOVA with post-test). N=9-15 biological replicates each replicate being one seedling. nd= not detected.

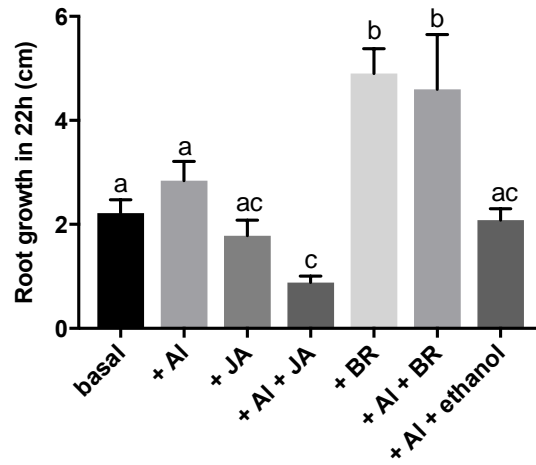


**Figure A14.** The effect of jasmonic acid (JA, 10 nM) and brassinosteroid (BR, 10 nM) on root growth of 3-day old ET8 wheat seedlings measured over 22 h. Brassinosteroid appeared to stimulate root growth. Different letter combination indicates significant difference ( $P < 0.05$ ) (one-way ANOVA with post-test).  $N = 5$  biological replicates each replicate being one seedling.

## References

- Bitterlich M, Krügel U, Boldt-Burisch K, Franken P, Kühn C** (2014) The sucrose transporter SISUT2 from tomato interacts with brassinosteroid functioning and affects arbuscular mycorrhiza formation. *The Plant Journal* **78**: 877-889
- Delhaize E, Ryan PR** (1995) Aluminum Toxicity and Tolerance in Plants. *Plant Physiology* **107**: 315-321
- Delhaize E, Ryan PR, Hebb DM, Yamamoto Y, Sasaki T, Matsumoto H** (2004) Engineering high-level aluminum tolerance in barley with the ALMT1 gene. *Proceedings of the National Academy of Sciences of the United States of America* **101**: 15249-15254
- Müssig C, Shin G-H, Altmann T** (2003) Brassinosteroids Promote Root Growth in Arabidopsis. *Plant Physiology* **133**: 1261-1271
- Ramesh SA, Tyerman SD, Xu B, Bose J, Kaur S, Conn V, Domingos P, Ullah S, Wege S, Shabala S, Feijo JA, Ryan PR, Gilliam M** (2015) GABA signalling modulates plant growth by directly regulating the activity of plant-specific anion transporters. *Nature Communications* **6**
- Ryan PR, Tyerman SD, Sasaki T, Furuichi T, Yamamoto Y, Zhang W, Delhaize E** (2011) The identification of aluminium-resistance genes provides opportunities for enhancing crop production on acid soils. *Journal of Experimental Botany* **62**: 9-20
- Sasaki T, Yamamoto Y, Ezaki B, Katsuhara M, Ahn SJ, Ryan PR, Delhaize E, Matsumoto H** (2004) A wheat gene encoding an aluminum-activated malate transporter. *The Plant Journal* **37**: 645-653
- Tian Q, Zhang X, Ramesh S, Gilliam M, Tyerman SD, Zhang W-H** (2014) Ethylene negatively regulates aluminium-induced malate efflux from wheat roots and tobacco cells transformed with TaALMT1. *Journal of Experimental Botany* **65**: 2415-2426
- Yang Z-B, He C, Ma Y, Herde M, Ding Z** (2016) Jasmonic acid enhances Al-induced root-growth inhibition. *Plant Physiology* **173**: 1420-1433
- Zhang W-H, Rengel Z** (1999) Aluminium induces an increase in cytoplasmic calcium in intact wheat root apical cells. *Functional Plant Biology* **26**: 401-409

## Chapter 4: General discussion and future directions

Being sessile, plants have evolved exquisite metabolic diversity that allows them to perceive the incoming stresses and rapidly regulate their physiology and metabolism to cope with them. Organic anion efflux e.g. malate via ALMTs is an important mechanism for providing tolerance from stresses such as  $\text{Al}^{3+}$  toxicity (Delhaize and Ryan, 1995; Sasaki et al., 2004; Zhang et al., 2008; Ryan et al., 2011) but unregulated and excess efflux may also lead to loss of valuable plant reserves such as carbon and energy. Conservation of resources under stress is important for continued plant growth and yield and thus it is intuitive that there exist mechanisms and molecules such as GABA that tightly regulate ALMT activity.

In Chapter 2 (Plant Cell paper), I contributed to the work that demonstrated that changes in endogenous concentrations of GABA in wheat root tips and heterologous systems can be facilitated by TaALMT1. The exogenous application of amino-oxyacetate (AOA), a GAD inhibitor and vigabatrin, a GABA-T inhibitor, to tobacco BY2 cells affected anion efflux via ALMTs. It was further demonstrated that the mechanism for reduction of endogenous GABA concentration upon  $\text{Al}^{3+}$  treatment at low pH was due to efflux of GABA via TaALMT1. The role of GABA efflux via TaALMT1 is currently not understood, but the following possibilities exist:

- 1) GABA may act as an extracellular pH buffer to increase the pH in acidic conditions. This buffering effect may also be the case under alkaline conditions where efflux of GABA may decrease external pH (Chapter 3 and see below).

- 2) The GABA efflux will elevate extracellular GABA concentration which may then act as a break on malate efflux, preventing a runaway situation of excessive malate release. This situation appears to be the case for the mutant TaALMT1<sup>F213C</sup> which is not sensitive to external GABA (Chapter 2).

- 3) Previously it had been shown that a low concentration (10  $\mu\text{M}$ ) of exogenous GABA, similar to concentrations measured in root media reported here (Chapter 3), improved root growth of barley seedlings in acidic conditions with and without  $\text{Al}^{3+}$  exposure (Song et al., 2010). It was proposed in this case that GABA had a protective role against oxidative damage. Interestingly GABA application at a much higher concentration (10 mM) at alkaline pH had a strong inhibitory effect on root growth (Supplementary material for Chapter 3).

- 4) It has been shown that in addition to aluminium tolerance, AtALMT1 also acted as a key regulator in the attraction of the beneficial *Bacillus subtilis* strain FB17 to Arabidopsis roots

(Lakshmanan et al., 2013). *Bacillus subtilis* positively affects root growth and there is positive chemotaxis to Arabidopsis roots with chemoreceptors that recognise a range of amino acids.

5) The results reported here provide evidence that regulation of anion channels by GABA may be an important aspect of adaptive signaling in plants to cope with abiotic stresses. The effect of mutations leading to unchanged GABA concentrations in transgenic plants such as wheat and barley and their effect on growth, yield and stress tolerance is a subject for further research.

### **3.1 Alkaline tolerance mediated by TaLMT1**

In Chapter 3 the role of TaALMT1 in alkaline tolerance was explored. Due to its devastating effects on plant growth, soil alkalinity is a major constraint to plant survival and productivity worldwide. It has negatively affected food production and has raised food security concerns. According to Food and Agriculture Organization of the United Nations (FAO), about 795 million people are undernourished globally. Beside this, the estimated world population is expected to be nine billion by 2050 (Nakashima et al., 2014). Considering this rapid increase in population, scientists suggest that, by 2050, the current rate of yield production must increase by 37% (Tester and Langridge, 2010). To meet the future world's food demands, crop yields need to be improved. Hence, alkaline soil tolerant plants have appeared to be one of the most demanding aims for modern agriculture.

Under alkaline conditions, anion nutrient uptake such as nitrate and phosphate via proton-coupled symporters may be inhibited, as well as cell wall expansion. To allow nutrient uptake and growth, acidification of the rhizosphere is required. In Chapter 3, it was shown that the TaALMT1 transporter can facilitate acidification of the rhizosphere in alkaline conditions linked to the release of malate and GABA. However, based on the amount of GABA released, which would not account for the reduction in pH, it was argued that there may be also a coupled proton efflux.

Several studies have shown the mechanism of alkaline soil tolerance based on PM H<sup>+</sup>-ATPase mediated H<sup>+</sup> efflux (Fuglsang et al., 2007; Yang et al., 2010; Xu et al., 2012; Xu et al., 2013; Li et al., 2015). Chapter 3 has demonstrated a new mechanism of acidification of the rhizosphere under alkaline conditions suggesting that TaALMT1 and possibly other ALMTs have broader functions than the well-known Al<sup>3+</sup> tolerance under acidic conditions.

#### **4.2 Root growth over 5 weeks is enhanced at high pH by the presence of the TaALMT1-V allele in ET8 plants but not in barley expressing TaALMT1 (Appendix Chapter 3).**

In contrast to the ET8/ES8 comparison, transgenic barley expressing *TaALMT1* showed no differences in root or shoot growth compared to the golden promise background plants (GP) at pH 6 or pH 9 over 5 weeks of growth (Figure A1A,B). However, there was a significantly higher root biomass for the TaALMT1-GP plants at pH 9 than at pH 6, while for GP there was no difference between these two pHs (Figure A1B). For leaf gas exchange there were some similarities in how chlorophyll and *A* responded to the high pH with TaALMT1-GP having significantly higher chlorophyll than GP at pH 9 and a correspondingly higher *A* for TaALMT1-GP though not significantly different to GP (Figure A1 E,F). In contrast to the ET8-ES8 comparison, *E* and *g<sub>s</sub>* were significantly higher in TaALMT1-GP plants compared with GP plants (Figure A1C,D). This is interesting in respect of stomatal control since *TaALMT1* is constitutively expressed in the TaALMT1-GP plants and there could be effects at the leaf level on both malate and GABA transport in guard cells.

The effect of GABA on root and shoot growth showed some similarities to that of ET8 and ES8 with greater inhibition by GABA at pH 9 than pH 6, but both genotypes showed similar responses at the two pHs (Figure A2 A,B). In contrast to ET8-ES8 comparison, there was no increase in *E* or *g<sub>s</sub>* with GABA (Figure A2 AC,D), but there was a greater degree of inhibition by GABA on chlorophyll and *A* for the TaALMT1-GP plants (Figure A2 E,F). Overall, although there were some interesting differences in leaf gas exchange and responses to GABA, the TaALMT1-GP results do not support a role for TaALMT1 in conferring alkaline tolerance. This is in contrast to the dramatic effect that TaALMT1 expression has on Al<sup>3+</sup> tolerance of barley at low pH (Delhaize et al., 2004). Barley is known to be quite tolerant of alkaline conditions (Kyoko et al., 2017) while it is less tolerant of low pH and Al<sup>3+</sup> (Delhaize et al., 2004). We can only speculate at this stage that the presence of TaALMT1 and its constitutive expression interferes with the normal alkaline pH tolerance mechanism of barley and that this may have something to do with GABA transport via TaALMT1.

There was however, higher malate and GABA efflux measured for TaALMT1-GP at pH 9 compared to GP (Figure A4B,F), but in contrast to ET8 there was not the expected higher exudation at pH 9 compared to pH 6, on the contrary, GP barley had very high rhizosphere concentrations of malate and GABA at pH 6 that were reduced at pH 9. This was in stark contrast to the behavior of the TaALMT1-GP, again suggesting that there is an interaction between the expression of *TaALMT1* and the alkaline pH tolerance mechanisms in barley.

Further experiments are required using appropriate controls, i.e. null segregants, rather than the wildtype for comparison.

#### **4.3 Higher root exudation of malate and GABA occurs at alkaline pH in wheat and barley associated with the expression of TaALMT1**

Associated with the greater root growth observed for ET8 over ES8 at pH 9 there was also a greater apparent rhizosphere concentration of malate and GABA for ET8 root systems sampled after 5 weeks of growth compared to that for ES8 (Figure A3A,B). The concentrations of malate and GABA were also higher for ET8 at pH 9 than for pH 6, while ES8 showed no differences. The values obtained cannot be attributed to actual rhizosphere concentrations, which are likely to be higher, but can be used for comparison between the genotypes. There was also higher malate and GABA concentrations measured for TaALMT1-GP at pH 9 compared to GP (Figure A3B,F), but in contrast to ET8 there was not the expected higher exudation at pH 9 compared to pH 6, on the contrary GP barley had very high rhizosphere concentrations of malate and GABA at pH 6 that were reduced at pH 9. This was in stark contrast to the behavior of the TaALMT1-GP, again suggesting that there is an interaction between the expression of *TaALMT1* and the alkaline pH tolerance mechanisms in barley.

There was no inhibitory effect of GABA treatment on the concentration of malate sampled from root systems, which is contrary to the expected effect of GABA as a blocker of malate efflux through TaALMT1 (Ramesh et al., 2015). Perhaps longer-term treatment by GABA has secondary effects as indicated by the alteration of leaf gas exchange. Interestingly for both ES8 and GP barley, there was a significant increase in malate rhizosphere concentration in response to GABA which was not observed for the genotypes with high *TaALMT1* expression (Figure 3C,D). It was previously shown that the expression of *TaALMT1* increased endogenous GABA concentrations by an unknown mechanism (Ramesh et al., 2018). This may account for the difference in malate exudation in response to GABA associated with TaALMT1 if GABA is a source for malate synthesis through the GABA shunt and tricarboxylate acid (TCA) cycle.

The efflux of malate and GABA from root apices were increased in the short term (1h) in response to pH 9 for the wheat ET8, (Figure A4). This effect was not dependent on solution buffering in ET8, but a weaker response in TaALMT1-GP for GABA efflux was dependent on buffering, where solution buffering resulted in a significant difference between pH 6 and pH 9. For malate efflux, there was no significant difference between TaALMT1-GP and GP at any pH while GABA efflux from TaALMT1-GP was significantly higher at pH 9. It is possible that TaALMT1 may be interacting with a barley ALMT that also effluxes malate at high pH, while the GABA efflux through TaALMT1 is not affected by this interaction. The weak response of

the TaALMT1-GP to high pH contrasts to the larger responses at low pH in the presence of  $\text{Al}^{3+}$  for both malate and GABA efflux (Ramesh et al., 2018), though one similarity between the two responses is the larger response in GABA efflux than malate efflux in TaALMT1-GP. These results reflect the situation observed for whole root systems of ET8 and ES8 but not for TaALMT1-GP and GP (Figure A3). A possible explanation is that the constitutive expression of *TaALMT1* in barley has disturbed the whole root response as opposed to the expected response of root apices.

#### **4.4 TaALMT1 might also be involved in aluminium tolerance at alkaline pH**

The malate and GABA efflux activation in ET8 and barley TaALMT1-GP in response to sodium aluminate over 22 hours is likely the result of the activation of TaALMT1 by aluminate (Figure A5). This needs to be confirmed in a heterologous system such as *Xenopus* oocytes expressing *TaALMT1*.

Better root growth over 22 h was also demonstrated by ET8 and TaALMT1-GP in response to aluminate (Figure A6) potentially linked to higher malate and GABA efflux. As was shown in Chapter 3, malate and GABA efflux is associated with lower rhizosphere pH. Previously, it has been suggested that it is not necessary to lower the rhizosphere pH to neutral to prevent aluminium toxicity under alkaline conditions. Rather, lowering soil pH to <9, at which point the concentration of negative species of Al is greatly reduced (Brautigan et al., 2014). This suggests that the possible pH decrease because of TaALMT1 mediated malate and GABA efflux resulted in better root growth in ET8 and TaALMT1-GP in response to aluminate at alkaline conditions and which raises a possible role of TaALMT1 in aluminium tolerance at alkaline conditions.

It is also possible that GABA is released to decrease pH while malate release controls the aluminate, though predictions of malate-aluminate complexation done by our collaborator (Dr Fien Degryse) showed a negligible complexation at alkaline pH. We know from Ramesh et al (2018) (Chapter 2 Supplementary data) that GABA doesn't complex with aluminium ( $\text{Al}^{3+}$ ) in acidic conditions. But we don't know if GABA can be complexed with aluminate at high pH.

#### **4.5 Exogenous GABA and muscimol blocked $\text{Al}^{3+}$ activated malate efflux at low pH, but the block didn't occur at high pH.**

Previously, it has been shown that exogenous GABA and muscimol blocked  $\text{Al}^{3+}$  activated malate efflux in acidic conditions from both ET8 roots and also in heterologous systems expressing TaALMT1 and other ALMTs (Ramesh et al., 2015). This was confirmed for ET8 roots (Figure A8 A,C). In contrast to low pH, GABA and muscimol block of malate efflux from

ET8 roots did not occur at high pH (Figure A8 B,D). This is likely to reflect the sensitivity of TaALMT1 which is highly expressed in ET8 roots, but the result needs to be confirmed using a heterologous system such as *Xenopus* oocytes. The observation does confirm the observation that GABA treatment in the long term had no effect on rhizosphere malate concentration at alkaline pH (Chapter 3). It is also possible that GABA has multiple effects particularly at high concentration.

#### **4.6 Is TaALMT1 calcium sensitive?**

It has been demonstrated that aluminium toxicity is linked with the disturbance of cytoplasmic Ca<sup>2+</sup> homeostasis in wheat which ultimately results in root growth inhibition (Zhang and Rengel, 1999). Previously it has been shown that a xylem parenchyma located QUAC channel, now considered to be ALMTs, are inhibited at high cytosolic calcium activity (Gilliham and Tester, 2005) while other ALMTs are activated by cytosolic calcium (Meyer et al., 2011). These reports indicate that there are likely to be links between ALMT activity and both extracellular and intracellular calcium concentrations.

In the presence of aluminium, except 0.1 mM CaCl<sub>2</sub>, all other CaCl<sub>2</sub> (0.5, 1, 3 and 5 mM) treatments showed a significantly increased Al<sup>3+</sup>-activated malate efflux in ET8 compared with ES8 (Figure A9). The 3 mM CaCl<sub>2</sub> concentration gave the largest response, and since this calcium concentration alone did not activate the malate efflux it suggests that Al<sup>3+</sup> activation of TaALMT1 is somehow potentiated by a high calcium concentration, possibly in the cytosol, since high external calcium can lead to high cytosolic calcium. That an optimum was observed at 3 mM may suggest a narrow range of cytosolic calcium for a maximum response. However it is possible that high media calcium concentration (5 mM) may reduce the free Al<sup>3+</sup> concentration, which is essential for TaALMT1 activation. The 3 mM CaCl<sub>2</sub> concentration was used routinely for the high pH experiments.

#### **4.7 Research questions and future directions**

My work has raised several important questions which I have discussed below with possible future experiments.

##### 4.7.1 What is the molecular mechanism (in a broader perspective) of alkaline soil tolerance?

Though I have studied the expression of a few genes in Chapter 3 (*TaALMT1*, *GAD*, *GAD1*, *GABA T*) in response to alkaline media it is vital to broaden this and understand the transcriptional events that may be important for alkaline soil tolerance.

Transcriptional events in ET8 and ES8 wheat could be compared upon transition of these plants to alkaline conditions using RNAseq analysis followed by quantitative RT-PCR on genes of interest. Although guided by the RNAseq results it may be anticipated that genes of interest could include those related to ALMTs. In addition, genes involved in the TCA cycle,  $Al^{3+}$  responses, pH regulation, J3 protein (Arabidopsis DnaJ homologous protein3) (Yang et al., 2010), TFT4 (member of 14-3-3 protein family) (Xu et al., 2013), protein kinase 5 (PKS5) (Fuglsang et al., 2007), and other genes that regulate the PM  $H^+$ -ATPase. Hormone markers should also be examined given the significant effects that ethylene, jasmonic acid and brassinosteroid have on TaALMT1 induced fluxes of malate and GABA (Chapter 3 Appendix). It would be profitable to examine expression of genes of interest emerging from the RNAseq in other cultivars of wheat that differ in sensitivity to alkaline conditions.

#### 4.7.2 Is TaALMT1-mediated GABA influx and efflux proton-coupled?

In Chapter 2 it was shown that GABA influx in *Xenopus* oocytes expressing *TaALMT1* is greatly stimulated by low pH (Chapter 2, Figure 6A). There was a significantly higher GABA influx in *TaALMT1* and *AtGAT1* (high-affinity GABA transporter) expressing oocytes compared with controls. At pH 7.5 (Chapter 2, Figure 6B), TaALMT1 loses its capacity to transport GABA, but when  $Na_2SO_4$  was added, which activates TaALMT1, there was a stimulated GABA influx. However, this stimulated flux was still much lower than that at low pH. This data may indicate that GABA influx is proton-coupled.

In Chapter 3 (Figure 3, 4 and 5) it was shown that in alkaline conditions, a higher concentration of both malate and GABA was found in root exudates from ET8 plants compared with ES8, which appeared to decrease the rhizosphere pH more rapidly in ET8 plants. Though there was a large difference in GABA concentrations between ET8 and ES8 in the early stages of the experiment (Chapter 3, Figure 6), the difference in the pH was quite small and not significantly different. This might be because bicarbonate was used as a buffer in the solution, which has a stronger buffer capacity at high pH. As the pH was lowered out of the range of the bicarbonate pKa, the greater capacity of ET8 roots to lower pH became clearer.

The role of TaALMT1 in acidification was verified by using microelectrode ion flux estimation (MIFE) on *TaALMT1* injected and water injected oocytes (Chapter 3 Figure 8). It was demonstrated that TaALMT1 was associated with greater acidification of the external medium associated with a large GABA release from *Xenopus* oocytes expressing *TaALMT1*. As *Xenopus* oocytes don't have a proton pump this raises an outstanding question: Is TaALMT1 mediated GABA efflux proton-coupled? In other words, as GABA effluxes it may be coupled

to the efflux of protons from the more acidic (relative) cytoplasm to the highly alkaline external media.

To address this, two models are proposed. In one model (Figure 1A), TaALMT1 is activated by high pH to release malate and GABA. GABA at pH 9 acts like a buffer and donates a proton from its amino group. GABA will release protons to the medium and a small proportion will become a negatively charged anion. In addition the malate efflux is allowing the proton pump to work faster (in plants) because malate<sup>2-</sup> efflux would balance the flux of positive charge through the pump. So in this way the proton pump helps in acidification of the apoplast along with the acidification caused by GABA efflux. This may be the situation accounting for the rapid reduction in pH observed for wheat root tips with high expression of TaALMT1 (Chapter 3 Figure 7). However, if we consider the *Xenopus* oocyte experiment (Chapter 3, Figure 8), where a proton pump does not operate (rather there is a Na<sup>+</sup>/K<sup>+</sup> ATPase (Setiawan\* et al., 2002), there is still an apparent proton efflux when TaALMT1 is activated. This strongly suggests that GABA efflux is coupled with proton efflux. Hence, an alternative model is suggested (Figure 1B) where protons are also effluxed with malate and GABA. This is in concordance with the observation that GABA influx is stimulated by low pH (Chapter 2, Figure 6A), i.e. based on the direction of the proton gradient. In other words, the movement of GABA is coupled to the movement of protons in both directions, either efflux or influx. There is one observation that does not match this hypothesis. When activated by Al<sup>3+</sup> at low pH there is an efflux of GABA in addition to malate via TaALTM1. This would be against the proton motive force. However, when one considers that GABA influx is blocked by Al<sup>3+</sup> at low pH (Figure 6C, Chapter 2) it is possible that Al<sup>3+</sup> is uncoupling the transport of protons with GABA.

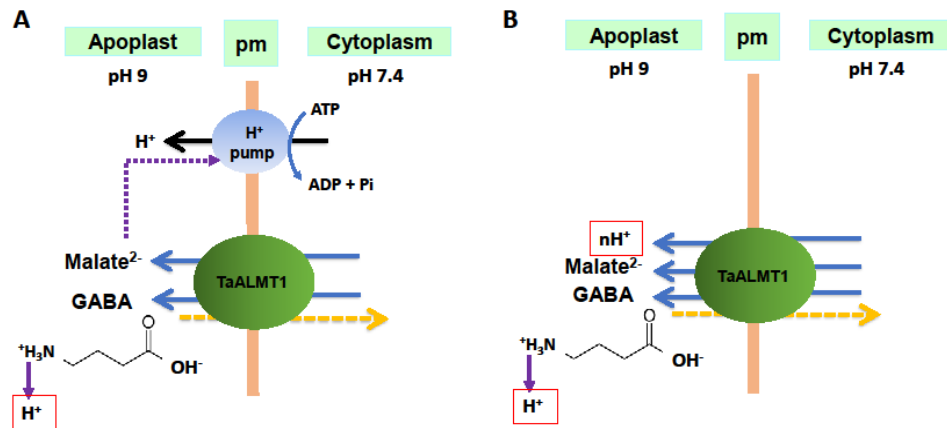


**Figure 1:** Two proposed models for external acidification via TaALMT1 under alkaline conditions. **A)** Shows a large GABA efflux through TaALMT1 in addition to malate at alkaline pH. Some acidification can occur from GABA release at high pH as GABA will donate a proton from its amino group ( $pK_a = 10.43$ ). In addition,  $H^+$  efflux via the PM  $H^+$ -ATPase is stimulated by malate<sup>2-</sup> efflux through TaALMT1 via membrane voltage (i.e. charge balance). **B)** shows malate and GABA efflux coupled with proton efflux.

Some basic calculations (for details see Discussion, Chapter 3) suggested that GABA efflux may be coupled with proton efflux (Model B) since the amount of GABA effluxed appeared to be higher than could be accounted for by the GABA concentration gradient from the oocytes. The following experiments, both with wheat roots and heterologous systems could be done to determine whether GABA efflux is proton-coupled.

In ET8 plants, the PM  $H^+$ -ATPase could be inhibited using vanadate, and then TaALMT1 could be activated by high pH and the acidification of the rhizosphere and proton efflux measured using MIFE (e.g. Chapter 3 Figure 7). If the same degree of acidification occurred as without the inhibitor and comparing also ES8 roots this would support the hypothesis of proton coupling. A similar experiment could be performed with *Xenopus* oocytes expressing TaALMT1 both for GABA efflux and influx. Since oocytes don't have a PM  $H^+$ -ATPase, using vanadate shouldn't affect the proton efflux. However they do possess a  $Na^+/H^+$  exchanger (Busch et al., 1995) which can be checked using the inhibitor amiloride.

Another possibility is to block TaALMT1 at high pH and measure the effect on the apparent proton efflux. The challenge here is to find a blocker that works at high pH since

muscimol was ineffective at high pH (Appendix Chapter 3). Vigabatrin (Chapter 2, Figure 5), niflumic acid (e.g. (Zhang et al., 2008)) might work as potential blockers of TaALMT1 at high pH.

#### 4.7.3 Can malate and GABA be complexed with aluminium at high pH?

Malate complexation with  $Al^{3+}$  in acidic conditions is a well-known mechanism which confers  $Al^{3+}$  tolerance in wheat (Delhaize and Ryan, 1995; Ma et al., 2001; Sasaki T, 2004). It was shown (Chapter 2, Supplemental Methods) that GABA does not significantly complex  $Al^{3+}$  in acidic conditions. In alkaline conditions, sodium aluminate ( $NaAlO_2$ ) activates TaALMT1 mediated malate and GABA efflux (App Figure A5). Despite the strong complexation of malate with  $Al^{3+}$  at low pH, with increase in pH, malate complexation decreases and above pH 7, the complexation is predicted to become negligible and there is no difference in  $Al^{3+}$  speciation (dominated by the  $Al(OH)_4^-$  ion above pH 7) whether malate is present or not (Dr F. Degryse Personal Communication).

Conversely to malate, it is possible that there might be complexation of  $Al(OH)_4^-$  with GABA at higher pH due to a possible interaction between the negative aluminate and the charged amino group.

Another possible experiment is to examine in detail the activation of TaALMT1 at high pH by aluminate in *Xenopus* oocytes. Aluminate may be acting like sulphate as an anion, which activates TaALMT1 at high pH (Ramesh et al 2015). TaALMT1 may be very sensitive to aluminate.

#### 4.7.4 What are the links between ALMTs and plant hormones?

Previously, it has been reported that plant hormones such as jasmonic acid (JA), auxin and ethylene are involved in Al-induced root growth inhibition in acidic conditions (Tian et al., 2014; Yang et al., 2016). It has also been observed that ethylene is a negative regulator of TaALMT1 by demonstrating that ethylene and ACC pre treatment inhibited ALMT1 mediated malate efflux in wheat roots and BY2 cells expressing TaALMT1 (Tian et al., 2014). More recently, it has been shown that JA modulates ALMT1 mediated malate efflux and hence, enhances aluminium induced root growth inhibition (Yang et al., 2016). These reports suggest that there may be links between ALMTs and other known regulatory pathways of root growth such as brassinosteroids, jasmonic acid, abscisic acid, ethylene, salicylic acid and auxin, which need to be explored further.

Preliminary experiments reported here show that BR and JA enhance  $Al^{3+}$ -activated malate efflux in ET8 roots (Figure A10, A11 and A12). Jasmonic acid in the presence of

aluminium also enhanced root growth inhibition in wheat, however, BR, increased root growth when aluminium was present (Figure A14). Although it is known that ethylene negatively regulates TaALMT1 mediated malate efflux (Tian et al., 2014), there is no information to date on the effect of ethylene on GABA flux via TaALMT1. Thus, it will be very interesting to see the effect of ethylene on GABA fluxes. Interestingly JA by itself increased GABA efflux from ET8 roots, but when aluminium was present, it decreased GABA efflux (App Figure 13). The BR effect was the other way around. These results demonstrate that the TaALMT1 transporter may be quite complex in the way it transports both malate and GABA, however, these results need to be confirmed in a heterologous system where the complication of other malate and GABA transporters which may be present in roots is decreased. Experiments with *Xenopus* oocytes (TEVC) could also indicate if direct hormone interaction occurs with the transporter since receptors for plant hormones are assumed to be absent in *Xenopus* oocytes. Further experiments are required to fully understand the links between ALMTs and these plant regulators and their possible role in extreme pH (acidic and alkaline) stress tolerance. Further links between plant hormones and ALMTs in extreme pH stress tolerance (both, low and high pH stress) may be explored using *Arabidopsis* wild type, *almt* mutants and ALMT over expresser plants.

#### 4.8 References

- Brautigan DJ, Rengasamy P, Chittleborough DJ** (2014) Amelioration of alkaline phytotoxicity by lowering soil pH. *Crop and Pasture Science* **65**: 1278-1287
- Busch S, Wieland T, Esche H, Jakobs KH, Siffert W** (1995) G Protein Regulation of the Na/H Antiporter in *Xenopus laevis* Oocytes: involvement of protein kinases A and C. *Journal of Biological Chemistry* **270**: 17898-17901
- Delhaize E, Ryan PR** (1995) Aluminum Toxicity and Tolerance in Plants. *Plant Physiology* **107**: 315-321
- Delhaize E, Ryan PR, Hebb DM, Yamamoto Y, Sasaki T, Matsumoto H** (2004) Engineering high-level aluminum tolerance in barley with the *ALMT1* gene. *Proceedings of the National Academy of Sciences of the United States of America* **101**: 15249-15254
- Fuglsang AT, Guo Y, Cuin TA, Qiu Q, Song C, Kristiansen KA, Bych K, Schulz A, Shabala S, Schumaker KS, Palmgren MG, Zhu J-K** (2007) Arabidopsis Protein Kinase PKS5 Inhibits the Plasma Membrane H<sup>+</sup>-ATPase by Preventing Interaction with 14-3-3 Protein. *The Plant Cell Online* **19**: 1617-1634
- Gilliam M, Tester M** (2005) The Regulation of Anion Loading to the Maize Root Xylem. *Plant Physiology* **137**: 819-828
- Kyoko H, Kota O, Satoru A, Shogo N, Tetsuya U, Taira M, Atsushi I, Takahiro H, Masayuki S** (2017) Elongation of barley roots in high-pH nutrient solution is supported by both cell proliferation and differentiation in the root apex. *Plant, Cell & Environment* **40**: 1609-1617
- Lakshmanan V, Castaneda R, Rudrappa T, Bais HP** (2013) Root transcriptome analysis of *Arabidopsis thaliana* exposed to beneficial *Bacillus subtilis* FB17 rhizobacteria revealed genes for bacterial recruitment and plant defense independent of malate efflux. *Planta* **238**: 657-668
- Li J, Xu H-H, Liu W-C, Zhang X-W, Lu Y-T** (2015) Ethylene Inhibits Root Elongation during Alkaline Stress through AUXIN1 and Associated Changes in Auxin Accumulation. *Plant Physiology* **168**: 1777-1791
- Ma JF, Ryan PR, Delhaize E** (2001) Aluminium tolerance in plants and the complexing role of organic acids. *Trends in Plant Science* **6**: 273-278
- Meyer S, Scholz-Starke J, De Angeli A, Kovermann P, Burla B, Gambale F, Martinoia E** (2011) Malate transport by the vacuolar AtALMT6 channel in guard cells is subject to multiple regulation. *The Plant Journal* **67**: 247-257

- Nakashima K, Yamaguchi-Shinozaki K, Shinozaki K** (2014) The transcriptional regulatory network in the drought response and its crosstalk in abiotic stress responses including drought, cold, and heat. *Frontiers in Plant Science* **5**: 170
- Ramesh SA, Kamran M, Sullivan W, Chirkova L, Okamoto M, Degryse F, McLauchlin M, Gilliam M, Tyerman SD** (2018) Aluminium-Activated Malate Transporters Can Facilitate GABA Transport. *The Plant Cell* **30**: 1147–1164
- Ramesh SA, Tyerman SD, Xu B, Bose J, Kaur S, Conn V, Domingos P, Ullah S, Wege S, Shabala S, Feijo JA, Ryan PR, Gilliam M** (2015) GABA signalling modulates plant growth by directly regulating the activity of plant-specific anion transporters. *Nature Communications* **6**: 7879
- Ryan PR, Tyerman SD, Sasaki T, Furuichi T, Yamamoto Y, Zhang W, Delhaize E** (2011) The identification of aluminium-resistance genes provides opportunities for enhancing crop production on acid soils. *Journal of Experimental Botany* **62**: 9-20
- Sasaki T, Yamamoto Y, Ezaki B, Katsuhara M, Ahn SJ, Ryan PR, Delhaize E, Matsumoto H** (2004) A wheat gene encoding an aluminum-activated malate transporter. *The Plant Journal* **37**: 645-653
- Sasaki T YY, Ezaki B, Katsuhara M, Ahn SJ, Ryan PR, Delhaize E, Matsumoto H.** (2004) A wheat gene encoding an aluminium-activated malate transporter. *The Plant Journal* **37**: 645–653
- Setiawan I, Henke G, Feng Y, Böhmer C, Vasilets LA, Schwarz W, Lang F** (2002) Stimulation of *Xenopus* oocyte Na<sup>+</sup>,K<sup>+</sup>ATPase by the serum and glucocorticoid-dependent kinase sgk1. *Pflügers Archiv* **444**: 426-431
- Song HM, Xu XB, Wang H, Wang HZ, Tao YZ** (2010) Exogenous gamma-aminobutyric acid alleviates oxidative damage caused by aluminium and proton stresses on barley seedlings. *Journal of the Science of Food and Agriculture* **90**: 1410-1416
- Tester M, Langridge P** (2010) Breeding technologies to increase crop production in a changing world. *Science* **327**: 818-822
- Tian Q, Zhang X, Ramesh S, Gilliam M, Tyerman SD, Zhang W-H** (2014) Ethylene negatively regulates aluminium-induced malate efflux from wheat roots and tobacco cells transformed with TaALMT1. *Journal of Experimental Botany* **65**: 2415-2426
- Xu W, Jia L, Baluška F, Ding G, Shi W, Ye N, Zhang J** (2012) PIN2 is required for the adaptation of *Arabidopsis* roots to alkaline stress by modulating proton secretion. *Journal of Experimental Botany* **63**: 6105-6114

- Xu W, Jia L, Shi W, Baluška F, Kronzucker HJ, Liang J, Zhang J** (2013) The tomato 14-3-3 protein TFT4 modulates H<sup>+</sup> efflux, basipetal auxin transport, and the PKS5-J3 pathway in the root growth response to alkaline stress. *Plant Physiology* **163**: 1817-1828
- Yang Y, Qin Y, Xie C, Zhao F, Zhao J, Liu D, Chen S, Fuglsang AT, Palmgren MG, Schumaker KS** (2010) The Arabidopsis chaperone J3 regulates the plasma membrane H<sup>+</sup>-ATPase through interaction with the PKS5 kinase. *The Plant Cell* **22**: 1313-1332
- Yang Z-B, He C, Ma Y, Herde M, Ding Z** (2016) Jasmonic acid enhances Al-induced root-growth inhibition. *Plant Physiology* **173**: 1420-1433
- Zhang W-H, Rengel Z** (1999) Aluminium induces an increase in cytoplasmic calcium in intact wheat root apical cells. *Functional Plant Biology* **26**: 401-409
- Zhang W-H, Ryan PR, Sasaki T, Yamamoto Y, Sullivan W, Tyerman SD** (2008) Characterization of the TaALMT1 Protein as an Al<sup>3+</sup>-Activated Anion Channel in Transformed Tobacco (*Nicotiana tabacum* L.) Cells. *Plant and Cell Physiology* **49**: 1316-1330